THE UNIVERSITY
of EDINBURGH

THE UNIVERSITY of EDINBURGH

The role of long non-coding RNA in atherosclerosis

Dr John David Hung

MBChB MRCP

PhD in Cardiovascular Science
The University of Edinburgh
2020

Author's Declaration

The thesis herein is solely my own work. Apart from where stated the experiments were performed entirely by me. I confirm that this work has not been previously submitted for any other degree.

Acknowledgement

Moving to Edinburgh to do a PhD at the Centre for Cardiovascular Science changed my life hugely, and in the 3 years I spent there I positively remodelled as a doctor a scientist and a person. For this I will always be grateful and indebted to my brilliant supervisors Professors Andy Baker, David Newby and Judith Sluimer. Andy and Dave took a chance on a doctor in science, who had never before held a pipette, and they guided me every step of the way with close and careful attention, both in and out of the lab. Time spent in Andy's office was balanced by time on our bikes, and although I now spend most of my time in a different sort of lab, I know we'll ride together many more times in years to come. Judith supported me greatly both in Edinburgh and in Maastricht, and introduced me to her fantastic team for a short but really fruitful placement in CARIM.

I thank all of the talented senior scientists and classmates of the Baker Lab past and present too numerous to mention individually, for their time, expertise and willingness to adopt a cardiologist into their fold, with particular thanks to Dr Julie Rodor for bioinformatic support. On the clinical side I worked with some of the best cardiology researchers in the world, and again I thank Dave and also Professor Nick Mills for the vast and valuable opportunities afforded to me. I helped to run and participate in some fantastic trials, and we will all remember how I once cured heart failure once and for all!

My friends and family, who all now understand the intricacies of long non-coding RNA biology, are I'm sure both proud and relieved that I have finished in equal measures, and of course I owe them all a depth of gratitude.

Table of Contents

List of Figures

List of Tables

Abstract

Coronary heart disease is responsible for around 2 million deaths across Europe each year. This is largely caused by atherosclerosis, a chronic inflammatory disease of the vasculature characterized by development of plaque in the arterial wall. Advanced plaques may become unstable, carrying a risk of rupture or erosion and manifest as acute myocardial infarction. In patients with type 1 and type 2 myocardial infarction, mortality rates remain high; up to 15% and 25%, respectively. Although risk stratification tools like the Global Registry of Acute Coronary Events (GRACE) 2.0 score can robustly predict outcome in these patients, new therapies targeting the unstable plaque are still needed to address this global epidemic.

Long non-coding RNAs (lncRNAs) are an emergent class of molecules with diverse functional roles, widely expressed in human physiology and disease. Although some lncRNAs have already been identified in cardiovascular disease, their potential as novel targets in the prevention of atherosclerosis remains unknown. The aim of this project was to discover important lncRNAs in unstable plaque and gain insight into their functional relevance.

Analysis of RNA sequencing previously performed on stable and unstable atherosclerotic plaque identified a panel of 47 differentially regulated lncRNAs. I focused on LINC01272, a lncRNA upregulated in unstable plaque previously detected in inflammatory bowel disease, and ultimately renamed it PELATON (plaque enriched lncRNA in atherosclerotic and inflammatory bowel macrophage regulation). PELATON is highly monocyte- and macrophage-

specific across vascular cell types, and almost entirely nuclear by cellular fractionation (90%–98%). In situ hybridization confirmed enrichment of PELATON in areas of plaque inflammation, co-localising with macrophages around the shoulders and necrotic core of human plaque sections. Consistent with its nuclear localization, and despite containing a predicted open reading frame, PELATON did not demonstrate any protein-coding potential in vitro. Functionally, knockdown of PELATON significantly reduced phagocytosis, lipid uptake and reactive oxygen species production in high- content analysis, with a significant reduction in phagocytosis independently validated. Furthermore, CD36, a key mediator of phagocytic oxLDL (oxidized low-density lipoprotein) uptake was significantly reduced with PELATON knockdown.

Taken together, these data demonstrate that a novel lncRNA (PELATON) is important to macrophage function in atherosclerotic plaque. Future work should focus on manipulation of PELATON, to reduce plaque instability, and prevent cardiovascular events.

Lay Summary

It is recently understood that RNA (ribonucleic acid) molecules have more significance in human physiology than previously known. Whilst it has long been accepted that RNA molecules are nature's middle man; between cellular DNA (deoxyribonucleic acid) and the body's manufacture of proteins - they play many other critical roles in healthy and disease processes, quite aside from regular transcription.

One particular type of RNA called long non-coding RNA is not extensively studied, but has already been associated with many disease processes, including atherosclerosis. Atherosclerosis or 'hardening of the arteries' is the disease process in the body that causes 'plaques' form in the walls of arteries which can suddenly rupture, to cause heart attacks or strokes. The objective of this project was to discover previously unknown long non-coding RNAs (lncRNAs) which are important in human atherosclerosis, and could be manipulated to reduce the risk of vascular diseases and complications.

Using RNA sequencing; a technique to identify all of the different RNAs within a sample, a panel of novel lncRNAs from the arteries of patients who had had strokes were identified. Of these, LINC01272, subsequently renamed PELATON, was studied further. PELATON (plaque enriched lncRNA in atherosclerotic and inflammatory bowel macrophage regulation) was mostly present in macrophages, one of the body's important immune system cell types. To further confirm this, sections of diseased arteries taken from patients' arteries were stained, and highlighted PELATON in the most critical regions.

Further experiments to investigate PELATON's function in macrophages then demonstrated it actually controls macrophage behaviour in certain aspects. In reducing the amount of PELATON in macrophages grown in petri dishes, the cells were less good at carrying out their usual functions. This included phagocytosis, the process of eating nearby foreign bodies; and lipid uptake, which occurs in the walls of diseased arteries contributing to plaque progression.

In summary, PELATON is a newly discovered and characterised species of long non-coding RNA. It has been shown to be important in controlling macrophage behaviour, which is a critical cell type in the plaques of diseased arteries. Future work should be aimed at manipulating levels of PELATON in human arteries to reduce the risk of heart attacks and strokes.

Definitions / Abbreviations

18F-FDG	18F Fluorodeoxyglucose
18F-NaF	18F Sodium fluoride
BSA	bovine serum albumin
CASMC	coronary artery smooth muscle cell
DCFDA	dichlorofluorescin diacetate
DTT	Dithiothreitol
EC	endothelial cell
ED	endothelial dysfunction
FPKM	fragments per kilobase million
GEO	gene expression omnibus
HA	haemagglutinin
ISH	in-situ hybridisation
LDL	low-density lipoprotein
Log2FC	Log2 fold change
lncRNA	long non-coding RNA
M-CSF	macrophage colony-stimulating factor
miRNA	micro-RNA
MLN	myoregulin
ORF	open reading frame
oxLDL	oxidised low-density lipoprotein
PAEC	pulmonary artery endothelial cell
PASMC	pulmonary artery smooth muscle cell
PBMC	peripheral blood mononuclear cell
PVD	Peripheral vascular disease
RNA	ribonucleic acid
RNA-seq	RNA sequencing
ROS	reactive oxygen species
SDS	Sodium dodecylsulfate
SMC	smooth muscle cell
SSC	saline-sodium citrate
T1MI	Type 1 myocardial infarction
T2MI	Type 2 myocardial infarction
TBS	tris-buffered saline
TBS-T	tris-buffered saline and Tween
VSMC	vascular smooth muscle cell

Chapter 1 Introduction

Hung J, Miscianinov V, Sluimer JC, Newby DE, Baker AH. Targeting Non-coding RNA in Vascular Biology and Disease.
Frontiers in Physiology. 2018;9:1655. Published 2018 Nov 22.
doi:10.3389/fphys.2018.01655

1.1 Atherosclerosis

Atherosclerosis is the principal driver of cardiovascular disease worldwide. Atherosclerotic plaques develop over decades in the arterial walls of susceptible individuals, in response to numerous well-known risk factors, including inflammation and high levels of circulating lipids. The clinical effect of atherosclerosis varies widely dependent on site, severity, and co-morbidity, and can range from completely asymptomatic to clinically catastrophic in the case of myocardial infarction (MI), stroke, and the acutely ischaemic limb. These acute events are usually sudden, often unexpected, and result from atherosclerotic plaque rupture. In its early stages, atherosclerosis is sub-clinical with endothelial dysfunction, intimal thickening, and plaque formation occurring silently and insidiously, only becoming clinically apparent when the plaque becomes large enough to impinge on luminal blood flow or becomes unstable and ruptures. In the coronary arteries, luminal stenosis results in angina, manifest most commonly as chest pain on exertion, and the equivalent in the peripheral vasculature, “intermittent claudication”, can be completely disabling to those affected. These chronic diseases, whilst not in themselves immediately life- threatening, reduce quality of life and consume large amounts of healthcare resources annually. Atherosclerosis in the carotid arteries is usually asymptomatic, until plaque rupture results in transient ischaemic attack (TIA) or stroke. Other sites of atherosclerosis result in chronic kidney disease and hypertension if present in the renal arteries; cognitive impairment in cerebrovascular disease in the brain; and abdominal angina in mesenteric disease.

1.2 Pathology of atherosclerosis

The precise and complete aetiology of atherosclerosis remains undiscovered, but there are multiple risk factors well-known to contribute to plaque formation, progression and rupture which may be genetic or acquired.

Risk Factors

In terms of genetics, the presence of a family history alone increases an individual's chances of atherosclerosis by up to 2.5-fold in some studies, particularly when occurring earlier in a parent or sibling's life (<60 years) (1-3). Whilst the genes and loci implicated in this condition are quite clear in specific scenarios such as familial hypercholesterolaemia (FH), a more general genetic susceptibility has never been identified (4, 5). In the particular case of FH, the most common abnormality is in the gene encoding the low-density lipoprotein receptor (LDLR) (60-80%), whilst aberrant genes encoding the apolipoprotein B (APOB), and proprotein convertase subtilisin/kexin 9 (PCSK9) are now also implicated. The syndrome was first characterised in 1939 by Muller, when high levels of circulating LDL and clinical evidence of xanthomata were correlated with an increased cardiovascular risk (6). It was in fact these early findings which, in no small part, contributed to the development of the 'diet–heart disease hypothesis', which is still commonly held today (7). Current recommendations in FH include familial screening and aggressive treatment with 3-hydroxy-3 methylglutaryl CoA (HMGCoA) reductase inhibitors (statins) to affected family members (8).

Hypercholesterolaemia

Whether it is hence considered genetic or acquired, hypercholesterolaemia has long been deemed one of the principal risk factors for cardiovascular disease. It would be considered household knowledge that “high-cholesterol” leads to atherosclerosis (and by extension cardiovascular disease) (9). Early insights from large epidemiological registries such as Framingham demonstrated the association in the 1960s, and the World Health Organisation still states that one third of ischaemic heart disease is attributable to high cholesterol, and it may cause up to 2.6 million deaths globally each year (10, 11). However, after decades of public health activity in the Western world directed at lowering cholesterol levels in the population, it is now clear that the involvement of lipids in the pathophysiology of atherosclerosis is more complex, and that the differing contributions of the different lipid particles in the human body ought to be recognised.

‘Cholesterol’ itself is the traditional lipid target for reduction in humans, to promote a healthy cardiovascular system. This sterol ($C_{27}H_{46}O$) is one of several major lipids, as well as triglycerides, that is actually essential for normal physiology in the production of steroid hormones and bile acids, and in the maintenance of cell membranes throughout the body. The majority of cholesterol (80%) is synthesised in the liver and intestines, with a relatively smaller contribution from dietary intake.

Triglycerides similarly are essential for cell membrane function, and are the storage form of fatty acids, an important energy source. Both triglycerides and

cholesterol are packaged and transported in lipoproteins, along with fat soluble vitamins, for delivery around the body.

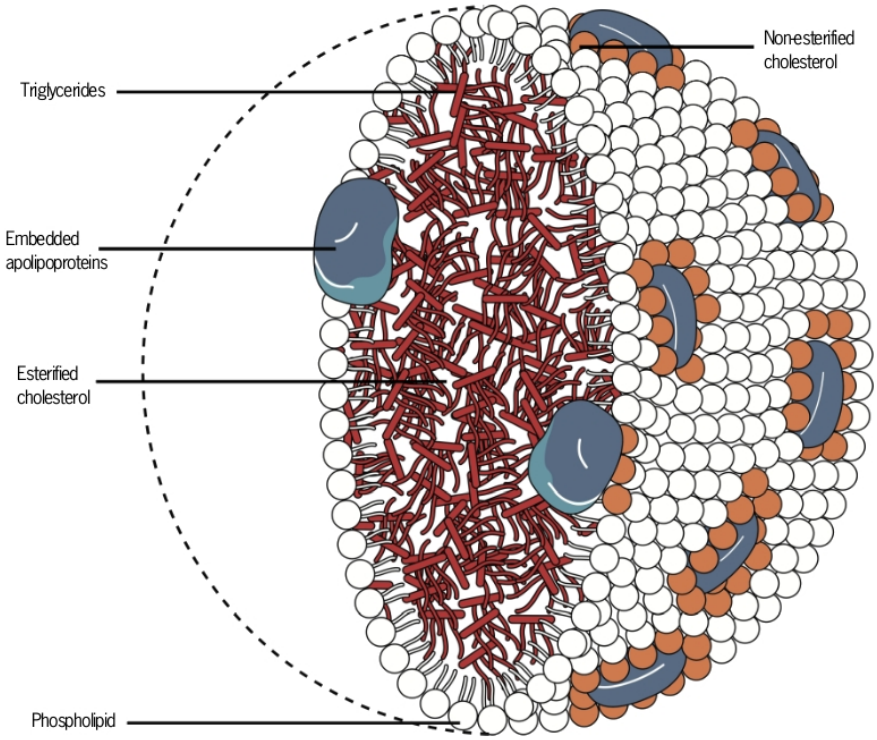

Figure 1-1: Lipoprotein structure
Adapted from British Journal of Cardiology lipids and metabolism module (12)
Lipoproteins have a common structure, comprised of an outer layer of phospholipids and embedded apolipoproteins, surrounding the inner cargo of cholesterol esters, triglycerides and fat-soluble vitamins.

Each of the lipoproteins share the same basic structure (Figure 1-1) but vary in their size and relative composition. They have been classified into the following well-known groups:

- Chylomicrons

- High-density lipoprotein (HDL)
- Intermediate-density lipoprotein (IDL)
- Low-density lipoprotein (LDL)
- Very low-density lipoprotein (VLDL)

Chylomicrons are the largest form of lipoprotein, formed by the intestine after ingestion of lipids from food. These large particles, which are of the lowest density of all the lipoproteins, are triglyceride rich and are rapidly digested into VLDL. HDL has the highest cholesterol density of the lipoproteins and primarily transports lipids to the liver; LDL transports lipids around the body and is the lipoprotein most closely associated with atherosclerosis (Figure 1-2).

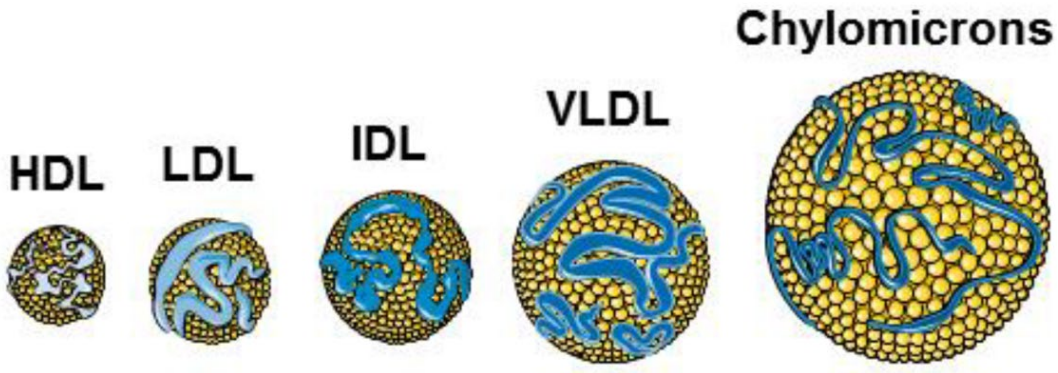

Figure 1-2: Human circulating lipoproteins
Chylomicrons are the largest and least dense of the lipoproteins, emanating from the intestines. HDL: high-density lipoprotein, LDL: low-density lipoprotein, IDL: intermediate-density lipoprotein, VLDL: very low-density lipoprotein (adapted from Chiva-Blanch G et al) (13)

Apolipoproteins have recently become recognized as important proteins in atherosclerosis and form the central structure of lipoproteins. They increase stability, whilst also serving as cell surface receptors and enzymatic activators. Lipoproteins that transport lipids to the liver (HDL) contain apolipoprotein-A, and those transporting lipids to the extra-hepatic tissues (LDL, VLDL) contain apolipoprotein-B. (14)

In maintenance of cholesterol homeostasis, the rates of cholesterol synthesis by the liver and absorption in the small intestine are principally regulated in a feedback mechanism by cellular levels of cholesterol via the HMGCoA reductase system. This is an important catalytic enzyme in the production of cholesterol, and of course the target of serum cholesterol lowering drugs statins.

Early Plaque Formation

The arterial wall is a trilaminar structure, consisting of tunica adventitia in the outermost layer; tunica media; and tunica intima with endothelium on the innermost aspect (Figure 1-3).

The adventitia is a layer comprised of fibroblasts and perivascular nerves within connective tissue, also containing the vasa vasorum – an important microvascular network, critical for maintenance of the adjacent medial layer (15).

The tunica media is itself composed of transversely laid down contractile smooth muscle cells in a well-organised matrix made of collagen, elastin and extra-cellular matrix. This smooth muscle structure allows constriction and relaxation of the vessel in response to local and neural stimuli.

The intima consists of an innermost single layer of endothelial cells, supported by an underlying network of connective tissue and elastic fibres.

Adaptive intimal thickening (AIT) or *intimal thickening* is defined by Virmani et al as the "*normal accumulation of smooth muscle cells (SMCs) in the intima in the absence of lipid or macrophage foam cells*" (16). Such lesions are well noted in children, and although not all progress to become atheromas, the majority of atheromas are thought to have arisen from areas of intimal thickening (17). It may represent a response to variability in shear stress, and indeed is commoner in sites of arterial bifurcation, where shear stress is lower, and flow is non-laminar (18). Whether AIT it is considered physiologic or pathologic remains an area of controversy. Pathologic intimal thickening (PIT) is different, currently defined by the absence of endothelium on histology, and the presence of thrombus. Of course, this is a histologic classification based on post mortem specimens, where a diagnosis of plaque erosion is given. Plaque classification is discussed later in this section.

The early atherosclerotic plaque begins to form when lipid particles are deposited in the intima triggering a cascade of events. In normal endothelial function, LDL which is the principal carrier of cholesterol passes through the arterial sub-intimal space in the delivery of cholesterol back to the liver. However, when there is endothelial dysfunction, LDL begins to aggregate (19).

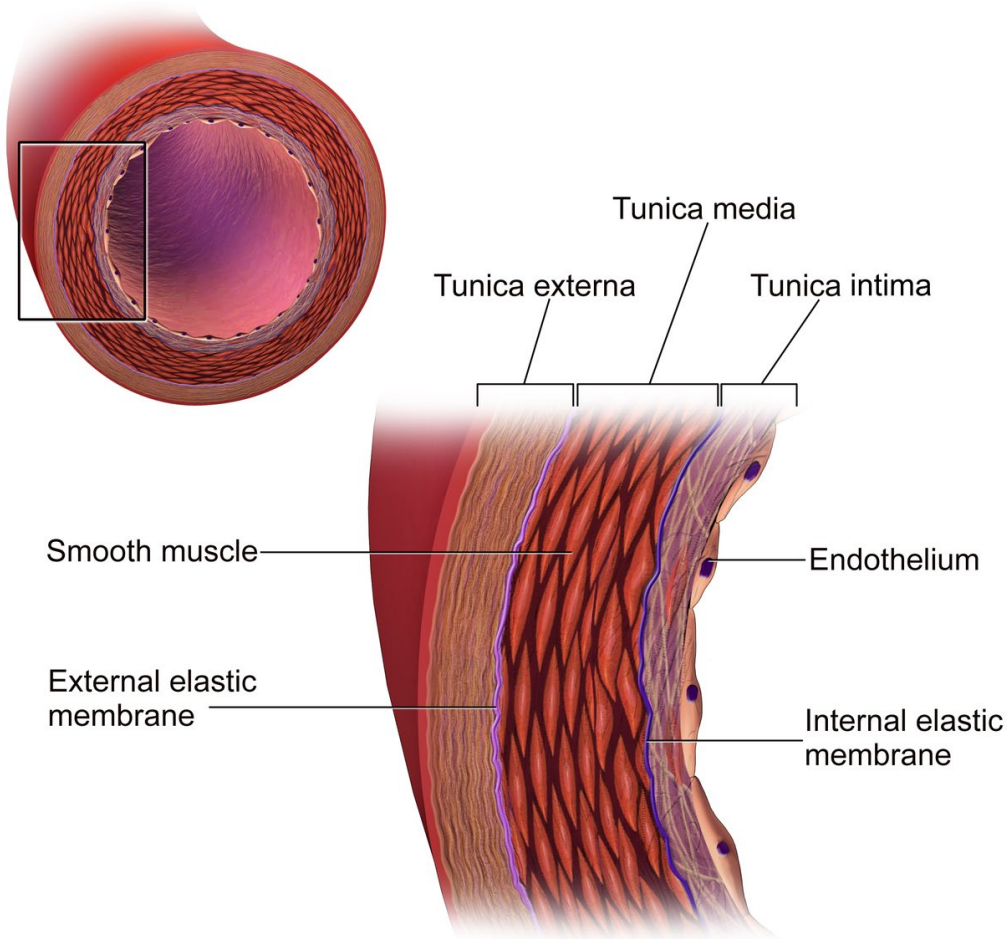

Figure 1-3: Normal arterial structure
Human arteries have a trilaminar structure consisting of adventitia, media and intima from outer to inner (adapted from [Blausen.com staff (2014). "Medical gallery of Blausen Medical 2014"])

When apoB-containing lipoproteins are retained in the sub-endothelial space they can be oxidized and in-turn activate endothelial cells to attract and recruit immune cells including monocytes, dendritic cells, mast cells, regulatory T cells, and T helper 1 (Th-1) cells via increased expression of vascular cell adhesion molecules (VCAMs) and selectins. Monocytes attach to the endothelium and begin to roll along it, before adhesion and finally trans-endothelial migration (20) (Figure 1-4).

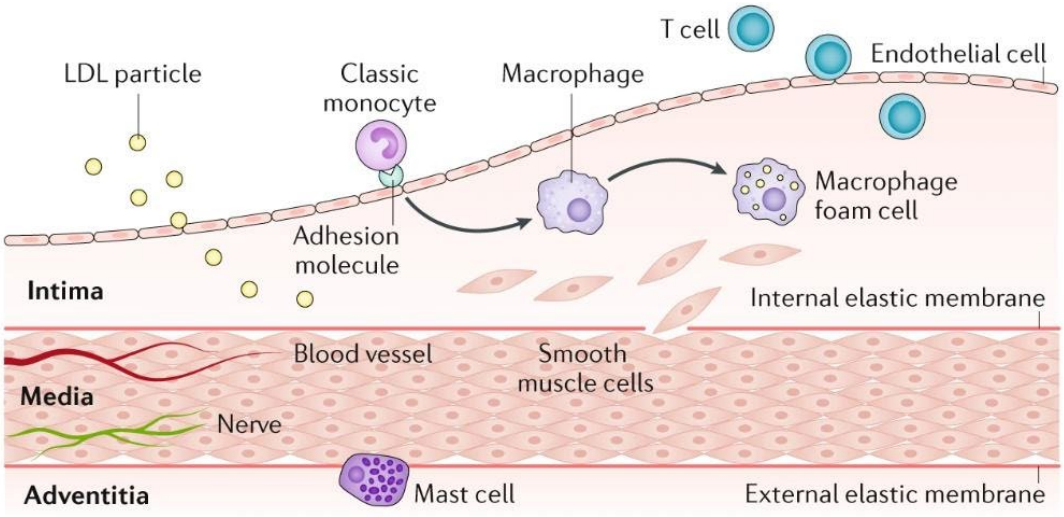

Figure 1-4: Early atherosclerotic plaque development
LDL particles invade the sub-endothelial space and monocytes begin to roll along the endothelium, before they are recruited into the plaque. Monocytes differentiate into macrophages, and macrophages absorb lipid particles to become foam cells. Smooth muscle cells migrate into the sub-endothelium and T-cells begin to invade (adapted from Libby et al (21))

Within the now expanding sub-endothelial space or plaque, monocytes then differentiate into macrophages, which sequester LDL, VLDL and ApoE remnants to become foam cells (22). Phagocytosis is the key mechanism by which the macrophages ingest the lipid via receptors including: CD36, CD68, SRA (scavenger receptor class A), and LOX-1 (lectin-like oxidized low-density lipoprotein receptor-1. LDL particles become oxidised to oxidised LDL (oxLDL), in the presence of oxidative stress, resulting in a higher affinity for these receptors. Once sequestered inside the macrophage the apoB-containing lipoproteins are degraded by lysosomes, when free cholesterol is transported to endoplasmic reticulum (ER) for esterification by acyl

CoA:cholesterol acyltransferase, and the resultant cholesteryl ester is packaged into characteristic lipid droplets. Foam cells then continue to activate inflammation and contribute to the inflammatory milieu.

Foam cells are just one subset of cells derived from the monocyte / macrophage lineage critical to the development of atherosclerotic plaque. Lesional subsets of each cell type are thought to have differing roles within the plaque and polarisation is thought to be determined by the particular micro-environment within it, encompassing a variety of signalling molecules. Whilst classical macrophage phenotypes ‘M1’ and ‘M2’ have been previously described, this is more a representation of simpler *in vitro* conditions, than the complex atherosclerotic plaque *in vivo* (23, 24).

The complex plaque

Plaque progression is a highly variable and complex process. Once lipid has started to deposit in the sub-endothelial space, and monocyte-macrophage infiltration has begun, the plaque can progress at variable rates into many different phenotypes. Further, each lesion can display characteristics of multiple different phenotypes at different points in time, due to the dynamic nature of their evolution in a patient’s (and a plaque’s) life (Figure 1-5).

Foam cells go on to further stimulate inflammation, as the plaque continues to grow with the retention of more lipid particles, and the invasion of more immune cells. Foam cells are not only evolved from the monocyte-macrophage

lineage, but also from vascular smooth muscle cells (VSMC) migrating into the sub-endothelial space from the media (25). These too can become engorged with lipid, and a adopt a foam cell phenotype (26). Much of the matrix accumulation of a growing atherosclerotic lesion is owed to an expanding mass of migrated VSMCs, which are large and undergo a transition into a more synthetic phenotype. Extra-cellular matrix is secreted, comprising collagen, elastin, proteoglycans and glycosaminoglycans, and contributes to the framework of the growing plaque.

Whilst lymphocytes and T-cells migrate from the luminal aspect, they can also infiltrate from the vasa vasorum, and may also proliferate within the plaque (27). They reside within the extracellular matrix, and TH1 cells secrete IFNγ – a pro-inflammatory cytokine, whilst TH2 cells secrete anti-inflammatory molecules including transforming growth factor beta (TGF-ß) and IL-10 which dampen the atherogenic response.

As foam cells of either origin begin to undergo programmed cell death, or apoptosis, the number and volume of dead cell bodies increases. Efferocytosis, or removal of dead cells, is characteristically impaired and this cellular debris adds to the necrotic core.

Calcification inevitably occurs as the plaque progresses. The process within the plaque bears many similarities with mineralisation and ossification of bones, and results from dysregulation of calcium deposition and impaired clearance (28). Spotty calcification develops first, and correlates with plaque instability (29), and develops into sheets and nodules.

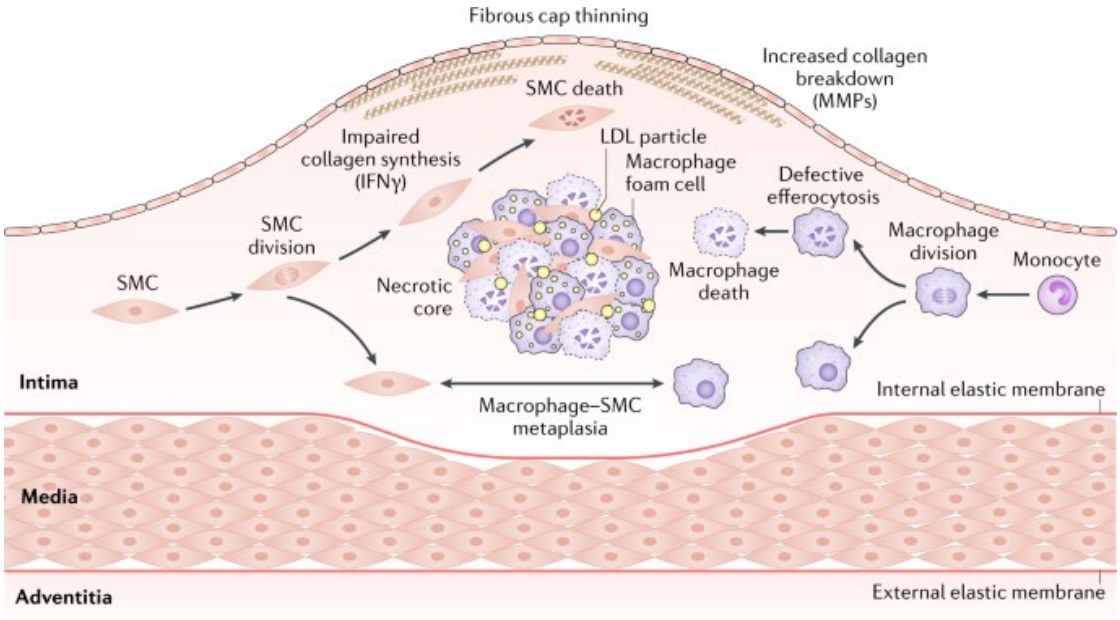

Figure 1-5: The complex plaque
A lipid and necrotic core forms in the sub-endothelial space, composed of macrophages, lipid particles and dead cells. Macrophages and SMCs undergo apoptosis and contribute to the volume of the core. A fibrous cap comprised of extra-cellular matrix forms between the core and the endothelium and begins to thin. SMC=smooth muscle cell (adapted from Libby et al (21)).

To rationalise the considerable variability and complexity observed in plaque morphologies, the American Heart Association proposed a classification system, published in Circulation in three parts by Stary et al in the mid-1990's. They described phenotypes I-VI, with some specific sub-types in group V and VI, to account for the heterogeneity found between lesions.

Each of the types of lesions they described were characterised as follows:

Type I (Initial) – Lipid deposits become detectable in the subintimal space. These features can be seen as early as infancy, and are not necessarily a pathological state (30). **Type II (fatty streak)** – Layers of foam cells form and

lipid droplets are taken up by intimal VSMCs. T-cells and mast cells invade the plaque. **Type III (preatheroma)** – A further increase in lipid droplets and foam cells which form separate pools, but no confluent lipid core has yet formed, this is an intermediate stage. **Type IV (atheroma)** – A lipid core which forms from the confluence of multiple smaller pools. This stage represents 'advanced' atheroma, which is potentially symptom producing. **Type V – (fibroatheroma)** – Characterised by thickening of the tissue between the core and the endothelium. There is luminal narrowing of the artery, and subtypes include Va – lipid core, Vb – calcium, Vc – fibrous. **Type VI (complicated)** – As V, but with surface defects of fissure / haematoma / thrombus.

Whilst this earlier classification provided the framework to build on, updates to to it have since been proposed and adopted. Notably, a classification system devised by Professor Renu Virmani et al, published in ATVB in May 2000 is the most frequently used (16). In this paper, several key problems with the original AHA classification were identified, and steps taken to try to address them. Modifications were principally in the description of intermediate and advanced plaques, which are heterogenous and complex, but also in the description of very early lesions initial xanthoma and intimal thickening. Virmani et al. recognised that plaque types IV, V and VI do not necessarily follow in order, and that thrombosis is observed to occur in circumstances other than plaque rupture, namely calcified nodule and plaque erosion (16).

Whereas the original AHA classification relied on a long list of Roman numerals to identify plaque types, the modified classification instead uses 7 categories of lesion: Initial xanthoma; intimal thickening (both pre-atheromatous); fibrous cap atheroma; pathologic intimal thickening, calcified nodule; thin fibrous cap atheroma; fibrocalcific plaque (Figure 1-6).

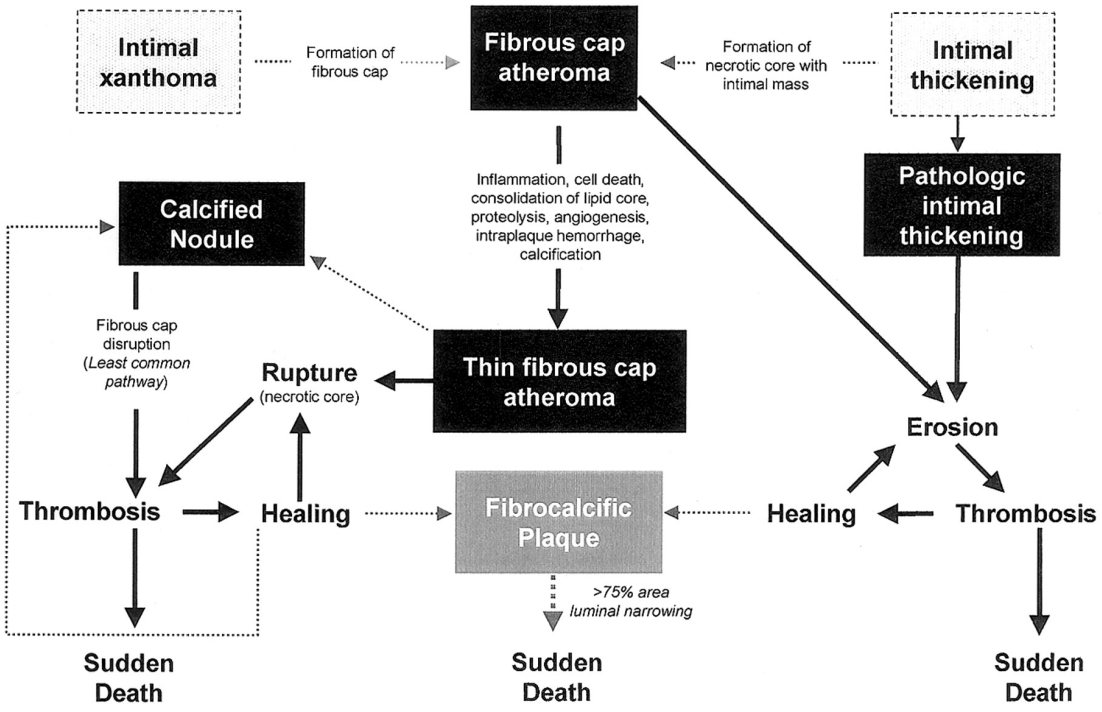

Figure 1-6: A Comprehensive Morphological Plaque Classification Scheme for Atherosclerotic Lesions (Adapted from Virmani et al, ATVB May 2000)
Boxed terminologies represent the 7 proposed plaque types. Dashed line boxes indicate that the role each of these types play in early plaque formation is controversial, and each may represent normal physiology. Lines represent how one process may progress to another, dashed lines indicating a lower strength of evidence to support it

This classification scheme relies on descriptive morphology rather than mechanistic implications, and can more simply be followed when considering

that classification relies largely on the accumulation of lipid and also the status of the fibrous cap.

1.3 The Vulnerable Plaque

The phenomenon of the vulnerable plaque has been the centre of much research endeavour in the last 2 decades. It was originally thought that the mechanism of coronary occlusion and resultant myocardial infarction was exclusively due to the rupture of unstable or vulnerable plaque, which exposed the enclosed thrombogenic material to platelets and clotting factors in the blood, precipitating clot formation and vessel occlusion. This is still held in the main, but it is an oversimplification, and other mechanisms such as plaque erosion and calcific nodule protrusion are now recognised (31-34). Studies at post mortem examination have demonstrated that acute thrombosis of the coronary artery in cases of sudden coronary death is associated with an obvious plaque rupture in 59-75% of patients (16, 35), and denudation of the endothelium (or erosion) in 36-44% of cases (16, 31). Calcified nodule causing luminal obstruction probably does lead to myocardial infarction, but in a minority of only 2-7% of cases (36).

Stage IV atherosclerotic plaques or atheromas are characterised by the presence of a large lipid pool or necrotic core which lies in the centre of the plaque, itself shielded from the lumen by a fibrous cap principally composed of collagen, secreted by smooth muscle cells. The perceived vulnerability of the plaque relates to its propensity to rupture, meaning the chance that the cap will be disrupted and either the necrotic core is exposed to the lumen triggering thrombosis, or arterial blood enters the plaque (or more likely a combination of the above).

When a plaque ruptures in a coronary artery causes thrombosis, the cascade of events is invariably rapid and devastating. Necrotic cores contain extremely thrombogenic material including various cell types, dead cells and oxidised lipids, but notably tissue factor (TF) (Figure 1-7). Tissue factor is produced by macrophages and smooth muscle cells within the plaque and is highly thrombogenic. When TF comes into contact with blood it triggers platelet activation and aggregation and the generation of thrombin (37, 38), leading to thrombosis and occlusion of the vessel.

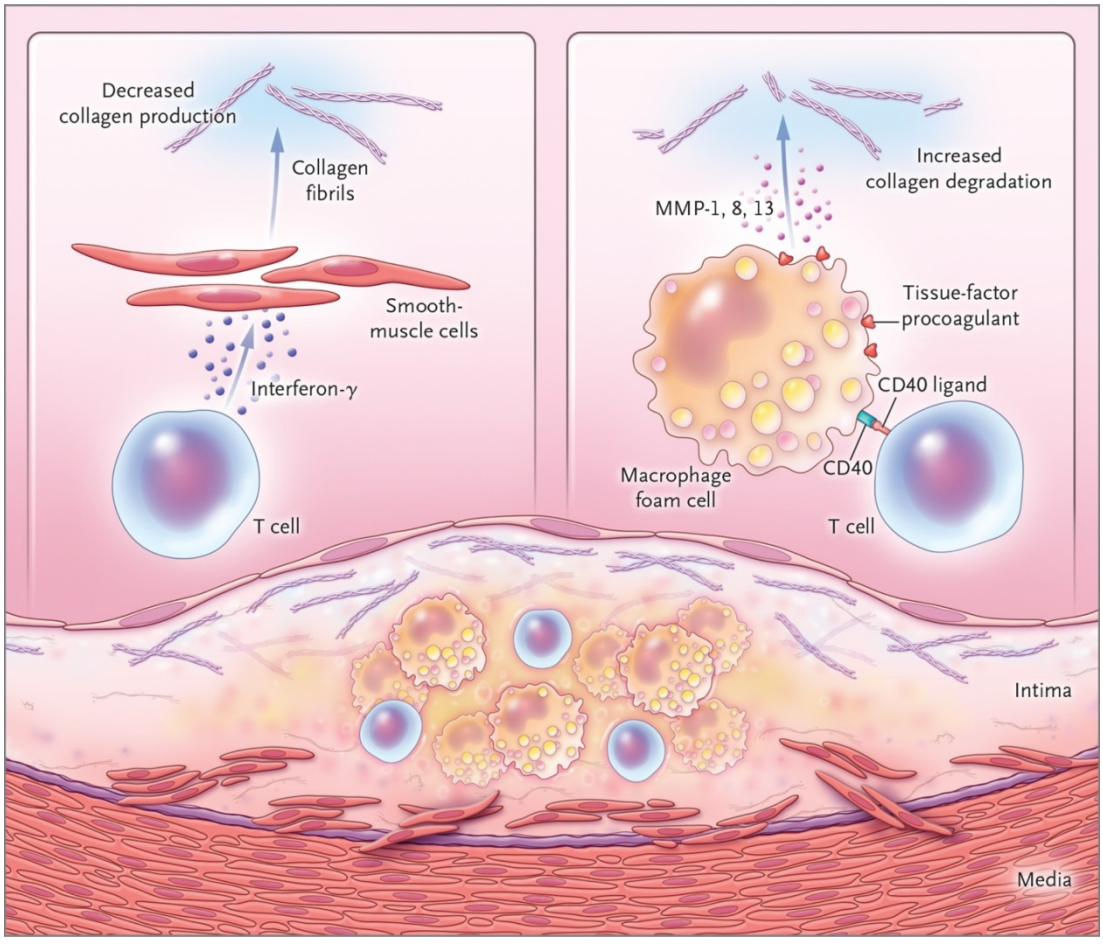

Figure 1-7: The mechanism of plaque rupture
MMPs secreted by macrophages degrade the collagenous matrix of the fibrous cap. Smooth muscle cells produce less collagen in response to IFNy secreted by T-cells (adapted from Libby (32))

The thickness of the fibrous cap in ruptured coronary plaques is observed to be just over 100 μm on both post-mortem and OCT studies (31, 39), and is recognised as one of the main factors in plaque rupture. The term thin-capped fibroatheroma (TCFA) was hence coined by Virmani et al (16). Gradual degradation of the collagenous cap structure is likely mediated by inflammatory cells macrophages and T-cells. Production of cytokines such as IFNy by T-cells is shown to downregulate production of extracellular matrix by VSMCs, even in the presence of TGFβ which are also found to fewer in number at sites of plaque rupture (40, 41). Further, macrophages secrete a family of enzymes known as matrix metalloproteinases (MMPs). Although collagen is generally resistant to the action of most organic proteases, MMP1, MMP8 and MMP13 over-production by activated macrophages has been demonstrated to cleave collagen, thus weakening and thinning the fibrous cap further (42-45). The weakest area of the cap is thought to be the shoulder region (46).

Plaque erosion attracts less attention than plaque rupture as a mechanism for coronary thrombosis but is likely causative in approximately one quarter of cases. More mature and complex plaques tend to be more proteoglycan rich, and fibrous as a result. There may be no lipid core at all, and the cap may not be thinned. Gradually there is desquamation of the superficial layer of endothelial cells overlying this tough internal plaque structure, which is thrombogenic when it comes into contact with the circulation and leads to thrombosis. The endothelial cells undergo apoptosis and as they do so produce tissue factor, and may sever their own underlying basement

membrane (47). This mechanism has now been well seen on both post-mortem and OCT studies *in vivo* (48-51).

However, the mere presence of a vulnerable plaque alone is not sufficient to generate thrombosis and myocardial infarction. In fact, most vulnerable plaques do not rupture. As complex plaques grow, the artery first undergoes 'positive remodelling' before there is luminal narrowing. Effectively the vessel grows outwards, to preserve its internal diameter (52, 53). As a result, only around half of culprit lesions actually cause luminal stenosis (54). It is the high-risk features of large lipid pool, thin-cap, and microcalcification which seem to be predictive of events, rather than luminal impingement.

Furthermore, it should be noted that not all plaque ruptures trigger thrombosis and result in fatality. Continual rupture and subsequent healing of plaques is part of the natural history of atherosclerosis, with only a minority of plaque ruptures resulting in clinical events. Studies of autopsy specimens demonstrate that healed plaque ruptures and the increasing number of healed plaque ruptures correlates with increasing luminal stenosis (55, 56). This mechanism may also explain why increases in luminal stenosis appear to be phasic rather than gradual, noted particularly when antecedent angiography had shown significantly less luminal narrowing (57).

The PROSPECT study followed up 697 patients using IVUS for 3 years after acute coronary syndrome to understand the natural history of non-culprit plaques. Strikingly, of over 3000 non-culprit lesions identified by IVUS at baseline, of which 595 were thin-capped fibroatheromas, only 6 were

subsequently related to myocardial infarction and death after 3 years. Other coronary features postulated to contribute to the perfect storm to precipitate coronary thrombosis include low shear stress, coronary vasospasm, inflammation, and micro-calcification (58-60). However multiple systemic and environmental features such as emotional stress, infections, temperature changes and even earthquakes have been associated with increased risk (61). Even the time of day is important as more myocardial infarctions are observed during the small hours of the morning. The common factor here is likely to be sympathetic nervous system activation, which increases blood pressure, heart rate and arterial stress. Hypercoagulability and platelet reactivity also seem to be higher at this time of day, and whether this is due to circadian rhythm or other factors such as cortisol release remains unknown (62, 63).

The identifiable features of a vulnerable plaque were first described by appearance on post-mortem as previously discussed, but subsequently more modern imaging techniques have characterised several hallmark appearances. Advances in the resolution of cardiac CT now permits detailed analysis of not only the vessel lumen to estimate stenosis, but also the structure of the arterial wall. When Motoyama et al followed up 1,059 patients who underwent coronary CT, features of either positive remodelling or low-attenuation plaque (<30 Hounsfield units [HU]) were predictive of acute coronary syndrome compared with neither with a hazard ratio of 22.8 (7-75, $p<0.001$) (64). These results were corroborated by similar CT studies, characterising the ‘napkin-ring’ sign and demonstrating microcalcification as predictive features (65-67).

1.4 Current therapies for atherosclerotic diseases

Besides lifestyle interventions, attempts at managing atherosclerosis have to date largely focused around the now well-accepted dogma that high levels of circulating lipid lead to accumulation of an expanding lipid-rich necrotic core in the sub-intimal space of the arterial wall forming predominantly in areas of low shear stress and endothelial dysfunction. Consequently, lipid lowering strategies have predominated with no less than 7 different available statins, other drugs like ezetimibe, fibrates, and most recently the development of monoclonal antibodies against the PCSK9 receptor, such as Evolocumab (68) and alirocumab (69). However, despite initially impressive results in the statin trials, some now doubt their efficacy in primary prevention, and staggering levels of LDL reduction as in the FOURIER trial (68) do not seem to translate into dramatically improved clinical outcomes. This suggests that lipid lowering may not be the only mechanism of action at play. The anti-inflammatory effect of statin drugs may be a major factor, and new drugs targeted at reducing inflammation such as canakinumab look promising. In the recently published CANTOS trial, canakinumab which targets interleukin-1β, reduced the relative risk of myocardial infarction in ischaemic heart disease patients by 16%, without affecting lipid levels (70).

1.5 The Universal Definition of Myocardial Infarction

The definition of myocardial infarction has evolved markedly over the last few decades. It is a condition which progresses rapidly and severely and can result in immediate fatality. When untreated there may be a shortened lifespan and for that a reduced quality of life. Critically it is also an eminently treatable condition, and modern therapies such as primary PCI (and earlier thrombolysis to a lesser degree) can halt it in its course, and potentially prevent all of the above adverse consequences. However, like many conditions the diagnosis remains a clinical one, and it is the role of the physician to assess the patient's history and examination, along with ECG findings and biomarkers to ascertain the likelihood of MI before instituting treatment. A type 1 or a type 2 error on the part of the physician would often be extremely costly. A false positive diagnosis would subject the patient to potent blood thinning drugs and quite likely an unnecessary invasive procedure carrying significant risks; whereas a false negative could be potentially worse, allowing the sequelae of an acute coronary syndrome to play out.

Furthermore, a diagnosis of myocardial infarction has significant psychological and legal implications for the individuals, groups and society. It is one of the leading health problems in the world, and an outcome measure in myriad clinical trials and studies.

The first Universal Definition of Myocardial Infarction (UDMI) was published in 2007 to unify the diagnosis of this important condition (Figure 1-8). The document published in Circulation described key diagnostic criteria to make a

diagnosis of myocardial infarction, and is now in its fourth iteration. The original criteria are detailed below:

Detection of rise and/or fall of cardiac biomarkers (preferably troponin) with at least one value above the 99th percentile of the upper reference limit (URL) together with evidence of myocardial ischaemia with at least one of the following:

- Symptoms of ischaemia
- ECG changes of new ischaemia
- Development of pathological Q waves on ECG
- Imaging evidence of new loss of viable myocardium, or new regional wall motion abnormality

The guidelines also described the criteria for post-mortem diagnosis, as well as peri-procedural diagnosis in and around PCI and surgical coronary artery bypass grafting.

Criteria for acute myocardial infarction

The term myocardial infarction should be used when there is evidence of myocardial necrosis in a clinical setting consistent with myocardial ischaemia. Under these conditions any one of the following criteria meets the diagnosis for myocardial infarction:

- Detection of rise and/or fall of cardiac biomarkers (preferably troponin) with at least one value above the 99th percentile of the upper reference limit (URL) together with evidence of myocardial ischaemia with at least one of the following:
  - Symptoms of ischaemia;
  - ECG changes indicative of new ischaemia [new ST-T changes or new left bundle branch block (LBBB)];
  - Development of pathological Q waves in the ECG;
  - Imaging evidence of new loss of viable myocardium or new regional wall motion abnormality.
- Sudden, unexpected cardiac death, involving cardiac arrest, often with symptoms suggestive of myocardial ischaemia, and accompanied by presumably new ST elevation, or new LBBB, and/or evidence of fresh thrombus by coronary angiography and/or at autopsy, but death occurring before blood samples could be obtained, or at a time before the appearance of cardiac biomarkers in the blood.
- For percutaneous coronary interventions (PCI) in patients with normal baseline troponin values, elevations of cardiac biomarkers above the 99th percentile URL are indicative of peri-procedural myocardial necrosis. By convention, increases of biomarkers greater than 3 × 99th percentile URL have been designated as defining PCI-related myocardial infarction. A subtype related to a documented stent thrombosis is recognized.
- For coronary artery bypass grafting (CABG) in patients with normal baseline troponin values, elevations of cardiac biomarkers above the 99th percentile URL are indicative of peri-procedural myocardial necrosis. By convention, increases of biomarkers greater than 5 × 99th percentile URL plus either new pathological Q waves or new LBBB, or angiographically documented new graft or native coronary artery occlusion, or imaging evidence of new loss of viable myocardium have been designated as defining CABG-related myocardial infarction.
- Pathological findings of an acute myocardial infarction.

Criteria for prior myocardial infarction

Any one of the following criteria meets the diagnosis for prior myocardial infarction:

- Development of new pathological Q waves with or without symptoms.
- Imaging evidence of a region of loss of viable myocardium that is thinned and fails to contract, in the absence of a non-ischaemic cause.
- Pathological findings of a healed or healing myocardial infarction.

Figure 1-8: Diagnostic criteria for myocardial infarction as per First Universal Definition of Myocardial Infarction.
Adapted from Thygesen et al (71) (CABG=coronary artery bypass graft; ECG=electrocardiogram; LBBB=left bundle branch block; PCI=percutaneous coronary intervention; URL=upper reference limit)

Thus far the term ‘myocardial infarction’ has been used almost exclusively to refer to what is known as a “type 1 myocardial infarction”. That is, infarction and myocardial necrosis resulting from a coronary plaque rupture or erosion event.

However, its worthy of note at this stage that nomenclature around myocardial infarction is variable, complex and to many quite confusing. At the time of writing there are several ways of semantically describing essentially the same thing, and how it is written or spoken about can depend highly on local culture, as well as knowledge of contemporaneous trends. This current section will go on to describe the UDMI types 1-5, with particular attention to types 1 and 2. However, myocardial infarction is still sometimes classified with respect to ECG changes: ST-elevation myocardial infarction (STEMI); non ST-elevation myocardial infarction (NSTEMI); or unstable angina, and might also generally be referred to in the context of ‘acute coronary syndrome’. The presence of myocardial injury (which implies no acute ischaemic event) can cloud matters even further.

Although the standard definitions will be adopted here and referred to throughout, its acknowledged that the most commonly used syntax in a clinical setting is that related to ECG change, and this is appropriate. The vast majority of chest pain presentations and suspected myocardial infarctions are owing to type 1 myocardial infarction, and the immediate management thereof is dependent on the severity of the ischaemia (indicated by ST change), rather than the underlying pathophysiological mechanism. STEMI is treated with

primary percutaneous coronary intervention, whereas NSTEMI is managed medically in the first instance, with a downstream invasive approach.

The different types of myocardial infarction as per the UDMI is summarised in Figure 1-9.

Table 1 Clinical classification of different types of myocardial infarction

Type 1
Spontaneous myocardial infarction related to ischaemia due to a primary coronary event such as plaque erosion and/or rupture, fissuring, or dissection
Type 2
Myocardial infarction secondary to ischaemia due to either increased oxygen demand or decreased supply, e.g. coronary artery spasm, coronary embolism, anaemia, arrhythmias, hypertension, or hypotension
Type 3
Sudden unexpected cardiac death, including cardiac arrest, often with symptoms suggestive of myocardial ischaemia, accompanied by presumably new ST elevation, or new LBBB, or evidence of fresh thrombus in a coronary artery by angiography and/or at autopsy, but death occurring before blood samples could be obtained, or at a time before the appearance of cardiac biomarkers in the blood
Type 4a
Myocardial infarction associated with PCI
Type 4b
Myocardial infarction associated with stent thrombosis as documented by angiography or at autopsy
Type 5
Myocardial infarction associated with CABG

Figure 1-9: Types of myocardial infarction as per the Universal Definition of Myocardial Infarction
Adapted from Stary et al (71)

Type 2 Myocardial Infarction

Type 2 myocardial infarction is now increasingly recognised and may even be as common as type 1 MI (72). In this condition, myocardial ischaemia is not caused by the classical plaque rupture phenomenon, but rather an imbalance between myocardial oxygen supply and myocardial oxygen demand. Common mechanisms reducing supply include hypoxia, anaemia, and some (possibly misplaced) coronary mechanisms including coronary spasm and embolism. Causes of an increase in demand include tachyarrhythmia, ventricular hypertrophy and hypertension (73) (Figure 1-10).

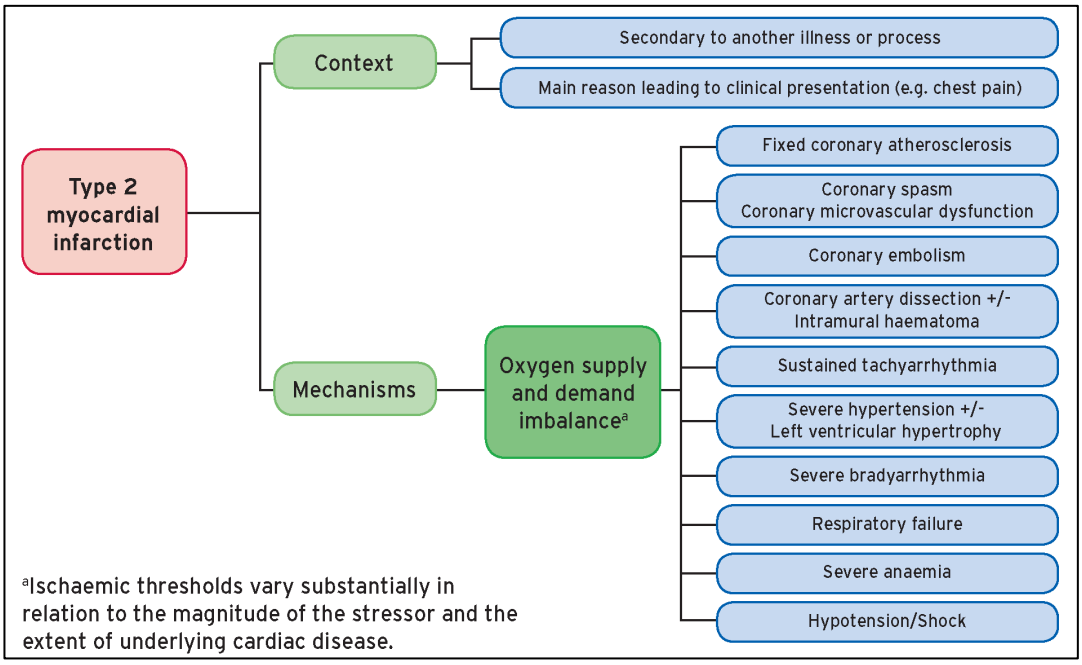

Figure 1-10: Supply demand mismatch in type 2 myocardial infarction
Type 2 myocardial is suspected when there are clinical features of cardiac ischaemia in the context of another illness or process (adapted from Stary et al (74))

Patients with type 2 myocardial infarction are older, more often have comorbidities and are at higher risk of adverse outcomes with as few as 30%

of patients alive at 5 years (75). Despite a significant increase in risk of non-cardiovascular death, patients with type 2 myocardial infarction appear to have a similar risk of future cardiovascular events as those with type 1 myocardial infarction (76).

Despite the severe consequences of type 2 MI, well-evidenced investigation, management and risk stratification pathways are still lacking. Presenting features differ from type 1 MI usually in that patients are less likely to have chest pain, have less impressive ECG changes, and generally lower magnitude biomarker increases (77). Coronary disease is less frequent than in type 1 MI (which is universal), but remains common, and when present portends a higher risk of future events (75). Distinguishing between type 1 and type 2 MI remains difficult, and novel diagnostic approaches are needed (78).

It may be that treatment with the usual regimen of anti-platelets, statins, beta-blockers and ACE-inhibitors are beneficial, as is well-established in type 1 MI, but whilst diagnosis and discrimination of the condition remains problematic, studies to identify the most appropriate management are not possible, and progress has been slow.

The Fourth Universal Definition of Myocardial Infarction is the most recent iteration, and has brought some changes with respect to type 2 myocardial infarction (74). The guideline characterises the aetiology of type 2 MI with respect to the coronary arteries and recommends consideration of the presence or absence of coronary artery disease when implementing treatments. Furthermore, high sensitivity troponin I and troponin T assays are

now recommended in diagnosis, and the guideline distinguishes between myocardial infarction, and acute or chronic myocardial injury. If there is absence of ischaemia in the way of symptoms, ECG changes, or regional wall motion abnormality, then a diagnosis of myocardial injury is more appropriate, If there is a rise or fall in troponin then it would be considered ‘acute myocardial injury’, and if it is static then ‘chronic myocardial injury’.

With the advent of highly sensitive troponin assays and their incorporation into the UDMI, much research is needed to define optimal diagnostic, investigative and treatment strategies for these groups of patients.

1.6 Non-coding RNA

The non-coding genome represents an exciting, yet complex layer in human physiology and pathology. Initially some function had been ascribed to ncRNAs as early as the 1950s as transfer RNA and ribosomal RNA. However, its only in the last few decades upon the discovery that approximately 98% of the human genome is non protein-coding (79) (Figure 1-11), that the potential biological significance of ncRNA has been even partly appreciated (80). MicroRNA (miRNA) is the best studied family of ncRNA, known to regulate thousands of protein-coding genes through messenger RNA (mRNA) degradation (81). MiRNAs are 20–25 nucleotides in length and form a characteristic “hairpin” structure. They are inherent in multiple pathologies, and due to their stability in plasma, miRNAs have also been proposed as biomarkers of atherosclerosis (82), MI (83), cancers (84), rheumatological, and other diseases. In terms of therapies, clinical trials are currently ongoing to determine the efficacy and safety of “antimiRs” in diseases such as cancer, hepatitis (85), and other conditions.

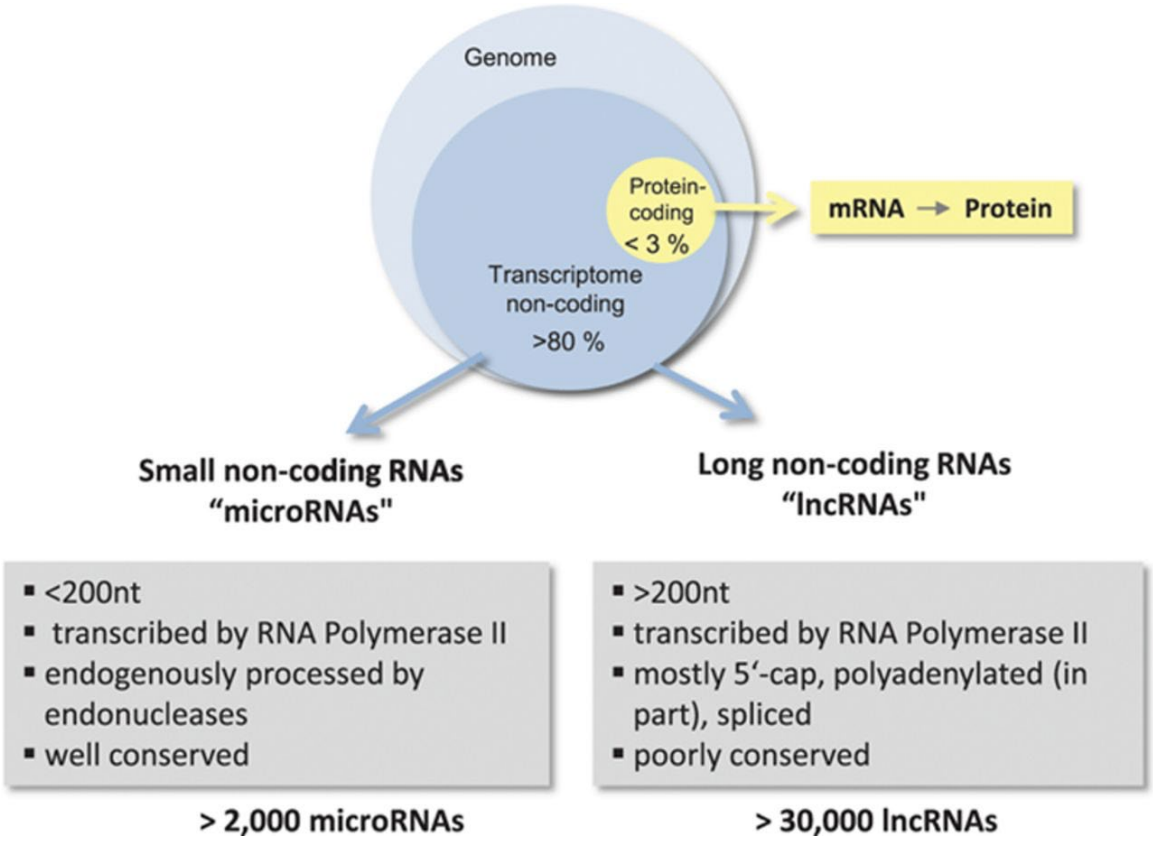

Figure 1-11: Contribution of coding vs noncoding RNAs in the human genome
The vast majority of the human genome is non-coding (adapted from Uchida et al(79))

1.6.1 Micro RNA

Since their discovery in 1993 in *C.elegans* nematode (86), miRNAs have now taken up an important niche in genomics with almost 2000 known sequences in the human genome. Usually, transcription of intronic miRNA is regulated by the same promoter as the host gene. Some miRNAs however, are shown to have multiple transcription start sites (87) and may be transcribed by a promoter distant from the gene they occupy (88). MiRNA transcription is controlled by RNA polymerase II and RNA Pol II-related transcription factors (89). The first product in the process is a primary miRNA (pri-miRNA) molecule, with a characteristic stem-loop structure, and lengths reaching up to

1 kilobase (kb). The next product in the sequence is a smaller precursor miRNA (pre-miRNA) molecule, which is generated by RNase III enzyme Drosha that cleaves the stem-loop of pri-miRNA (90). The small, hairpin-shaped pre-miRNA is then transported into the cytoplasm by exportin 5, where the Dicer enzyme further processes it to generate a double-stranded molecule, ready for assembly with the Argonaute (Ago) protein (91, 92). The final product in the miRNA biogenesis pathway is formation of the RNA-induced silencing complex (RISC), consisting of a mature, single-stranded miRNA molecule and Ago protein, which induces post-transcriptional gene silencing (93). Importantly, human miRNA lacks Ago specificity and can bind to all Ago variants (93). Recent evidence demonstrates that the Ago-unbound miRNA strand isn't always cleaved, and both the 5p and 3p strands are found in different sorts of tissues (94). The mature miRNA then facilitates gene silencing, whereby mRNA degradation occurs in 66-90% of cases (81) and mechanistically depends on mRNA deadenylation, decapping and cleavage by XRN1 nuclease (95). On the contrary, miRNA-induced repression of translation targets only 6-26% of genes (96) using primarily RNA helicases eIF4A and DDX6, which repress cap-dependent translation (81).

1.6.2 Long non-coding RNA

Long non-coding RNAs (lncRNAs) are much less well characterised to date, but their importance in gene expression is increasingly being recognised. In contrast to miRNAs, lncRNAs are much longer at >200 nucleotides, with more complex secondary structures. They may act both to activate and to repress genes, exerting their effects by a variety of mechanisms at both transcriptional and translational levels (97, 98).

Remarkably, lncRNAs outnumber not only miRNAs, but also protein-coding genes. In fact, the number of lncRNAs annotated continues to rise, due to recent advances and new strategies in RNA sequencing and bioinformatic techniques, and hence a much greater depth of sequencing (99). Despite this, there is still no strict classification method, and the most accurate definition of lncRNA at present is “long RNA transcripts that do not encode proteins” (100). It is generally accepted that lncRNAs are longer than 200 nucleotides, separating them from other shorter ncRNA molecules such as miRNAs, snoRNAs, an piRNAs amongst others, but confusingly, some lncRNAs do actually contain cryptic open reading frames (ORFs) (101), and short open reading frames (sORFs) encoding micropeptides. These micropeptides can act independently from large proteins, regulating essential biological processes (102). For example, a skeletal muscle-specific RNA, annotated as lncRNA LINC00948, encodes a cryptic micropeptide ‘myoregulin’ (MLN). MLN interacts with sarcoplasmic reticulum Ca2+-ATPase (SERCA), preventing Ca2+ uptake into the sarcoplasmic reticulum in skeletal muscle, while MLN silencing improves Ca2+ handling (103). Similarly, it was reported that lncRNA

LINC00961 also encodes a polypeptide termed ‘small regulatory polypeptide of amino acid response’ (SPAR). Mechanistically, SPAR prevents mTORC1 activation via interaction with lysosomal v-ATPase while SPAR deletion induces mTORC1 leading to muscle regeneration (104). Sanders et al found that although SPAAR (AKA SPAR in previous reference) is transcribed from within the LINC00961 locus, the micropeptide and the lncRNA actually have opposing roles in endothelial cell biology (105).

Given these clear mechanistic roles for encoded micropeptides, one might consider then that the parent lncRNA transcripts are in fact ‘misannotated’. How can a transcript that is experimentally proven to contain genetic code for a protein be referred to as ‘non-coding’? Nomenclature naturally evolves with new knowledge over time, and perhaps this will change. Clearly though there are differences between a simple mRNA which has one function only, to produce a peptide, and the complex lncRNA molecule, with its myriad of interactions and functions, which remain largely undiscovered.

Within the class of lncRNA, there are different sub-classes of lncRNAs which include long intervening/intergenic ncRNAs (lincRNAs), promoter upstream transcripts (PROMPTs), enhancer RNAs (eRNAs) and natural antisense transcripts (NATs). These are transcribed from intergenic and promoter upstream regions, enhancers and reverse strand of protein-coding genes, respectively (106). Interestingly, lncRNAs do not require polyadenylation to be functional and upon transcription a significant proportion of lncRNA remains non-polyadenylated. In fact, many lncRNA are bi-morphic and can exist in both

polyadenylated and non-polyadenylated states (107). Furthermore, lncRNAs can exist in different forms and structures: some lncRNAs are capped by snoRNAs at 5' (108) or both ends (109); others can occur in a circular form as circular intronic RNAs (ciRNAs) and circular RNA from back-splicing of exons (circRNAs) (110-112). ANRIL (discussed in more detail later) is the most well-known ncRNA that can take a circular form. Currently considered to be a form of ncRNA, these transcripts exist in loops with a bond between the 3' and 5' ends. Much like other lncRNA, they are thought to regulate gene transcription and expression, acting as sponges for miRNA, and are extremely abundant in the circulation.

It is now accepted that lncRNAs can modulate gene expression on transcriptional, post-transcriptional and translational levels. The function of a specific lncRNA depends much on its cellular localization and context of the cell (i.e. basal/stressed). In particular, nuclear lncRNAs mainly act on transcription, while cytoplasmic lncRNAs modulate expression of gene post-transcriptionally. In the nucleus, lncRNAs regulate the epigenome, facilitate transcriptional control and participate in alternative splicing (113). A good example of lncRNA-mediated epigenetic control is ANRIL, which facilitates the recruitment of the chromatin-modifying complex PRC2 and promotes silencing of p15INK4B tumour suppressor gene (114). Interestingly, after the discovery of enhancer RNAs (eRNA) (115), it has been further suggested that eRNAs are able to modulate chromatin and facilitate its assembly (116) and interact directly with DNA structure to guide the enhancer to its promoter (117). A similar type of lncRNA, termed activating ncRNAs (ncRNA-as), can also

regulate transcription and are expressed from independent genes (118). Further, lncRNAs modulate different aspects of transcriptional control ranging from modulating the expression of transcription factors, such as ncRNA-a7 (118) and OCT4 pseudogene 5 (119), to acting as co-activators and repressors independently, such as Alu RNA inhibiting RNA polymerase Pol II directly (120). MALAT1 is an example of lncRNA modulation of alternative splicing. Specifically, MALAT1 is enriched in nuclear speckles and upon interaction with sarcoplasmic reticulum (SR) splicing factors promotes alternative splicing (121). Within the cytoplasm, lncRNAs can stabilise or lead to mRNA decay and promote/inhibit translation. Cytoplasmic lncRNAs can also act as miRNA precursors or sponges, mimicking mRNA for miRNA binding (113). Mainly, lncRNA-induced mRNA degradation occurs via Staufen1 (STAU1)-mediated mRNA decay (SMD), where STAU1 binds to the pairing of mRNA 3'-UTR sequences with lncRNA due to complementary Alu elements (122). On the other hand, a natural antisense lncRNA BACE1-AS forms a bond with mRNA of BACE1 and protects it from miR-485-5p-induced degradation by masking the miRNA binding site (123). LncRNA such as Uchl1-AS can recruit ribosomes to Uchl1 mRNA and thus facilitate protein translation (124). Conversely, a subset of lncRNAs termed translational regulatory lncRNA (treRNA) can repress translation. TreRNA facilitates the assembly of a new ribonucleoprotein (RNP) complex, which interacts with translation initiation factor eIF4G1 resulting in translational repression of E-cadherin (125). Finally, a well-studied lncRNA in cancers, H19, has been recently demonstrated to be a precursor for miR-675, which targets a tumour suppressor RB (126). H19 is

considered to be an effectual molecule itself, rather than just the primary transcript giving rise to miR-675. In the setting of keratinocyte differentiation H19 acts as a sponge to miR-130b-3p, its target (127). Further to that, it has been reported that circRNA CDR1-as contains 63 binding sites for miR-7 and can act a “sponge” or decoy for miR-7, thus reactivating the expression of its target genes in neuronal tissues (110, 128).

1.6.3 Long non-coding RNA in atherosclerosis

Discovery of novel non-coding RNAs in disease-specific context continues to increase, largely due to the widespread application of high-throughput gene expression arrays and development of next generation RNA sequencing. By far the most studied field in this area is cancer, but already a significant number of miRNAs are implicated in vascular disease and biology, and although much less studied, several long non-coding RNAs have been discovered and are currently being investigated (See Table 1-1 for a list of important non-coding RNAs in atherosclerosis). Development, cellular differentiation and commitment is a logical starting point to identify novel RNA candidates, and evidence of endothelial cell growth and phenotype regulation in a long non-coding transcript such as in the case of *MALAT1* would suggest a strong likelihood of an important function in pathology for this. Below are described some of the most important long non-coding RNAs findings to date..

Increasingly, long non-coding RNAs emanating from multiple sources are shown to be implicated in cardiovascular disease. The long non-coding RNA anti-sense noncoding RNA in the *INK4* locus (*ANRIL*) is transcribed from the now well-known 9p21 locus, which has been strongly implicated in vascular disease (129-131) and ANRIL itself has been associated with pathogenic changes in atheroslerotic plaques (130).

It was initially discovered through genome-wide association studies detecting several polymorphisms, which were predictive of myocardial infarction (132, 133). Notably, important tumour suppressor genes *CDKN2A* and *CDKN2B* are

also found near this region, but are not found to be dysregulated in atherosclerosis models and patients, unlike *ANRIL* (134). *ANRIL* was one of the first lncRNAs described in atherosclerosis, and multiple interactions have now been demonstrated, although the full extent of its regulation in vascular disease remains unclear. As is the case with most long non-coding RNAs, *ANRIL* is alternatively spliced, and expressed as multiple 'isoforms'. Ensembl currently reports 21 splice variants, each of which may interact differently to the others. Further adding to its complexity, *ANRIL* is found in multiple cell types including VSMCs, ECs, and inflammatory cells. Initially *ANRIL* appeared to be grossly associated with pathogenic changes; reduced cell viability and proliferation in VSMCs (131), upregulation of inflammation and apoptosis in endothelial cells (135), and a consistent correlation with atherosclerotic burden in human PBMCs and plaque samples (130). More recently though a circular variant has been characterised, *circANRIL*, which seems to be atheroprotective in its behaviour; by controlling ribosomal RNA biogenesis and modulating some atherogenic processes in VSMCs and macrophages (136). Unless otherwise stated, *ANRIL* would hence usually refer to the linear transcript (*linANRIL*). This alternatively structured RNA from the same locus exemplifies the added layers of complexity in lncRNA biology compared with smaller micro and other non-coding RNAs.

Table 1-1: Non-coding RNA in atherosclerosis

	Vascular Examples	Biological context	Reference
miRNA	miR-21	Biomarker of coronary artery disease, upregulated in vein grafts	(137-139)
	miR-126	Promotes endothelial cell proliferation, atheroprotective	(140, 141)
	miR-92a	Endothelial inflammation, atherogenic	(142)
	miR-33a/b	Inhibits *ABCA1* translation, atherogenic	(143, 144)
	miR-143/145	Complex interaction in atherosclerosis and pulmonary hypertension: upregulated in human unstable carotid plaque, knockout blocks pulmonary hypertension in murine model	(145, 146)
	miR-221/222	Dysregulated in acute plaque	(145, 147)
	miR-1	Biomarkers for myocardial infarction	(148, 149)
	miR-133a		
	miR-499		
	miR-208a		
	miR-192	Predictive of heart failure post-myocardial infarction	(150)
	miR-194		
	miR-34a		
lncRNA	ANRIL	Transcribed from 9p21 locus, associated with pathogenic changes in atherosclerotic plaques	(130)
	MIAT	Biomarkers for myocardial infarction	(151-153)
	MIRT1/2		
	HIF1-AS2		
	KCNQ1OT1		
	SENCR	Downregulated in human critical limb ischemia and in premature coronary artery disease	(154)
	SMILR	Induces smooth muscle cell proliferation, upregulated in human carotid plaques	(155)
	meXis	Improves cholesterol efflux, atheroprotective	(156)
	MALAT1	Downregulated in plaque, endothelial phenotypic switch	(157)
	LIPCAR	Predictive of heart failure post myocardial infarction	(158)

Until now, *in vitro* work has led to limited characterisation of some other vascular lncRNAs in relevant cell types, but translation into definite therapeutic targets in humans requires complex mechanistic unravelling, which in most

cases is in the early stages. Long non-coding RNAs identified in circulatory samples from atherosclerosis patients, or from GWAS may provide a starting point for vascular targets, but confounding processes such as myocardial injury and repair, or the general upregulation of inflammation are equally likely to account for these correlative findings. Notable examples include myocardial infarction associated transcript (*MIAT*) (151), another transcript discovered by large case-control genome association study in patients with MI, and myocardial infarction related transcript 1 and 2 (*MIRT1*, *MIRT2*) in a murine MI model (152). Whilst dysregulation in myocardial infarction has been demonstrated has been demonstrated, mechanistic work to understand if these transcripts are important in atherosclerosis or a different pathway is needed.

As with miRNAs, a certain insight has been achieved from *in vitro* cellular models. Although cultured cell lines representing one cell type are not truly analogous to the multicellular *in vivo* environment, it is possible to investigate candidate novel transcripts, and to identify at least if these are important in cellular function in the first instance. In coronary artery smooth muscle cells, the smooth muscle and endothelial cell–enriched migration / differentiation-associated long non-coding RNA (*SENCR*) is an example of a transcript discovered by RNA sequencing, and functionally characterised in relevant cell types. *SENCR* was shown to be anti-migratory in VSMCs, and subsequent RNA-Seq after *SENCR* knockdown then demonstrated a reduced expression of myocardin and numerous contractile genes, consistent with the observed phenotype (159). Subsequently, lower levels of *SENCR* in human critical limb

ischemia and in the endothelial cells of patients with premature coronary artery disease were observed (154), again supporting that hypothesis that *SENCR* is downregulated in pathology. As SENCR appears to be a regulator of VSMC behaviour, it could be hypothresised that targeted delivery of *SENCR* in areas of deficiency might then ameliorate maladaptive smooth muscle cell behaviours in atherosclerosis. Another vascular lncRNA, smooth-muscle induced long non-coding RNA (*SMILR*), was investigated in a similar manner, but in this case upregulation of *SMILR* was associated with vascular smooth muscle cell proliferation, and in human atherosclerotic plaque *SMILR* is enriched. Mechanistic investigation showed that *SMILR* may exert its effects by interaction with *cis* protein *HAS2*, which codes for hyaluronic acid. *HAS2* was also reduced on *SMILR* knockdown, and the VSMC phenotype was of reduced proliferation (155). Therapeutic targeting of *SMILR* with *in vivo* locked nucleic acids (LNAs) might prove useful in preventing neointima formation in clinical settings.

Aside from the cells which are inherent to the vascular wall, immune cells monocytes and macrophages, are known to be key regulators of lipid handling within the plaque, and recently it was shown that the lncRNA *meXis* is an amplifier of the *ABCA1* gene, via the sterol activated liver X receptors (LXRs). LXRs are sterol-activated nuclear transcription factors, and may be important in the pathology of atherosclerosis, as key regulators of genes involved in cholesterol transport. *MeXis* interacts with and guides promoter binding of the transcriptional coactivator *DDX17*, so loss of the gene resulted in impaired cholesterol efflux, and accelerated atherosclerosis in murine models. As

discussed, any novel target for improving cholesterol efflux (which is beneficial in plaque disease) certainly warrants further investigation (156).

Utilising human samples excised at coronary endarterectomy a recent study compared lncRNA expression from diseased left anterior descending (LAD) artery plaque with inferior mammary artery control tissue. This is a rarely performed procedure, and coronary artery samples from live patients are not usually readily available. The inferior mammary artery used as a control here is preferentially used for LAD coronary artery bypass and tends to be quite resistant to atherosclerosis with low failure rates (160). Differential lncRNA expression was observed in 3 of the 5 plaques chosen for analysis, with upregulation of *ANRIL* and *MIAT* whilst metastasis-associated lung adenocarcinoma transcript 1 (*MALAT1*) was downregulated (157). This reinforces the initial premise that these lncRNAs which had been previously proposed as atherosclerosis related lncRNAs, and had been found in the circulation of patients with acute myocardial infarction (153), are in fact reproducibly found in human atherosclerotic tissue.

MALAT1 briefly described above is frequently cited in vascular disease and widely in multiple pathologies (primarily cancer) is a very well-conserved and highly expressed long non-coding RNA (161). Having initially been demonstrated as a prognostic marker in non-small cell lung cancer (162), *MALAT1* may also be relevant in vascular disease, and was shown to control phenotypic switch in endothelial cells, as well as impair vessel recovery in a hind-limb ischaemia model when knocked down using *in vivo* GapmeRs (163,

164). In atherosclerosis, MALAT1 has been shown to be downregulated in atherosclerotic plaque (157). The use of *in vivo* GapmeRs to knock down chosen ncRNAs will be discussed later.

1.6.4 Non-coding RNA therapies

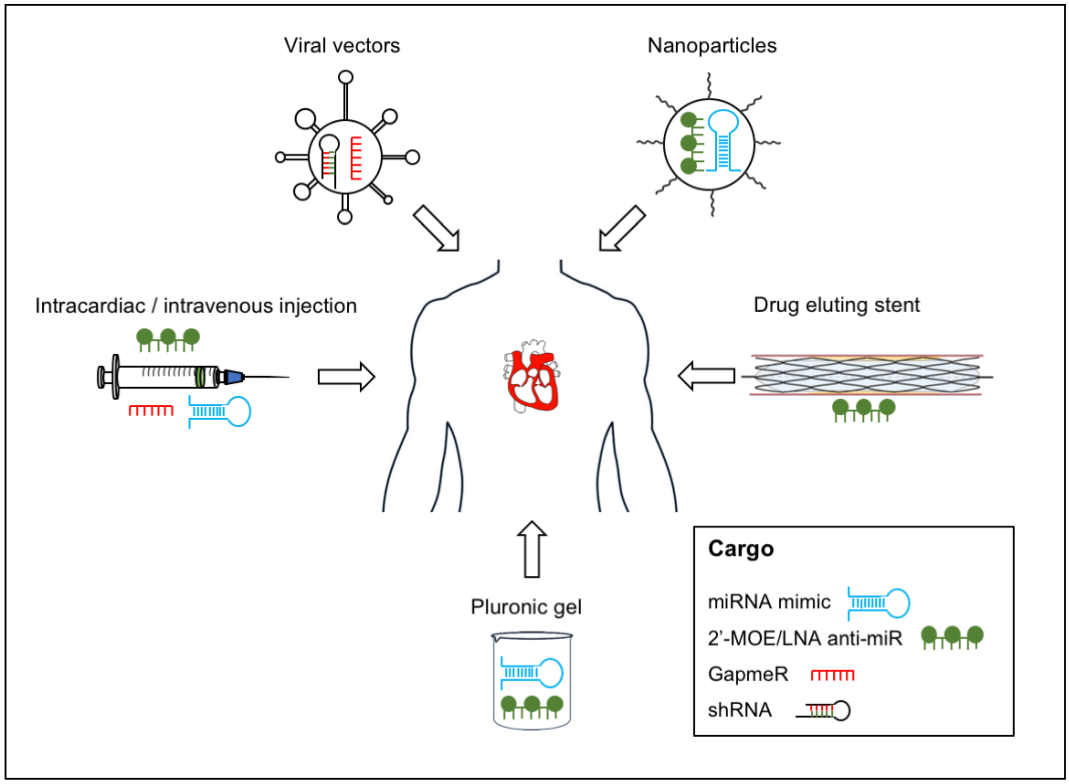

Figure 1-12: Proposed delivery methods of non-coding RNA-based therapeutics in vascular disease.
RNA therapeutics can be delivered to the vascular system using vehicles such as viral vectors, nanoparticles and pluronic gel; intravascular devices such as drug eluting stents; or by direct injection.

MiRNA as therapeutic agents

In the large class of non-coding RNAs, miRNAs currently possess the strongest therapeutic potential due to our greater knowledge of them, clearer mode of action and ability to regulate multiple genes in multiple molecular pathways. Moreover, due to their pleiotropic mechanism of action, a manipulation of a single miRNA could potentially induce a therapeutic effect within several cells and tissues. With re-emerging interest in RNAi therapeutics (165), it is possible that miRNA-based therapies will progress further in the

coming years. Figure 1-12 summarises current and proposed approaches to non-coding RNA therapy and delivery.

Ultimately, efficacy depends on both modification of the RNA molecule, and its vehicle for delivery. The two principal strategies for miRNA therapeutics include overexpression of miRNA by synthetic oligoribonucleotide (ORN) delivery or targeted miRNA inhibition using single-stranded antisense oligonucleotides (anti-miRs). In order to obtain better delivery efficiency, the ORNs can be subjected to chemical modifications, such as 2′-O-methoxyethyl (2′-MOE) substitutions and LNA bases, which stabilise the oligoribonucleotides (166-168). In particular, the 2′-MOE modification is generally used to prevent degradation of ORN as well as to mask it from the immune response, whereas LNA enhances the affinity of miRNA and stabilises the ORN further (169, 170). The use of such modifications to improve expression modulation of certain miRNA has been validated numerously in the vascular disease setting, including examples such as delivery of 2′OMe-miR-21 to rat carotid artery (171), systemic downregulation of miR-92a with LNA-anti-miR to induce re-endothelialisation (172) as well as intravenous delivery of LNA-anti-miR-15b to reduce cardiac remodeling in mice post-MI (173).

In addition to ORN modifications, efficient RNA delivery vehicles are required to facilitate their uptake. There are several studied thus far, as discussed below. The most common delivery method to date is the use of lipid-based nanocarriers, which package the RNA, allowing it to cross the cellular membrane (174, 175). Notably, in a study carried out by Weber‘s group it was

shown that miR-126-5p mimics packaged in this way were effectively and efficiently transfected *in vivo*. The cargo was delivered intravenously to high cholesterol diet mice, resulting in a marginal decrease in atherosclerotic lesion formation, and an increase in luminal EC proliferation. They reported in the same study that using pluronic gel-based delivery was also effective, in this case for local delivery of anti-miRs injected around the mouse carotid artery (141). Pluronic gel can be used internally or topically and was also used effectively in a recent study by Miscianinov et al., where miR-148b mimics were topically administered to efficiently enhance angiogenesis and wound healing *in vivo*. It was noted in this case however that the delivery of anti-miR-148b within the pluronic gel had impaired wound closure and induced EndMT in the wound vasculature, possibly a result of the target manipulation more-so than the mode of delivery (176). Alternative methods to package and deliver RNA based therapies involve polymer- and peptide-based systems, such as polylactic-co-glycolic acid (PLGA) and Polyamine-co-ester terpolymer (PACE) nanoparticles. The latter are able to release the oligoribonucleotides steadily over time (177, 178). PLGA was used in the vascular setting when an anti-miR to miR-92a encapsulated by PLGA microspheres was delivered directly to pig coronary arteries. MiR-92a expression was downregulated locally, preventing left ventricular remodeling in a model of reperfused MI (179).

Of course, viral vectors such as adenovirus (AV) and adeno-associated virus (AAV) are amongst the best-known vehicles for gene therapies due to their natural ability to infect and transfer genetic information. Viruses have been used to efficiently deliver many different cargoes *in vivo* previously like the

tissue inhibitor of metalloproteinase-3 (TIMP3) in vein graft failure, which reduced neointimal formation consistently (180). The commonly used vector AAV has been equally well-studied, and delivery of hsa-miR-590 and hsa-miR-199a pre-miRs to the neonatal rat heart was shown to significantly reduce infarct size and improve cardiac function post-MI (181). Despite concerted efforts to optimise this process however, viral delivery can be hampered by several drawbacks, namely the triggering of immune response (especially in the case of AV), off target effects, and the sometimes undesirable long-term incorporation of the virus's genes into those of the host.

Specificity of site action hence represents one of the major barriers to developing successful miRNA therapies, as in both of the above classes of examples. Some success has been seen with attempts to deliver miRNA therapies locally. In the vasculature in particular, drug-eluting stents (DES) were already widely used in percutaenous coronary intervention, releasing anti-proliferative and immunosuppressive drugs to prevent re-stenosis. In a similar approach, it was shown that delivery of LNA anti-miR-21 by DES significantly attenuated in-stent restenosis in the humanised rat myointimal hyperplasia model (182). Photoactivatable antimiRs, which have photolabile cages attached to the oligonucleotide structure are only activated by light, therefore generating an inducible model (183, 184). This ensures that the miR treatment is only efficiently released at the intended site. Clearly this is useful in skin, but perhaps less so internally. Efficacy of a miR-92a light-inducible compound was demonstrated in superficial mice wounds and was able to enhance proliferation and angiogenesis (185). Finally, incorporation of miRNA

therapy with a thioaptamer, specifically interacting with a chosen ligand, E-selectin in this example, may be useful to ensure specificity. The aptamer binds to the chosen molecule and guides the miR therapy, miR-146a and miR-181b to inflamed endothelium, reducing atherosclerosis in mice (186).

Non-nascular ncRNA therapeutics

As there are currently no clinical trials focused on ncRNAs in vascular disease, we will describe studies in liver and heart and translational relevance for vascular disease. The most successful example of miRNA-based therapeutics to date is anti-miR-122 compound for hepatitis C. It has been demonstrated in Jopling et al. study that miR-122 is highly and specifically expressed in human liver. Moreover, it has been shown that inhibition of miR-122 was able to strongly decrease viral RNA of hepatitis C, introducing the novel idea for a potential miR-122-modulating therapy (187). Since then a lot of work has been done to achieve an efficient miR-122 inhibition method *in vivo*, primarily using 2′-MOE-modified anti-miR (188, 189). Furthermore, anti-miR-122 LNA modification approach was efficient in downregulating miR-122 expression in mice, which was delivered intravenously (190). Notably, the preclinical trials on chimpanzees have confirmed that LNA-anti-miR-122, now known as SPC3649 or Miravirsen, leads to significant reduction in hepatitis C viral load with no side-effects (191). Currently, Miravirsen is being developed by Santaris Pharma and is since 2017 in Phase II clinical trials (192).

In other translational studies, direct intra-cardiac injection of miR-21, miR-1 and miR-24 reduced infarct size in mice, with LAD ligation, at 24 hours (193). The mice underwent ischaemic preconditioning, forcing an altered miRNA expression profile, with the hypothesis that these miRNAs would be protective in the case of infarct. The miRNAs were then extracted and injected into the infarct model, resulting in an increase of eNOS, HSF-1, and HSP70. Direct injection of miRNA seems to be effective therefore in altering tissue expression of important mRNAs and proteins. In a mesenchymal stem cell vector, miR-1 was overexpressed and injected into infarcted myocardium again in a mouse model of infarct, resulting in enhanced cell survival and improved cardiac function (194). In a similar way but with a different mode of delivery, polyketal (PK3) nanoparticles (a solid polymer) were used to deliver miRNA mimics miR-106b, miR-148b and miR-204 to macrophages in mice hearts, all targeting Nox2 expression. Infarct size was significantly reduced, and function improved (195). The alternative approach of miRNA inhibition has also been shown to be effective in the cardiovascular setting, and in some cases may be technically easier to achieve. Anti-miRs can be quickly designed and developed, and *in vivo* delivery of the anti-miR-143 is protective in the development of pulmonary arterial hypertension in mice (196). MiR-143-3p is selectively upregulated in cell migration, and its modulation significantly reduces cell migration and apoptosis.

Coronary artery bypass vein graft failure has been a longstanding problem, and the setting for some significant advances in ncRNA therapy. The underlying pathologies are of neointima formation and superimposed

atherosclerosis. MiR-21 expression is elevated in mice, porcine and human *ex vivo* models of vein graft failure and localises to the smooth muscle cell layers of the forming neointima in the failing grafts. Delivery of anti-miR-21 to inhibit miR-21 was effective to reduce expression and attenuate the pathological neointima formation in a model of vein graft failure (139), and now further clinical investigation is needed before this can be applied in patients. In a completely different disease system its also been reported that inhibition of miR-21 using anti-miR can prevent Alport syndrome in mice. This disease which is characterised by glomerulonephritis and progressive renal failure also results in sensorineural deafness in the human form (197). As a result of these findings, Regulus Therapeutics is now carrying out a Phase II clinical study (NCT02855268) of the safety and efficacy of RG-012 drug (anti-miR-21) administered to patients with Alport syndrome.

In another important study, from the Dimmeler group, they demonstrated that downregulation of miR-92a expression using 2′O-methyl anti-miR oligoribonucleotides enhanced *in vivo* angiogenesis, neovascularisation as well as enhanced post-MI recovery in mice (198). The pro-angiogenic and cardioprotective effect of anti-miR-92a therapy was further confirmed in a further study from the same group. Specifically, it has been demonstrated that the catheter-based delivery of anti-miR-92a with LNA modification (LNA-92a) led to the decrease in the infarct size in pig hearts and improved cardiac function (199). A recent publication by the same group demonstrated that delivering a LNA-based antisense oligonucleotide that targets miR-92a-3p did

in fact reduce circulating levels of the same. This is one step closer to a human *in vivo* study, to quantify the effects of this transcript knockdown (200).

With the advances of CRISPR/Cas9 technology and the ability to modify the genome at the base pair level, this method has become a very attractive and promising approach to generate both gain- and loss-of-function miRNA phenotypes. Interestingly, an *in vitro* transfection of CRISPR/Cas9 vectors, which contain sgRNAs, targeting the biogenesis processing sites of miR-17, miR-200c, and miR-141, decrease the expression of these miRNAs up to 96% (201), an impressive knockdown. Moreover, subcutaneous injection of HT-29 cells with CRISPR/Cas9-mediated *miR-17* knockdown into nude mice resulted in almost complete knockout of miR-17 expression in the *in vivo* environment after 28 days (201). Despite the clear benefits of the CRISPR/Cas9 approach in modulating miRNAs *in vivo*, the usual obstacles, such as off-target effects and lack of delivery vehicles with tissue specificity are yet to be overcome.

LncRNA based intervention strategies

Given the fact that lncRNAs guide gene expression from start of transcription to protein translation, this class of molecules possess a promising therapeutic potential. The first study involving modulation of lncRNA expression for therapeutic purposes described the oncogenic lncRNA *H19*. In particular, it has been reported that *H19* is specifically expressed in over 30 tumors. Based on those findings, a plasmid expressing diphtheria toxin under control of the *H19* promoter (BC-819) has been intra-tumorally injected into bladder tumour

leading to a significant reduction in size in mice (202). This led to initiation of phase I and II human clinical trials, in which a *H19* promoter-based plasmid is used to treat patients with different malignancies such as bladder, pancreatic and ovarian cancers (202). Recently reported results seem promising, including in the treatment of early stage bladder cancer, BioCanCell report that BC-819 treatment resulted in 54% of patients recurrence-free at 24 months (203).

Currently, there are two main approaches to silence lncRNA expression, which are employed in pre-clinical models: the use of RNAi-based methods, such as siRNA, and LNA-GapmeR antisense oligonucleotides (ASOs), which induce RNase cleavage. Generally, the RNAi approach, including siRNA and short hairpin RNA (shRNA), which can be delivered via viral vectors, is used predominantly for lncRNA that are localised in the cytoplasm. In particular, it has been demonstrated that siRNA targeting cytoplasmic lncRNA *SMILR* can reduce *SMILR* expression and attenuate pathological human saphenous vein smooth muscle cell proliferation (155). On the other hand, GapmeRs can be used for nuclear-localised lncRNA due to the fact that it induces degradation by RNase-H and is RISC-independent (204). Furthermore, GapmeRs can be used to modulate lncRNA expression *in vivo*. In particular, intraperitoneal injection of GapmeRs in mice model of hindlimb ischemia was able to significantly reduce *MALAT1* expression in the muscle tissue leading to poor blood flow recovery and diminished capillary density (205). In another study GapmeRs were used to inhibit the lncRNA *Chast*, which is upregulated in hypertrophic heart tissue from aortic stenosis patients. Notably, the *in vivo*

delivery of GapmeR targeting *Chast* resulted in a decrease in pathological cardiac remodelling with no significant side effects (206). Finally, the CRISPR/Cas9 genome editing method is an attractive emerging tool for modulation of gene expression including manipulation of lncRNAs. To date, the CRISPR-inhibition (CRISPRi) approach has been shown to knockdown the expression of six lncRNAs including *GAS5*, *H19*, *MALAT1*, *NEAT1*, *TERC* and *XIST* (207). The CRISPR/Cas9 method is in its nascent stages but coupled with viral-based delivery systems, it holds much potential in terms of non-coding RNA-based therapeutics.

1.7 Hypothesis

This thesis will incorporate clinical and pre-clinical studies, to combine the strengths of large clinical data and fundamental laboratory research. It is my overall hypothesis that:

'*Long non-coding RNAs play important roles in the pathology of atherosclerosis*'

The results chapters detailed below aim to address this hypothesis step-by-step, to identify areas of need in the management of myocardial infarction, and understand how lncRNAs could be used investigatively and or therapeutically to improve the care of patients with atherosclerosis.

Aims

- In Chapter 3, the risk stratification of patients with type 2 myocardial infarction using the GRACE 2.0 score will be analysed. The aim of this chapter is to explore how patients with different clinical syndromes within myocardial infarction are risk stratified, to gain insight into the gaps that exist in scientific knowledge, and what potential there is for development of new strategies to improve their care. The existing GRACE 2.0 score is well-validated in patients with type 1 myocardial infarction, but its performance in patients with type 2 myocardial infarction is unknown. The objective of this analysis is to assess the utility of GRACE 2.0 score in a large population of patients with type 1 and type 2 myocardial infarction to

investigate if patients with type 2 myocardial infarction can be risk stratified using the GRACE 2.0 score.

- In chapter 4, a large RNA-sequencing dataset from human carotid stable and unstable atherosclerotic plaque will be validated and analysed to derive a shortlist of dysregulated long non-coding RNAs. Candidates will be selected for further investigation in the following chapter.

- In chapter 5, a candidate lncRNA will be manipulated *in vivo* by modulation of expression (knockdown), to investigate its role in atherosclerosis. The objective of this series of experiments is to understand if knockdown of the candidate lncRNA changes the phenotype of its host cells, to demonstrate that long non-coding RNAs are important in the biology of unstable plaques.

Chapter 2 Materials and methods

2.1 Ethics

Carotid plaques were harvested in accordance with Bioresource local ethical approval (15/ES/0094, 15/HV/013). All studies were approved by East and West Scotland Research Ethics Committees, and all experiments were conducted according to the principles expressed in the Declaration of Helsinki.

Blood harvested by venepuncture was taken in accordance with local Blood Bank conditions, under ethical approval via the Centre for Inflammation Research, University of Edinburgh (AMREC Reference number 15-HV-013).

The High-STEACS trial was approved by the Scotland A Research Ethics Committee, the Public Benefit and Privacy Panel for Health and Social Care, and by each National Health Service (NHS) Health Board. All data were collected prospectively from the electronic patient record, deidentified and linked within secure NHS Safe Havens. In the Karolinska University Hospital cohort, the study protocol was approved by the Regional Ethical Review Board in Stockholm. Both studies were conducted in accordance with the Declaration of Helsinki.

2.2 GRACE 2.0 Score in Type 2 Myocardial Infarction Study

2.2.1 Study populations

We assessed the performance of the GRACE 2.0 score in two cohorts of consecutive patients presenting to the Emergency Department with suspected acute coronary syndrome in Scotland and in Sweden.

High-Sensitivity Troponin in the Evaluation of patients with suspected Acute Coronary Syndrome (High-STEACS) is a stepped-wedge cluster randomized controlled trial to evaluate implementation of a hs-cTnI assay in consecutive patients with suspected acute coronary syndrome across 10 hospitals in Scotland (76). Troponin was measured using the Abbott ARCHITECT STAT high-sensitive troponin I assay (Abbott Diagnostics, Chicago, IL, USA). This assay has an inter-assay coefficient of variation of <10% at 4.7 ng/L and a 99th centile of 16 ng/L in women and 34 ng/L in men (208). All patients attending the Emergency Department between June 2013 and March 2016 were identified as having suspected acute coronary syndrome by the attending clinician at the time troponin was requested. using an electronic form integrated into the clinical care pathway. Patients were excluded if they had been admitted previously during the trial period or were not resident in Scotland. We used regional and national registries to ensure complete follow-up.

The study population from the Karolinska University Hospital in Stockholm was derived from an observational cohort study of all patients >25 years old with a visit to the Emergency Department with chest pain and at least one hs-cTn measurement from January 2011 to October 2014 (209, 210). Troponin was measured using the Roche Elecsys hs-cTnT assay (Roche Diagnostics, Mannheim, Germany). This assay has a limit of detection of 5 ng/L, and a limit of blank of 3 ng/L. The 99th percentile cut-off point is 14 ng/L, and the coefficient of variation is <10% at 13 ng/L. The hospital's local administrative database was used to identify eligible patients. Patients were excluded if they

had an estimated glomerular filtration rate of <15 mL/min/1.73 m^2. The obtained data, together with laboratory data, were sent to the Swedish National Board of Health and Welfare who linked information on comorbidities and outcomes, use of medication, and dates and causes of death from the National Patient Register, the Prescribed Drug Register, and the Cause-of-Death register, respectively. The Patient Register has nationwide coverage on diagnoses at discharge and surgical procedures coded according to the International Classification of Disease.

2.2.2 Adjudication of myocardial infarction and outcomes

All diagnoses were adjudicated in accordance with the Fourth Universal Definition of Myocardial Infarction (74). In both cohorts two physicians independently reviewed all clinical information with discordant diagnoses resolved by a third reviewer (Scotland) or by consensus discussion (Sweden). Type 1 myocardial infarction was defined in those with suspected acute coronary syndrome with symptoms or signs of myocardial ischaemia on the electrocardiogram and evidence of myocardial necrosis: hs-cTnI concentration above the sex-specific 99th centile with a rise and/ or fall in concentration where serial testing was performed (Scotland); hs-cTnT concentration above the uniform 99th centile with a delta of 3 ng/L (Sweden). Patients with myocardial necrosis, symptoms or signs of myocardial ischaemia, and evidence of increased myocardial oxygen demand or decreased supply secondary to an alternative condition without evidence of acute atherothrombosis were defined as type 2 myocardial infarction. Patients with

hs-cTn concentrations above the 99th centile without symptoms or signs of myocardial ischaemia were classified as having myocardial injury. All non-ischaemic myocardial injury was classified as acute, unless a change of < 20% was observed on serial testing (74), or the final adjudicated diagnosis was chronic heart failure or chronic renal failure, where the classification was chronic myocardial injury.

The primary outcome was all-cause death at 1 year, and the secondary outcome was all-cause death or type 1 myocardial infarction at 1 year. All in-hospital and community deaths are recorded on the National General Register of Scotland, and the Swedish Patient Register. Subsequent myocardial infarction events were identified through the electronic patient record in Scotland with adjudication as for the index diagnosis, and using ICD-10 coding (I21 and I22) from the Swedish Patient Register in the Swedish cohort.

2.2.3 Statistical Analysis

Baseline characteristics were summarized for each cohort and in groups according to adjudicated diagnosis. Group-wise comparisons were performed using x^2, Kruskal–Wallis, or one-way analysis of variance tests as appropriate. We determined the GRACE 2.0 score for all-cause death, and for all-cause death or type 1 myocardial infarction at 1 year. This score includes age, heart rate, systolic blood pressure, creatinine as continuous variables, with categorical variables for Killip class, cardiac arrest at admission, ST-segment deviation, and elevated cardiac biomarkers (defined here as any hs-cTn concentration above the 99th centile). Where data were missing within the

Scottish cohort, this was assumed to be at random, and we applied multiple imputation using chained equations with five imputations of the dataset. For imputation, we applied Bayesian linear regression models for continuous data (creatinine, heart rate, and systolic blood pressure), multinomial logistic regression for ordinal data (Killip class) and logistic regression for binary data (e.g. cardiac arrest status). We assessed overall GRACE 2.0 model discrimination by determining the area under the receiver operating curve (AUC) and compared performance in patients with type 1 and type 2 myocardial infarction using the DeLong method. We assessed model calibration both graphically, and by using the Hosmer–Lemeshow goodness of fit test. In addition, we assessed GRACE performance by evaluating previously defined categories of mortality risk (<3% low, >_3 and <_8% intermediate and >8% high risk) using the Kaplan–Meier method. We explored the impact of multiple imputation by performing a sensitivity analysis in which we evaluated the complete dataset only. These results were similar to the primary analysis and are presented in Table 7-1. In post hoc analyses, we also determined performance of the GRACE 2.0 score for in-hospital death and of hs-cTn alone to predict all-cause death at 1 year. All analyses were performed in R (Version 3.5.1), with thanks to Dr Andrew Chapman for statistical support.

2.3 Carotid Artery Plaque Samples for RNA

Excised carotid plaque tissue was harvested from patients undergoing carotid endarterectomy following acute neurovascular event. Local ethical approval was obtained via the NHS Lothian BioResource Tissue Governance

committee (15/ES/0094). Plaques were assessed macroscopically for dissection into stable and unstable sections. Areas of plaque rupture with associated intraplaque haemorrhage were considered ‘unstable’, and relatively healthy adjacent sections taken to be ‘stable’. Samples were stored in RNA later (Sigma-Aldrich) for 30-60 minutes, before snap freezing and storage at -80°C, until use for downstream validation of RNA sequencing candidates. Patient characteristics are described below (Table 2-1).

Table 2-1: Carotid endarterectomy patient characteristics
Carotid endarterectomy patient demographics, clinical presentation, past medical history and serum parameters. Data presented as mean and either standard deviation (SD) or percentage (%) in brackets, as stated. TIA= transient ischemic attack, ACEi/ARB= angiotensin-converting enzyme inhibitor/angiotensin receptor blocker.

Carotid Endarterectomy Patients (n=5)	
Age in years, mean (SD)	74 (7.1)
Men, n (%)	5 (100)
Systolic BP (mmHg), mean (SD)	144 (15.2)
Diastolic BP (mmHg), mean (SD)	86 (15.4)
Presenting syndrome, n (%)	
Stroke	2 (40)
TIA / amaurosis fugax	4 (80)
Cardiovascular history, n (%)	
Ischaemic heart disease	3 (60)
Myocardial infarction	0 (0)
Risk factors	
Hypertension	3 (60)
Diabetes	0 (0)
Hypercholesterolaemia	1 (20)
Smoker	0 (0)
Medication	
Aspirin	2 (40)
Clopidogrel	2 (40)
Anticoagulant	1 (20)
Statin	3 (60)
ACEi/ARB	1 (20)
B-blocker	3 (60)
Haematology, mean (SD)	
Hb	146 (15.2)
WBC	7.2 (0.9)
PLT	236 (32)
Biochemistry, mean (SD)	
Creatinine (mmol/L)	85.6 (22.3)
Total cholesterol (mmol/L)	4.4 (1.1)
HDL	1.2 (0.45)
LDL	2.3 (0.88)
Trig	1.9 (1.3)

2.4 Normal aortic samples for RNA analysis

Aortic tissue was harvested from patients undergoing coronary bypass grafting, with no known aortic disease. Local ethical approval was obtained via the NHS Lothian BioResource Tissue Governance committee (15/ES/0094). Punch biopsy samples taken from grafting sites were stored in RNA later (Sigma-Aldrich), for 30-60 minutes, before being snap frozen and stored at -80°C, until use.

Table 2-2: Normal aorta patient characteristics
Patient demographics, clinical presentation, past medical history and serum parameters. Data presented as mean and either standard deviation (SD) or percentage (%) in brackets, as stated. TIA= transient ischemic attack, ACEi/ARB= angiotensin-converting enzyme inhibitor/angiotensin receptor blocker.

Normal Aorta Patients (n=3)	
Age in years, mean (SD)	65 (7.2)
Men, n (%)	3 (100)
Cardiovascular history, n (%)	
Ischaemic heart disease	3 (100)
Myocardial infarction	3 (100)
Risk factors	
Hypertension	2 (67)
Diabetes	2 (67)
Hypercholesterolaemia	2 (67)
Smoker	0 (0)
Medication	
Aspirin	0 (0)
Clopidogrel	0 (0)
Anticoagulant	0 (0)
Statin	1 (34)
ACEi/ARB	1 (34)
B-blocker	1 (34)
Haematology, mean (SD)	
Hb	122 (17.0)
WBC	8.7 (5.4)
PLT	254 (45)
Biochemistry, mean (SD)	
Creatinine (mmol/L)	79 (6.9)
Total cholesterol (mmol/L)	4.0 (1.1)
HDL	1.1 (0.1)

LDL	2.1 (0.8)
Trig	1.7 (0.9)

2.5 Human carotid plaque sections for ISH/IHC

Human atherosclerotic plaque samples were obtained from patients undergoing carotid endarterectomy. The tissue was part of the 'Maastricht Pathology Tissue Collection', and collection, storage, and use of tissue and patient data were performed in agreement with the Dutch Code for Proper Secondary Use of Human Tissue, the Declaration of Helsinki, and was approved by the local Medical Ethical Committee (protocol number 16-4-181). Immediately after resection, each atheroma was divided into parallel segments of 5mm. Formalin-fixed segments were stained with haematoxylin-eosin and according to Virmani et al (16), fibrous cap atheroma with or without intraplaque hemorrhage, termed stable or unstable respectively, used for ISH/IHC.

2.6 Human Tissue Panel

A commercially available human tissue panel, Human MTC™ Panel I (Takara Clontech), was used to characterise expression of LINC01272 across different human tissue RNA samples, from healthy organs.

2.6.1 Venepuncture

Healthy volunteers were selected based on their availability from the University blood donor bank, Centre for Inflammation Research, University of Edinburgh (AMREC Reference number 15-HV-013). Blood was collected from healthy

volunteers using standard venepuncture equipment including 50ml syringe and 16g needle, into 50ml Falcon tubes, and anticoagulated with sodium citrate 3.8%.

2.7 Cell Culture

Cell culture was undertaken in standard biological safety class II vertical laminar flow cabinets under sterile conditions. Cabinets were sterilised before and after use with 70% ethanol.

Peripheral blood mononuclear cells (PBMCs) were isolated from whole blood of anonymised healthy control subjects, for use in fractionation RNA-FISH, phagocytosis and efferocytosis assays, with local ethical approval (15/HV/013). All studies were approved by East and West Scotland Research Ethics Committees, and all experiments were conducted according to the principles expressed in the Declaration of Helsinki. In Edinburgh, porous membrane separation tubes (Greiner Bio-One GmbH, Germany) were used to isolate human PBMCs, and monocytes were isolated by positive selection performed with lyophilised CD14 microbeads (Miltenyi Biotech, Gladbach, Germany). The protocol in Maastricht differed slightly, with PBMCs isolated by Ficoll-Paque gradient, using buffy coat samples from Uniklinik RWTH Aachen, Germany, rather than the porous membrane tubes. Purification with CD14 microbeads and subsequent steps were the same.

For differentiation to macrophages, monocytes were cultured for 1 week at 37°C, 5% CO_2, and stimulated with 10ng/ml M-CSF (Immunotools, Friesoythe,

Germany) in RPMI 1640 Glutamax (Life Technologies, Netherlands, Europe) supplemented with 10% FBS (Gibco / Thermo Fisher, UK) and 1% Pen/Strep (Gibco), with one medium change after 4 days of culture. Coronary artery, pulmonary artery and saphenous vein smooth muscle cells and endothelial cells included in cell expression panel were cultured using supplemented Smooth Muscle Cell Growth Medium 2 (PromoCell, Heidelberg, Germany) and endothelial cell growth medium (EGM-2 BulletKit™) (Lonza, Basel, Switzerland) respectively, at 37°C, 5% CO_2.

2.8 GapmeR knockdown

For selective knockdown of LINC01272 (PELATON), GapmeRs were designed using a sequence common to all isoforms (Table 2-3) (Exiqon, Denmark). GapmeRs were resuspended with RNase free water to a stock concentration of 10μM, and frozen at -20°C until use. Macrophages were transfected with Lipofectamine RNAiMax (ThermoFisher Scientific) with GapmeR concentration of 20nM for 6 hours, followed by quiescence for 18 hours.

Table 2-3: GapmeR sequences

Gapmer ID	Sequence
GapmeR control	AACACGTCTATACGC
GapmeR 1	GAAGGGCTTGGGTCG
GapmeR 2	AAGGAATCCGAGGGT

2.9 Macrophage polarisation

Macrophages were polarised into 4 different subtypes, M1, M2a, M2b and MoxLDL (foam cells), achieved by incubation for 24 hours at 37°C with the relevant stimuli for each; IFNγ 20ng/ml and LPS 10ng/ml for M1; IL-4 for M2a at 50ng/ml; IL- 10 at 10ng/ml for M2c and human oxLDL at 50μg/ml for MoxLDL (Table 2-4). Polarisation was confirmed by qRT-PCR for subtype specific markers (M1, CD86; M2a, CD200R; M2b, CD163; MoxLDL, iNOS) (Chapter 5.3.3).

Table 2-4: Polarisation stimuli

ID	Supplier	Cat no
LPS	Thermo, UK	00-4976-93
IFNγ	Immunotools	11343534
IL-4	Immunotools	11340042
IL-10	Immunotools	11340102

2.10 RNA isolation

Total RNA was isolated from human tissue and cultured cells using the miRNEasy kit (Qiagen, Hilden, Germany).

For tissues, disruption was performed in 700μL of Qiazol for each sample using TissueLyser II (Qiagen) for normal aortic samples, and pestle and mortar in liquid nitrogen for carotid plaque samples.

For cultured macrophages, the yield is notoriously low when cells are differentiated and harvested from plates with small wells. To optimise the number of cells needed to obtain adequate quantities of RNA, wells were

pooled at the Qiazol stage, and various numbers of wells compared for yield and quality of RNA (Table 2-5).

Table 2-5:Optimising RNA extraction from macrophages in 96 well plates

96 well plate
Likely approx. 150,000 cells p/w (double usual)
Qiagen miRNeasy kit, eluted 30µL water

# wells	Nanodrop yield (ng/µl)	Qubit yield (ng/µl)	Nanodrop quality 260/280
x2	9.2	6.0	1.76
x4	17.0	14.0	1.88
x6	21.3	22.0	1.92
x8	40.4	47.8	2.02
x10	45.3	43.5	1.9

So approx 2.26 ng/µL per 75,000 cells / per (normal) well

For enough RNA for x1 optimal cDNA synth (400ng), need 12 wells
For enough RNA for x1 minimum cDNA synth (200ng) , need 6 wells

DNase treatment was also carried out during the extraction with a complimentary RNase- free DNase Kit (Qiagen). As per standard protocol, 140µL chloroform was added for separation of RNA fraction over 3 minutes. Samples were then centrifuged at 12,000 x g 4°C for 15 min, allowing separation into 3 phases: upper aqueous phase containing total RNA; middle interphase containing DNA; lower organic phase, containing protein. The upper aqueous phase was carefully transferred without disturbing the interphase and transferred to a new tube for precipitation with 550µL of absolute alcohol. Samples were passed through columns, when RNA should bind to the column, and a DNase treatment was performed. DNase solution

was prepared with 10µL of enzyme and 70µL of buffer per sample. 80 µL of the mix was then added directly to each column and incubated for 15 minutes at room temperature. RWT and RPE washes were then added to each column, and briefly centrifuged, to wash away contaminating phenol. The flow through was discarded following each wash. Finally, RNase free water was added to each column, quantity dependent on the expected yield of RNA. RNA concentration was estimated using a NanoDrop 1000 spectrophotometer (Thermo Scientific, Paisley, UK) and samples stored at -80°C until use.

2.11 cDNA Preparation

For quantitative gene expression analysis, cDNA was prepared from total RNA using the Multiscribe Reverse Transcriptase kit (Life Technologies, Paisley, UK).

Each reaction contained 200-400ng of total RNA. Constituents of the Multiscribe mix were added as follows: 1x reverse transcription buffer, 5.5 mM MgCl2, 0.5 mM of each dNTP, 2.5 µM random hexamers, 0.4 U/µL RNase inhibitor enzyme, 1.25 U/µL Multiscribe Reverse Transcriptase. A final total volume of 20µL was achieved with addition of nuclease-free water.

Samples were then placed on a thermal cycler (Thermo) adhering to the following protocol:

- 10 min at 25°C to allow for annealing of random primers
- 30 min at 48°C for reverse transcription
- 5 min at 95°C to inactivate the reverse transcriptase

Samples were then stored at -20°C until required.

Quantitative real time polymerase chain reaction (qRT PCR) was performed using SYBR green (Life Technologies) and custom PCR primers (Eurofins MWG, Ebersberg, Germany) or Taqman Master Mix™ (Applied Biosystems) with Taqman probes (primer and probe sequences. Ubiquitin C (UBC) was used as housekeeping gene for normalisation. Relative quantifications were calculated by using the 2-ΔΔCT method (211). When ‘undetermined’, a cycle threshold of 40 was used arbitrarily.

2.12 Real-time Quantitative PCR

For novel lncRNAs quantitative real time polymerase chain reaction (qRT PCR) was performed using SYBR green (Life Technologies) and custom PCR primers (Eurofins MWG, Ebersberg, Germany) or Taqman Master Mix™ (Applied Biosystems) with Taqman probes for known protein targets (primer and probe sequences Table 2-6 + Table 2-7). Ubiquitin C (UBC) was used as housekeeping gene for normalisation. Relative quantifications were calculated by using the 2-ΔΔCT method (211). When 'undetermined', a cycle threshold of 40 was used arbitrarily.

2.12.1 SYBR

Primers were designed to span intron-exon boundaries when possible, and were reconstituted and used at [100μM], stored at -20ºC. SYBR green dye in the PCR mixture fluoresces when it binds to double stranded DNA, which is formed by annealing of the primer to any available transcript in the mixture. The level of fluorescence detected is therefore proportional to the quantity of the target.

cDNA 2.5μl was added to a standard PCR mastermix as follows:

- Power SYBR Green master mix - 5 μL
- Nuclease-free H_2O - 4.9 μL
- Forward (fw) and reverse (rv) SYBR green primers - 0.05 μL each (at [100 μM])

All reactions incorporated housekeeping control genes, to compare relative expression between samples. A non-template control with no cDNA was also

tested, when there should be no fluorescence. All samples were performed in triplicate, or duplicate when sample quantities were less plentiful. Once pipetted, qPCR plates were centrifuged briefly to ensure all mixture was sent to the bottom of the well. Samples were analysed on the Quantstudio 7 or Quantstudio 12 real time PCR system with the following protocol:

- 10 min at 95°C before undergoing
- 40 cycles of denaturing at 95°C for 15 s
- 60 s at 60°C for primer annealing and primer extension

Primer sequences are listed below (Table 2-6).

Table 2-6: SYBR Primer sequences

Gene ID	Sequence
LINC01272_Fw	CCTTCCTTCTGCCTCCACTG
LINC01272_Rv	TTGCTGTGGACTGATGTGGG
NEAT1_Fw	TTGGGACAGTFFACGTGTGG
NEAT1_Rv	TCAAGTCCAGCAGAGCA
PELATON+HA_Fw	GCCTCCACTGCCACCACTGC
MLN+HA_Fw	AAGATGAAATTGTGGGAAGA
HA_only_Rv	AGCGTAATCTGGAACATCGT
BCAS4_Fw	GAGCTCGCGCTCTTCCTGAC
BCAS4_Rv	AGGGGCTGGCTCTCATTGGT
UBE2V1_Fw	TGGAGTGGTGGACCCAAGA
UBE2V1_Rv	TAACACTGTCCTTCGGGCG
PARD6B_Fw	GGGCACTATGGAGGTGAAGA
PARD6B_Rv	TCCATGGATGTCTGCATAGC
SPATA2_Fw	AGCCAGACTTTGTTGGATTTG

SPATA2_Rv	TTTACTGGCGATGTCAATAGG
RIPOR3_Fw	TCCATTGAAGAGGAGGCTCG
RIPOR3_Rv	TCCCCTCCTAAGTTCCTCCA
CD200R_Fw	TGGATGAAAAACAGATTACACAGAA
CD200R_Rv	TAATGCGATAGGAGGGCAAC
CD163_Fw	GATGTGGATCTGCACTCAAA
CD163_Rv	TCCAGAGAGAAGTCCGAATC
iNOS_Fw	CTTTGATGAGGGGACTGGGC
iNOS_Rv	ATGTTCTTCACTGTGGGGCTTG

Standard curves with serial dilutions were performed to assess the optimum concentration of cDNA per reaction, at a given concentration of primer (10μM). Amplification of samples at 20ng/uL and 4ng/uL would be adequate, yielding CT values within the desired range (20-30). My usual input of 400 ng of total RNA into a final reaction of volume 40 μL means 10 ng/ μL, would yield a CT in a measurable and detectable range.

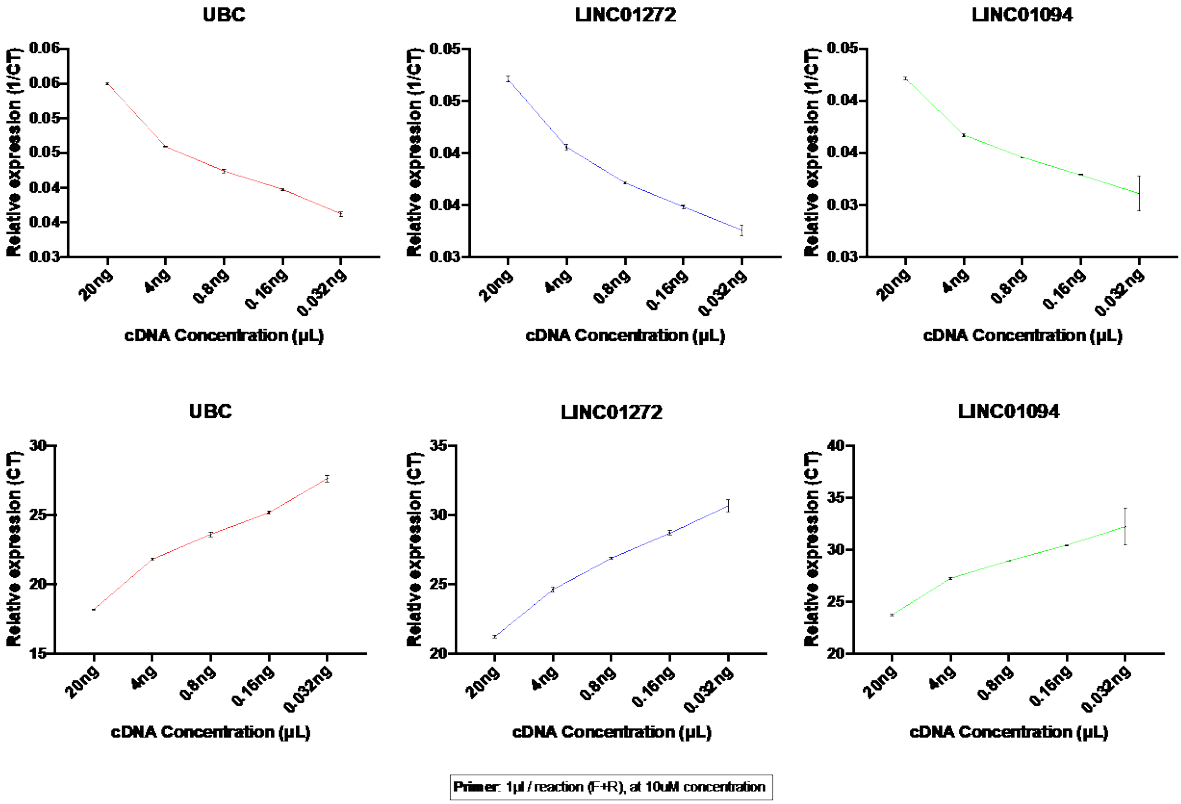

Figure 2-1: Standard curves for SYBR primers: RNA input
Amplification of samples at 20ng/uL and 4ng/uL would be adequate, yielding CT values within the desired range (20-30)

To determine the optimum concentration of primer, standard curves were produced, indicating that the standard concentration of 10uM would allow detection of the target in the desirable range, without primer-dimer effects.

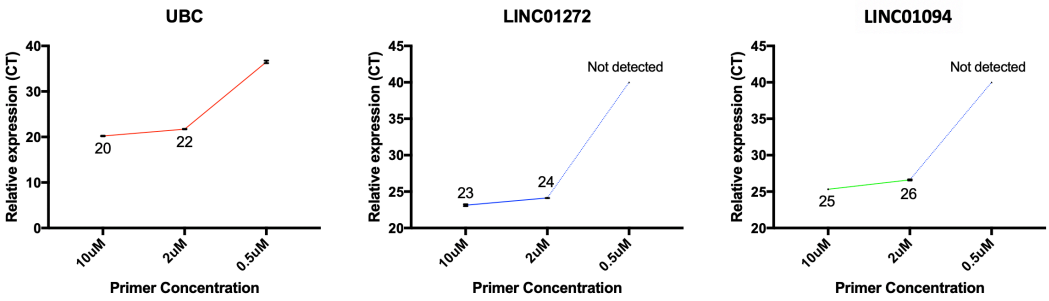

Figure 2-2: Standard curves for SYBR primers: Primer concentration
The standard concentration of 10uM would allow detection of the target in the desirable range

2.12.2 Taqman®

TaqMan® qRT-PCR was performed using TaqMan® Gene Expression assays and TaqMan® Universal Master Mix II (both Thermo Fisher). TaqMan® qRT-PCR assays are labelled with a 5' fluorescent reporter dye (FAM) and quencher molecule at the 3' end. When the TaqMan® probe is intact, fluorescence released from the 5' dye is transferred to the 3' quencher molecule 88 by a phenomenon known as fluorescence resonance energy transfer (FRET). During the amplification process, if the target sequence is present in the sample, the probe anneals and the quencher is cleaved via the action of Taq DNA polymerase – present in the reaction mixture. The Taq polymerase enzyme contains a 5' nuclease domain, which allows degradation of DNA bound to the target, downstream of DNA synthesis. This results in the degradation of the TaqMan® probe, and cleavage of the 3' quencher molecule, therefore preventing FRET and allowing for the detection of the reporter fluorophores. The strength of the fluorescence is increased with each

amplification cycle and is relative to the amount of a specific mRNA within a sample.

Reactions were performed in 384-well plates using the following mixture:

- *1 x Taqman® assay (5 µL)*
- *1 x TaqMan® master mix (0.5 µL)*
- *1.5 µL cDNA*
- *3 µL nuclease free H2O – total reaction volume of 10 µL.*

As per SYBR qPCR, samples were pipetted in triplicate where possible, and reactions performed using the the Quantstudio 7 or Quantstudio 12 real time PCR system with the following protocol:

- *10 min at 95°C*
- *40 cycles at 95°C for 15 seconds*
- *60 seconds at 60°C*

Table 2-7: Taqman probes

Gene ID	Catalogue Number
PTPN1	Hs00942477_m1
CEBPB	Hs00942496_s1
IL-6	Hs00174131_m1
IL-1β	Hs01555410_m1
TNFα	Hs00174128_m1
CD68	Hs02836816_g1

2.13 Cellular Fractionation for LINC01272 Localisation

Fractionation of monocytes and macrophages was carried out using the Ambion PARIS kit (Thermo Fisher, UK), as per the manufacturer's guidelines. Cells were initially treated with cell fractionation buffer, resulting in a nuclear and cytoplasmic fraction. Nuclear material was further subjected to cell disruption buffer, and then both fractions processed for RNA isolation using a column purification method.

2.14 Cloning and in vitro translation

Open reading frame sequences from PELATON and LINC00948 were incorporated into pcDNA 3.1 (+) vectors (Geneart, Thermo Fisher), with Kozak sequence upstream, and haemagglutinin (HA) tag downstream, and flanking restriction enzyme sites (Supplementary Material – Table 3). Translation potential was assessed using the PURExpress In Vitro Protein Synthesis Kit (New England Biolabs, Massachusetts, US).

Table 2-8: Open reading frame sequences.
Both genes were flanked with restriction enzyme digestion sites, Kozak sequence, appended with HA tag, and inserted into pcDNA 3.1 (+) vectors.

Gene	Inserted sequence
PELATON	AAGCTTGGATCCCCACCATGAAGCTACTTGCCAAGGTCACGCAGCACA GTCACATCCTACTGAACATCATCCTGTTCTCTGGGTGGAATGTCACCAT CGCCCAGGTGGGGATTTTTGTGTGTTTTGTTCACTGCTGTACACCCAGC CCCCAGCACAGCGCCTGTCCAGGACAAGTGCCCAGTAAACACTTGGGA AGCAATGCAAGCGTCCTCCCAGCAGCTCCTGCAAACAGACCCCCGACC CAAGCCCTTCCTTCTGCCTCCACTGCCACCACTGCTGCTCATCTCTGCT GGCACAGAAGTCTCTTCCCTGGTCTTCCAGAAATCCCCTCTCCACACTC AGCCAGAGGGAGCTATTACCCATACGATGTTCCAGATTACGCTTAACTC GAGGATATC
LINC00948	GGATCCCCACCATGACTGGTAAAAACTGGATATTAATTTCTACTACTACT CCCAAAAGTCTAGAAGATGAAATTGTGGGAAGACTTCTAAAAATTTTGTT TGTTATCTTTGTTGACTTAATTTCTATTATATATGTTGTGATAACTTCTTA CCCATACGATGTTCCAGATTACGCTTAACTCGAG

2.15 Western Blot

Protein lysates were prepared in Novex™ Tricine sodium dodecylsulfate (SDS) sample buffer, (Thermo Fisher Scientific, Massachusetts, USA) and Dithiothreitol (DTT), incubated at 85°C, centrifuged briefly, and loaded onto a Novex™ 10-20% Tris-Glycine Mini Gel, alongside a the Spectra™ low range multicolour protein ladder (1.7 – 40 kDa range). Electrophoresis was performed at 120V, 300A, for 1 hour, in Novex™ Tris-Glycine SDS Running Buffer. Membrane transfer was carried out in a Mini Blot transfer module at 20V, 300A for 1 hour in Novex™ Tris-Glycine Transfer Buffer. Membranes were incubated overnight at 4°C with anti HA-tag (Abcam, ab9110, 1/1000). After washing, membranes were incubated with the appropriate Licor IRDye® 680 secondary antibody (1:10,000) at room temperature for 1 hour. Following additional washing, protein levels were visualised via Licor.

2.16 High content analysis

For all screening high content assays primary human monocytes were seeded at a density of 75-100,000 cells per well in Corning Falcon 96-Well Imaging Microplates (Fisher Scientific), from 3 biological donors. In the initial high content analysis, 7-day differentiation into macrophages was performed and cells were then transfected with LNA GapmeR targeting LINC01272, as described above. Functional assays were then carried out and are described below. In each case Hoechst nuclear staining was used to identify nuclei, and images were acquired using BD Pathway 855 High Content Bioimager (BD Biosciences, California, USA). Nine images were taken of each individual well. Using Attovision software, stitched images were corrected for background variations and Attovision cell segmentation (Polygon based on Hoechst signal) was carried out using appropriate threshold, watershed and object size in- and exclusion criteria. Data was further analysed using DIVA software (BD Biosciences) to enable quantification of output parameters.

Apoptosis of macrophages was first assessed at 24 hours post-transfection (baseline) and after a further 24 hours treatment with 300nM staurosporine (Sigma, Dorset, UK) for chemical induction of apoptosis. Apoptosis was detected by binding of Annexin-V-OG (locally prepared, courtesy of C. Reutelingsperger, MUMC) at 2.5ng/ml, incubated for 15 minutes at 37°C in binding buffer. Images were acquired and apoptotic cells expressed as a proportion of total cells.

Phagocytosis was assessed by incubation with pHrodo™ Red Zymosan Bioparticles™ (Life Technologies) at 5µL in 150µL per well for 1 hour. Cells shown to have positive uptake of the particles were considered positive, and expressed as a percentage of total cells in each well. For validation experiments the same protocol was used, but images acquired with the Operetta High-Content Imaging System (Perkin-Elmer, Ohio, USA) and image analysis was performed using Columbus (Perkin-Elmer, Ohio, USA) software. Image analysis produced an image that pseudo labelled cells positive (green) and negative (red) for bead uptake to allow for clear visual representation.

Lipid uptake was assessed by incubation with a mixture of 0.8µg oxidised LDL (derived locally) and 0.2µg Topfluor (Avanti Polar Lipids, Alabama, US) for 3 hours. Cells with uptake of Topfluor and oxLDL were expressed as a percentage of total cells in each well.

Mitochondrial stress was induced using 1.2µM staurosporin for 2 hours. Mitotracker mitochondrial stain (Thermo Fisher, UK) was then added at 250nM, and cells incubated for 30 minutes. Reduced mitochondrial membrane potentials result in less uptake of Mitotracker and so a lower signal intensity. Relative average intensity was compared between wells.

Reactive Oxygen Species (ROS) production was stimulated using 10µM menadion (Sigma, Dorset, UK) for 30 min, and ROS were detected with 20µM DCFDA (Invitrogen, California, USA). ROS positive cells were expressed as a percentage of total cells per well.

2.17 Operetta High Content Analysis

Primary human monocytes were seeded at a density of 75-100,000 cells per well in Corning Falcon 96-Well Imaging Microplates (Fisher Scientific), N=3 biological replicates, 4-5 wells per condition, 9 images per well acquired.

Columbus software was used to analyse the fluorescence based assays, in a similar manner to previous. Populations of cells were identified by nuclear Hoechst stain, and subsequently the cytoplasm was identified surrounding each nucleus by autofluorescence. ‘Spots’ or areas of TRITC intensity identified in each cell were identified, and intensity <100 excluded. The number of spot positive cells were then calculated.

2.18 Efferocytosis Assay

Monocytes were differentiated to macrophages and transfected with LNA GapmeR as described previously. Jurkat T cells (JC) (ATCC), were induced to undergo apoptosis by incubation with 20nM Staurosporine for 1.5hrs at 37°C, then labelled with Calcein (ThermoFisher). The macrophages were incubated with the JC for 1 hour with and washed thoroughly. Macrophages were then detached on ice with 0.05% EDTA in phosphate buffered saline, and run on an Attune NxT Flow Cytometer to quantify the percentage of cells which have taken up the Calcein labelled JC (FITC+ cells) with analysis performed on FlowJo software. Apoptosis of JC was confirmed with Annexin V.

2.19 In-situ Hybridisation + Immunohistochemistry

For in-situ hybridisation (ISH), formalin-fixed, paraffin embedded tissue sections were firstly deparaffinised and rehydrated by washing in Xylene for 5 min, followed by sequential washes in 100%, 96% and 70% ethanol respectively, for 5 min each, then washed in water, followed by PBS for 5 min. The miRNA buffer set (Qiagen, 339450) was then used, providing proteinase K for tissue digestion (incubated 1:1000 at 37°C for 4 min) and hybridisation buffer which was used to dilute the ISH probes (Supplementary Material – Table 5) to 25nM. The ISH probes were incubated on the sections overnight at 55°C, sealed using coverslips and rubber glue to prevent drying out. The sections were washed with 5X saline-sodium citrate buffer (SSC) at 55°C and room temperature to increase hybridisation specificity. Subsequently, the sections were washed with PBS, and incubated for 1hr with Digoxigenin wash and block buffer set (Roche, 11585762001), which was subsequently used to dilute anti-Digoxigenin-AP (Roche, 11093274910) at 1:500 and left for 1hr at room temperature. After washing with TBS-T, NBT/BCIP AP tablets (Roche, 11697471001) were used for detection to visualise probe in the presence of levamisole to reduce background staining (Vector laboratories, Peterborough, UK). Detection occurred at approximately 3 hours. For immunohistochemistry co-staining, slides were incubated in 0.3% hydrogen peroxide for 15 minutes, washed with TBS-T 0.1% BSA, before incubation in 5% goat serum for 1 hour. Antibodies were then added (Supplementary Material – Table 6) for 30 minutes, before washes with TBS, and incubation with anti-mouse-HRP Brightvision (Immunologic, Netherlands) for 30 minutes.

After TBS washes, Polydetector HRP green kit (Bio SB, California, USA), 1 drop in 2ml was added to tissues and allowed to develop for 3 minutes. After rinsing with water, tissues were counterstained with nuclear fast red (Sigma Aldrich), before further washing. Rehydration was done with sequential washes of 70%, 96% and 100% ethanol respectively, followed by xylene and mounting with Pertex.

Table 2-9: In-situ hybridisation probes

Probe ID	Sequence
Scramble control	GTGTAACACGTCTATACGCCCA
PELATON	TTATTCTCCAAGCAACAGAGAT

Table 2-10: Immunohistochemistry probes

Antibody	Supplier	Concentration	Dilution
CD68	Dako	185mg/L	1:500
SMA	Dako	71mg/L	1:8000
IgG	Invitrogen	3000mg/L	1:4000

2.20 RNA-Fluorescent In-Situ Hybridisation (RNA-FISH)

Custom RNA-FISH probe sets were generated to the full sequence of PELATON (Thermo Fisher Scientific). Monocytes were differentiated to macrophages as previously described, grown on 16-mm coverslips for one week, before being washed in PBS and fixed in 4% paraformaldehyde. RNA-FISH was performed according to manufacturer's instructions (ViewRNA™ cell FISH, ThermoFisher Scientific). Briefly, the coverslips were permeabilised using detergent QS and digested in protease solution at 1:4000, then incubated with a probe sets at 1:100 (PELATON, SNORD3 (small nucleolar RNA, C/D box 3A) and UBC). The coverslips were then subsequently incubated with pre amplifier, and amplifier, before finally being incubated with the label probe, which provides the fluorescent signal. Coverslips were then mounted onto glass slides using Prolong Gold Antifade Mounting Medium with DAPI (Vector Laboratories).

2.21 Microscopy

An Axioscan slidescanner (ZEISS) was used to image both *in situ* and immunofluorescence, using Zen software (ZEISS). All settings for the Axioscan and software were optimised and then maintained for each set of experiments, so that sections can be compared accurately. RNA-FISH was imaged using the Andor Revolution XDi spinning disk confocal microscope.

2.22 Pseudo Fluorescent Image Analysis

Bright field images for PELATON (Purple *in-situ* staining) and CD68/aSMA (green immunohistochemistry staining) in human plaque were converted into pseudo fluorescent images using Image J Software. Images were opened in Image J, and the colour deconvolution tool used, selecting regions of interest for each stain (Purple *in situ* staining, green immunohistochemistry staining, and pink nuclear red counterstain), generating RGB values for each colour, and splitting the images into these components. The RGB values generated for each colour were kept consistent for further analysis across all samples. Once the images were split into the 3 colours, the nuclear stain was discounted, so that the *in-situ* and immunohistochemistry staining could be seen clearly. These were then inverted, and given pseudo colours of red and green respectively, and the resulting images merged to create a dual fluorescent image.

2.23 Statistical analysis

Statistical analyses in chapters 4 and 5 were performed according to figure legends using Graphpad Prism version 8.0. Data are expressed as mean ± standard deviation. Normality of data was assessed using the Shapiro-Wilks test. Statistical difference between 2 groups was assessed using 2-tailed unpaired or paired t-test for parametric data and Mann-Whitney or Wilcoxon matched pairs signed rank tests for non-paired and paired non-parametric data

respectively. One-way ANOVA ± multiple comparisons was used for ≥ 3 groups. Post-hoc testing with Dunnett's test has been performed as appropriate. Statistical significance is indicated when p value of less than 0.05 ($p<0.05$=*, $p<0.01$=**, $p<0.001$=***, $p<0.0001$=****).

2.24 RNA Sequencing Analysis

For sample and library preparation see GEO database: GSE120521. Data was analysed using RSEM and DESeq2 packages to derive FPKM, fold change, and p-values, with thanks to Dr Julie Rodor (senior scientist) for bioinformatic support in conducting this analysis, and production of some figures. Filtering was performed using Microsoft Excel for Mac, version 16.

Chapter 3 Results – Performance of the GRACE 2.0 score in patients with type 1 and type 2 myocardial infarction

Hung J, Roos A, Kadesjö E et al. Performance of the GRACE 2.0 score in patients with type 1 and type 2 myocardial infarction.
European Heart Journal,
ehaa375, https://doi.org/10.1093/eurheartj/ehaa375

3.1 Introduction

Coronary heart disease is responsible for around 2 million deaths across Europe every year (212). To improve prognostication and promote consistency in the investigation and management of patients with acute coronary syndrome, the Global Registry of Acute Coronary Events (GRACE) score was developed (213-216). The score applies clinical variables, the electrocardiogram, and cardiac biomarkers to estimate risk of future all-cause mortality and myocardial infarction. The use of the GRACE 2.0 score in patients with non-ST-segment elevation acute coronary syndrome has a class Ia recommendation for guiding prognosis and IIa recommendation for guiding management across all international guidelines (217-219).

Since the introduction of the GRACE score, there have been significant changes in the way we diagnose myocardial infarction, driven by major improvements in the sensitivity of cardiac troponin. The Fourth Universal Definition of Myocardial Infarction recommends the use of high-sensitivity cardiac troponin (hs-cTn) assays and a sex- specific 99th centile diagnostic threshold for myocardial injury and infarction (74). These assays have the ability to quantify myocardial injury at a threshold 10-fold lower than was in use at the time of the original GRACE study. This increase in diagnostic sensitivity has led to an understanding that myocardial infarction can occur in a number of different clinical settings (73, 220, 221).

The Fourth Universal Definition recognises that myocardial infarction may occur due to atheromatous plaque rupture and thrombosis (type 1 myocardial

infarction), or secondary to an imbalance in myocardial oxygen supply or demand without coronary atherothrombosis (type 2 myocardial infarction) (74). Patients with type 2 myocardial infarction are older, more often have comorbidities and are at higher risk of adverse outcomes with as few as 30% of patients alive at 5 years (75). Despite a significant increase in the risk of non- cardiovascular death, patients with type 2 myocardial infarction appear to have a similar risk of future cardiovascular events as those with type 1 myocardial infarction (222). To date, there are no validated prognostic tools to estimate all-cause mortality or future cardiovascular events in this population. Our aim was to evaluate the performance of the GRACE 2.0 score for the prediction of all-cause death in patients with type 1 and type 2 myocardial infarction.

3.2 Methods

We assessed the performance of the GRACE 2.0 score in two cohorts of consecutive patients presenting to the Emergency Department with suspected acute coronary syndrome in Scotland and in Sweden (see full description in Chapter 2.2.1). In brief, the Scottish cohort was derived from the High-STEACS study, which included patients with suspected ACS from 10 hospitals across Scotland between June 2013 and March 2016. The Swedish cohort comprised patients presenting to Karolinska University Hospital, Stockholm with chest pain and at least one hs-cTn measurement from January 2011 to October 2014 (209, 210).

All diagnoses were adjudicated in accordance with the Fourth Universal Definition of Myocardial Infarction (74), (see Chapter 2.2.2 for full details). In both cohorts two physicians independently reviewed all clinical information with discordant diagnoses resolved by a third reviewer (Scotland) or by consensus discussion (Sweden).

The primary outcome was all-cause death at 1 year, and the secondary outcome was all-cause death or type 1 myocardial infarction at 1 year. All in-hospital and community deaths are recorded on the National General Register of Scotland, and the Swedish Patient Register. Subsequent myocardial infarction events were identified through the electronic patient record in Scotland with adjudication as for the index diagnosis and using ICD-10 coding (I21 and I22) from the Swedish Patient Register in the Swedish cohort.

We determined the GRACE 2.0 score for all-cause death, and for all-cause death or type 1 myocardial infarction at 1 year. We assessed overall GRACE 2.0 model discrimination by determining the area under the receiver operating curve (AUC) and compared performance in patients with type 1 and type 2 myocardial infarction using the DeLong method. We assessed model calibration both graphically, and by using the Hosmer–Lemeshow goodness of fit test. In addition, we assessed GRACE performance by evaluating previously defined categories of mortality risk (<3% low, >_3 and <_8% intermediate and >8% high risk) using the Kaplan–Meier method (see Chapter 2.2.3 for full statistical methods).

3.3 Results

Study Populations

The Scottish cohort consisted of 48 282 consecutive patients (61 ± 17 years, 47% women) with suspected acute coronary syndrome of whom 10 360 (21%) had hs-cTnI concentrations above the 99th centile. It was possible to adjudicate the diagnosis in 88% (9115/10 360) of patients. The final diagnosis was type 1 myocardial infarction in 55% (4981/9115), type 2 myocardial infarction in 12% (1121/ 9115), and acute or chronic myocardial injury in 18% (1676/9115) and 14% (1287/9115), respectively. The remainder of patients had type 4a (9/9115) or 4b (41/9115) myocardial infarction.

The Swedish cohort consisted of 22 589 consecutive patients with suspected acute coronary syndrome of whom 3853 (17%) patients had hs-cTnT concentrations above the 99th centile. The final diagnosis was type 1 myocardial infarction in 28% (1080/3853) of patients, and type 2 myocardial infarction in 6% (247/3853), with acute or chronic myocardial injury in 30% (1144/3853) and 35% (1347/3853), respectively.

Patient characteristics

Compared to patients with a diagnosis of type 1 myocardial infarction, those with type 2 myocardial infarction were older (74 ± 14 vs.68 ± 14 years), more likely to be women (55% vs. 40%), and more likely to have a history of cardiovascular disease. Similar differences were apparent in both cohorts

(Table 3-1). Patients with type 2 myocardial infarction were less likely to be offered coronary angiography, revascularization or secondary prevention than those with type 1 myocardial infarction (Table 3-2). There were differences in the covariates which influence the GRACE 2.0 score between groups, with higher heart rates (101 vs. 77 b.p.m.), lower systolic blood pressures (130 vs. 141 mmHg) and a higher proportion of patients with increased Killip class observed in those with type 2 myocardial infarction (Table 3-3).

Table 3-1: Characteristics of the Scottish and Swedish cohorts of patients diagnosed with type 1 and type 2 myocardial infarction

	Scottish cohort			Swedish cohort		
	All patients	**Type 1 myocardial infarction**	**Type 2 myocardial infarction**	**All patients**	**Type 1 myocardial infarction**	**Type 2 myocardial infarction**
No. of participants	48,282	4,981	1,121	22,589	1,080	247
Age (years), mean (SD)	61 (17)	68 (14)	74 (14)	56 (17)	69 (13)	72 (13)
Men, n (%)	25,720 (53)	2,995 (60)	501 (45)	11,817 (52)	743 (69)	122 (49)
Past medical history						
Myocardial infarction, n (%)	4,214 (9)	667 (13)	163 (15)	1,885 (8)	184 (17)	47 (19)
Ischemic heart disease, n (%)	11,912 (25)	1,519 (30)[a]	454 (40)	2,570 (11)[b]	-	-
Cerebrovascular disease, n (%)	2,949 (6)	368 (7)	135 (12)	940 (4)	66 (6)	20 (8)
Diabetes mellitus, n (%)	3,518 (7)	802 (16)	147 (13)	2,191 (10)	204 (19)	54 (22)
Heart failure hospitalisation, n (%)	4,322 (9)	792 (16)	292 (26)	1,244 (6)	86 (8)	40 (16)
Previous revascularisation						
Previous PCI or CABG, n (%)	4,464 (9)	592 (12)	129 (12)	1,979 (9)	210 (19)	53 (22)
Medications at presentation						
Aspirin, n (%)	13,163 (27)	1,694 (34)	471 (42)	4,258 (19)	414 (38)	101 (41)
Statin, n (%)	19,366 (40)	2,377 (48)	632 (56)	4,265 (19)	362 (34)	86 (35)
ACE inhibitor or ARB, n (%)	15,618 (32)	1,995 (40)	514 (46)	5,547 (25)	456 (42)	130 (53)
Beta-blocker, n (%)	13,173 (27)	1,598 (32)	489 (44)	5,508 (24)	441 (41)	140 (57)
Oral anti-coagulant, n (%)	3,253 (7)	292 (6)	170 (15)	-	-	-
Electrocardiogram[c]						
Myocardial ischemia	-	1,872 (38)	383 (34)	-	281 (26)	67 (27)
Physiological parameters[d]						
Heart rate, beats per minute	-	79 (20)	105 (35)	-	76 (17)	94 (31)
Systolic blood pressure, mmHg	-	142 (28)	132 (30)	-	153 (28)	142 (34)
Hematology and clinical chemistry						
Haemoglobin, g/L	136 (22)	136 (22)	126 (29)	-	139 (17)	130 (20)

eGFR, ml/min	54 (13)	51 (14)	46 (15)	88 (23)	74 (23)	66 (25)
Peak hs-cTnI, ng/L	4 [2, 16]	855 [104, 6775]	125 [48, 604]	-	-	-
Peak hs-cTnT, ng/L	-	-	-	-	182 [49, 616]	77 [32, 173]

eGFR calculated according to the MDRD equation (mL/min).
[a]Defined as prior angina, myocardial infarction, or revascularization.
[b]Defined as prior myocardial infarction or revascularization.
[c,d]Electrocardiogram findings and physiological parameters provided for patients with myocardial infarction only.

Table 3-2: Rates of angiography, revascularisation and prescription for medical therapy on discharge in the Scottish and Swedish cohorts

	Scottish cohort		Swedish cohort	
	Type 1 myocardial infarction (n=4,981)	**Type 2 myocardial infarction (n=1,121)**	**Type 1 myocardial infarction (n=1,064)**	**Type 2 myocardial infarction (n=228)**
Coronary Angiography†	3,083 (62)	123 (11)	-	-
PCI or CABG†	2,217 (45)	24 (2)	543 (51)	7 (3)
Aspirin	3,934 (79)	588 (52)	918 (86)	101 (44)
P2Y12 inhibitor	3,544 (71)	319 (28)	871 (82)	26 (11)
ACE or ARB	3,572 (72)	618 (55)	725 (68)	118 (52)
Beta-blocker	3,476 (70)	708 (63)	169 (74)	946 (89)
Statin therapy	4,141 (83)	700 (62)	883 (83)	92 (40)

Information from the Swedish cohort available in 99% (1064/1080) with type 1 and 92% (228/247) with type 2 myocardial infarction.
Values are number (%). † Angiography and revascularisation within 30 days of presentation.
P <0.001 for all treatments in patients with type 1 versus type 2 across both cohorts. P values obtained from group-wise comparisons using Chi-square test

Table 3-3: Components of the GRACE 2.0 risk score in patients with type 1 and type 2 myocardial infarction

	Type 1 myocardial infarction		**Type 2 myocardial infarction**	
	Scottish cohort	**Swedish cohort**	**Scottish cohort**	**Swedish cohort**
Age	68 (14)	69 (13)	74 (14)	72 (13)
Heart rate (bpm)	77 [65-92]	73 [64-84]	101 [81-125]	89 [72-109]
Systolic blood pressure (mmHg)	141 [123-160]	152 [135-170]	130 [111-150]	140 [120-160]
Creatinine	0.93 [0.80-1.19]	0.93 [0.79-1.13]	1.05 [0.82-1.39]	0.98 [0.78-1.27]
Killip class (%) I / II / III / IV	4,419 (88.7) 279 (5.6) 205 (4.1) 78 (1.6)	1014 (93.9) 64 (5.9) 2 (0.2) 0 (0.0)	852 (76) 126 (11.2) 130 (11.6) 13 (1.6)	188 (76.1) 51 (20.6) 8 (3.3) 0 (0.0)
Cardiac arrest (%)	278 (5.6)	8 (0.1)	30 (2.7)	1 (0.4)
Troponin >99th centile at presentation (%)	4,092 (82.2)	929 (86.0)	881 (78.6)	199 (80.6)
ECG ischaemia (%)	1,627 (32.7)	281 (26.0)	311 (27.7)	67 (27.1)
STEMI (%)	915 (18.4)	0 (0)	5 (0.5)	0 (0)
GRACE 2.0 risk of death at 1 year, %	4.9% [2.3 - 11.7%]	3.8% [1.9 - 8.2%]	11.2% [5.4 - 22.1%]	7.7% [3.5 - 19.9%]
GRACE 2.0 risk of death or MI at 1 year, %	9.4% [5.6 - 18.2%]	7.7% [4.9 - 14.0%]	17.8% [10.2 - 29%]	13.3% [7.4 - 25.9%]

Values are Mean (SD) or Median [IQR].

GRACE risk score and prediction of death at 1 year

We obtained follow-up in 100% of participants for primary and secondary outcomes at 1 year. In patients with type 1 myocardial infarction, 15% (720/4981) and 10% (112/1080) died from any cause at 1 year in the Scottish and Swedish cohorts, respectively. The GRACE 2.0 score was higher in those with type 2 compared to type 1 myocardial infarction across both cohorts (Table 3-3) and had good discriminative ability with an AUC of 0.83 [95% confidence interval (CI) 0.82–0.85] and 0.85 (95% CI 0.81–0.89), respectively (Figure 3-1).

In patients with type 2 myocardial infarction 23% (258/1121) and 23% (57/247) died from any cause at 1 year in the Scottish and Swedish cohorts respectively. The GRACE 2.0 score had moderate discriminative ability, with an AUC of 0.73 (95% CI 0.70–0.77) and 0.73 (95% CI 0.66–0.81), respectively, and performed less well than in patients with type 1 myocardial infarction (DeLong test $p<0.001$ and $p<0.008$ vs type 1 myocardial infarction in Scottish and Swedish cohorts respectively (Figure 3-1) .

Similar performance was observed in men and women with type 1 and type 2 myocardial infarction in both cohorts (Appendix, Table 7-3). Calibration plots and the Hosmer–Lemeshow test indicated the GRACE 2.0 score underestimated future all-cause death across all deciles of risk in both type 1 and type 2 myocardial infarction (Figure 3-2, Appendix Table 7-2).

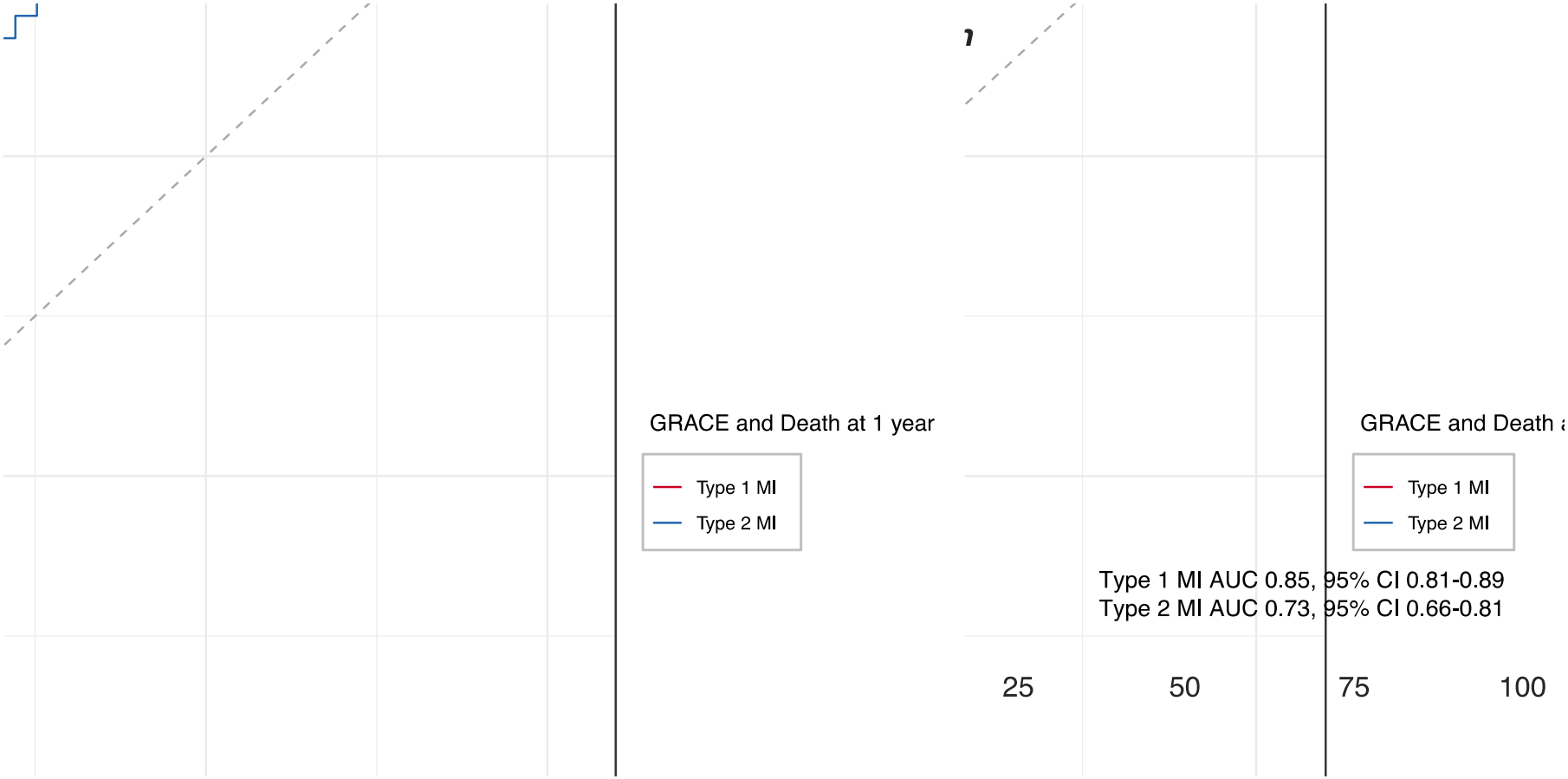

Figure 3-1: Receiver-operator-curve for GRACE 2.0 score.
ROC curve to predict all-cause death at 1 year in patients with type 1 and type 2 myocardial infarction in the Scottish and Swedish cohorts

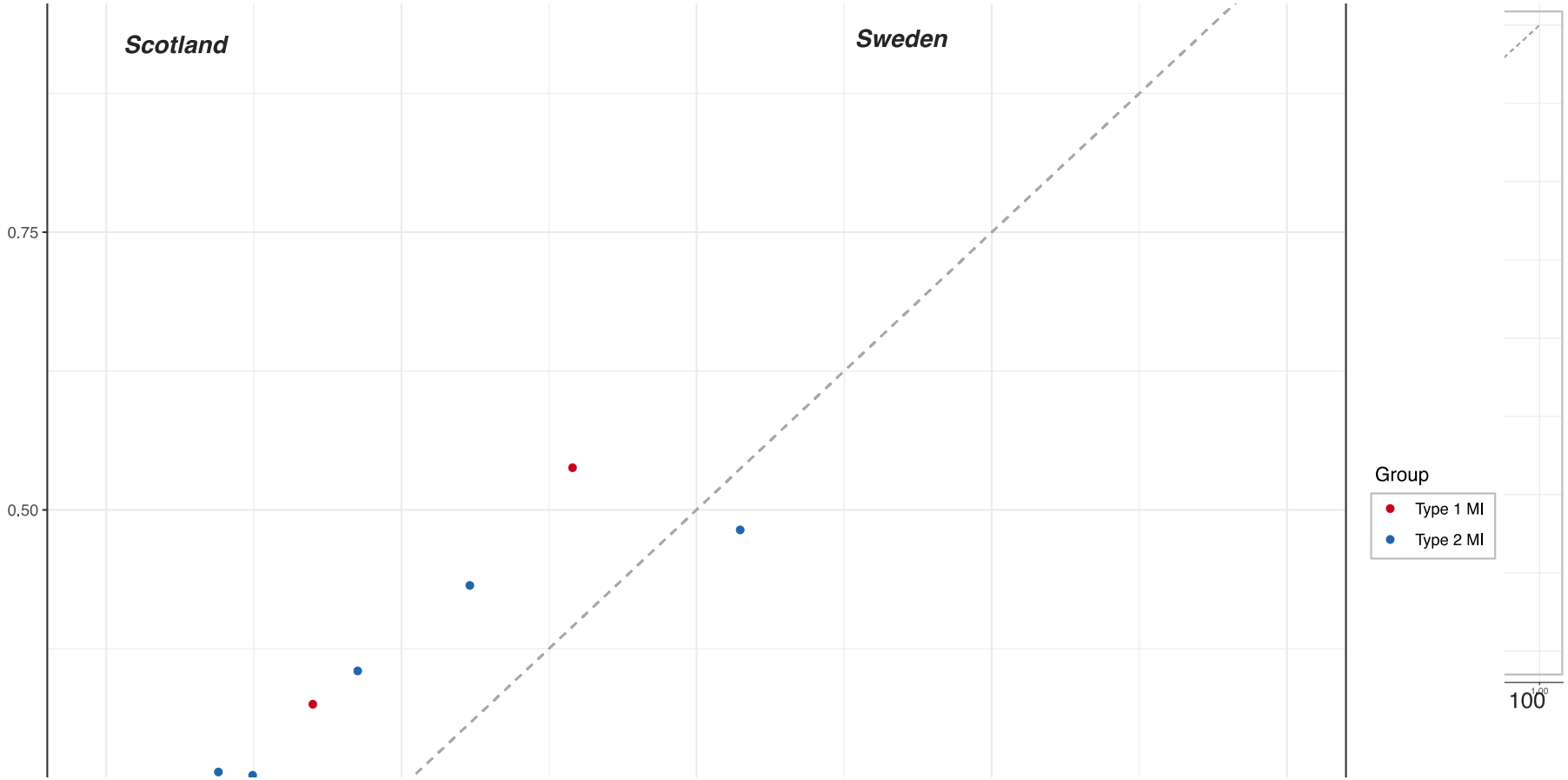

Figure 3-2: Calibration plot.
Observed versus predicted all-cause mortality in type 1 and type 2 myocardial infarction according to the GRACE 2.0 score in the Scottish cohort

GRACE risk categories

In the Scottish cohort, we evaluated conventional GRACE categories of low, intermediate, and high predicted risk of mortality. Observed event rates were higher in patients with type 2 myocardial infarction who had a low or intermediate predicted risk of death (Figure 3-3). Baseline demographic information was similar across all categories of risk irrespective of the diagnosis of type 1 and type 2 myocardial infarction (Appendix Table 7-4). In patients with type 2 myocardial infarction in the Scottish cohort at low risk of death, there were fewer new prescriptions for aspirin (25% vs. 67%), statin (11% vs. 56%), angiotensin-converting enzyme inhibitor or angiotensin II receptor blocker (15% vs. 49%) compared to those with type 1 myocardial infarction. Similar patterns were observed in patients at intermediate or high risk of death.

GRACE score and prediction of death or myocardial infarction

In patients with type 1 myocardial infarction, a total of 22% (1075/4981) and 16% (173/1080) of patients died or had a myocardial infarction at 1 year in the Scottish and Swedish cohorts, respectively. The AUC for the GRACE 2.0 model incorporating death or future myocardial infarction was 0.76 (95% CI 0.74–0.77) and 0.81 (95% CI . 0.77–0.85), respectively.

In patients with type 2 myocardial infarction, there were 27% (297/1121) and 26% (63/247) deaths or myocardial infarctions at 1 year. Here, the GRACE 2.0 score gave an AUC of 0.70 (95% CI 0.67– . 0.74) and 0.72 (95% CI 0.65–

0.80), respectively (P = 0.007 and P = 0.042 vs. type 1 myocardial infarction). Calibration plots showed the GRACE 2.0 model underestimated future risk in type 1 and type 2 myocardial infarction in both cohorts. (Appendix Figure 7-1).

Post hoc analysis

In a post hoc analysis, the GRACE 2.0 score had better discrimination for in-hospital death in patients with type 1 compared to type 2 myocardial infarction, where performance was moderate (Appendix Table 7-5). When applied as a continuous variable, both hs-cTnI and hs-cTnT were moderate predictors of all-cause death at 1 year (Appendix, Table 7-6)

3.4 Discussion

We evaluated the performance of the GRACE 2.0 score for the prediction of all-cause death, and all-cause death or myocardial infarction in consecutive patients with type 1 and type 2 myocardial infarction from two independent cohorts across two countries. We observe that the GRACE 2.0 score provides good discrimination for all-cause death in patients with type 1 myocardial infarction diagnosed using hs-cTn assays and for both cardiac troponin I and T. Consistent with the original validation study (215), discrimination for all-cause death was better than for death or myocardial infarction. In patients with type 2 myocardial infarction, the GRACE 2.0 score provided moderate discrimination in the prediction of all-cause death and performed less well in the prediction of all-cause death or myocardial infarction. As the GRACE 2.0

score performed better in patients with type 1 myocardial infarction, there may be opportunities to develop a bespoke model for risk prediction in patients with type 2 myocardial infarction.

The GRACE 2.0 score was derived prior to the publication of the first Universal Definition of Myocardial Infarction (71), which introduced a classification based on the underlying mechanism. Whilst type 1 myocardial infarction is caused exclusively by atherosclerotic plaque rupture and thrombotic coronary artery occlusion, type 2 myocardial infarction is a heterogeneous condition, occurring due to an imbalance in myocardial oxygen supply or an unmet need in myocardial oxygen demand in the context of another acute illness. A type 2 myocardial infarction may occur due to coronary pathology such as vasospasm, spontaneous dissection or coronary embolism, or with bystander stable coronary artery disease or normal coronary arteries in the context of tachyarrhythmia, severe hypoxia or hypotension. Whilst we have a strong evidence base for treatments which reduce all-cause mortality and future cardiovascular events in patients with type 1 myocardial infarction, at present, we have no guidelines to support investigation or management of patients with type 2 myocardial infarction, and in these patients clinical outcomes are worse, with as few as 30% of patients alive at 5 years(223-228).

We recently demonstrated future cardiovascular risk was increased in all patients with myocardial injury and infarction, irrespective of diagnostic classification, despite a vast excess in non-cardiovascular death in patients without type 1 myocardial infarction. Patients with type 2 myocardial infarction

were at almost four-fold increased risk of cardiovascular events relative to those without myocardial injury. This risk appears to be highest in those with a history of prior coronary artery disease, suggesting underlying coronary atheroma may at least in part be driving future cardiovascular risk (229, 230). In order to identify patients with type 2 myocardial infarction who may benefit from further investigation and treatment, accurate risk stratification is required.

In this analysis, we demonstrate the GRACE 2.0 score performed well in the prediction of all-cause mortality and future cardiovascular events in patients with type 1 myocardial infarction, but discrimination was lower in those with type 2 myocardial infarction. At the time the GRACE score was derived, the diagnosis of myocardial infarction was based on contemporary cardiac biomarkers with a diagnostic threshold at least 10-fold higher than advocated in current guidelines (74). The subsequent increase in sensitivity of cardiac troponin led to a reduction in the diagnostic threshold, and an increase in the recognition of myocardial injury and infarction in other conditions (222). A number of studies indicate a phenotypic distinction between patients with type 1 and type 2 myocardial infarction(222-229, 231) Those with type 2 myocardial infarction are older, more often female, with lower haemoglobin and impairment in renal function. The GRACE 2.0 score was not derived in these patients, and although we found its performance to be acceptable with an AUC of 0.72 for all-cause death, it is perhaps not surprising it performed less well when compared with type 1 myocardial infarction.

Some attempts have been made to derive risk stratification tools in patients with type 2 myocardial infarction. The TARRACO risk score was derived in 611 patients with type 2 myocardial infarction and myocardial injury (230). This score applies troponin concentrations from a contemporary sensitive assay and the covariates age, hypertension, dyspnoea, anaemia, and the absence of chest pain and had moderate discrimination for future major adverse cardiovascular events (AUC 0.74, 95% CI 0.70–0.79). However, in a recent direct comparison of the GRACE, TIMI, and TARRACO scores in 359 patients with type 2 myocardial infarction from a single tertiary cardiac centre, only the GRACE score was predictive of all-cause mortality at 90days (AUC 0.70, 95% CI 0.63–0.77), performing better than the bespoke TARRACO score (AUC 0.52, 95% CI 0.46–0.58) (230, 231).

Analysis of the calibration of the GRACE 2.0 model in type 1 and type 2 myocardial infarction identified underestimation of risk across all outcomes. This likely reflects differences between the population of consented patients recruited into the GRACE registry, and the consecutive patient cohort evaluated here. There are a number of potentially important comorbidities not included in the GRACE 2.0 score which are common in clinical practice and could influence survival, particularly in those with type 2 myocardial infarction. These include atrial fibrillation, chronic obstructive pulmonary disease, heart failure, malignancy, dementia, and frailty. Furthermore, as suggested in a post-hoc analysis, incorporating troponin concentration as a continuous variable could offer improved performance. Whether the inclusion of absolute troponin

concentration, comorbidities or additional covariates, such as haemoglobin concentration, could improve model performance requires exploration.

Given that implementation of hs-cTn assays has been shown to increase recognition and the prevalence of type 2 myocardial infarction, there is an urgent and unmet need to improve risk prediction in these patients. Until bespoke risk prediction tools are available for patients with type 2 myocardial infarction, the GRACE 2.0 score allows identification of patients at increased risk of death, both in-hospital and at 1 year. This may be helpful to guide clinicians when reviewing patients with type 2 myocardial infarction and deciding who may benefit from more intensive monitoring or further investigation for underlying coronary disease. We observed lower prescription rates for secondary prevention therapy in patients with type 2 myocardial infarction. This was most evident in those classified by GRACE as low- or intermediate risk, where rates of prescriptions for new anti-platelet or statin therapies in type 2 myocardial infarction were half those of type 1 myocardial infarction, and outcomes were worse. In those classified as high risk, prescription rates and outcomes between patients with type 1 and type 2 myocardial infarction were similar. Whether secondary prevention therapy in patients with type 2 myocardial infarction will improve clinical outcomes requires evaluation in prospective trials (222).

We acknowledge some limitations. Firstly, whilst the GRACE 2.0 score was derived and validated across 14 countries, we only evaluate performance in Scotland and Sweden. However, we included consecutive patients across two

different healthcare systems using different high-sensitivity troponin assays and found consistent results. The consistency in results was evident despite differences in the original study design and in the selection of patients between the two healthcare sites. Second, whilst we adjudicated all diagnoses according to the latest Fourth Universal Definition of Myocardial Infarction using all available clinical information, we acknowledge that diagnostic misclassification is possible. In the Scottish cohort, where there was consensus amongst the adjudication panel that there was insufficient clinical information to make a definitive diagnosis because of missing admission or discharge letters, we did not attempt to adjudicate the diagnosis. Third, where information on covariates required for calculating the GRACE score was missing this was determined to be at random, and to minimize bias we applied multiple imputation. As data were missing in patients with type 1 and type 2 myocardial infarction in equal proportion, and we observed consistent performance in a sensitivity analysis restricted to the dataset where complete case data were available, we do not think this impacted on the results observed. Fourth, we acknowledge that our analysis of in-hospital events was post hoc and is limited by a small number of events. Finally, we acknowledge that the rates of coronary angiography were lower here than in other registries or clinical trials of selected patient populations (232, 233). We enrolled all consecutive patients in both cohorts, where older patients with comorbidities managed out with the coronary care unit were included rather than excluded. This improves the generalisability of our findings, and whilst angiography is not required for the diagnosis of myocardial infarction, lower rates may have

contributed to diagnostic misclassification and influenced performance of the GRACE 2.0 score.

The GRACE 2.0 score provided good discrimination for all-cause death at 1 year in patients with type 1 myocardial infarction, and moderate discrimination for those with type 2 myocardial infarction. Until specific risk prediction tools are derived and validated, clinicians should consider applying the GRACE 2.0 score to guide prognosis and subsequent management in type 2 myocardial infarction.

Further Study

Future work to derive a bespoke risk stratification score for type 2 myocardial infarction may allow more accurate risk prediction, and allow clinicians to treat patients accordingly. At present, those in low and intermediate risk groups according to GRACE have worse outcomes in type 2 MI than type 1, and there is a marked discrepancy in the medications prescribed. Further work must define new parameters to better predict outcome in type 2 MI, and novel or adapted risk scores may incorporate known parameters such as troponin or frailty. Both are already known and utilised as predictors of outcome and could improve the predictive strength of risk-stratification scores.

Pathways for diagnosis of type 2 MI are in their naissance, and the Fourth Universal Definition of Myocardial Infarction now incorporates an element of subjectivity when determining if there has been a supply / demand imbalance. Troponin and other indices of myocardial damage are not specific to ‘type’ of MI, whereas a biomarker that is specific to plaque rupture would enable discrimination from other types, and allow clinicians to employ the most appropriate treatment strategies.

Treatment of type 2 myocardial infarction remains highly variable and remains an area where further evidence is required to determine the most appropriate invasive and pharmacological strategies. In many cases of type 2 MI, the most important intervention is to treat the underlying cause, such as in cases of anaemia or sepsis for example. However, the high rates of coronary artery disease in type 2 MI patients suggests that interventions and medications to

quiesce and improve the coronary vasculature may yield improved outcomes. Further study is needed to define the profile of type 2 myocardial infarction patients, particularly with respect to coronary artery disease and the potential benefit of treatment with aspirin, statins, beta blockers and ace inhibitors. Further study should help to guide clinicians as to which patients should undergo and invasive strategy, and which would be better managed conservatively.

Chapter 4 Results – RNA-sequencing validation and lncRNA selection

4.1 Introduction

RNA sequencing is a well-established transcriptome profiling approach which has been used to great effect to study the transcriptome of eukaryotic and prokaryotic organisms. Using high-throughput 'next-generation sequencing' (NGS) technology provides accurate, quantitative data, describing the relative abundance of each transcript and its isoforms in a given sample (234, 235). The increased depth and resolution this platform provides allows not only more accurate quantification than the previous 'Sanger' or micro-array hybridisation based technologies, but also allows discovery of novel transcripts, alternatively spliced genes, and detection of allele specific expression (236).

Total RNA is isolated from each sample, converted into cDNA, then used to prepare a RNA sequencing library which involves selection of the RNA population of interest. Ribosomal and other small RNAs can account for more than 95% of the total RNA sample, hence it is important to either positively or negatively select out these transcripts to ensure adequate read-depth of the remainder of the sample, if that is where the interest lies. Polyadenylation selection is useful for study of mRNA, but perhaps less useful for non-coding RNAs when only around 16% may be polyadenylated. In this case, ribosomal depletion is more likely to ensure a representative library of the non-coding transcriptome (237).

4.1.1 RNA-sequencing of carotid artery plaque

The starting point for novel long non-coding RNA discovery was to utilise the output of a previously conducted RNA-sequencing experiment from our laboratory in human carotid atherosclerotic plaque. Plaque samples were obtained from patients undergoing clinically indicated carotid endarterectomy for stroke or transient ischaemic attack (TIA), and dissected into ‘stable’ and ‘unstable’ regions for comparison of RNA transcriptome by RNA-sequencing (238). Each patient had undergone 18F-NaF and 18F-FDG positron emission tomography combined with computed tomography scans to demonstrate plaque instability before surgery and had signs and symptoms consistent with a cerebrovascular event, most likely resulting from ischaemia caused by embolisation of plaque material to a cerebral artery. Each of the 4 patients’ plaques was macroscopically divided into ‘stable’ and ‘unstable’ sections, giving 2 groups of 4 matched samples. Patient 1 having donated a stable and unstable section, patient 2 the same etc (Figure 4-1). High-depth Illumina RNA sequencing was performed, with poly-A enrichment for library preparation.

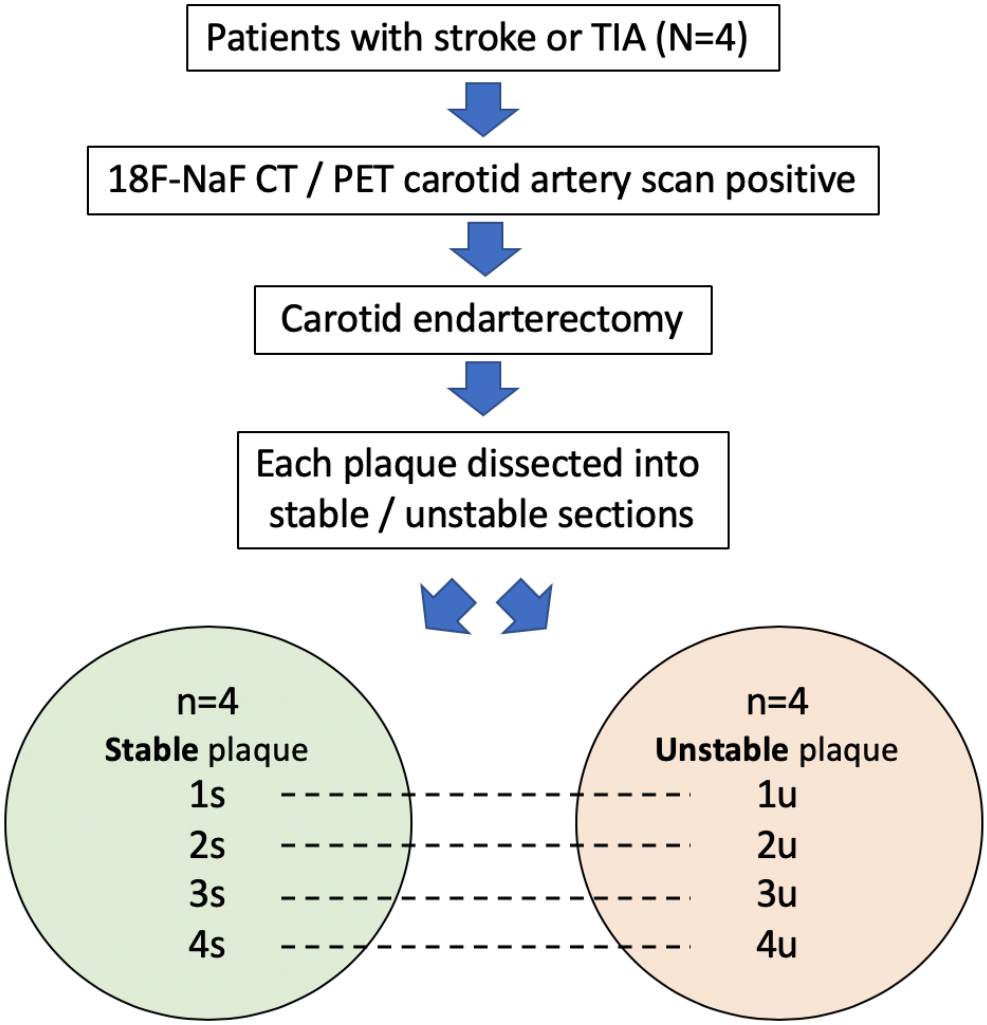

Figure 4-1: RNA sequencing design
Patients with stroke / TIA who had positive 18F-NaF CT/PET and underwent carotid endarterectomy. Plaques were dissected into stable and unstable sections, resulting in 4 paired samples

4.2 Aims

- RNA sequencing validation
- Analyse RNA sequencing data to shortlist interesting lncRNAs
- Preliminary characterisation of candidates

4.3 Results

4.3.1 18FNaF Micro PET/CT

Ruptured plaques typically demonstrate disruption of the fibrous cap and haemorrhage into the lipid core on a macroscopic level (239), features which had enabled dissection of the plaques into what were defined as ‘stable’ and ‘unstable’ regions.

To further validate this approach, fresh endarterectomy specimens were harvested and dissected in the same manner as before (Figure 4-2) and subjected to 18FNaF Micro PET/CT imaging (Figure 4-3).

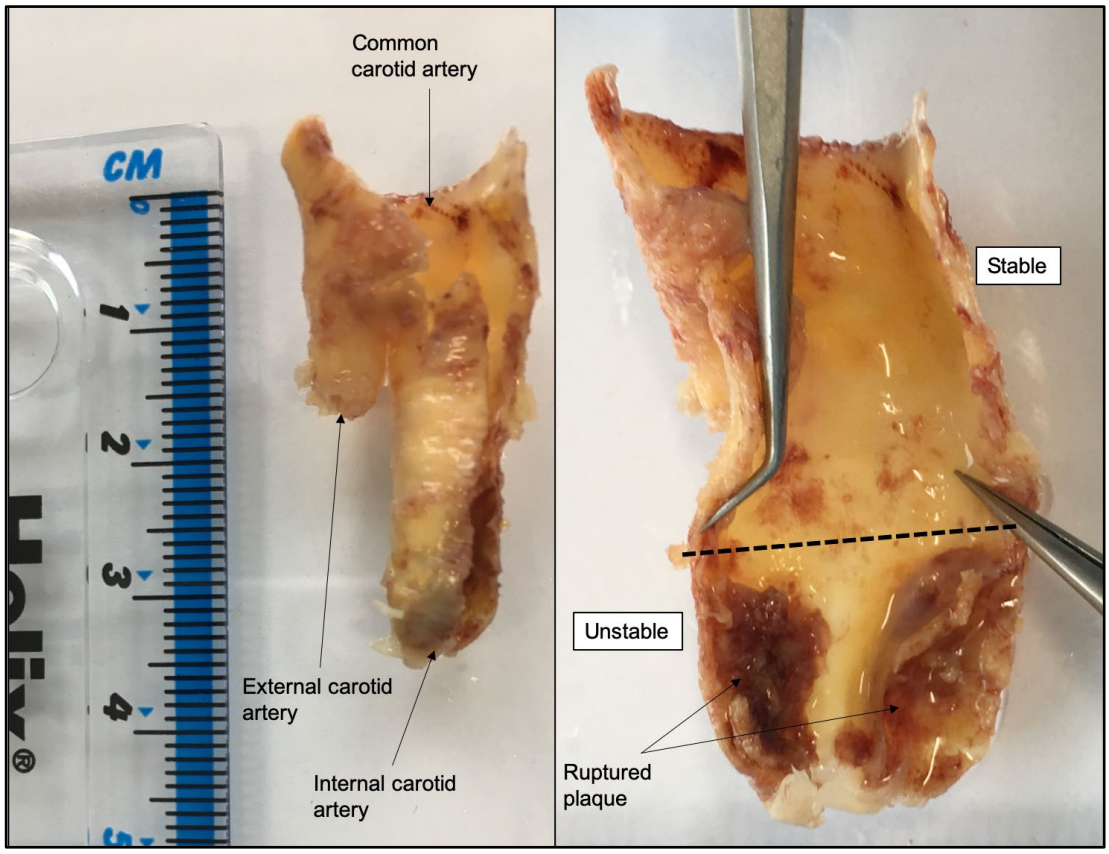

Figure 4-2: Carotid plaque dissection.

Atherosclerotic plaque specimens harvested at carotid endarterectomy were dissected into ‘stable’ and ‘unstable’ regions. ‘Unstable’ regions are characterised by disruption of the fibrous cap, and intraplaque haemorrhage. The surrounded relatively healthy areas were considered ‘stable’.

Unstable plaques are easily identified by the constellation of luminal encroachment of the plaque with evidence of fibrous cap disruption and red discolouration resulting from intraplaque haemorrhage. Although adjacent areas cannot be described as truly “healthy”, in relative terms these areas are best described as ‘stable’ plaque.

Imaging with PET/CT and the tracer 18F-NaF has been shown to identify and localise high risk and ruptured plaques in patients with carotid and coronary atherosclerosis (240-242). When used in ex vivo specimens on a microscopic level, it can also accurately detect areas of active calcification (243).

Images of plaques excised as described above demonstrate that 18F-NaF uptake it observed at sites of active calcification, in what would be determined as the unstable regions. There was no tracer uptake observed in ‘stable’ regions.

This additional ex vivo validation step confirms that the macroscopic method used previously to generate phenotypically distinct groups of samples is likely to be representative of ‘stable’ and ‘unstable’ atherosclerotic plaque.

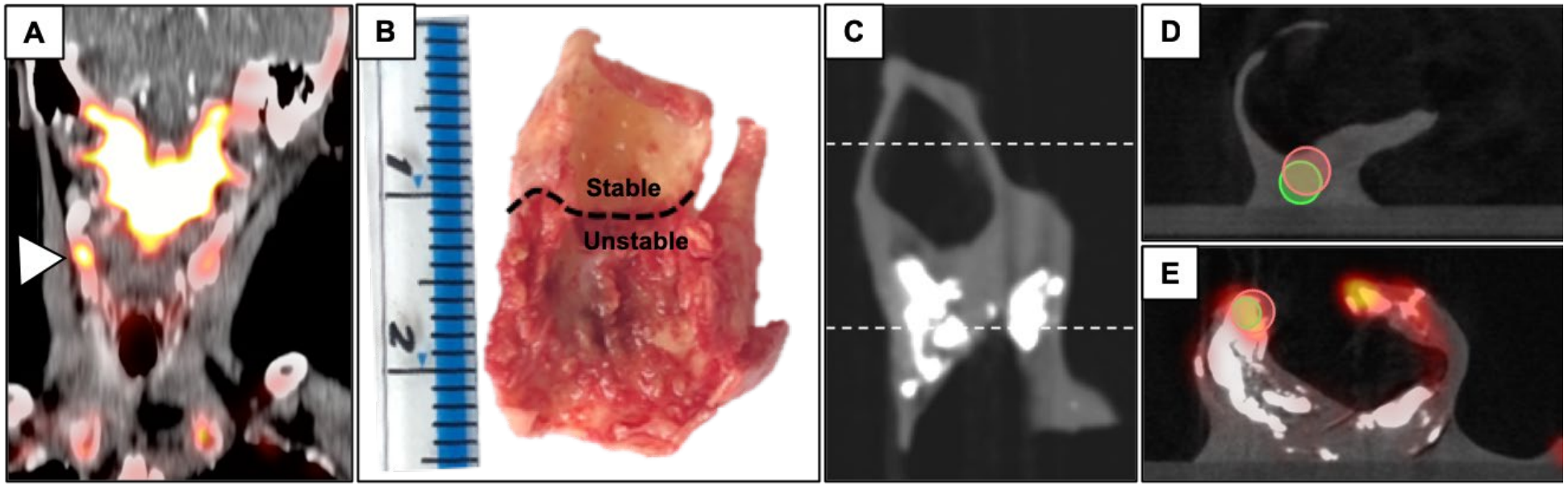

Figure 4-3: Micro CT/PET of human atherosclerotic plaque.

(A) Positive 18F NaF CT/PET scan in patient with stroke, white arrow: high fluoride uptake in right common carotid artery. Plaque tissue excised during carotid endarterectomy (B) divided macroscopically into unstable and stable regions. Ex-vivo micro CT/PET demonstrates calcification in unstable region (C), low uptake of radio tracer in stable region (D), and high uptake of tracer and heavy calcification in unstable region (E).

4.3.2 Bioinformatic validation

Before in-depth analysis of the RNA-sequencing data is undertaken it is possible to demonstrate similarities and differences in the clustering of genes from each patient sample using *principle component analysis*.

Visualisation of data generated from RNA-sequencing is complex, because typically multiple levels of data are yielded from multiple patient samples, resulting in multi-dimensional results. In this case, there are 4 patients in each group, and each patient sample will result in quantification of thousands of RNA species. Broadly speaking, each sample should contain approximately the same number of different RNAs, but it is expected that each RNA will be represented in a different quantity for each sample. The precise differential levels of each of these species between the 2 phenotypic groups is ultimately what the experiment is designed to prove.

Principal component analysis is a mathematical algorithm that reduces the dimensionality of the data, whilst retaining the majority of the variation within the dataset. This simplification is achieved by identifying a few key ‘directions’ within which, most of the variation of the data is contained. In-so-doing, each sample can be represented by relatively few numbers (rather than thousands), to demonstrate gross similarities between datasets from each sample (244).

Each of these ‘principal components’ can be used to plot samples against each other. The output then demonstrates how each of the samples compare relatively, according to the variables of the identified principal components.

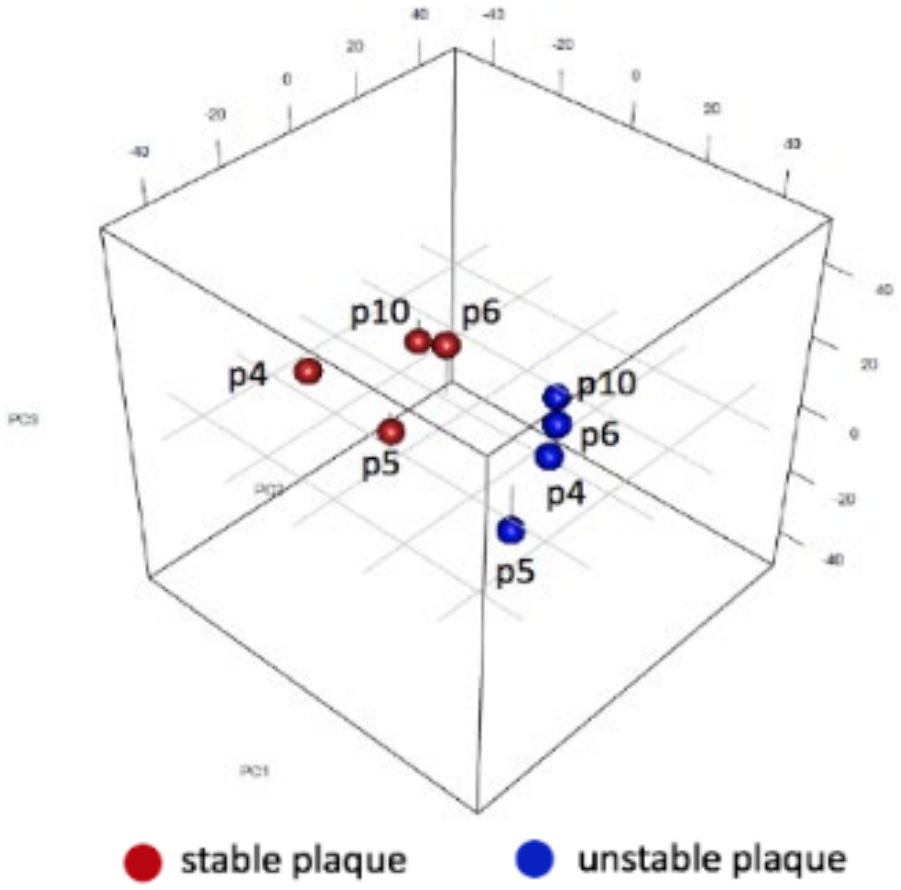

Figure 4-4: Principal component analysis of RNA-sequencing data

Stable plaque samples (red) and unstable plaque samples (blue) cluster together, indicating similarity in gene expression profiles within the groups, and differences in the principal components between the 2 groups of samples. Thanks to Dr Julie Rodor, senior scientist for contribution of this Figure.

A stable and unstable sample from each plaque was analysed resulting in 4 matched pairs. The principal component analysis demonstrates clustering of the stable samples (red) and the unstable samples (blue). This indicates mathematically that the principal components (variables where most deviation between samples exists) identified for these samples as a whole, vary most between the group of stable vs unstable samples. This result gives confidence that the method of dissection had at least yielded consistent results across plaque specimens.

4.3.2.1 RNA sequencing analysis and filtering

The carotid plaque RNA-seq identified a total of 58,037 genes, according the GRCh37 annotation of the human genome. A filtering process was then undertaken to first start to characterise the RNA population in the sample in broad terms, and second to narrow down a candidate list of long non-coding RNAs suitable for further study (Figure 4-5).

The first cut-off applied was mean FPKM > 1, resulting in 18,101 remaining transcripts. 'Fragments per kilobase million' is a normalised quantification of gene expression commonly used in RNA-seq data which is taken to approximate to 'copy number per cell'. Transcripts with a lower mean FPKM would be too low in quantity to allow their study, and less likely to be biologically important.

Of these 18,101 transcripts which were deemed to be present in sufficient quantity, only those that were differentially expressed between the stable and unstable groups were carried forwards, resulting in 1,822 transcripts. Differential expression between the conditions is a key discriminator, as this indicates some role for the transcript, whether active or passive, in the pathology (or whatever phenotypic differences exist between the groups). A lenient log2 fold change of ≤1 or ≥1 ($p<0.01$) was applied to capture transcripts which were downregulated and upregulated respectively. For the purpose of this project it should be taken that the 'stable' condition is considered to be the baseline (control) and that 'unstable' is the disease condition. Hence if a transcript is deemed to be 'upregulated', it is expressed more highly in the unstable group compared with stable.

Of the well expressed and differentially regulated genes, 1,655 (90.8%) were protein coding; 135 (7.4%) long non-coding; 30 (1.6%) pseudogenes; 2 (0.001%) small RNA.

A final filter was then applied to the long non-coding category, mean FPKM > 5, to eke out the most highly expressed transcripts amongst them. The principle again being that greater expression is likely to correlate with functionality. This resulted in 47 candidate lncRNAs.

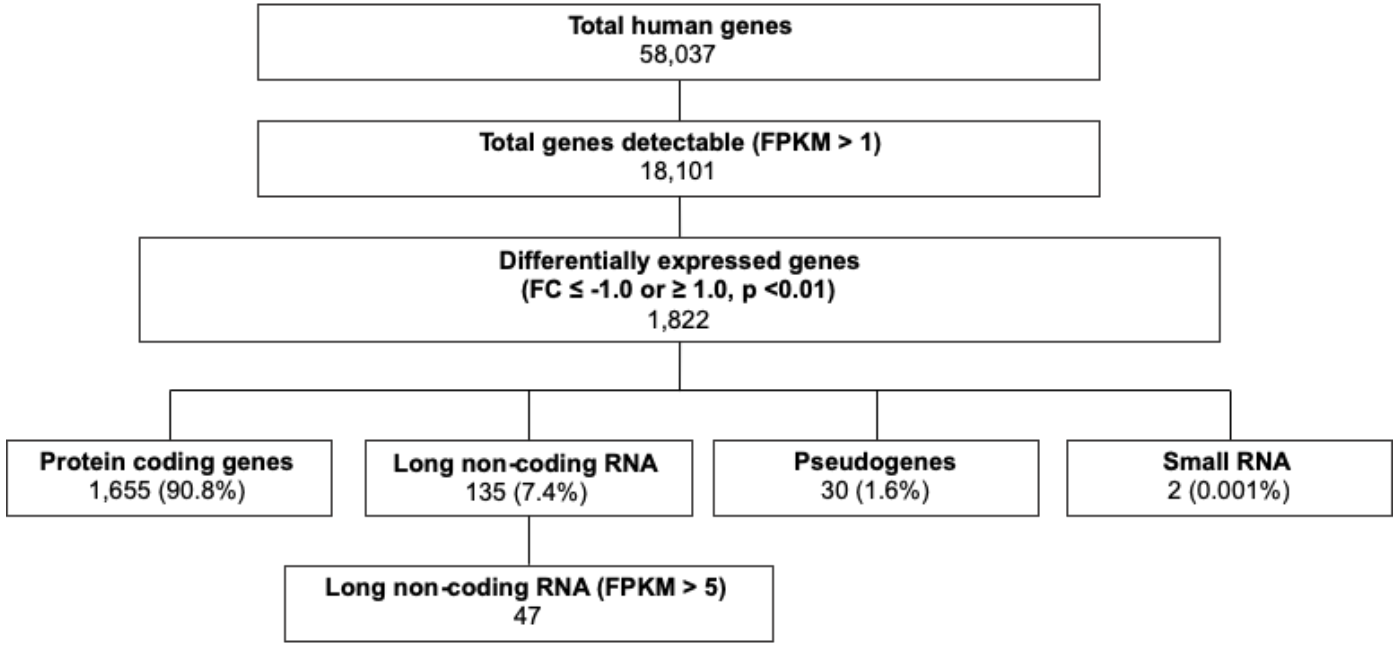

Figure 4-5: RNA seq filtering strategy.
The complete set of genes mapped to the genome were filtered by mean FPKM and differential expression to identify well-expressed / differentially expressed transcripts. They were then classified by type into protein coding genes, long non-coding RNA, pseudogenes, small RNA. Highly expressed lncRNA mean FPKM > 5 were then shortlisted for further study.

4.3.3 Protein coding gene analysis

The protein-coding gene component of the well- and differentially regulated transcripts identified is in the majority, at 90.8%. For further validation of the dataset, a panel of the most dysregulated protein-coding genes was analysed for Gene Ontology (Go) term enrichment. The top 200 terms for upregulated coding genes corresponded largely with immune system processes and inflammation (Figure 4-6), whilst downregulated genes were involved mainly in muscle system processes as expected (Figure 4-7). [http://www.geneontology.org]

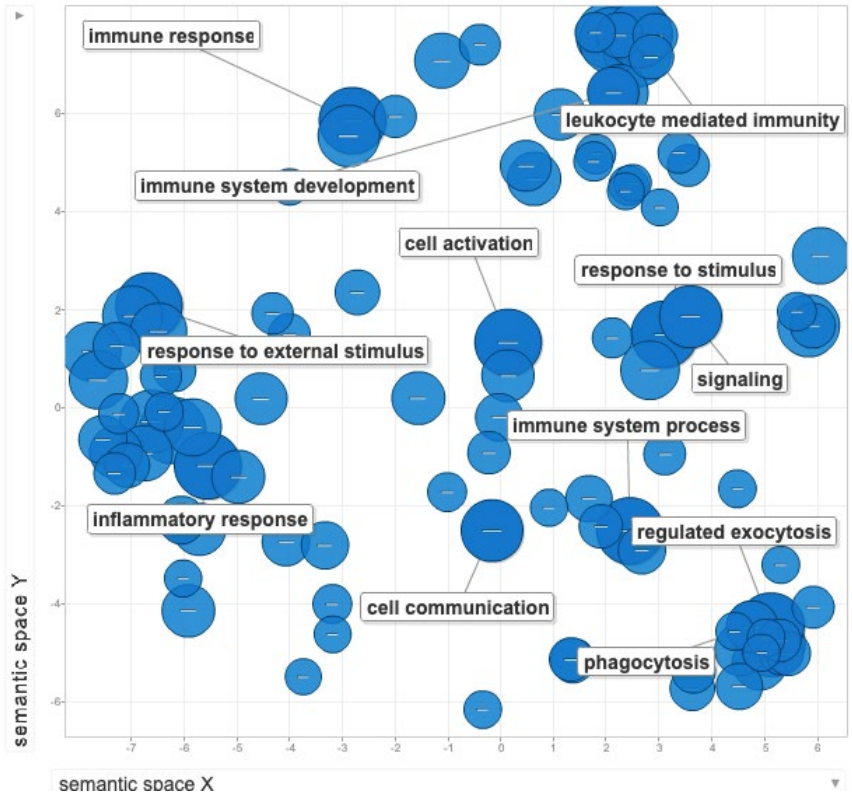

Figure 4-6: GoTerm analysis, up-regulated protein-coding genes.
Processes involved in immune response and inflammation are associated with upregulated genes

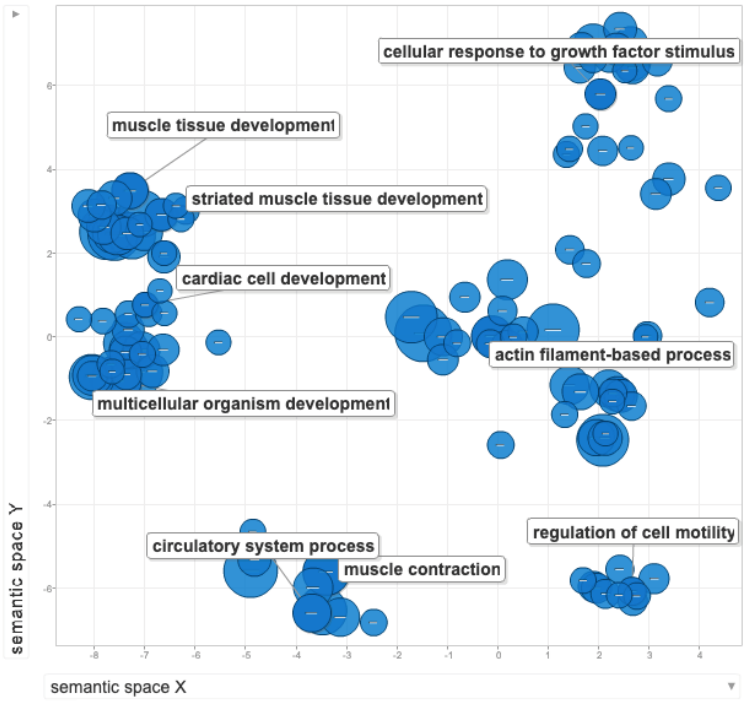

Figure 4-7: GoTerm analysis, down-regulated protein-coding genes.
Processes involved in muscle structure and function are associated with down-regulated genes

In a more selective approach, a panel of important protein-coding genes associated with key pathophysiological processes in plaque instability, which would be expected to be dysregulated were examined for differential regulation.

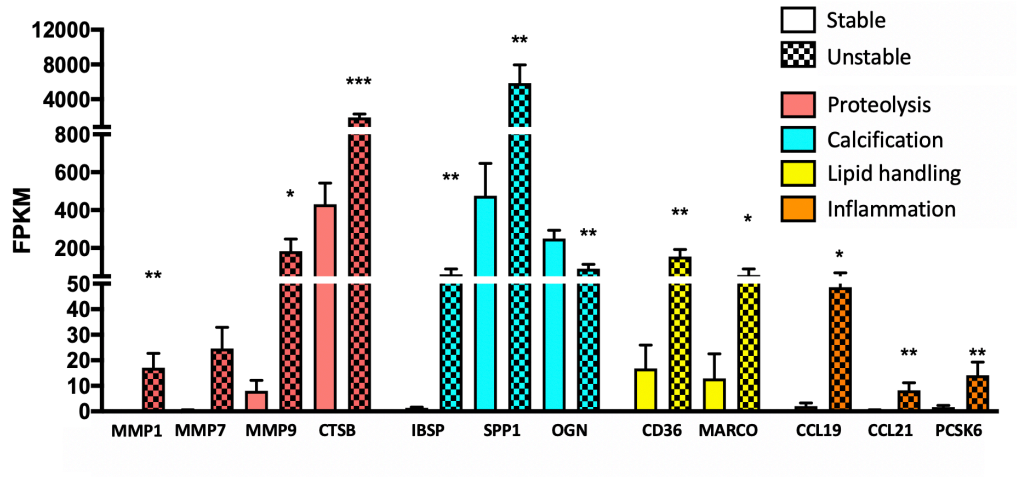

Figure 4-8: Protein coding gene expression in RNA-sequencing.
Protein coding genes associated with plaque rupture, calcification, lipid handling and inflammation are dysregulated. (n=4 paired samples, paired t-test for parametric data for statistical significance, mean (+SD), p<0.05=*, p<0.01=**, p<0.001=***, p<0.0001=****)

Matrix metalloproteinases (MMP1, MMP7, MMP9) and cathepsin (CTSB) which are genes associated with degradation of the fibrous cap were up-regulated in unstable plaque (42, 43, 245, 246).

Proteins associated with the process of active plaque calcification (IBSP, SPP1) were upregulated in unstable plaque. Osteoglycan, which has been shown to be upregulated in patients with atherosclerosis, was decreased.

There was a significant increase in the expression of lipid transport proteins (CD36 and MARCO) and also in pro-inflammatory molecules (CCL19, CCL21). PCSK6 has been strongly implicated in the degradation of the fibrous cap in symptomatic carotid plaques and was also upregulated (247).

4.3.4 Candidate lncRNAs

The shortlist of 47 lncRNAs with expression levels of mean FPKM > 5 as demonstrated in the heatmap in Figure 4-9 comprised 8 upregulated and 39 downregulated lncRNAs. This indicates that the majority of 'well-expressed' lncRNAs are well-expressed in the stable condition, but then less so in the unstable condition.

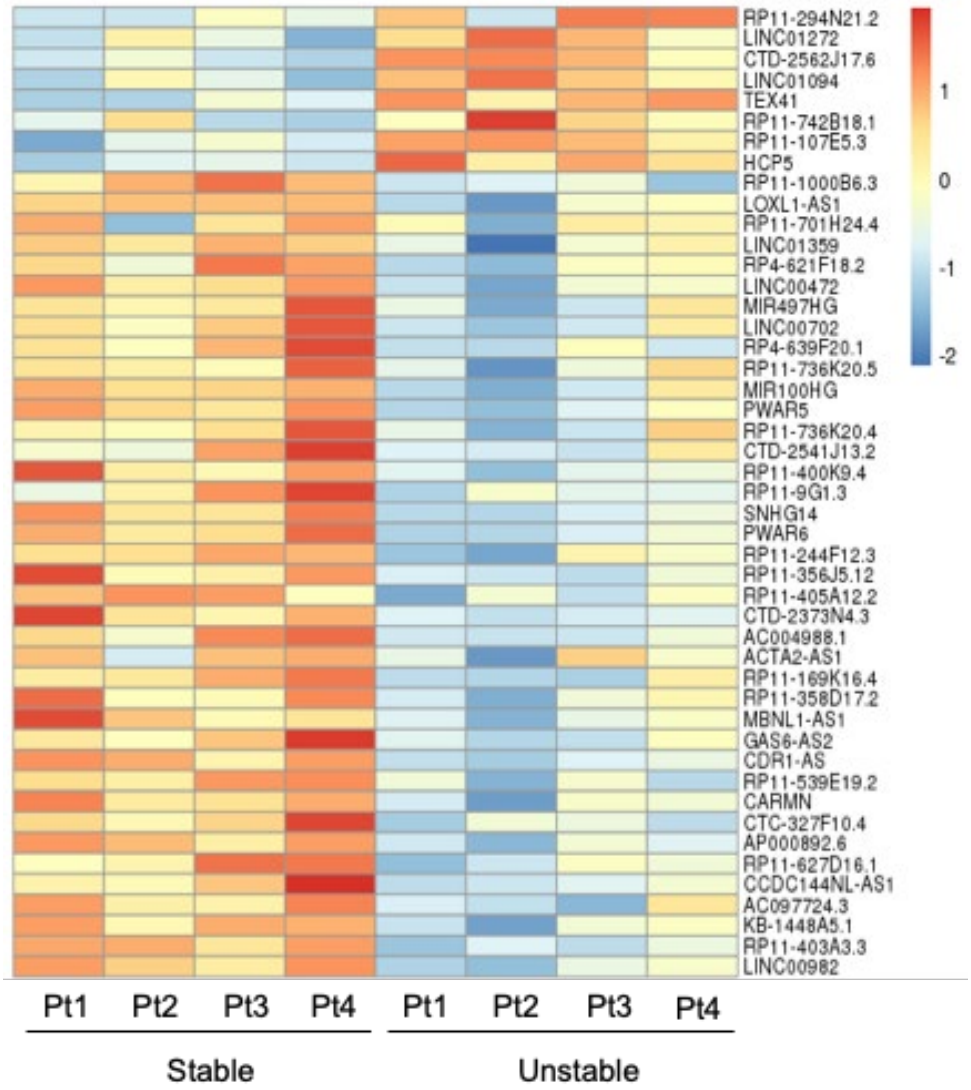

Figure 4-9: Heatmap showing differentially expressed transcripts across 4 paired patient samples.
Red through to blue colour indicates high to low expression level. Each column represents one sample, and each row indicates a transcript. Top 8 rows demonstrate mostly higher expression of genes in unstable samples compared with stable. Thanks to Dr Julie Rodor, senior scientist for contribution of this Figure.

To further narrow down the selection of candidate lncRNAs, the top 5 up- and downregulated lncRNAs were examined more closely (Table 4-1 and 4-2).

Table 4-1: Top 5 upregulated candidate lncRNAs

#	Gene ID	Gene symbol	Log^2FC	p-value
1	ENSG00000280096.1	RP11-294N21.2	+ 2.47	5.86×10^{-4}
2	ENSG00000224397	LINC01272	+ 2.23	2.36×10^{-8}
3	ENSG00000279117.1	CTD-2562J17.6	+ 1.72	3.8×10^{-13}
4	ENSG00000251442.5	LINC01094	+ 1.49	3.17×10^{-11}
5	ENSG00000226674.8	TEX41	+ 1.26	6.44×10^{-8}

Table 4-2: Top 5 downregulated candidate lncRNAs

#	Gene ID	Gene symbol	Log^2FC	p-value
1	ENSG00000233098.8	LINC00982	- 2.65	1.85×10^{-12}
2	ENSG00000275830.1	RP11-403A3.3	- 2.53	6.26×10^{-8}
3	ENSG00000253105.5	KB-1448A5.1	- 2.21	6.88×10^{-8}
4	ENSG00000226833.5	AC097724.3	- 2.13	3.76×10^{-6}
5	ENSG00000233098.8	CCDC144NL-AS1	- 2.09	1.55×10^{-11}

From this starting point with a shortlist of candidate lncRNAs, the decision on which lncRNA to study is complex and multifactorial.

A significant fold change in either direction is suggestive of an important role in pathophysiology. However, an increase in concentration in the diseased pathology does represent a more attractive prospect for study.

The top upregulated lncRNA RP11-294N21.2 had a log2FC of +2.47 and mean FPKM 65.5 in unstable plaque. However, on close inspection of the raw read mapping profile for each sample, read coverage extends outside the annotation and thus likely corresponds to background signal emanating from the nearby intron of MAPRE2 a protein coding gene (Figure 4-10).

On this basis the result was considered a false positive and RP11-294N21.2 excluded from further study.

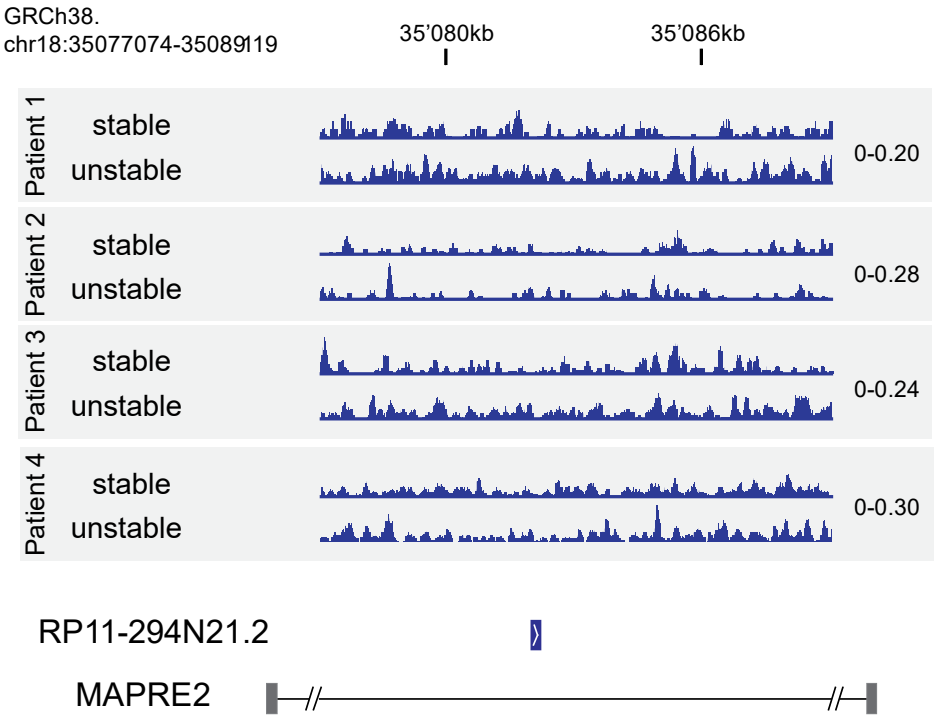

Figure 4-10: RP11-294N21.2 read coverage from RNA sequencing.
Mapped reads for RP11-294N21.2 are randomly distributed, not consistent with an exonic structure and likely emanate from the nearby protein coding gene MAPRE2, and therefore represents a false positive.

The second most upregulated lncRNA, LINC01272, was then analysed in the same way.

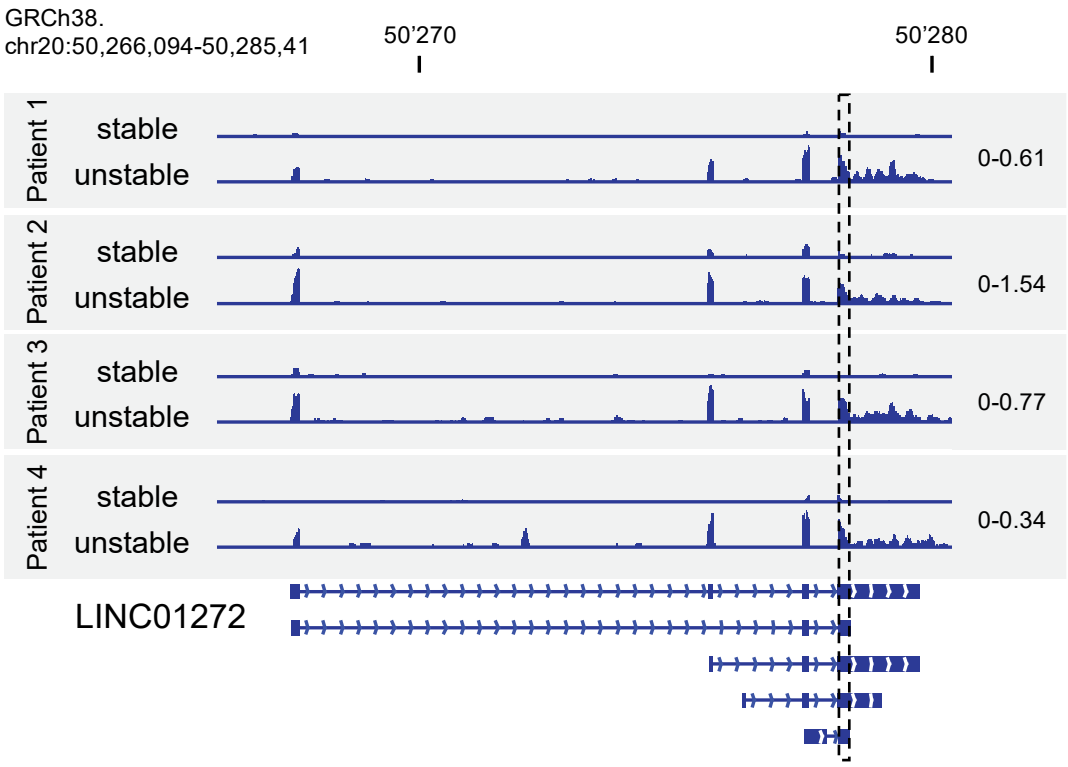

Figure 4-11: LINC01272 read coverage from RNA sequencing.
Stable vs unstable read coverage for each patient, with annotated exonic structure underneath (GRCh 38), scale to right. Thanks to Dr Julie Rodor, senior scientist for contribution to this figure.

The read profile of LINC01272 is consistent with the up-regulation in unstable plaque and shows the expression of a 4 exon-transcript, corresponding to the longest annotated isoform (203, ENST0000425497.5) (Figure 4-11). Each isoform shares a common region at the start of the final exon, which was subsequently used for primer and GapmeR design (dashed box, Figure 4-11).

One other previously annotated lncRNA 'LINC01094' was also upregulated in unstable plaque, log2FC 1.49 (p =3.17x10-11) and detected in good quantity (mean FPKM 21.8) in unstable samples.

4.3.5 lncRNA validation in plaque qPCR

From the RNA sequencing dataset, LINC01272 expression was 4.6-fold higher (log2FC 2.2) in the unstable condition (p=2.36 x 10-8, Figure 4-12).

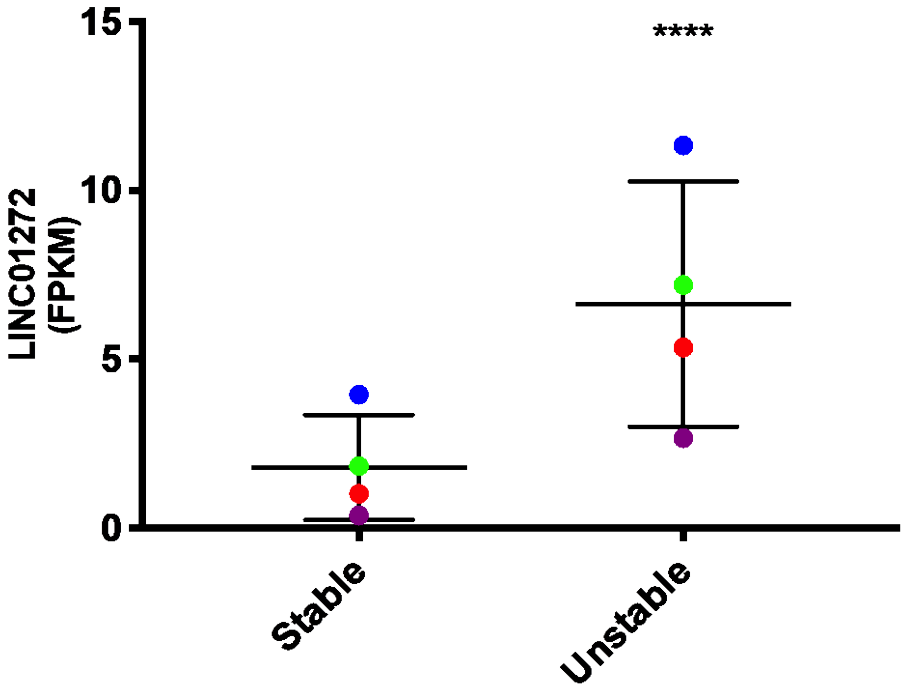

Figure 4-12: LINC01272 expression in RNA sequencing dataset (as FPKM).
Stable versus unstable plaque, p-value of 2.36x10-8 obtained using DESeq2 based on the raw read count. (Coloured dots represent each biological replicate, mean (+SD), p<0.05=*, p<0.01=**, p<0.001=***, p<0.0001=****)

This differential expression was further confirmed in a qRT-PCR validation set of 5 independently collected carotid plaque samples (Figure 4-13). Each paired sample demonstrated higher LINC01272 levels in the unstable condition, compared with stable.

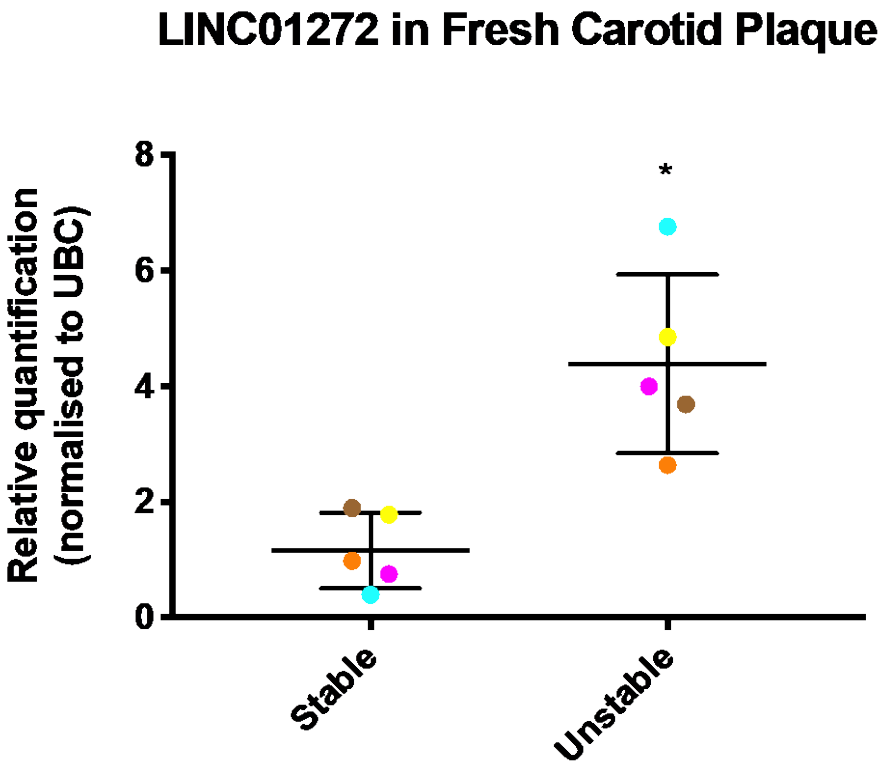

Figure 4-13: LINC01272 expression in fresh carotid plaque samples
Relative quantification of LINC01272 expression determined by qRT-PCR in additional samples of stable and unstable plaque (N=5) obtained by qRT-PCR (p=0.02, t-test, paired, two-tailed), mean (+SD), p<0.05=*, p<0.01=**, p<0.001=***, p<0.0001=****).

Similarly, LINC01094 was uniformly upregulated in the unstable condition, validating the findings of the RNA-seq.

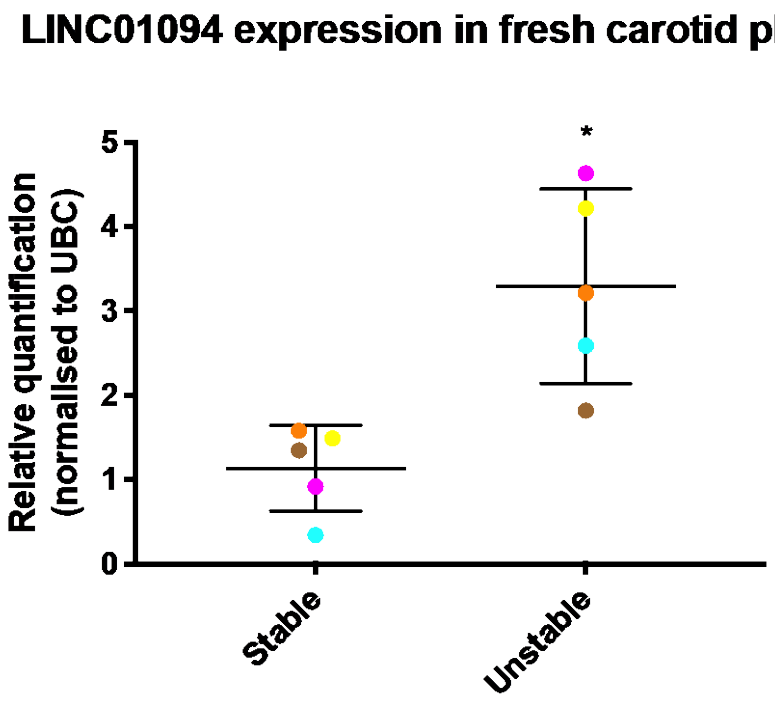

Figure 4-14: LINC01094 expression in fresh carotid plaque samples
Relative quantification of LINC01094 expression determined by qRT-PCR in additional samples of stable and unstable plaque (N=5) obtained by qRT-PCR (p=0.02, t-test, paired, two-tailed, mean (+SD), p<0.05=*, p<0.01=**, p<0.001=***, p<0.0001=****)

Novel lncRNAs in unstable plaque: **LINC01272 and LINC01094**

Both candidate lncRNAs were considered ‘novel’, having been annotated but not interrogated in any detail as to their character, role in physiology, disease, or mechanism previously. To begin to predict if a role in atherosclerosis is likely, their loci were then studied closely. Long non-coding RNA regulation of genes in *cis* is well understood to be a common mechanism by which they can exert effects on physiologic or disease processes. ‘*Cis’* is a terminology used to describe genes whose activity is based at, and is dependent on the loci from which they are transcribed (248). If protein coding genes that were already known to be important in atherosclerosis were nearby and showing signs of interaction, this would raise suspicion of a function for the lncRNA.

LINC01272 has 5 isoforms and is situated on Chromosome 20 (50,267,483-50,279,795). The locus it occupies is busy, with several interesting nearby genes (Figure 4-15):

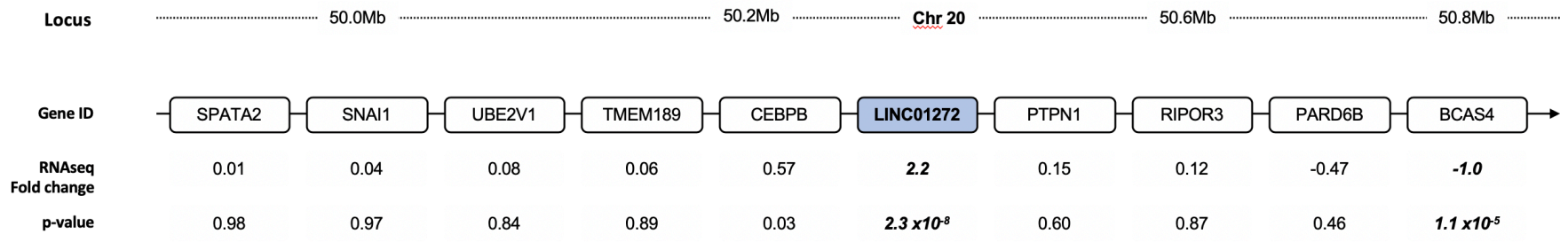

Figure 4-15: Locus of LINC01272
LINC01272 is transcribed in a 'sense' direction, from a locus with several interesting nearby genes. The RNA-seq fold change of nearby genes is denoted underneath. Only BCAS4 is significantly dysregulated in the RNA-seq.

- CEBPB situated 73kb upstream from LINC01272 has a role in macrophage inflammation by regulation of M2 activation, likely interacting with Arg1 and Il10 promoters (249-251). There was a slight but significant trend to upregulation in unstable plaque in the RNA-seq, log2FC 0.57 (p=0.03).

- PTPN situated 226kb downstream is theorised to have a role in atherosclerosis as a major regulator of insulin resistance, and has been shown to reverse atherosclerosis in mice when inhibited (252, 253). In the RNA-seq it was not significantly dysregulated, log2FC 0.15 (p=0.6).

- BCAS4 is the only gene within a 1Mb span of LINC01272 that was significantly dysregulated in the RNA-seq, log2FC -1.0 ($p=1.1x10^{-5}$). It is a gene previously characterised in the pathology of breast cancer (254).]

Due to their potential for interaction with LINC01272 these genes were later assessed for dysregulation in macrophages when LINC01272 was knocked down by GapmeR. None exhibited a significant change in expression.

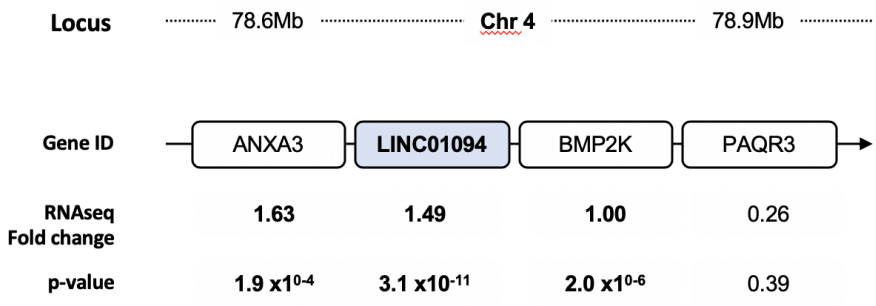

Figure 4-16: Locus of LINC01094
LINC01094 is transcribed in a 'sense' direction, from a locus with several interesting nearby genes. Both ANXA3 and BMP2K were significantly upregulated in the RNA-seq.

LINC01094 has 6 isoforms and is situated on Chromosome 4 (78,645,903-78,682,699) (Figure 4-16). Nearby genes are described below.

- BMP2K situated 94kb immediately downstream was upregulated, log2FC 1.0 ($p=2x10^{-6}$). Bone morphogenic proteins (BMPs) are growth factors that belong to the TGF superfamily. Thought to have a regulatory role in osteoblast differentiation.

LINC01272 was henceforth chosen for deeper investigation, based on its relatively higher expression, differential regulation and interesting locus.

4.3.6 Atherosclerotic cell type expression

Both the magnitude of expression, and specificity to particular cell types within the atherosclerotic plaque are critical features in ascribing the likelihood of importance to the novel lncRNAs.

A panel of relevant cell types including immune cells, smooth muscle cells and endothelial cells of multiple origins demonstrated that LINC01272 expression is very high in monocytes and macrophages, but barely expressed by other common vascular cell types (Figure 4-17).

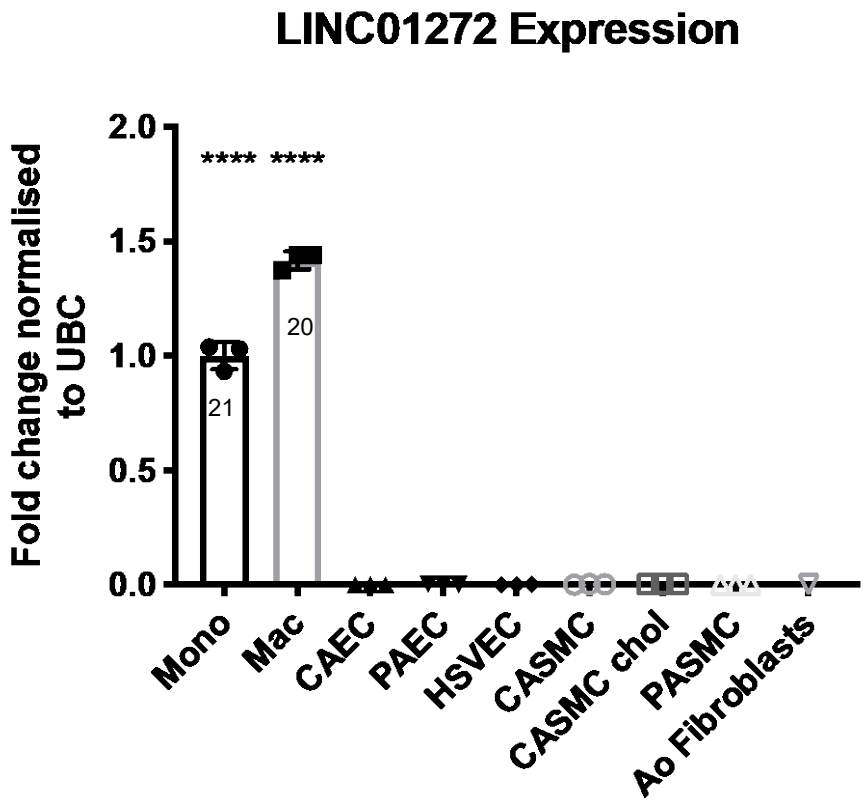

Figure 4-17: LINC01272 expression across different cell types
LINC 01272 is highly expressed on monocytes and macrophages, but not other atherosclerotic cell types. Raw CT values of 21 in monocytes and 20 in macrophages indicate a relative abundance of transcript within the sample (n=3 for each cell type, ANOVA with multiple comparisons, mean (+SD), p<0.05=*, p<0.01=**, p<0.001=***, p<0.0001=****). Mono=CD14 monocytes, Mac=monocyte derived macrophages, CAEC=coronary artery

endothelial cells, PAEC=pulmonary artery endothelial cells, HSVEC=human saphenous vein endothelial cells, CASMC=coronary artery smooth muscle cells, CASMC chol=coronary artery smooth muscle cells + oxLDL, PASMC=pulmonary artery smooth muscle cells, Ao=aortic

Human tissue expression

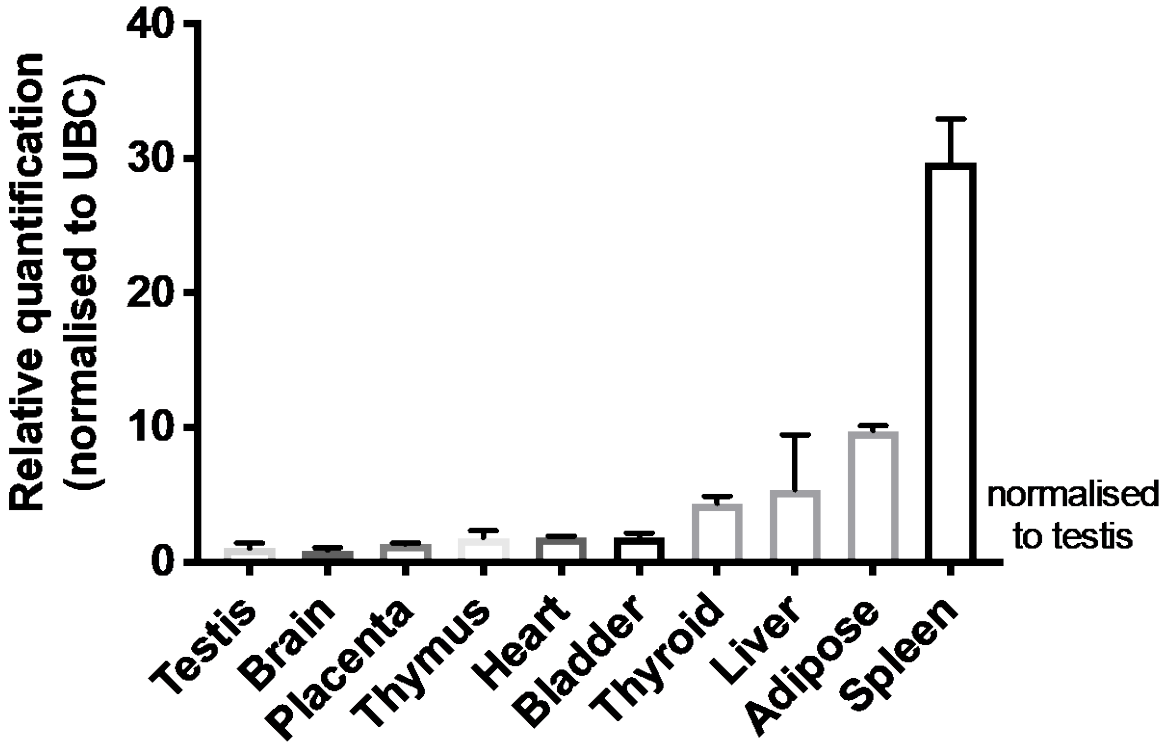

Figure 4-18: Expression of LINC01272 in human tissues
Highest expression of LINC01272 in panel of healthy human tissue was seen in adipose, liver and spleen (n=1 sample with 3 technical replicates for each, mean (+SD), p<0.05=*, p<0.01=**, p<0.001=***, p<0.0001=****)

To corroborate the finding that LINC01272 expression is specific to the circulating monocyte and monocyte derived macrophage lineage, a panel of healthy human tissue RNA was examined for relative expression by PCR.

LINC01272 expression was highest in spleen, adipose tissue and liver (Figure 2F), all macrophage-rich tissues, consistent with the cell panel findings

Expression of LINC01272 in Unstable Plaque vs Normal Aorta

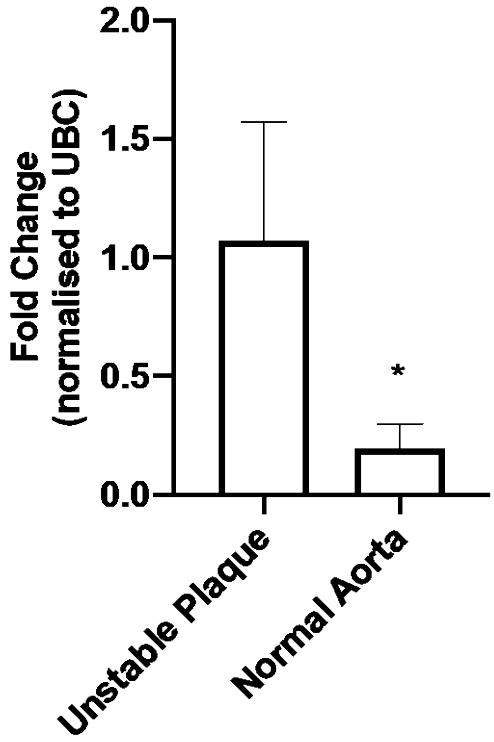

Figure 4-19: LINC01272 expression is higher in unstable plaque compared with normal aortic samples
Normal samples obtained from punch biopsy samples in otherwise normal aortic tissue, in patients undergoing coronary artery bypass grafting.
(N=3 biological replicates per group, p=0.05 by Mann Whitney test for non-parametric data, mean (+SD), p<0.05=*, p<0.01=**, p<0.001=***, p<0.0001=****).

Normal aortic tissue, without overt atherosclerosis or high-grade arterial inflammation, had significantly reduced LINC01272 expression when compared to unstable plaque. This again is consistent with most LINC01272 emanating from monocytes and macrophages, as normal aortic tissue should not contain significant numbers of these inflammatory cells.

4.4 Discussion

Using data from an existing RNA-seq experiment, it was possible to identify several novel, long non-coding RNAs upregulated in unstable atherosclerotic plaque. Several additional validation techniques then added to confidence that the experimental design and interpretation of the results of the RNA-seq were valid, and that the candidate lncRNAs ‘LINC01272’ and ‘LINC01094’ were suitable for more detailed and extensive investigation.

The paired-sample design of the RNA sequencing experiment was important in ensuring the discovery of differentially expressed lncRNAs in plaque. Using paired stable and unstable samples from the same patient overcomes the inherent variability in gene expression between human subjects, which may otherwise mask significant fold changes. This is particularly important in lowly expressed transcripts such as lncRNAs, when absolute copy numbers per cell may be lower than protein coding genes (255). Further, a high read-depth enabled accurate alignment of reads to the most recent human genome annotation (GRCh37 at time of study). Notably, lncRNAs represent a relatively small proportion of all of the differentially expressed genes (7.4%), and protein coding genes predominate (90.8%), as would be expected in these atherogenic, pro-inflammatory conditions.

Exploratory experiments that are designed in an unbiased manner such as the RNA-sequencing experiment in question inherently have an unknown and uncertain outcome. The fundamental intention of the experiment is to discover something completely new. The results therefore are by their very nature

unexpected and have no precedent to compare with. Naturally this approach carries risk. Scientifically speaking, there is no control measure that can be employed to ensure that the results are true beyond any doubt. There is no gold standard that can be prospectively deployed to compare with. Hence, it might not be possible in the first instance to know conclusively that the “novel findings” of such an experiment are a true representation of the actual biological situation, or merely a quirk of experimental design, or an anomaly or outlier because of an unknown variable or experimental factor not accounted for. It has to be thus, otherwise discovery could never occur.

In the current example, the information already known includes some species of long non-coding RNA which have already been annotated by others. There are limited data on these lncRNA indicating their abundance and function in certain atherosclerotic environments. However, as this field is in its infancy, there should still be a healthy amount of scientific apprehension applied to much of this knowledge, and the contribution from the given experiment may be as, or more valid.

To mitigate the risk of over- or under-interpretation of this exploratory RNA-sequencing experiment a number of additional validation measures were performed to confirm that the experimental design at least ensured that the input had been appropriate, and that the output, whatever it showed could be regarded as reliable.

Gene Ontology analysis of the most dysregulated protein coding genes provides further validation of the RNA-sequencing output, demonstrating an increase in terms related to inflammatory and immune processes in the unstable tissue, whilst muscle cell processes were down (Figure 3-6 and 3-7). Though these groupings are typically broad, a reduction in the smooth muscle fibrous cap is characteristic in plaque instability, as is enhanced infiltration by inflammatory cells (239, 256).

Following the logical short-listing process by filters of expression levels and dysregulation (Figure 4-5) the decision on which lncRNAs to pursue with an in-depth investigative strategy is critical, as it is an expensive, time-consuming and risky exercise. Although the RNA-seq demonstrates species that are differentially regulated between the two experimental conditions, the relationship at this stage represents merely an association. In fact, their up- or down-regulation could well reflect a distant and unrelated process; or that they are only passengers rather than drivers in a large and complicated milieu of undiscovered interactions. Further to this, even if a biologically important novel species is taken forwards, it may prove too difficult to validate experimentally or just open up a new direction which is outside of the usual expertise of the investigating scientist.

LINC01272 and LINC01094 were therefore chosen based on both the hard evidence of their existence and expression in unstable atherosclerotic plaque and on presumed biological significance. Specifically, their relatively high expression (compared to other lncRNAs); seemingly relevant protein coding

genes at their loci; and preliminary minor prior knowledge from the literature demonstrating their previous identification, and a suggestion of biological importance in relevant diseases. Whilst neither of the 2 candidate lncRNAs had previously been characterised in any detail, both had been identified in RNA profiling experiments. Although the objective of the present study was to identify 'novel' RNA species, the presence of some prior acknowledgement of the transcripts' existence can be taken as minor experimental proof of their veracity, over and above a false positive result from the RNA-seq.

LINC01272 had in fact been known by several identities. In a study of gastric cancer and tumour tissue it was found to be up-regulated compared to healthy controls and had been termed "GCRL1" (although initially named RP11-290F20.3). In vitro experiments had subsequently shown it was capable of acting as a sponge, post-transcriptionally sequestering miR-885-3p, which affected cellular proliferation (257). A different study by Wang et al. aimed at identifying biomarkers of inflammatory bowel disease (IBD) had also earmarked LINC01272 and several other lncRNAs as potential candidates. They too had demonstrated up-regulation of LINC01272 and KIF9-AS1 in plasma and tissue of patients in the disease condition compared with healthy controls (258). No further characterization was undertaken. To be clear at this point, such experiments confirm *only* an association, without any suggestion of biological mechanism or any substantive evidence of a *cause and effect* relationship at all. However, whilst acknowledging the possibility of chance, the involvement of LINC01272 in atherosclerosis, another disease process associated with inflammation was in-keeping with the best evidence to hand.

Comparatively high expression of LINC01272 was found in monocytes and macrophages compared to other cell types (Figure 4-17). This panel includes a range of smooth muscle and endothelial cells, but is limited in that other immune cells such as T-cells, B-cells and other dendritic cells, or fibroblasts are not represented. It is possible that LINC01272 is also well expressed in these other species of immune cells, and this would warrant further investigation. Cycle threshold values were quite high in all of the endothelial and smooth muscle cell types tested however, which is consistent, and does not rule out expression of the transcript in these cells, but suggests it would be very lowly expressed, if at all. It should also be noted that these cells *in vitro* are not subject to the regulation and 'cross-talk' that they would be *in vivo*, which would also be likely to affect their expression levels.

However, enrichment in monocytes and macrophages is in keeping with previous data, which has shown upregulation in inflammatory bowel disease tissue (258), and also with the higher expression levels seen in human tissues with high levels of immune cells within (Figure 4-18). The human spleen which demonstrates highest expression is a reservoir for immune cells, with the purpose of filtering blood for ageing red blood cells, pathogens, and regulating the immune response. Large populations of macrophages reside in the red pulp of the spleen, whereas white pulp is generally restricted to T-cells, B-cells and dendritic cells (259). The liver is known for a large population of resident macrophages (Kupffer Cells), comprising around 80-90% of the body's fixed macrophages (260); and adipose tissue hosts large fractions of macrophages involved in adipose cell inflammation (261).

Cell type specificity is a characteristic of lncRNA which may be advantageous in their use as biomarkers and in therapeutics (98). Off-target effects of therapies can then be prevented or limited, and changes in expression may be more attributable to the cell type or tissue in question. With the above evidence of LINC01272 enrichment in monocyte and macrophages, this cell line was then selected for the cell model to conduct further experiments in. It cannot be confirmed by these data that these are the only cells LINC01272 is well-expressed in, as other immune cells lines have not been investigated, however, it is a commonly used cell line, with established protocols, known to be critically important in atherosclerosis.

Limitations

Although the RNA-sequencing experiment design is now shown to have been appropriate, a limitation of this approach was in defining what is ‘stable’ and what is ‘unstable’. Due to the macroscopic method of carotid plaque dissection by eye, it was critical to retrospectively analyse both the validity of the technique used for input, and the quality of the data output from the RNA-seq.

The micro-CT/PET scans provide reassurance that fresh carotid plaques which were harvested and dissected in the same manner did exhibit the expected distribution of 18F-NaF uptake in ‘unstable’, and much less so in the ‘stable’ sections (Figure 4-3). As the radiolabelled sodium fluoride is absorbed by actively calcifying cells, it is possible to identify these areas of active micro-calcification, which are the hallmark of a developing plaque (241). Additionally, each of these sections were bordering the site of a visually and clinically

evident plaque rupture, which had led to symptoms of stroke or TIA. Hence, this tissue can be considered ‘unstable’ by definition, having been identified as such after the defining event had occurred. The surrounding tissue, which demonstrated less or no active micro-calcification on micro CT/PET and had been visually ‘normal’ to inspection at the time of dissection was considered ‘stable’. These areas were not haemorrhagic macroscopically, were less thickened, and represent the border regions of the plaque. In the absence of micro-calcification and intra-plaque haemorrhage, these sections were considered ‘stable’, although because histological confirmation was not available, it is not possible to know the stage of plaque development beyond “normal” tissue.

In the context of a comparative experiment, it was necessary to divide the plaques into these two phenotypically distinct groups based on the subjective criteria described. Whilst there are multiple other ways of defining what constitutes unstable atherosclerosis, including histological assessment ex vivo which would be the gold standard method, it is essential that during whatever process used that the RNA in the plaque was not degraded. Once excised from the artery, RNA within plaque degrades rapidly, particularly long non-coding RNAs which are less stable. Whilst measures can be taken to preserve the RNA as much as possible, such as rapid freezing with liquid nitrogen and temporary storage in RNA Later® solution, some degradation is accepted. It wouldn’t be technically feasible therefore to histologically examine specimens for dissection, nor was it possible to scan with radiotracers first.

It was henceforth reassuring to bioinformatically demonstrate that the ‘stable’ and ‘unstable’ groups were broadly dissimilar from each other, and transcriptionally similar between samples within group, using principle component analysis (Figure 4-4). On deeper assessment of genes within the groups it became apparent that protein coding genes were regulated appropriately to the condition and in-line with sodium fluoride imaging, with inflammatory and calcification genes upregulated in ‘unstable’, and smooth muscle genes upregulated in ‘stable’ plaque.

With these limitations considered, there are then several other reasons that LINC01272 could be upregulated in unstable plaque RNA. The proposition in the first place is that monocytes and macrophages within the unstable plaque express the transcript more highly than their counterparts in stable plaque, due to an as-yet undiscovered reason related to their role in plaque instability. This is plausible, and seems likely based on pre-existing literature, but two alternative hypotheses must be borne in mind. One is related simply to raw cell numbers in the stable and unstable plaques. Due to experimental design, it was not possible to control the proportion of cells making up each sample, and it is conceivable that there are more monocytes and macrophages in the unstable compared with stable. If so, this could result in more LINC01272 in the unstable sample, merely because of more cells, rather than an increase in expression per cell. If this were true it wouldn’t necessarily rule out an important role for LINC01272, and could still reflect the fact that more macrophages still results in more of the transcript in the given location, regardless.

The other potential reason is also related to proportions of cells within samples, and relates to the phenotype of the “stable” plaque. Due to the rapid and crude dissection method employed, tissue was not phenotyped by histology before dissection, and therefore not definitely characterised as atherosclerotic plaque, beyond intimal thickening or even normal vascular tissue, beyond reproach. This could result in a comparison more akin to “normal tissue” vs unstable plaque, which would predictably yield more immune cells in the unstable sample, and again result in more LINC01272 due to higher cell nunbers, rather than higher expression by each cell.

With these factors considered, a potentially important role for LINC01272 within the atherosclerotic plaque remained probable, and investigations were taken to the next logical stage, as detailed in the next chapter.

Conclusion

In conclusion, the data mined from a well-conducted RNA-sequencing experiment using unstable human atherosclerotic plaque samples revealed several interesting, novel long non-coding RNA candidates. Validation of expression in fresh carotid plaque samples confirmed the bioinformatic results, and the small amount of existing literature supported some likelihood of an important biological role in disease. Finally, LINC01272 is highly enriched in monocyte and macrophages, and this cell line was selected for use in further experimental approaches.

Chapter 5 Results – LINC01272 characterisation and role in atherosclerosis

Hung J, Scanlon JP, Mahmoud AD, et al. Novel Plaque Enriched Long Noncoding RNA in Atherosclerotic Macrophage Regulation (PELATON). ***Arterioscler Thromb Vasc Biol***. 2020;40(3):697-713. doi:10.1161/ATVBAHA.119.313430

5.1 Introduction

Long non-coding RNAs are diverse in their distribution, function and mechanism, and their discovery has become commonplace since major recent advances in, and adoption of high-throughput sequencing technologies. However, whilst many scientific papers report the relative abundance of these transcripts in various pathological conditions, relatively fewer go on to describe their precise role in pathology, and even less their molecular mechanism.

Elucidating the function and mechanism of a novel lncRNA is a challenging prospect. This is because lncRNAs are known to exist in most or all human cell types and can exert their effects at any number of stages in a disease process. Given that it is impossible to study all pathophysiological processes in all cells and systems, its vital therefore to look for and identify any cues in preliminary data that hint at specificity to a particular system, cell type, or process. Knowledge of these factors can narrow down the scope of the experimental approach, and a relevant disease model can be selected as a basis for study.

To deduce a functional role, the commonest experimental approach is by either knock-down or overexpression. A well conducted knock-down experiment ensures that the only independent variable is the quantity of the target, and hence any functional change can be attributed to it. This is commonly achieved in non-coding RNA using silencing RNAs (siRNAs) and more recently oligonucleotides known as LNA GapmeRs (204, 262). These small, specifically designed sequences are added to the cells or tissues with

or without transfection reagents and can achieve high levels of lncRNA depletion within minutes to hours. Unfortunately, human organisms are inherently complicated, highly variable in phenotype, and ethically complex to experiment on, so this type of approach is reserved for *in vitro* experiments only in the earlier stages.

Although both LINC01272 and LINC01094 both emerged as potential candidate lncRNAs, this chapter will focus principally on LINC01272 which was later renamed PELATON. Preliminary data set out in the previous chapter, had already defined LINC01272 as a transcript upregulated in the unstable plaque, and also highly enriched in monocytes and macrophages (Figure 4-17). Such enrichment in this cell lineage is an important feature which enabled the focus of study to be narrowed down to the well-studied processes that monocytes and macrophages are known to affect in the unstable plaque.

Before progressing then to more complex knock-down experiments, some further characterisation of LINC01272 would be necessary. An understanding of expression patterns within the plaque and within the cell itself would give valuable insight to further concentrate down on function and mechanism, as well as inform the most appropriate experimental conditions.

5.2 Aims

- Characterise LINC01272's expression pattern in the cell, and in unstable atherosclerotic plaque
- Discover what function LINC01272 performs in human macrophages
- Investigate potential mechanistic pathways underpinning its function
- Explore the non-coding nature of the transcript

5.3 Results

5.3.1 Intracellular localisation

Several lncRNAs have now been described on a mechanistic level, and they have been demonstrated to act in all compartments of the eukaryotic cell. Transcripts which are principally expressed in the nucleus may function as post-transcriptional regulators of gene expression (263), whereas cytoplasmic lncRNAs may have roles in modulating mRNA stability, regulating mRNA translation, serving as competing endogenous RNAs, functioning as precursors of miRNAs, and mediating protein modifications (264).

To determine the intracellular expression pattern of LINC01272 in monocytes and macrophages, both fractionation and in fluorescent in situ hybridization were performed.

Fractionation

Human monocytes and monocyte-derived macrophages were extracted and cultured *in vitro*. Cellular fractionation in both monocytes and monocyte-derived macrophages revealed that LINC01272 was localised predominantly within the nucleus of the cell (91 and 98% respectively).

NEAT1 is a well-described lncRNA known to only exist in the nucleus of the cell (265, 266). The quantity of LINC01272 in both of the cell types is not dissimilar.

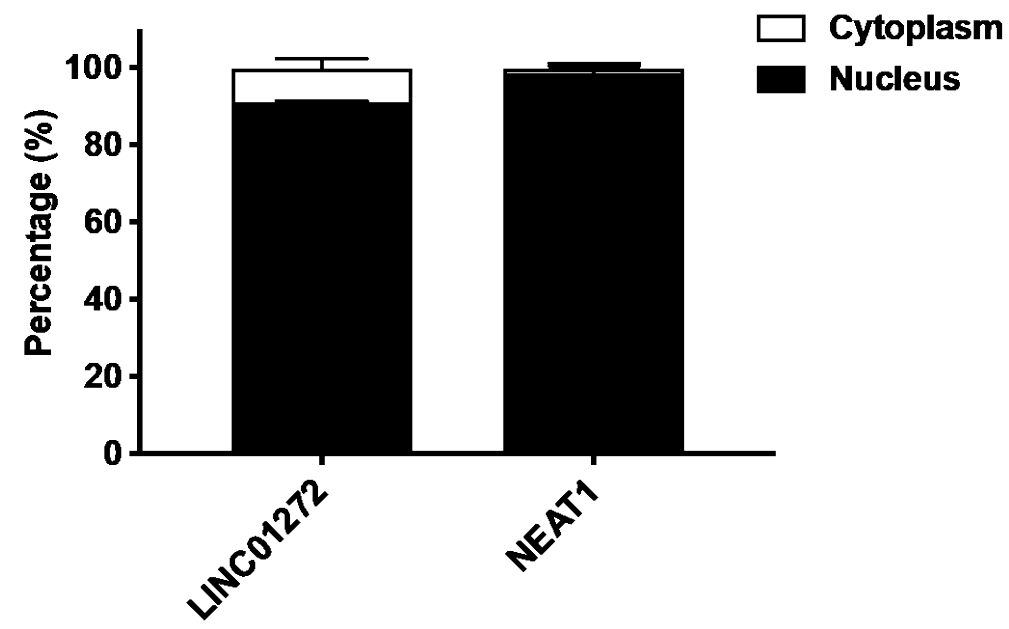

Figure 5-1: Intracellular localisation of LINC01272 in monocytes
Fractionation by PARIS kit and RTqPCR demonstrates intra cellular localisation of LINC01272 is 91% nuclear in monocytes, NEAT1 is a completely nuclear lncRNA (n=3 technical replicates, mean (+SD))

Intracellular Expression of LINC 01272 and NEAT1 In Macrophages

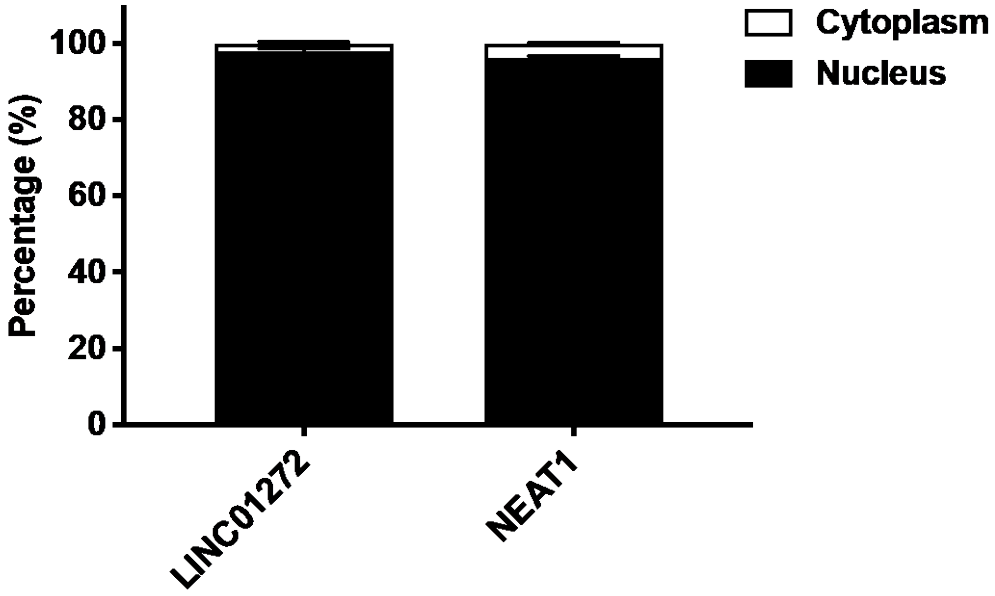

Figure 5-2: Intracellular localisation of LINC01272 in macrophages
Fractionation by PARIS kit and RTqPCR demonstrates intra cellular localisation of LINC01272 is 98% nuclear in macrophages, NEAT1 is a completely nuclear lncRNA (n=3 technical replicates, mean (+SD)).

RNA Fluorescent *In Situ* Hybridisation

Following on from the fractionation findings, RNA fluorescent *in situ* hybridisation (RNA-FISH) was undertaken in monocyte derived macrophages. LINC01272 was targeted alongside the cytoplasmic and nuclear protein UBC, and the nuclear target SNORD3. Whilst UBC is seen on both cytoplasm and nucleus, SNORD3 is entirely nuclear, as is LINC01272.

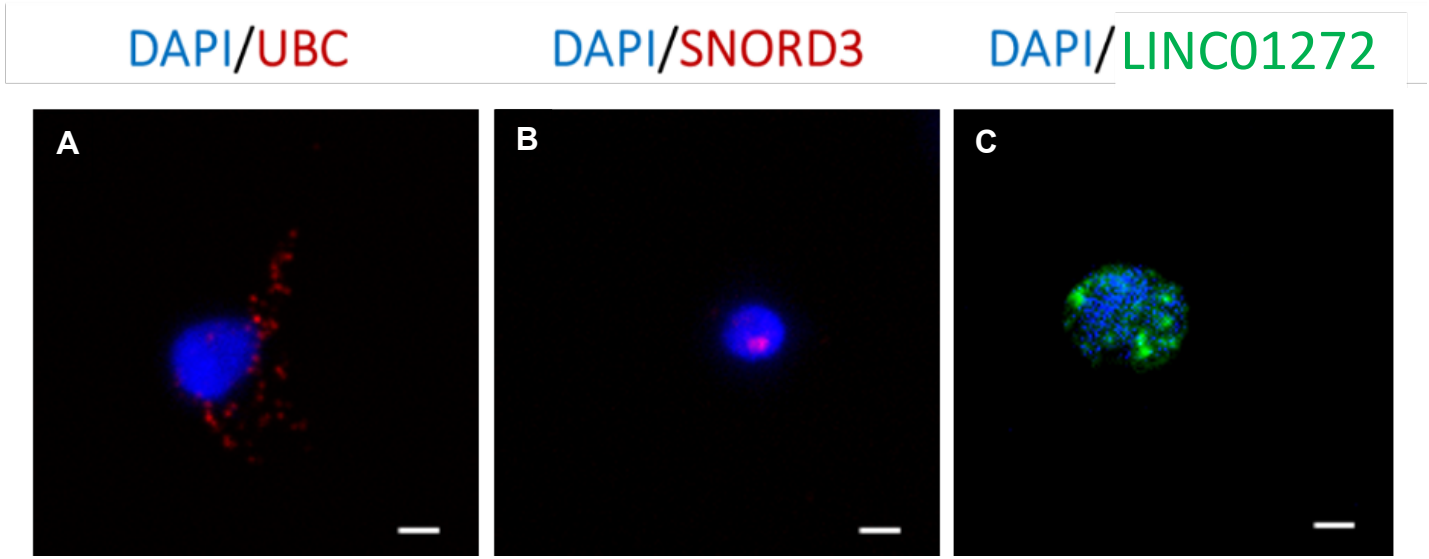

Figure 5-3: RNA-FISH for LINC01272 in monocyte derived macrophages
RNA-FISH in human monocyte derived macrophages of PELATON. Cytoplasmic/nuclear (UBC) and nuclear (SNORD3) markers used as controls. Scale bar represents 5μm. (Macrophages differentiated from CD14 monocytes as per Methods section 2.7)

5.3.2 Intra-plaque localisation - In situ hybridisation

Having confirmed the nuclear location of LINC01272, in situ hybridisation was performed to localise its expression *in vivo*, within human atherosclerotic plaque. In situ hybridisation allows detection of target mRNAs by hybridisation with an anti-sense RNA probe, labelled with a reporter dye.

Unstable atherosclerotic plaque excised at carotid endarterectomy from 3 patients was stained. In all specimens LINC01272 co-localised with CD68, mainly around the plaque shoulder regions, and also running alongside the necrotic core (Figure 5-4 B,E,H,K). In the smooth muscle regions there was very strong αSMA staining, and little to no LINC01272 (Figure 5-4 C,F,I,L). A non-specific hybridisation probe (scramble) sequence, and immunohistochemistry IgG control probe confirmed absence of non-specific staining (Figure 5-4 A,D,G,J)

To increase the intensity of the visually represented results, pseudo fluorescent images were produced in Image J from the in situ hybridisation originals. These images allow for better visualisation of co-staining (Figure 5-4 D-F, J-L)

These data therefore provide *in vivo* confirmation that LINC01272 expression is predominantly in macrophages in unstable atherosclerotic plaque, and localises to shoulder regions and areas adjacent to the necrotic core.

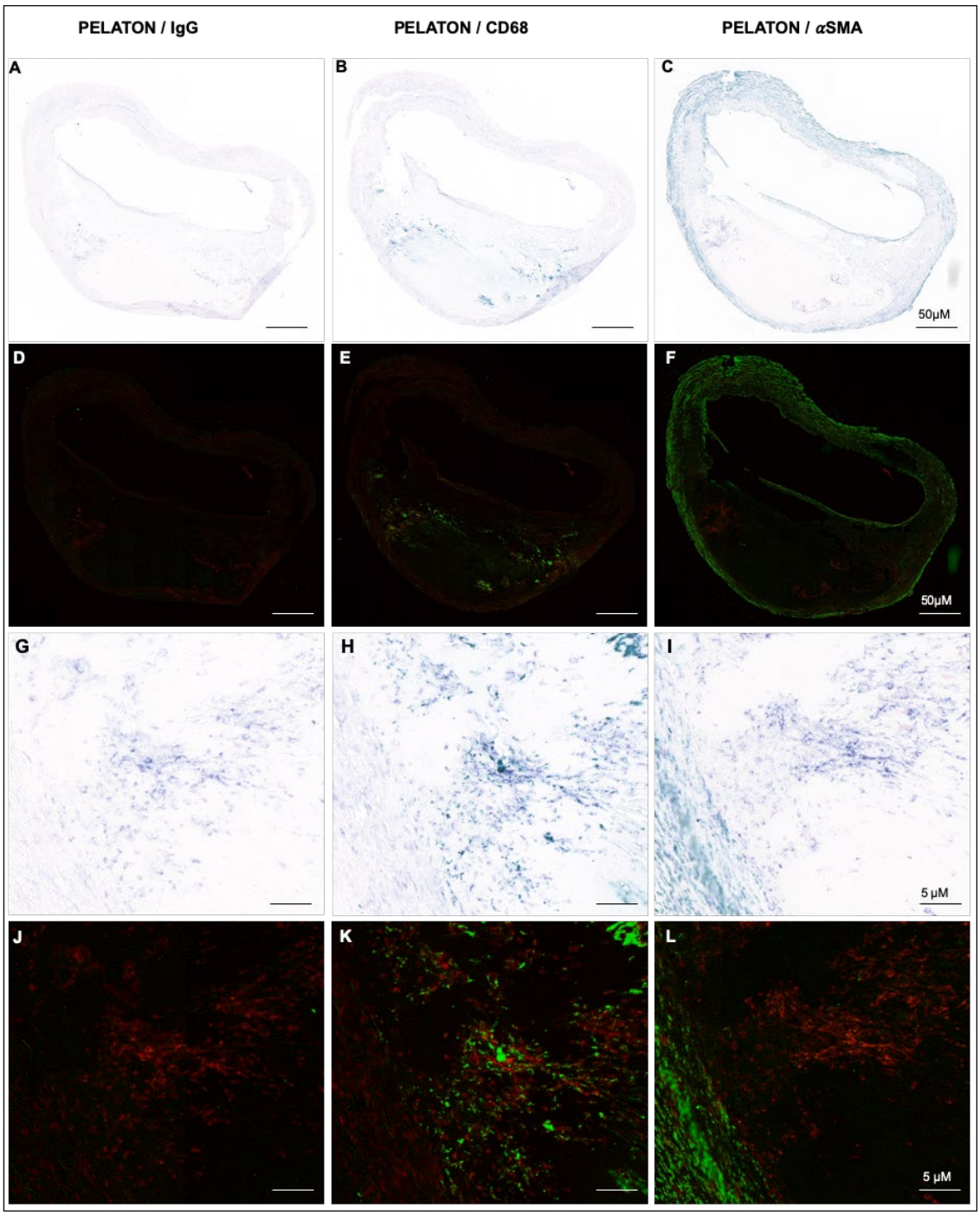

Figure 5-4: In situ hybridisation and immunohistochemistry in human carotid atherosclerotic plaque with pseudo fluorescent images.
PELATON expression (purple A-C, G-I, Red D-F, J-L) is enriched alongside the necrotic core and plaque shoulders. PELATON co-localised with CD68 (green) (B, E, H, K), but not with αSMA (green) (C, F, I, J). Pseudo fluorescent images (D-F, J-L) were produced with Image J, to allow for clearer visualization of PELATON and CD68/aSMA staining and co-localisation. n=3 biological replicates Scale bars represent 50μm in large plaque images (A-F) and 5μm in magnified images (G-L).

5.3.3 Macrophage phenotype expression

Macrophages perform a number of important roles in the atherosclerotic plaque (267, 268). Once circulating monocytes invade the subintimal space and differentiate into macrophages they begin to accumulate modified lipids and further modify accumulating lipid particles and secrete chemo-attractants. As foam cells they have a limited ability to migrate, and secrete pro-inflammatory cytokines producing reactive oxygen species. Apoptosis then occurs and dead cells release their lipid rich debris into the expanding necrotic core.

Plaque macrophages have previously been sub-categorised into classically activated M1 macrophages, and alternatively activated M2 macrophages (269). M1 macrophages are thought to be pro-inflammatory and contribute to plaque progression (270, 271), and can secrete cytokines including IL-1, IL-23, TNF-α, and nitric oxide (272, 273).

M2 macrophages have the opposite, protective effect, and are thought to be anti-inflammatory (274-277). M2 polarised cells inhibit pro-inflammatory chemokines by inhibiting STAT1 and the p65 subunit of NFκB (278).

More recently, this binary classification has been considered somewhat of an oversimplification, as macrophages in the plaque are more likely to exist somewhere on a spectrum, exhibiting varying degrees of transcriptional plasticity dependent on their environment.

As a preliminary experiment to achieve some understanding of the potential role of LINC01272, human monocyte-derived macrophages were differentiated into classical phenotypes (M1, M2a, M2c and MoxLDL). Sufficient polarisation was confirmed by modulation of appropriate markers in the expected direction for M1 and M2a macrophages, but changes in expression were not statistically significant in M2c and MoxLDL macrophages (Figure 5-4).

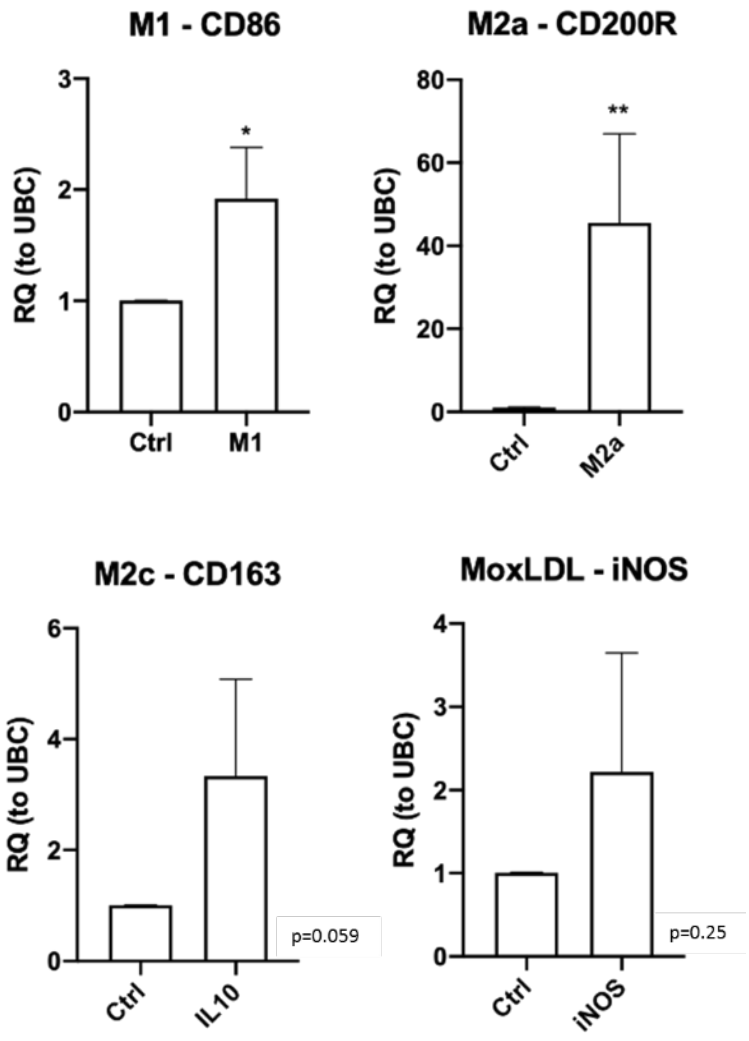

Figure 5-4: Markers of macrophage polarisation.
The expression of macrophage subtype specific markers was quantified by qRT-PCR on samples which had undergone phenotypic differentiation. For M1, M2a, M2c and MoxLDL

phenotypes, M0 (control) macrophages were stimulated with IFNγ +LPS, IL-4, IL-10 and oxLDL, respectively (N=3 biological replicates, t-test for statistical significance, bars represent mean (+SD), p<0.05=*, p<0.01=**, p<0.001=***, p<0.0001=****

LINC01272 expression was unaltered across most subtypes but was significantly reduced in M1 stimulated macrophages (Figure 5-5).

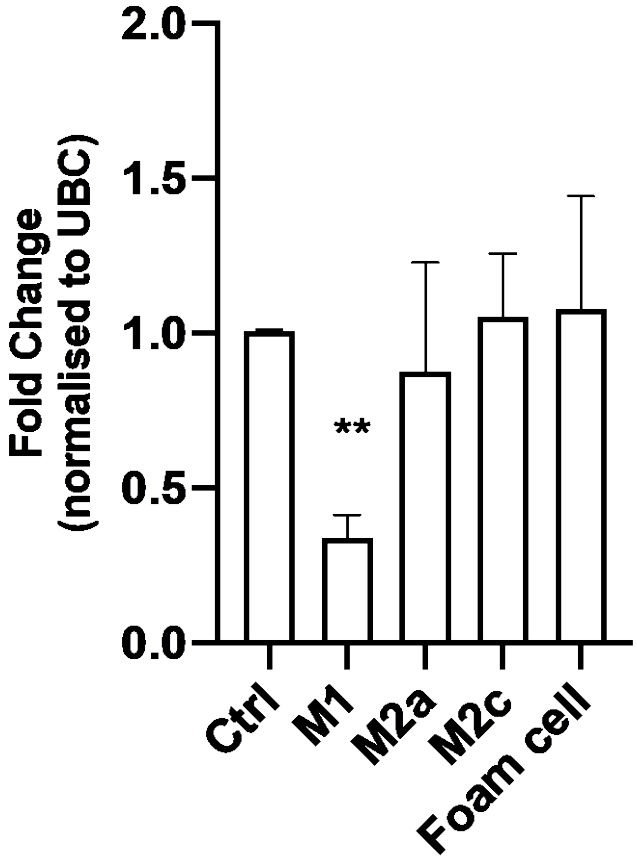

Figure 5-5: LINC01272 expression in classical macrophage phenotypes
Expression of LINC01272 was reduced in M1 macrophages compared to controls, and alternatively stimulated phenotypes. (N=3 biological replicates, t-test for statistical significance, bars represent mean (+SD), p<0.05=*, p<0.01=**, p<0.001=***, p<0.0001=****)

Across this panel of classically and alternatively stimulated macrophages the only phenotype with a change in LINC01272 regulation was M1 macrophages.

5.3.4 Long non-coding RNA confirmation

Ensembl.org is routinely used as the reference genome browser, to support research in genomics. It displays the current reference library for all known transcripts mapped to the human genome (and others), and archives historical versions. To the surprise of the investigators, Ensembl.org changed the annotation for LINC01272, designating it as a protein coding gene 'small-membrane integral protein 25' (SMIM25), towards the end of the project. A literature search did not yield any publications demonstrating the transcript as protein coding or otherwise, and the name was likely the result of in silico prediction.

Several protein coding prediction tools exist, and all that were explored predicted no protein coding potential (Table 5-1).

Table 5-1: Tools to predict likelihood of protein coding potential

Prediction Score	Result	Interpretation
Phylo CSF	-2.17	Non-coding
CPC2	0.14	Non-coding
CPAT coding probability	18.2%	Non-coding
PRIDE reprocessing	0	Non-coding
Bazzini small ORFs	0	Non-coding

To confirm experimentally if LINC01272 had any protein coding potential, the putative open reading frame (ORF) NP_001265584, as predicted by Refseq was inserted into a pcDNA 3.1(+) vector with a haemagglutinin (HA) tag and cloned for in vitro translation assay (Figure 5-6).

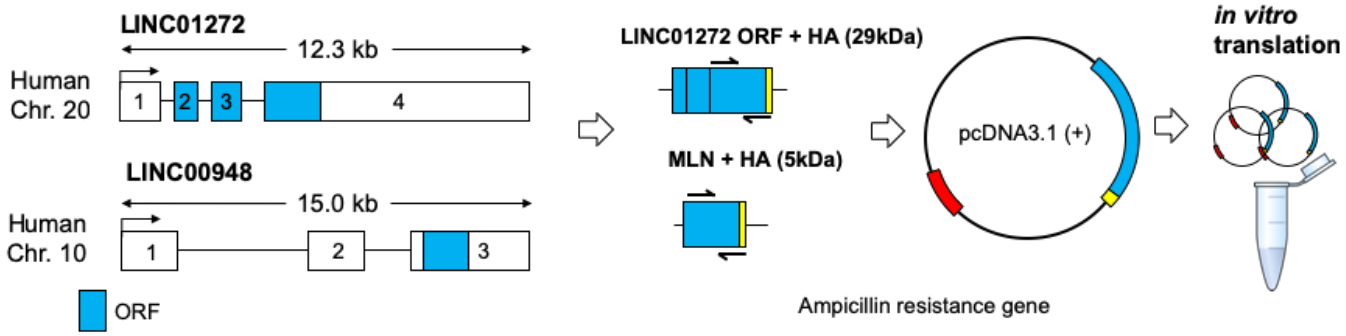

Figure 5-6: In vitro translation of LINC01272
LINC01272 predicted ORF (blue) appended with an HA tag (yellow) was inserted into pcDNA 3.1(+) plasmid for in vitro translation assay. LINC00948 was used as a +ve control, known to encode the micropeptide MLN. ORF=open reading frame, MLN= myoregulin, HA= haemagglutinin,

Sequencing of the resultant plasmid confirmed the intended base pair sequence was present, along with the transcription start site and standard Kozak sequence upstream. The plasmid was then inserted into a proprietary in vitro translation kit, with all the cellular components necessary for translation contained. Successful transcription of messenger RNA (mRNA) was detected for both LINC01272 and positive control by RT qPCR (Figure 5-7) (using primers across the ORF sequence and HA

tag boundary), but the LINC01272 transcript was not translated to a peptide, confirmed by western blotting. A positive control, LINC00948 known to encode the micro-peptide Myoregulin (MLN) indeed encoded a peptide of the expected size of 5 kDa (Figure 5-8).

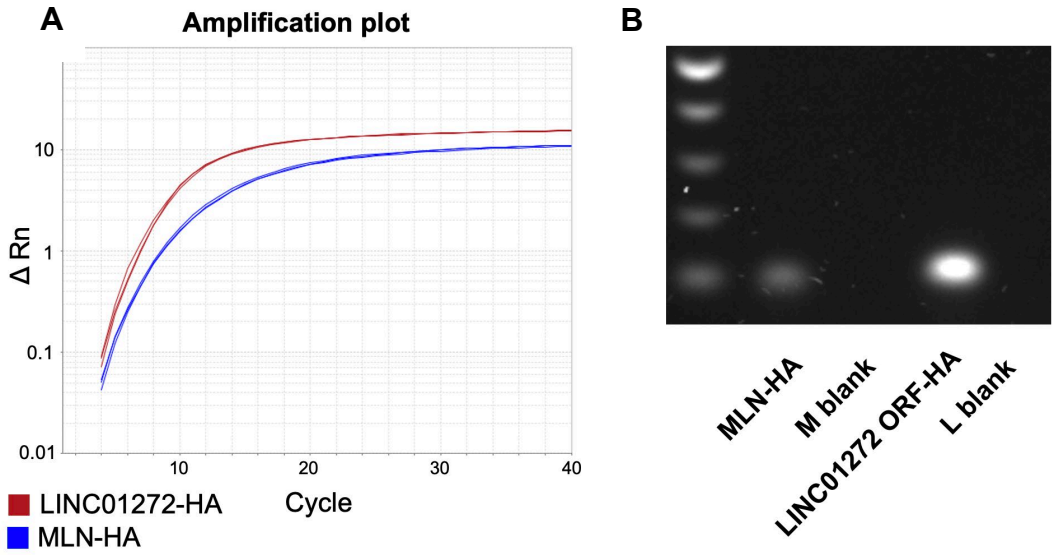

Figure 5-7: Confirmation of lncRNA-HA mRNA transcription from plasmids
(A) RT qPCR with custom primers spanning ORF/HA boundary (left) and (B) gel electrophoresis (right) confirm presence of mRNA and the PCR product, respectively M blank, L blank=RT qPCR negative controls for MLN-HA + LINC01272 ORF-HA, respectively.

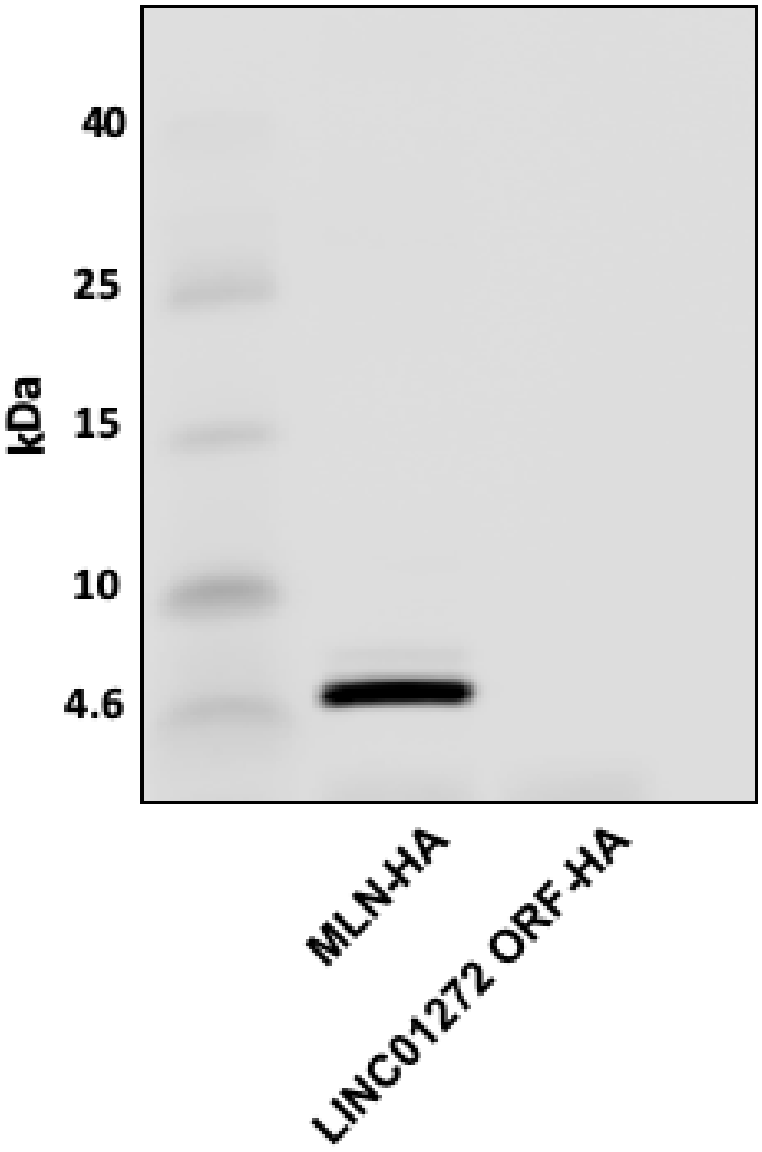

Figure 5-8: Western blot showing protein coding potential of MLN and LINC01272 from *in vitro* translation
In vitro translation product of MLN-HA sequence demonstrates a protein around 5kDa, LINC01272 ORF-HA lane is blank indicating absence of protein.

Together, these data strongly support the non-coding nature of LINC01272.

5.3.5 GapmeR Knockdown of LINC01272

Monocyte-derived macrophages treated with LNA GapmeRs targeting LINC01272 were tested for knockdown efficiency. RT-qPCR demonstrated a good, consistent level of knockdown with 2 GapmeR sequences which were selected for further experiments. To ensure that any generic effects of treatment with LNA GapmeR oligonucleotides were accounted for, a GapmeR control sequence was used as the standard comparator for all knockdown experiments. Both GapmeRs achieved a good level of LINC01272 knockdown (Figure 5-9).

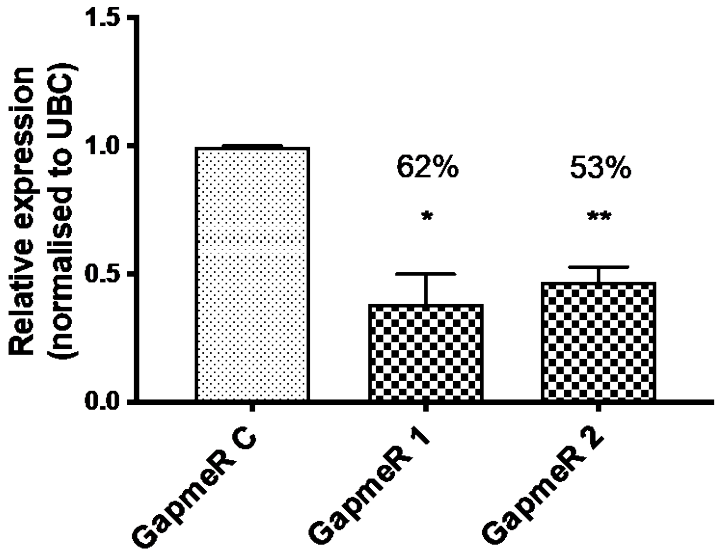

Figure 5-9: Efficacy of knockdown for high content analysis experiments
GapmeRs 1 and 2 achieve a 62% and 53% LINC01272 knockdown, respectively (N=3 biological replicates, t-test for statistical significance, bars represent mean (+SD) p<0.05=*, p<0.01=**, p<0.001=***, p<0.0001=****)

5.3.6 Nearby Gene Expression in Knockdown

As several lncRNAs are known to act on nearby genes at the same locus (in cis), neighbouring genes on chromosome 20 were further analysed for regulation when LINC01272 levels were reduced by GapmeR knockdown (Figure 5-10) (279). The protein coding gene CEBPB, occupying a locus 74 kb upstream from PELATON, is implicated in the human immune response, and in macrophage function, and was therefore a potential candidate for LINC01272 regulation (280). However, none of the genes in a 1 megabase span around LINC01272 were observed to be dysregulated in monocyte-derived macrophages under LINC01272 knockdown conditions

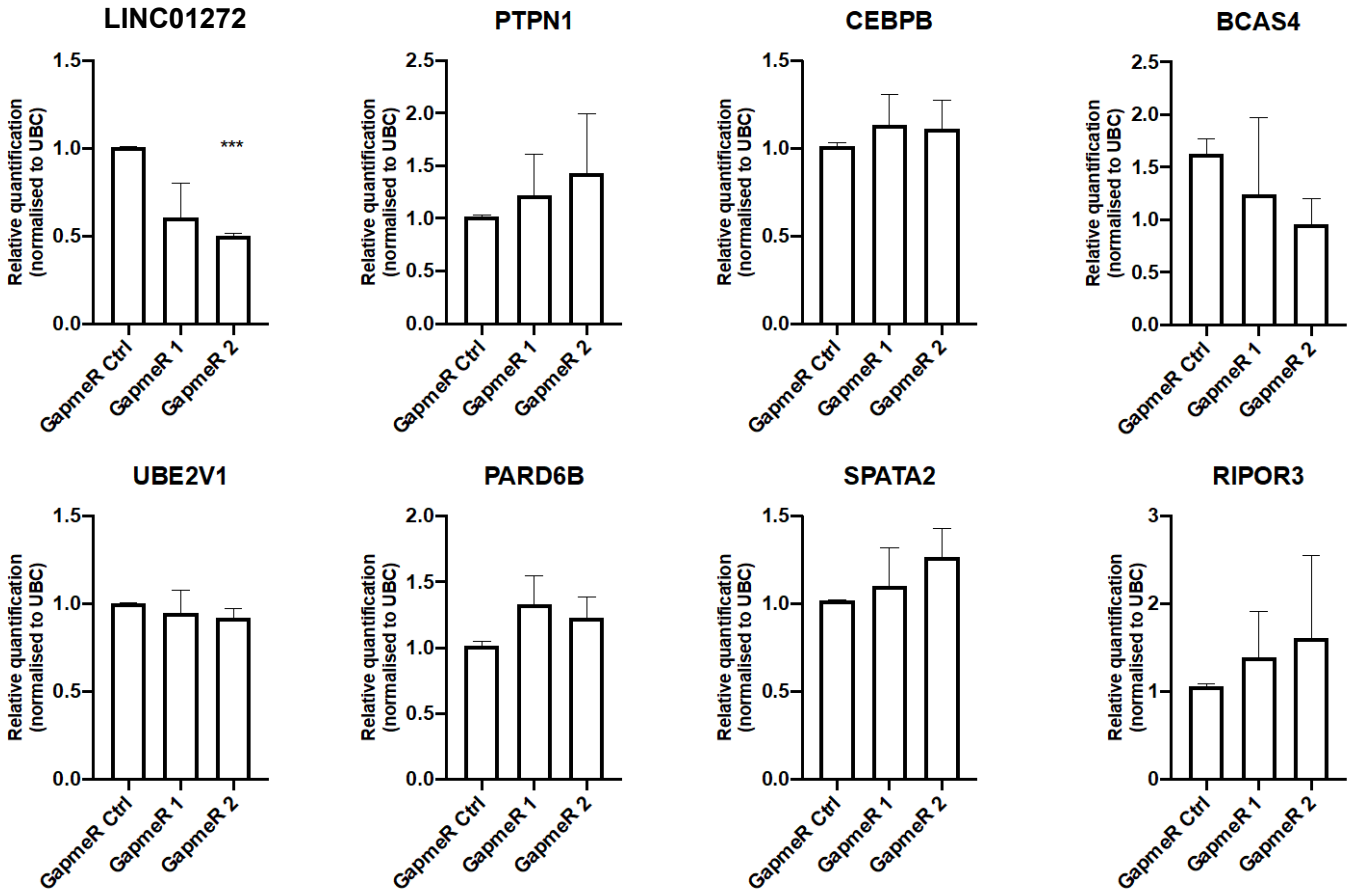

Figure 5-10: Nearby gene expression in LINC01272 knockdown
None of the genes within 1 megabase of the LINC01272 locus were significantly reduced by LINC01272 knockdown with x2 GapmeRs, bars represent mean (+SD), N=3 biological replicates, t-test for statistical significance, p<0.05=*, p<0.01=**, p<0.001=***, p<0.0001=****)

5.3.7 Phenotype discovery

High content analysis

High content analysis is a method in scientific research now commonly employed to identify how candidate RNAs (or other targets such as proteins) affect the function of a cell or tissue. They may also be known as a phenotypical screen, or high content screening (281). The variables can be the targets or the phenotypes (in this case 1 target and multiple phenotypes), and the common method across various platforms is the use of automated microscopy, usually with fluorescence. Automated image analysis is then undertaken and yields high statistical validity due to large numbers of replicates, and deep image interrogation (282, 283).

Human monocyte-derived macrophages lend well to the high content platform, as they can be cultured *in vitro* in standard optical 96-well plates, and have RNA manipulating treatments performed (such as GapmeR knockdown) in the well, before the phenotypic assay is applied.

Using the 2 GapmeR sequences described above, a high content analysis experiment to determine any phenotypic effects of LINC01272 knockdown was undertaken (Figure 5-11). Assays modelling atherosclerosis-related pathophysiology were performed, using well-established locally optimised protocols in the cardiovascular research Institute Maastricht (CARIM), the Netherlands.

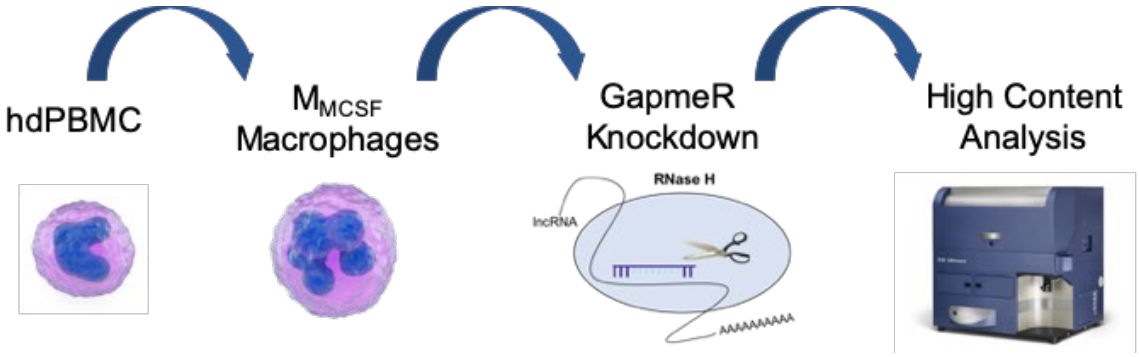

Figure 5-11: Schematic of high content analysis workflow:
Human-derived peripheral blood mononuclear cells (hdPBMCs) were differentiated to macrophages with MCSF. After 7 days of incubation GapmeR knockdown was performed and followed by phenotype specific assays.

As described in Chapter 2.15, a standard approach to each assay was undertaken. Monocytes from 3 biological donors were seeded in 96 well optical plates and cultured to macrophages over 7 days using human cytokine MCSF, at a density of 75,000-100,000 cells per well. Transfection was performed with GapmeRs for 24 hours, before phenotypic assays were performed in parallel (Figure 5-8). Each well was imaged independently with 9 separate segments, GapmeR control wells were compared with GapmeRs 1 and 2 for each phenotype. Statistical analysis for each was by one-way ANOVA and multiple comparisons.

Size and shape

As long non-coding RNAs are known to act at all levels in eukaryotic cell behaviour, simple assessment of cell size and shape were performed to identify any major fundamental effects on cell structure.

There was no significant effect on either cell area, or cell perimeter length (Figure 5-12).

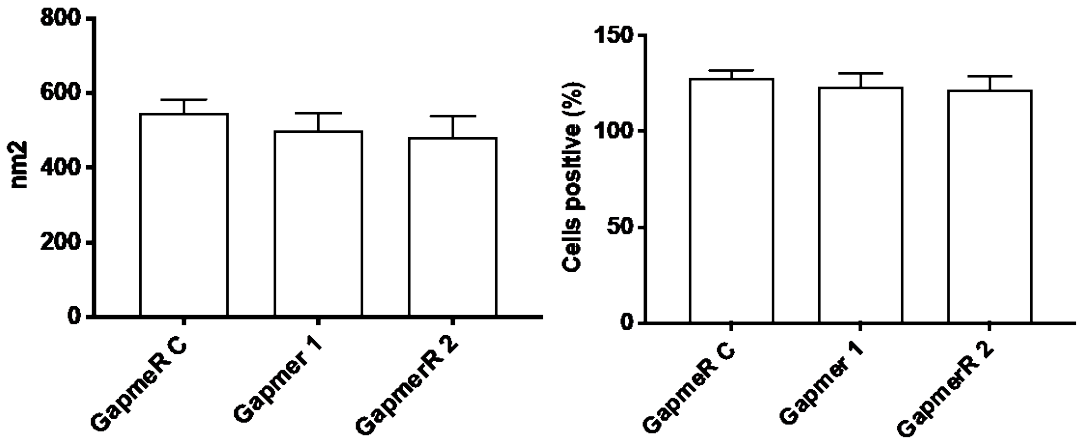

Figure 5-12: Cell area and perimeter
No difference in mean (+SD) cell area or perimeter was observed when LINC01272 was knocked down with x2 different GapmeRs.N=3 biological replicates, 5 wells per condition, each well imaged in 9 independent sections. (mean (+SD), ANOVA and multiple comparisons used for statistical analysis).

The atherosclerosis related macrophage functions tested in the phenotype screen included:

- Apoptosis
- Phagocytosis
- Lipid uptake
- Reactive oxygen species production

Apoptosis

Apoptosis of macrophages and other cells is a major factor in the development of the unstable plaque. Apoptosing macrophages and the cellular debris they release are extremely pro-inflammatory and contribute largely to the expanding necrotic core, combined with a failure of efferocytosis (clearance of dead cells).

Furthermore, if LINC01272 was an important factor in any basic cellular functions high levels of apoptosis could be seen at baseline.

Apoptosis was not affected by LINC01272 knockdown either at baseline, or after 24 hours of induction with Staurosporine (Figure 5-13 and 5-14).

Baseline

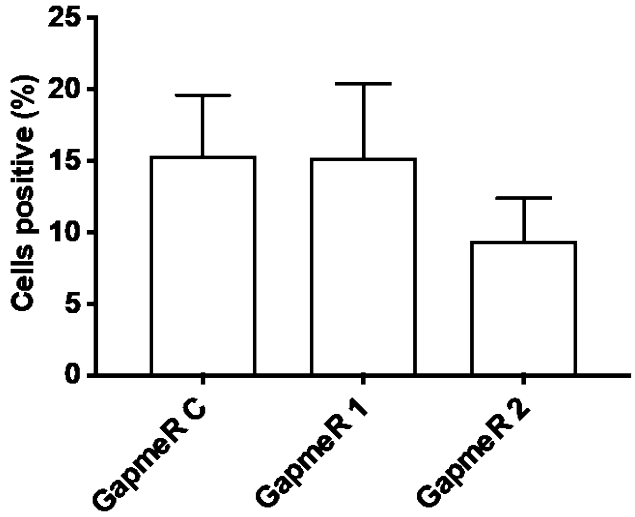

Figure 5-13: High content analysis - apoptosis at baseline
The proportion of cells positive for annexin uptake (Y axis) was not significantly different after knockdown of LINC01272 with x2 different GapmeRs. (N=3 biological replicates, 5 wells per condition, each well imaged in 9 independent sections, mean (+SD), ANOVA and multiple comparisons).

24 hours incubation with Staurosporine

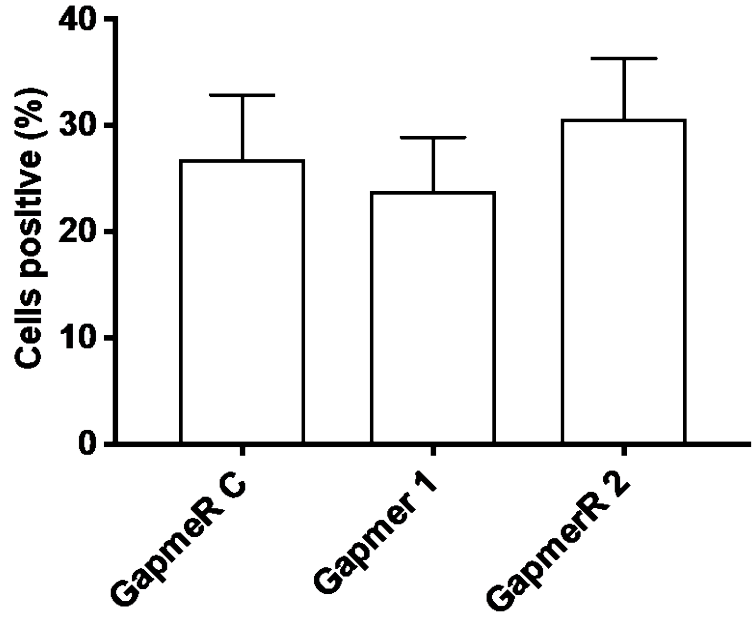

Figure 5-14:High content analysis: apoptosis at 24 hours

The proportion of cells positive for annexin uptake (Y axis) was not significantly different after knockdown of LINC01272 with x2 different GapmeRs and after 24 hours of incubation with Staurosporine [300nM]. (N=3 biological replicates, 5 wells per condition, each well imaged in 9 independent sections, mean (+SD), ANOVA and multiple comparisons).

Although overall levels of apoptosis were higher after Staurosporine incubation than at baseline, neither of the apoptosis assays demonstrated a significant difference under LINC 01272 knockdown conditions.

Phagocytosis

Phagocytosis is a critical macrophage function in the atherosclerotic plaque. Although the overall effect of phagocytosis on the plaque is nuanced and has been an area of debate, the mechanisms of phagocytosis are relatively well-studied.

Within the plaque, phagocytosing macrophages are known to ingest unwanted and dead cells including erythrocytes and platelets as well as cellular debris, and in-so-doing become more pro-inflammatory. They also ingest dead macrophages, in a process known as efferocytosis (284, 285). Further, phagocytosis is also the mechanism by which macrophages ingest oxidised lipids such as oxidised low-density lipoprotein (oxLDL) and become foam cells. This is largely via surface receptors including CD36, SRA, CD68 and LOX-1. Once overladen, the cells then undergo programmed cell death themselves and rupture their pro-inflammatory contents into the necrotic core, expanding it in size, and providing more cellular debris for other phagocytes to ingest.

This positive feedback loop continues to upregulate inflammation within the plaque, which can ultimately lead to instability and plaque rupture.

Whether phagocytosis has a net positive or negative effect towards plaque instability depends largely on the particular stage of development the plaque is in. Early on the uptake of harmful debris may be considered helpful, but later the increasing effects on inflammation, necrotic core growth, and secretion of fibrous cap degrading proteins almost certainly push the burgeoning plaque towards greater levels of instability and increase its chances of rupture.

The diagram below (Figure 5-15) adapted from Schrijvers at al (2007) summarises the pattern of macrophage surface receptors responsible for the phagocytosis of particles including LDL, platelets (PLT), red blood cells (RBCs) and apoptotic cell bodies.

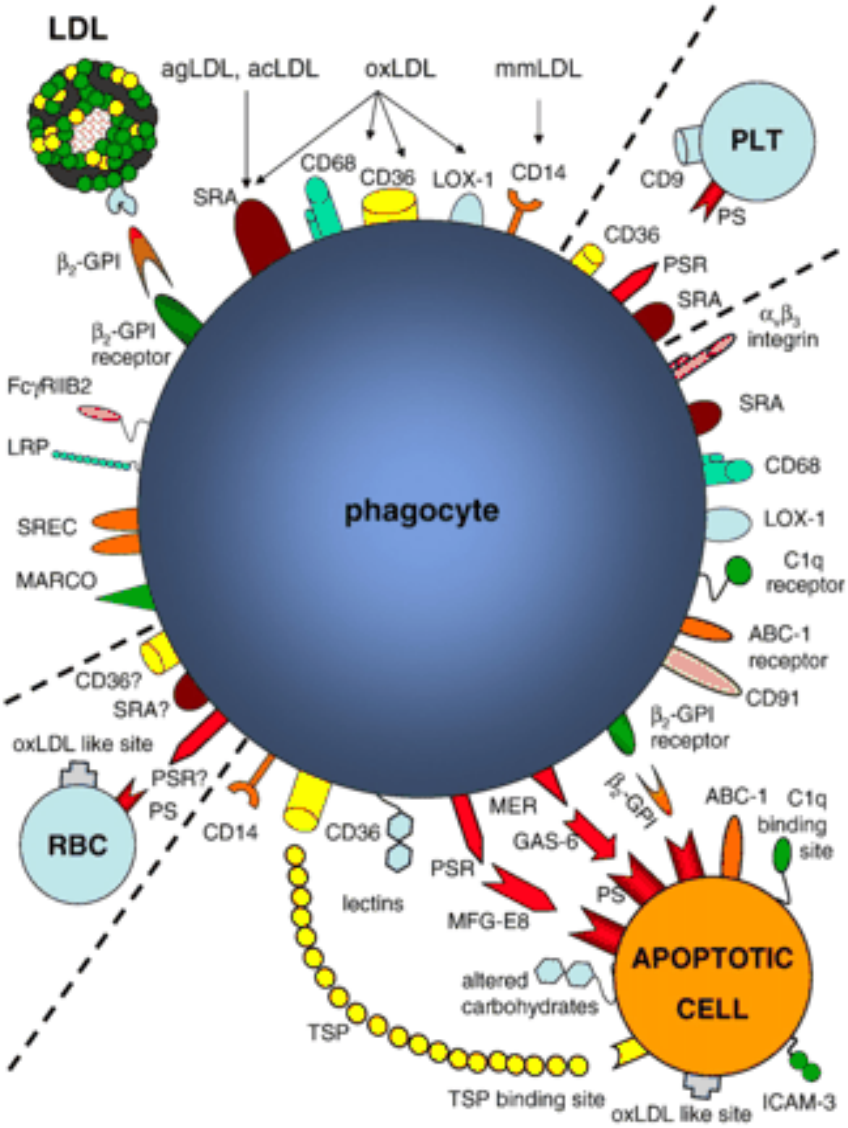

Figure 5-15: Phagocyte recognition of lipoproteins
Adapted from Schrijvers et al, Cardio Res 2007 (285)
Phagocyte recognition of lipoproteins (LDL), apoptotic cells (AC), red blood cells (RBC) and platelets (PLT). Several receptors on the phagocyte membrane are involved in the phagocytic process. They interact either directly with their ligands or via bridging molecules. CD14, lipopolysaccharide receptor; LOX-1, lectin-like oxidized low density lipoprotein receptor-1; CD36, thrombospondin receptor; CD68, macrosialin; SRA, scavenger receptor class A; FcR, Fc fragment of immunoglobulin G receptor; LRP, LDL receptor-related protein; SREC, scavenger receptor of endothelial cells; MARCO, macrophage receptor with collagenous structure; CD91, calreticulin; GAS-6, growth arrest-specific gene 6; β2-GPI, beta 2-glycoprotein 2; ABC-1, ATP-binding cassette-1; TSP, thrombospondin; PS, phosphatidylserine; PSR, PS receptor; αvβ3, vitronectin receptor.

Phagocytosis assays in cell culture models are a widely used method to assess the effects of modulating RNAs and proteins. Commercially available particles such as pHRodo beads are readily taken up by macrophages in vitro, and are labelled with fluorescent markers (286).

When LINC01272 was knocked down the GapmeRs 1 and 2, both demonstrated a reduction in phagocytosis (Figure 5-13).

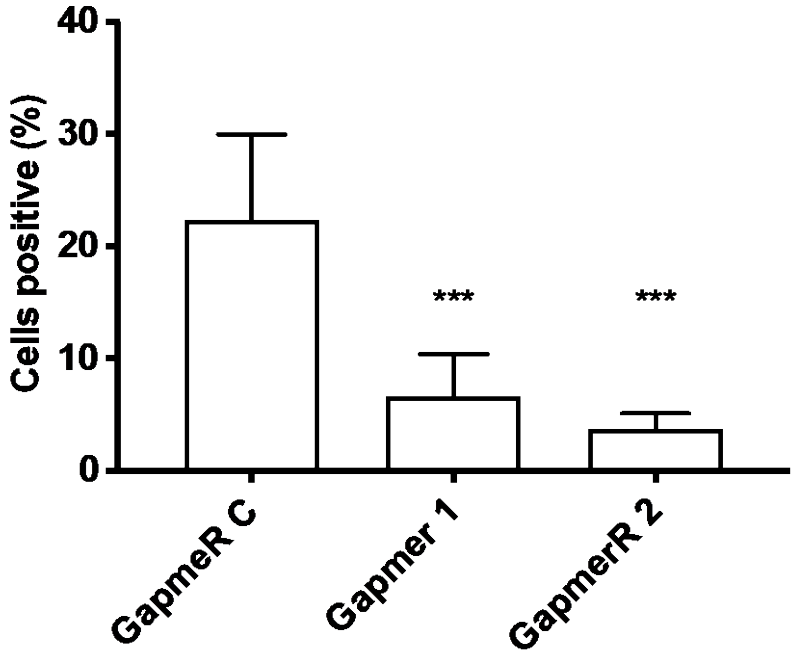

Figure 5-16:High content analysis – phagocytosis
Phagocytosis of PHrodo beads was reduced in macrophages when LINC01272 expression was knocked down with x2 different GapmeRs, when compared to non-specific GapmeR controls. N=3 biological replicates, 5 wells per condition, each well imaged in 9 independent sections. (mean (+SD), ANOVA and multiple comparisons, $p<0.05$=*, $p<0.01$=**, $p<0.001$=***, $p<0.0001$=****).

Lipid uptake

The accumulation of lipoproteins in plaque macrophages is principally by phagocytosis and via the scavenger receptors CD36, SRA1, CD68 and LOX-1 (285, 287). Within the subintimal space, modification of LDLs by oxidization, acetylation or aggregation allows the macrophage to accumulate excessive amounts, and avoid the negative feedback mechanism to stop (288). This leads to engulfment and classical foam cell formation. Although oxidized LDL (oxLDL), acetylated LDL (acLDL) and aggregated LDL (agLDL) are all characteristically scavenged by the plaque macrophage, oxLDL accounts for the majority (288-291).

Monocyte-derived macrophages were fed with oxLDL (produced locally) labelled with Topfluor. Under LINC01272 knockdown conditions, there was a significant reduction in lipid accumulation (Figure 5-17).

Given the close relationship between the lipid uptake and phagocytosis assays, this represents a scientifically consistent finding. A reduction of the process of phagocytosis would lead to less uptake of oxidised LDL.

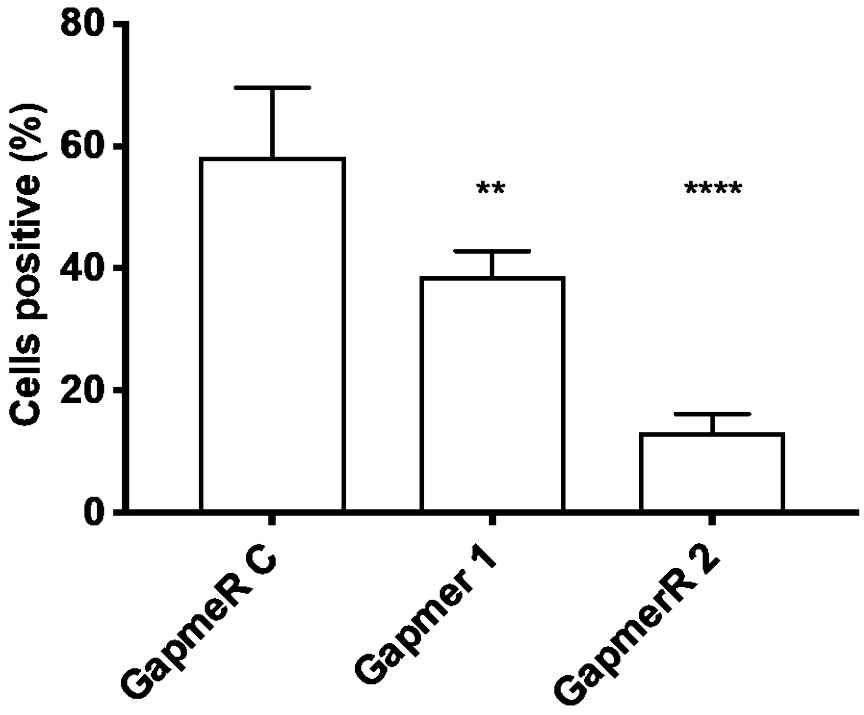

Figure 5-17: High content analysis – lipid uptake
Uptake of oxLDL in macrophages was reduced when LINC01272 expression was knocked down with x2 different GapmeRs, compared to a non-specific GapmeR control.
N=3 biological replicates, 5 wells per condition, each well imaged in 9 independent sections. (Bars represent mean (+SD), ANOVA and multiple comparisons, $p<0.05$=*, $p<0.01$=**, $p<0.001$=***, $p<0.0001$=****).

Reactive oxygen species

Reactive oxygen species (ROS) are important molecules in the pathology of the unstable plaque, and regulation of ROS and their effects remains an area of ongoing study (292). Reactive oxygen species are produced by macrophages, endothelial cells, smooth muscle cells and stem cells within the plaque. They exist both intra- and extra-cellularly, and some level of oxidative stress is normal and necessary for normal cellular signalling. However, too much oxidative stress is atherogenic (293).

When ROS production in monocyte-derived macrophages was measured at baseline there was no difference under LINC01272 knockdown conditions (Figure 5-18).

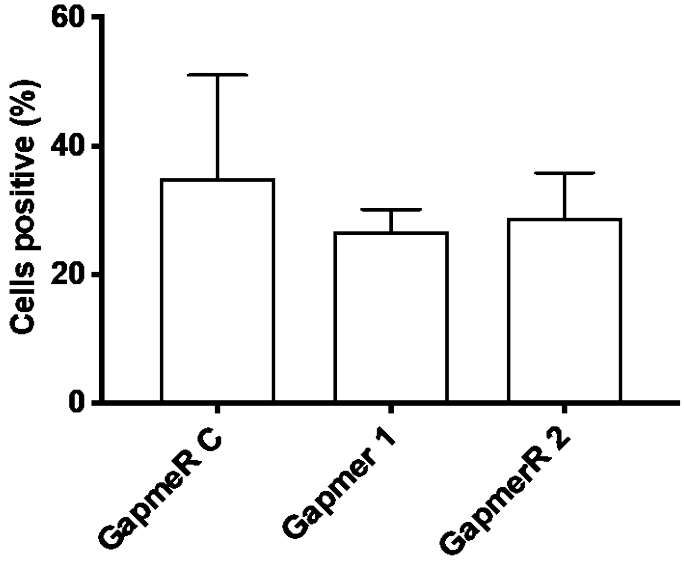

Figure 5-18: High content analysis – Reactive oxygen species production at baseline
ROS production was not reduced in macrophages with LINC01272 knockdown with x2 different GapmeRs, compared with GapmeR control. N=3 biological replicates, 5 wells per condition, each well imaged in 9 independent sections. (Bars represent mean (+SD), ANOVA and multiple comparisons, $p<0.05$=*, $p<0.01$=**, $p<0.001$=***, $p<0.0001$=****).

After stimulation with the radical stress generator menadione for 30 minutes, ROS production was reduced with LINC01272 knockdown (Figure 5-19).

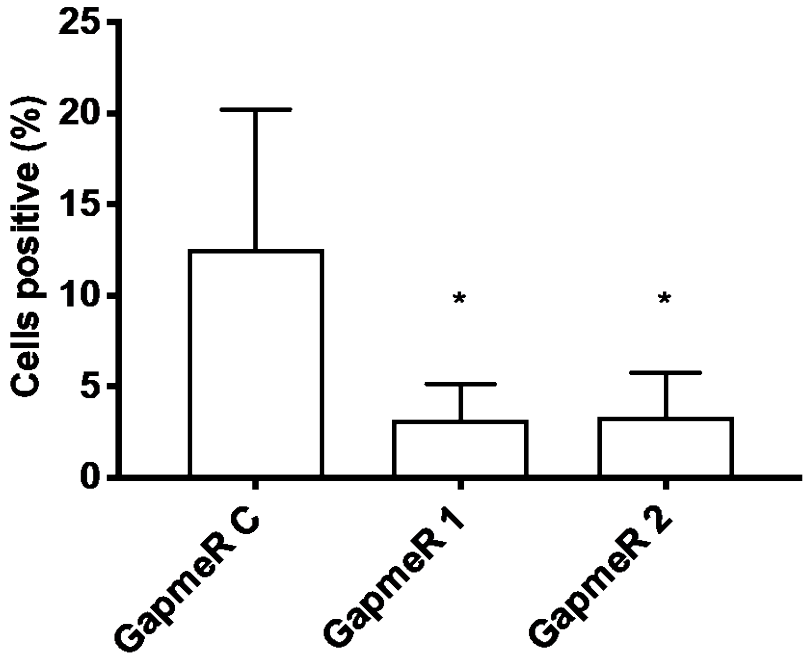

Figure 5-19: High content analysis – Reactive oxygen species production with menadione stimulation
ROS production when stimulated with menadione [10μM] was significantly reduced in macrophages with LINC01272 knockdown with 2 different GapmeRs, when compared with GapmeR control. N=3 biological replicates, 5 wells per condition, each well imaged in 9 independent sections. (ANOVA and multiple comparisons, $p<0.05$=*, $p<0.01$=**, $p<0.001$=***, $p<0.0001$=****).

5.3.8 Phenotype validation

Findings of reduced lipid uptake and phagocytosis in LINC01272 knockdown are consistent and suggest an important functional role for LINC01272 in this critical macrophage process within the atherosclerotic plaque.

To confirm and validate these data, further assays in phagocytosis and efferocytosis were undertaken separately, in Edinburgh.

Phagocytosis validation

A high content approach was again used, this time on an Operetta microscope and images analysed using Columbus software. Cells were identified by Hoechst nuclear staining, and their cytoplasm area defined by autofluorescence. Identified cells were then analysed for TRITC fluorescence within, which would only be present if containing pHRodo beads, through phagocytosis. Cells with TRITC fluorescence over the significance threshold were considered positive, and those below it negative (Figure 5-20 and 5-21).

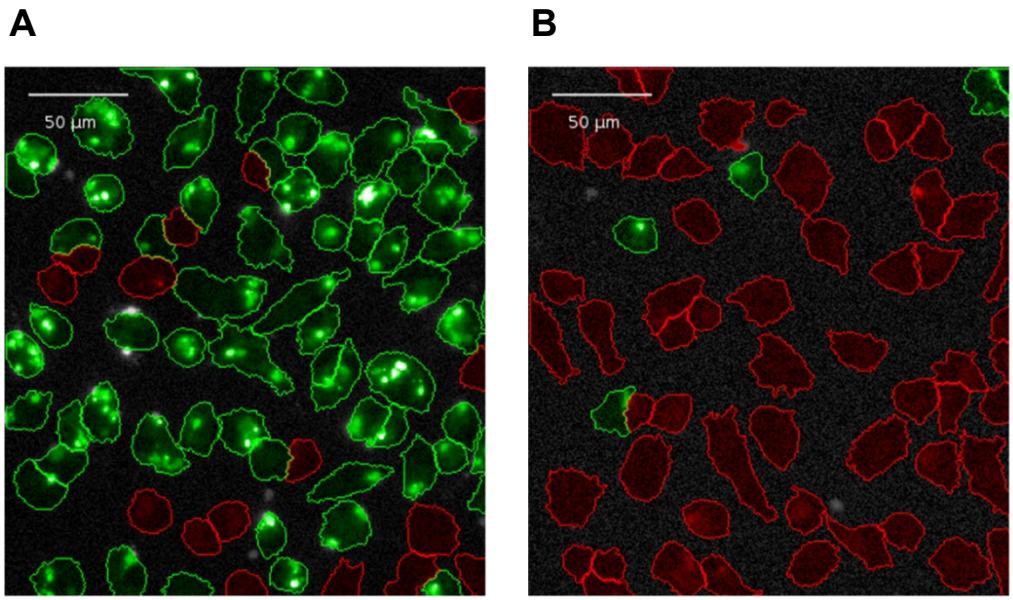

Figure 5-20:Columbus software analysis of phagocytosis high content analysis
Columbus software identifies cells within each image by cytoplasmic autofluoresence and draws a cell membrane accordingly. If TRITC fluorescence from pHRodo beads is detected above the threshold for significance within the cell membrane the cell is pseudo-labelled by the software as positive, and those below it are marked as negative. Cells pseudo labelled as positive are represented in *green*, and negative cells *red*, Representative images demonstrate high (A) and low levels of phagocytosis (B), white scale bar 50µm.

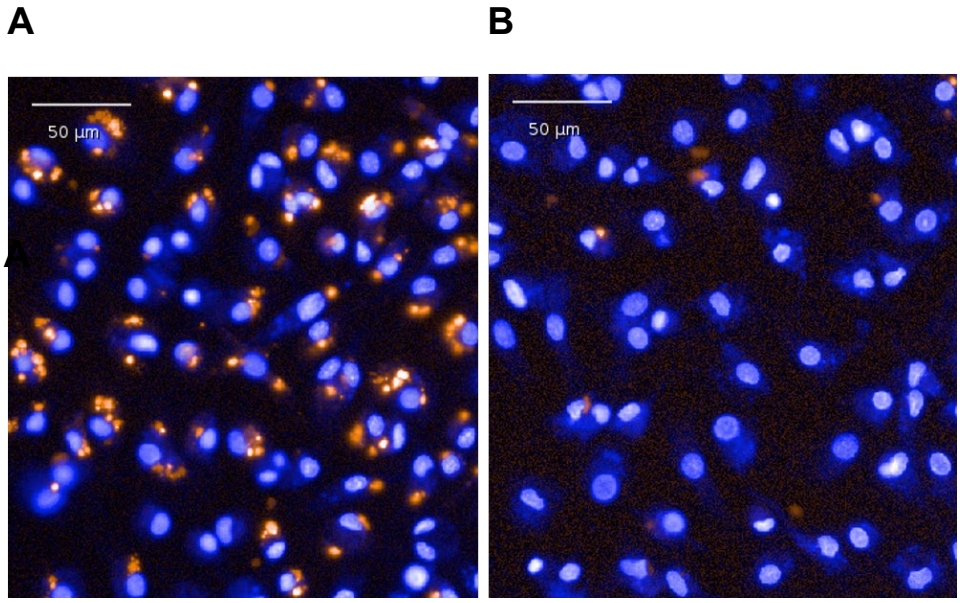

Figure 5-21: Phagocytosis of PHrodo beads
Representative images of high uptake (left) and low uptake (right). Macrophages (blue with pale nucleus) autofluoresce, and PHrodo beads exude TRITC fluorescence and are seen within macrophage cytoplasm when phagocytosed *in vitro* (white scale bar 50µm).

Consistent with previous findings, phagocytosis was reduced in the presence of LINC01272 knockdown (Figure 5-22).

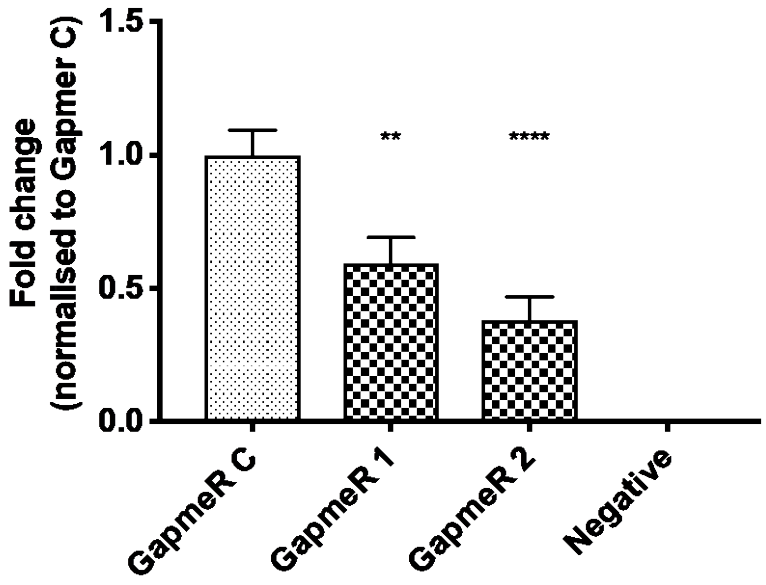

Figure 5-22:Phagocytosis validation in high content analysis
Phagocytosis was significantly reduced in LINC01272 knockdown (One-way ANOVA with multiple comparisons). N=3 biological replicates for each condition, 4-5 wells per condition, 9 images per well acquired for analysis with Columbus software (see Methods section 2.17). (Mean (+SD), ANOVA and multiple comparisons, p<0.05=*, p<0.01=**, p<0.001=***, p<0.0001=****).

5.3.9 Efferocytosis

Efferocytosis is the process by which dead and apoptotic cells are removed from the plaque, and is a process which is carried out to a large extent by macrophages (294). It is closely related to phagocytosis, and refers specifically to apoptotic cell bodies that self-signal for removal.(295) In this assay, labelled apoptotic Jurkat cells (JCs) were fed to macrophages with LINC01272 knockdown, and fluorescence-activated cell sorting (FACS) used to count the number of macrophages positive for JC ingestion.

Efferocytosis was not affected by LINC01272 knockdown (Figure 5-23).

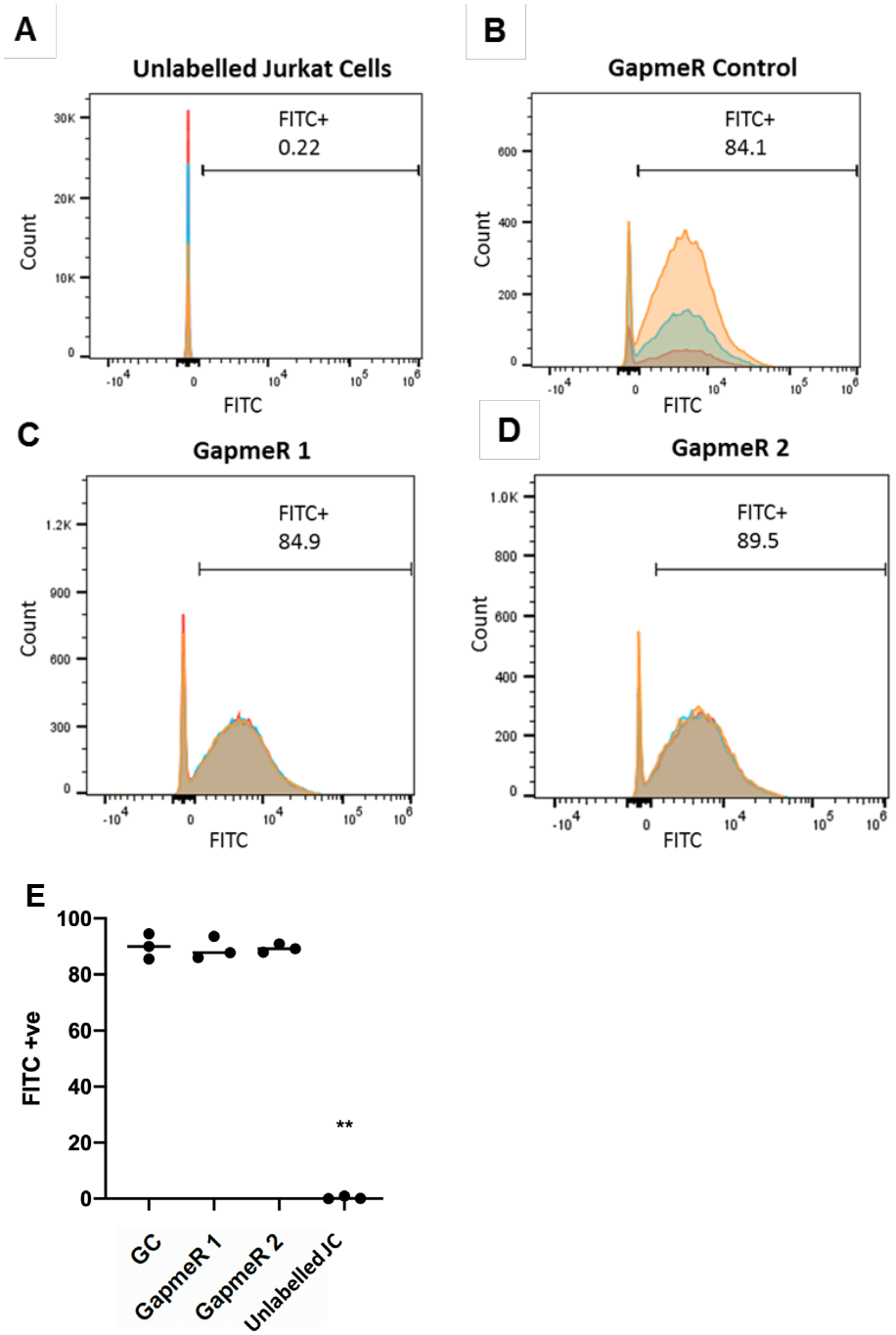

Figure 5-23: The effect of LINC01272 knockdown on efferocytosis.
FACS histogram, to show the presence of Calcein labelled (FITC+) Jurkat cells within macrophages, shown as percentage labelled in macrophages. (A) Unlabelled jurkat cells are used as a negative control. The percentage of FITC+ macrophages in (B) GapmeR control, and (C, D) LINC01272 knockdown. Each plot shows an overlay of 3 replicates (orange, blue, red lines). FITC+ =Fluorescein positive cells. (E) GapmeR knockdown of LINC01272 did not affect overall percentage of Jurkat cell uptake, mean, ANOVA and multiple comparisons.

5.3.10 Correlation with CD36

CD36 is key receptor in oxLDL uptake and phagocytosis (296), both of which were downregulated by LINC01272 knockdown (Chapter 5.3.6). To determine if CD36 could be involved in the mechanism of action of LINC01272, its expression in control and LINC01272 knockdown conditions was assessed.

The expression of CD36 in LINC01272 knockdown macrophages was reduced by an average of 39% compared with controls (Figure 5-24).

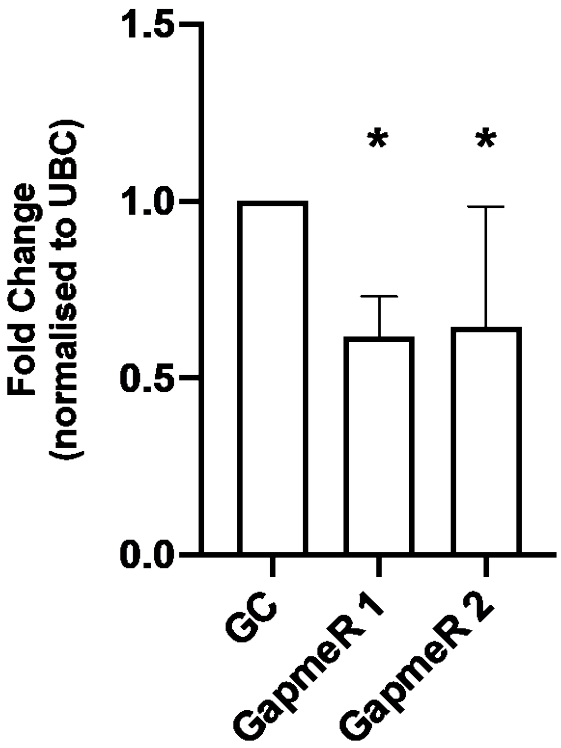

Figure 5-24: CD36 expression in LINC01272 knockdown monocyte-derived macrophages.
CD36 was significantly reduced with both GapmeRs (N=5 biological replicates, mean (+SD), ANOVA and multiple comparisons used for statistical analysis, p<0.05=*, p<0.01=**, p<0.001=***, p<0.0001=****)

In Chapter 4 the RNA sequencing experiment which formed the basis for lncRNA discovery described how LINC01272 was upregulated in unstable plaque compared with stable. After describing CD36 as a potential mediator of the phagocytosis and lipid uptake phenotype, the same RNA nseq was again interrogated for correlation between CD36 and LINC01272.

There was a very strong positive correlation (R2=0.9287, p=0.0001) between PELATON and CD36 (Figure 5-25).

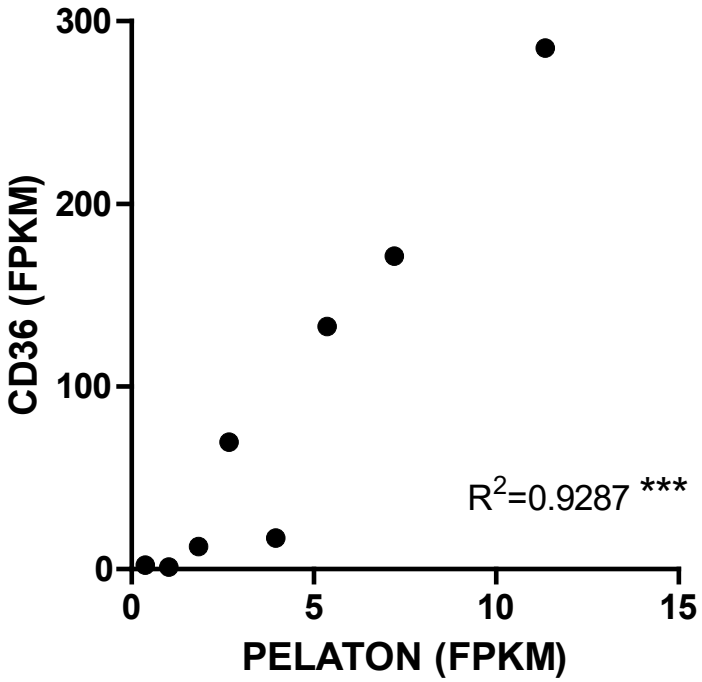

Figure 5-25:Correlation of LINC01272 and CD36 expression in stable vs unstable RNA sequencing
Very good correlation between expression values was observed, R^2 = 0.93 by Pearson's correlation.

5.4 Discussion

Using a wide variety of scientific techniques, LINC01272 has been characterised as a bonafide lncRNA with no protein coding potential, expressed highly in the monocyte and macrophage cell line. Within the human atherosclerotic plaque it co-localises with CD68 cells alongside the necrotic core and plaque shoulder regions, and fluorescent in situ hybridisation confirms nuclear expression within the cell. Upon knockdown, several important macrophage functions were reduced, including phagocytosis and oxLDL uptake, and ROS production. Basic mechanistic investigation revealed an interaction with CD36, a potential mechanism for the phenotypic changes observed.

The vivid in vitro hybridisation images confirmed the findings of the previous cell panel PCR, that LINC01272 is highly enriched in macrophages within the plaque. Furthermore, the predominance for the transcript around the necrotic core and the shoulder regions is in keeping with the general pattern of macrophage infiltration (297). CD68 is a common marker of macrophages, and itself is a scavenger receptor with an affinity for oxLDL and apoptotic cell bodies. Whilst it is contained primarily in the endosomal / lysosomal compartment it can rapidly transfer to the cell's surface (298). The lack of correlation between LINC01272 and αSMA also further confirms that smooth muscle cells, at least in a pre-foam cell phenotype, do not strongly express LINC01272.

As described previously, macrophages are responsible for more than just plaque progression, and likely have a role in plaque rupture. It is hence possible that LINC01272 has a role in the same. Macrophages are shown to directly induce this process by secretion of matrix metalloproteinases (MMPs) which actively degrade the collagenous extra-cellular matrix of the fibrous cap (299, 300). Whether LINC01272 is involved in this process would be an interesting future area of research.

When expression of LINC01272 was compared in classical and alternatively stimulated macrophages (Figure 5.5), macrophages stimulated with IFNγ and LPS (M1), express LINC01272 significantly less than controls (M0 macrophages) and the other phenotypes. This is somewhat against the prevailing hypothesis that LINC01272 is a pro-inflammatory lncRNA, a theory thus far supported by its upregulation in inflammation in existing literature, and in the earlier described RNA-seq data from stable and unstable plaque. One clear limitation of this assay is that simple stimulation by 1 or 2 cytokines significantly oversimplifies the plaque environment. Plaque macrophages are constantly stimulated by a plethora of signalling molecules, and within the constraints of the simple cell model used, it's possible only to extrapolate the findings speculatively. Furthermore, given that the M2c and MoxLDL stimulated macrophages were not well polarised, the relative differences in expression between them could be misinterpreted. A larger sample size and a wider range of stimuli would be beneficial to further investigate this point. To better understand the differential regulation of LINC01272 between different

macrophage phenotypes along the transcriptional spectrum an *in vivo* model would be preferred.

This series of experiments hence relied heavily on the human derived monocyte-derived macrophage (hdMDM) cell model, which formed the basis for the majority of the assays. As LINC01272 is highly enriched in these cells, it is clear that a monocyte lineage would be suitable to perform the *in vitro* analyses. However, there are several alternatives, and the hdMDM system is not the simplest to culture and maintain. Unlike the immortalised THP-1 cell line, which was derived from childhood leukaemia cells, hdMDMs have a once only usage. For fresh cells, each culture requires a donation of blood from healthy volunteers or study subjects, which is then followed by a 7-day culture with expensive cytokines, and variable cell senescence. Despite this, they are likely a superior solution to THP1 cells which may be transcriptionally quite different from plaque monocytes and macrophages, and as with any immortalised cell line, less analogous to the inherent variability of human subjects (301, 302).

Targeted GapmeR knockdown within the hdMDMs against a specific sequence common to all annotated isoforms of LINC01272 achieved a good level of transcript depletion (Figure 5-9). This knockdown model provided the basis for a well-controlled high content analysis experiment, which identified several important effects on macrophage function.

Phagocytosis, oxLDL uptake and ROS production are all critical, and indeed related macrophage functions within the atherosclerotic plaque. Macrophages

are known to produce ROS, which in-turn oxidise lipids, which are then taken up into the macrophage by the mechanism of phagocytosis (284, 285, 293).

A reduction in phagocytosis, which was also replicated in different conditions, is entirely in-keeping with the observed reduction in oxLDL uptake and in ROS production. These hypothesis generating results suggest that LINC01272 has a role in these functions, and that normal or higher levels of the transcript would upregulate all 3 of these atherogenic and plaque de-stabilising mechanisms.

Whilst efferocytosis is a similar and related process, it differs from phagocytosis. The substrate for encapsulation is an apoptotic cell body, rather than a modified lipid, and it can be performed via a number of different cell receptors (Figure 5-15). Whilst LINC01272 is apparently an important molecule in several atherosclerosis processes, it is unlikely to regulate all that occurs in the pathology.

To strengthen the hypotheses generated in the phenotypic experiments, an association with CD36 has been demonstrated both in LINC01272 knockdown, and also in the original RNA sequencing experiment. As a major cell receptor in phagocytosis, this is indeed a plausible interaction. Given that depletion of LINC01272 in cells resulted in a reduction in CD36 mRNA, it could be speculated that the lncRNA has a role in CD36 regulation. Long non-coding RNAs can regulate protein expression at the transcriptional and post-transcriptionally by interaction with the apparatus of transcription and transcription factors, alternative splicing, micro-RNA regulation and several other mechanisms (116-118, 120, 248, 303). As depletion of LINC01272

reduces the expression of CD36, it may be that LINC01272 is a promoter of CD36 and enacts its effects on phagocytosis via this pathway. Further study into this mechanism represents one of the important next steps in elucidating LINC01272's mechanism.

Finally, a plasmid cloning experiment was undertaken using an *in vitro* translation kit to confirm the non-coding nature of LINC01272. By combining a HA tag with the predicted ORF for the proposed protein within LINC01272, it would be possible to detect and anneal it in a Western Blot, and hence demonstrate its presence (or absence). The control sequence was taken from LINC00948 which contains an ORF coding for micro peptide myoregulin. Reassuringly, there was no protein translated from the LINC01272-HA mRNA (Figure 5-8), whilst the analogous control MLN clearly produced a protein of the expected size.

Based on these data and the publication of the paper describing them (304), LINC01272 was renamed by the HUGO Gene Nomenclature Committee as 'plaque enriched lncRNA in atherosclerotic and inflammatory bowel macrophage regulation' or PELATON.

This name reflected the data demonstrating PELATON's role in the atherosclerotic macrophage, as well as referring to its previous association with inflammatory bowel disease.

In conclusion, the data presented in this chapter define LINC01272 as a lncRNA in macrophage phagocytosis and formed the basis to rename it as PELATON. A potential mechanistic link was identified in the well-studied cell

membrane protein CD36, which is reduced in expression when PELATON is depleted.

Chapter 6 Discussion

6.1 General discussion

As the global pandemic of ischaemic heart disease continues to grow, this thesis identifies the need for new understanding in the pathology, diagnosis, risk stratification and treatment of myocardial infarction. In an analysis of the GRACE 2.0 score in type 2 MI, it is demonstrated that existing risk models perform reasonably well, but there is still work to be done in the classification of MI, which would allow the much-needed development of risk stratification tools, and novel approaches in this area. Further, in an exploratory programme of pre-clinical investigation, a novel long non-coding RNA involved in the regulation of macrophages in the atherosclerotic plaque is described. New discoveries about this previously uncharacterised long non-coding RNA demonstrate the extent to which atherosclerosis pathology remains poorly understood and adds to the small but growing body of evidence that non-coding RNAs may be important players in future development of this area.

GRACE 2.0 Score Performance in Type 2 Myocardial Infarction

For the clinical aspect of the project, the predictive strength of the GRACE 2.0 score was assessed in 2 large, European cohorts of patients with type 2 myocardial infarction. The study found that GRACE 2.0 performed well in prediction of all-cause mortality at one year (AUC 0.73) but not as well as in type 1 myocardial infarction (AUC 0.83-85). Further study to refine the GRACE 2.0 score for type 2 myocardial infarction or derive a new score altogether could improve risk stratification in these high-risk patients.

The Global Registry of Acute Coronary Events (GRACE) was originally conceived in 2000, designed to collate and analyse the data of ACS patients all around the world (305). Through characterising the acute coronary syndrome (ACS) population in more than 100,000 patients in 30 countries, the investigators derived a risk stratification tool to predict outcomes of death, MI and in-hospital mortality using just 8 data points readily available at the bedside (213-215). Since then, newer iterations of the GRACE score have been added, and it has been validated as a clinical tool in the management of ACS many times over, as well as in other pathologies such as pulmonary embolism and contrast renal nephropathy (216, 306-308). Critically however, these studies do not differentiate the type of myocardial infarction as per the new 'Fourth Universal Definition of Myocardial Infarction' (74), and patients with type 2 myocardial infarction are likely under-represented.

Our present study (309) was devised to assess the performance of the GRACE 2.0 Score in patients with both type 1 and type 2 myocardial infarction. As expected, discrimination of death was better than death/MI, and performance was superior in type 1 myocardial infarction, the population in which the score was originally devised.

The performance of any risk stratification tool is highly dependent on the reference population from which it was devised and the patients in which it is applied. Patients with type 2 myocardial infarction differ significantly from the cohort of patients that were included in the original GRACE registry. Modern high-sensitivity troponins detect significantly more patients with myocardial

injury, resulting in a shift in the characteristics of the population defined as having had myocardial infarction (222). Recent evidence suggests that implementing a high-sensitivity troponin in a population of patients with suspected acute coronary syndrome increases diagnosis of type 1 MI, type 2 MI, and acute and chronic myocardial injury by 11%, 22%, 36% and 44% respectively (222).

This relatively newly characterised population of patients with type 2 myocardial infarction is demographically older and more female (223, 226), and clinical factors other than those related to the cardiovascular system such as frailty may be important in prediction of outcome (310). Further study to develop new risk prediction tools must include parameters like frailty which encompass non-cardiovascular risk factors and are easily measurable at the bedside.

A limitation of the present study and of others which have attempted to devise risk scores for type 2 myocardial infarction is in the inherent heterogeneity of patients in this group (230, 231). Unfortunately, this is owed largely to what has become a slightly confusing classification system, whereby patients who have completely disparate pathologies can be given the same diagnosis of type 2 myocardial infarction. Although the Universal Definition of Myocardial Infarction was published in multiple iterations with the intention of unifying diagnosis, investigation and management of patients with MI, developments in biomarker technology have now completely changed the landscape. Small

magnitude troponin elevations are now commonly detected in the presence of relatively minor ischaemia, and evidence on optimal management is lacking.

Clearly, a patient with type 2 myocardial infarction who sustains myocardial injury due to profound anaemia should not be treated in the same manner as a patient with type 1 MI due to atherothrombosis. However, neither should patients with type 2 MI due to other diverse pathologies, such as atrial fibrillation, or aortic stenosis. Although the same diagnosis should be applied to such patients (type 2 myocardial infarction), quite different underlying pathologies would require different investigational strategies, and of course different treatments.

Whilst development of better risk stratification tools in type 2 myocardial infarction are scientifically within reach, it may be difficult to unify investigation and treatment strategies because even though patients could be grouped by risk, their underlying pathologies would be different.

The DEMAND-MI study has now completed recruitment and aims to characterise a contemporary cohort of patients with type 2 myocardial infarction with respect to coronary artery disease prevalence, patterns of myocardial injury and cardiovascular outcome. These findings should clarify the distribution of myocardial injury mechanisms in this diverse group of patients and inform further randomised studies into how type 2 myocardial infarction patients should be optimally investigated and managed. Further, appropriate risk stratification parameters will be identified, to inform further attempts at good risk stratification in this group.

Ultimately, it may become too difficult to generalise in patients with type 2 myocardial infarction, and it may be necessary to change how myocardial injury is classified and managed altogether. Grouping patients with myocardial injury by more specific, individual characteristics would allow a more personalised approach to work towards improving patient outcomes.

PELATON Discovery

The mechanisms of long non-coding RNA in atherosclerosis were studied, to gain insight into new pathways for treatment of patients with myocardial infarction. Based on interrogation of existing RNA sequencing data in unstable human carotid endarterectomy samples, a novel long non-coding RNA in unstable atherosclerosis was discovered, characterised and renamed PELATON. Through its interaction with the membrane protein CD36, this important lncRNA represents a new target for unstable plaque detection and treatment.

To explore new pathways and gain new insights into mechanisms underpinning myocardial infarction, it is important to consider translational applications of rapidly developing technologies, not least in the area of high throughput genetic screening, and high content analysis. Insight into undiscovered mechanisms can lead to novel diagnostic pathways, treatments, and risk prediction models. It is possible that new biomarkers could distinguish the mechanism of myocardial injury upstream in the diagnostic pathway, and allow new classification methods, leading to improved, targeted treatments.

Advances in understanding of non-coding RNA have recently uncovered a potentially rich new layer of complexity to almost all human pathologies, and multiple completely novel non-coding RNAs have now been shown to have critically important roles in vascular pathologies, including PELATON (304, 311).

The data presented above describe PELATON as a monocyte and macrophage enriched lncRNA, that regulates phagocytosis, lipid uptake and reactive oxygen species production (Chapter 5). Early indications suggest that the macrophage surface marker and scavenger receptor CD36 may mediate these effects (Chapter 5.3.9).

Although PELATON had been predicted to encode a micro-peptide called SMIM25 part way into the study, robust in vitro translation data was able to disprove this (Chapter 5.3.10). This intervention was timely, as several contemporaneous publications had very recently described ‘bifunctional long non-coding RNAs’. These are transcripts which function both as non-coding RNA transcripts, but also contain functional open reading frames which encode micro-peptides (312). Anderson et al. reported an interesting micro-peptide called Myoregulin (MLN), which is transcribed from LINC00948 (103), and was used to good effect as an experimental control in the *in vitro* translation experiment in Chapter 5 (Figure 5-23). Much like LINC00948, PELATON contains a possible open reading frame within it, but in the case of PELATON it is simply not transcribed, and PELATON will maintain its non-coding status. Other examples of lncRNAs encoding micro-peptides include

lncRNA PNUTS which functions both as mRNA for PNUTS and as a lncRNA sponge for miR-205 (313); and the lncRNA steroid receptor RNA activator (SRA1), which also encodes protein whilst functioning as a hormone activating lncRNA (314). At the time of writing, no micro-peptide encoding lncRNAs have yet been described in atherosclerosis.

Further to this, PELATON is quite highly expressed for a lncRNA, more in the range of a protein, as lncRNAs are usually much less abundant in cells. Raw CT values of 20 and 21 in macrophages and monocytes, respectively in RT qPCR with cDNA (produced using standard protocols) are low and indicate abundance (Figure 4-17). This is a factor which makes PELATON attractive as a substrate for study, but also as a therapeutic target. The cell-type enrichment of PELATON is typical for a lncRNA, and is an advantageous feature of lncRNAs that also make them good targets for novel therapies (315).

However, whilst PELATON is reliably upregulated in unstable vs stable plaque, certain limitations acknowledged principally in Chapter 4 should be considered before accepting the explanation for this. Various issues in RNA-seq design could lend to a degree of variability in the proportion of monocytes and macrophages between stable and unstable samples, and there is a possibility that differences between groups exist because of a difference in cell number rather than levels of expression within the cells. If this is the case, it would not rule out an important role for PELATON, which was studied in more depth afterwards, but a more nuanced approach to understanding its expression in different subsets of immune cells would prove extremely valuable. To

underline this, an unexpected reduction in PELATON expression in M1 macrophages was observed in Chapter 5 when monocyte-derived macrophages were classically and alternatively stimulated (Figure 5-5). This experiment was limited by small sample size, and likely incomplete polarisation of all phenotypes, but again emphasises that a more complete picture of PELATON expression in immune cells with differing polarisation would be desirable.

In the ensuing experiments however, LNA-GapmeR knockdown achieved adequate depletion of PELATON in macrophages, which was sufficient to reduce phagocytosis of pHRodo beads and oxidised LDL.

A reduction in lipid uptake by PELATON knockdown, as a novel therapy, may possibly therefore reduce plaque progression to instability, as it would interfere with multiple atherogenic mechanisms within the plaque. Macrophage differentiation to foam cell is a key factor in almost all of the processes which result in plaque growth and instability(24, 268, 289). Attenuation of this process in the human vasculature could potentially slow the rate of atherosclerotic progress, and thereby reduce the risk of plaque rupture. No therapies are currently licensed for this specific indication, except statins (and more recently PCSK9 inhibitors (68, 316)) which were originally given really for their lipid lowering properties. Contemporary data has suggested however that the reduction in cardiovascular risk achieved with statin treatment might actually

be ascribed to their pleiotropic effect of a reduction in inflammation rather than just a reduction in circulating LDL (317).

Whilst macrophages are extremely well studied in atherosclerosis, no other study as yet reports a potential therapeutic agent to act on lipid uptake (318, 319). Whilst statins significantly reduce circulating lipids and are well known to reduce cardiovascular risk more generally, they have no effect on lipid uptake within the plaque. Other recent evidence of lncRNA modulation of macrophage behaviour relates to regulation of apoptosis (320-322) rather than lipid regulation, and none have yet progressed as far as phase 2 studies in human.

Translation of these *in vitro* and animal model findings is fundamentally possible, and necessary, but relatively few have progressed to clinical use. Just as in the majority of experimental science in this field, the basic diametric options are to either over-express or deplete the target in the pathologically relevant cell or tissue. Earlier attempts at over-expression have seen limited success using viral vectors, but off-target effects remain a problem (323, 324). Depletion using silencing RNAs (siRNAs) and antisense oligonucleotides such as GapmeRs hold promise and have been more successful on an experimental level. Both methods manipulate endogenous RNA transcription machinery to knock-down expression of target genes by different mechanisms. SiRNAs are delivered as a double-stranded RNA molecule which binds with RISC, allowing the passenger strand to dissociate and anneal their target to be degraded. GapmeRs and other anti-sense nucleotides bind directly to target RNAs and recruit endogenous nucleases to cleave it (325, 326).

One notable example of a siRNA in atherosclerosis which has been clinically proven and is about to be introduced is a drug called Inclisiran (327, 328). Inclisiran targets the mRNA of PCSK9, depletion of which has already been shown in RCTs to significantly reduce circulating LDL levels, and translates to a reduction in cardiovascular endpoints (68, 69, 316).

Evidence thus far suggests strongly that PELATON is highly enriched in the monocyte / macrophage cell line in the plaque, but more evidence is needed to understand other sources of expression including other immune cells, and other important roles in human physiology and pathology. Given the previously cited evidence of upregulation in gastric cancer and in inflammatory bowel disease it is quite evident that PELATON exists outside of the atherosclerotic plaque. However, exactly which cell types express it in these conditions is not demonstrated, and it may well be the same cell lines, which are in fact implicated in both pathologies. Assuming that PELATON is expressed more widely in the body than in the vasculature, it is likely that depletion would have some off-target effects. This unquantified risk of off-target side effects may be difficult to avoid when therapies are delivered systemically, particularly when the target cell line is ubiquitous to multiple different tissues around the body, and represents a significant limitation of the approach. Whilst the siRNA or ASO might reliably penetrate the target cells and deplete the lncRNA within, further study would be necessary to develop methods to avoid unwanted action on cells in other organs or territories. In the case of PELATON, given that the demonstrated phenotype affects phagocytosis, which is an important

process in innate immunity, careful study in animal models would be a necessary next step to understand how the immune system would be affected.

One peculiarity of coronary artery disease compared to other pathologies is that there is already a therapy which facilitates extremely precise, localised delivery of drugs, and is already in routine clinical practice. Percutaneous coronary intervention with stents is performed as a class 1a treatment for angina and acute coronary syndromes in all developed healthcare systems and is extremely mature in terms of technology and operator experience. Modern drug eluting stents are impregnated with immunosuppressant compounds such as everolimus and sirolimus, designed to prevent endothelial overgrowth known as in-stent restenosis. As this technology already exists, there is logically already a vehicle to target an ASO to the culprit vessel, and increase the chance of avoiding off target, systemic effects.

A barrier to this approach is that primary prevention of plaque rupture with “prophylactic” implantation of stents for vulnerable plaque has never been shown to be beneficial. Stent implantation carries a risk of re-stenosis of approximately 1% per year, and immediate complications such as coronary dissection, peri-procedural myocardial infarction, stroke and even death affect around 1% of patients. The risk of stenting may well exceed the risk of myocardial infarction, especially in primary prevention. If PELATON is capable of causing plaque regression, which is of course unknown, the risk-benefit profile of an intervention may be more favourable in a secondary prevention

setting. Here the culprit plaque would be already identified, and the benefits of PCI to culprit lesions is well established.

Another potential mode of delivery which avoids the complication of early stent thrombosis and later re-stenosis is the bioresorbable stent. Bioresorbable stents or scaffolds were once thought to be advantageous over tradition bare metal and drug-eluting stents, as they are physically resorbed over time, leaving no physical remnant, and also facilitate delivery of local immune-suppressant drugs. Studies are still ongoing in this field, as clinical benefit was not shown in earlier studies, and the technology is still in a relatively early phase.

6.2 Concluding remarks

The data presented above confirm that myocardial infarction remains one of the world's major health problems. Despite the advances of contemporary science and medicine, patients with type 1 and type 2 myocardial infarction still have a 10-25% risk of death at 1 year. Analysis of the GRACE 2.0 score in risk stratification of patients with type 2 MI demonstrates that although existing models of care perform reasonably well, the complexity of this condition is still unfolding, and much is still to be learned about type 2 myocardial infarction.

In an exploratory study of long non-coding RNAs in unstable atherosclerosis, PELATON was discovered to be a novel regulator of macrophage behaviour

in the atherosclerotic plaque. Further study is now needed to understand if PELATON depletion in vivo is clinically beneficial, and safe to perform.

6.3 Future perspectives

Type 2 myocardial infarction is a burgeoning area of research, and several groups internationally continue to generate data in this area. As the Universal Definition of Myocardial Infarction (UDMI) has evolved over years, and the diagnosis of type 2 MI becomes ever more common, the magnitude of the clinical problem continues to expand.

There are several domains within type 2 myocardial infarction where evidence is desperately needed to improve not only patient outcomes, but first the scientific understanding of this condition needs to improve.

Currently, the grouping of such diverse pathologies within the umbrella terminology of type 2 myocardial infarction renders generalisation of investigation and management strategies impossible. Whilst all patients have features of myocardial injury and ischaemia in common, the mechanisms underlying are diverse. Further work into a more suitable classification system is urgently needed to facilitate good quality research into the optimum management of each individual patient who falls into this awkward category.

As previously discussed, the DEMAND-MI study for which the author is a lead investigator should hopefully produce valuable data on the profile of type 2 MI patients and form the basis for RCTs of optimum investigation and management. It is likely that the presence or absence of coronary artery disease in this population is an important and useful discriminator, which would at least inform the use of primary prevention medications such as aspirin and

statins. How best to diagnose this anatomically, whether invasive or non-invasive is another research question, which we intend to address.

For the patients with coronary disease, PELATON represents an interesting new possible target with the potential to regress atherosclerosis and reduce plaque instability.

Whilst a phenotype has been well-identified, further work is now needed to understand the mechanism by which PELATON interacts with CD36, and by what pathway macrophage functions are regulated. This understanding is not absolutely necessary to bring a new drug to market, but mechanistic insights allow better prediction of clinical effects, both intended and unintended. Furthermore, a fuller appreciation of the multiple molecular interactions in this pathway, which are inevitable, widens the scope for therapeutic interventions.

Investigation into PELATON is very early stage, and several key milestones need to be achieved before it could be considered for phase 2 studies. In parallel, mechanistic and in vivo studies should be carried out. Both systemic and local delivery should be performed in animal models, and effects on vasculature, and more generally the immune system investigated.

Murine genetic knockout models are often considered at this stage but are frequently hampered by significant unintended harm to the organism, and in fact full gene knockout is quite likely to be deleterious in an important and highly expressed transcript.

If proven safe and efficacious in animal models, studies into the optimum delivery method, including bioresorbable stents would be an attractive prospect for the future.

Chapter 7 Appendix

7.1 GRACE supplementary material

Table 7-1: Performance of the GRACE 2.0 score for death and death or myocardial infarction in the Scottish cohort with and without multiple imputation.

	Scottish cohort			
	Type 1 MI		Type 2 MI	
	Complete only (n=2,538)	With imputation (n=4,981)	Complete only (n=642)	With imputation (n=1,121)
Death	378 (15%)	720 (15%)	144 (23%)	258 (23%)
AUC for Death (c-statistic)	0.85 (0.83-0.87)	0.83 (0.82-0.85)	0.71 (0.66-0.75)	0.73 (0.70-0.77)
Death or MI	560 (22%)	1,075 (22%)	166 (26%)	297 (27%)
AUC for Death or MI (c-statistic)	0.78 (0.76-0.80)	0.76 (0.74-0.77)	0.69 (0.64-0.74)	0.70 (0.67-0.74)

AUC: area under the receiver-operator-curve; HL: Hosmer-Lemeshow test.

As we used electronic records and enrolled consecutive patients into the High-STEACS trial, some variables required for the calculation of the GRACE score were missing from our dataset. This was most commonly due to the omission of routine observations which was assumed to be at random. To maximise the available dataset and to minimise bias from excluding participants, we applied multiple imputation using chained equations with five imputations of the dataset, using the mice package in R. For imputation we applied Bayesian linear regression for continuous data (creatinine, heart rate, systolic blood pressure), multinomial logistic regression for ordinal data (Killip class) and logistic regression for binary data (cardiac arrest status). Data was missing for

the following variables (n,%) ; creatinine (64, 1%), cardiac arrest status (460, 7.5%), ECG ischaemia (718, 11.8%), Killip class (1,079, 17.7%), heart rate (1,360, 22.3%) and systolic blood pressure (2,444, 40.1%).

Table 7-2: Performance of the GRACE 2.0 score for all-cause death and all-cause death or myocardial infarction at one year in the Scottish and Swedish cohorts
AUC: area under the receiver-operator-curve; CI = confidence interval, HL: Hosmer-Lemeshow test. The principle of the Hosmer-Lemeshow test is to compare the concordance between predicted and actual event rates. Based on the predicted probability, the data is divided into ten groups. In each of these groups the predicted and actual are calculated, and a χ2 statistic is calculated to compare the differences between predicted and actual event rates (sum of [actual-expected]2/expended). Small χ2 values with a p-value close to 1 indicates a good calibration

	Type 1 myocardial infarction		**Type 2 myocardial infarction**	
	Scottish cohort (n=4,981)	**Swedish cohort (n=1,080)**	**Scottish cohort (n=1,121)**	**Swedish cohort (n=247)**
All-cause death	720 (15%)	112 (10%)	258 (23%)	57 (23%)
AUC	0.83	0.85	0.73	0.73
(95% CI)	(0.82-0.85)	(0.81-0.89)	(0.70-0.77)	(0.66-0.81)
χ2 and P-value for HL	159.4 <0.001	27.3 <0.001	77.9 <0.001	54.2 <0.001
P-value for DeLong test	Reference	Reference	<0.001	0.008
All-cause death or MI	1,075 (22%)	173 (16%)	297 (27%)	63 (26%)
AUC	0.76	0.81	0.70	0.72
(95% CI)	(0.74-0.77)	(0.77-0.85)	(0.67-0.74)	(0.65-0.80)
P-value for HL	244.5 <0.001	52.9 <0.001	46.6 <0.001	14.8 0.064
P-value for DeLong test	Reference	Reference	0.007	0.042

Table 7-3: Performance of the GRACE 2.0 score for all cause death and death or myocardial infarction by sex

	Type 1 myocardial infarction				Type 2 myocardial infarction			
	Scottish cohort		Swedish cohort		Scottish cohort		Swedish cohort	
	Men (n=2,995)	Women (n=1,986)	Men (n=743)	Women (n=337)	Men (n=501)	Women (n=620)	Men (n=122)	Women (n=125)
All-cause death AUC (95% CI)	0.85 (0.83-0.87)	0.81 (0.79-0.84)	0.85 (0.81-0.90)	0.84 (0.77-0.90)	0.74 (0.69-0.78)	0.73 (0.69-0.77)	0.74 (0.65-0.84)	0.72 (0.60-0.84)
P-value for DeLong test (Men versus Women)	0.04		0.70		0.86		0.77	
All-cause death or MI AUC (95% CI)	0.76 (0.74-0.78)	0.74 (0.72-0.77)	0.81 (0.77-0.86)	0.79 (0.73-0.86)	0.71 (0.66-0.76)	0.70 (0.65-0.74)	0.76 (0.66-0.85)	0.69 (0.57-0.80)
P-value for DeLong test	0.23		0.61		0.59		0.36	

	Low Risk GRACE (<3%)		Intermediate Risk GRACE (≥3 and ≤8%)		High Risk GRACE (>8%)	
	Type 1 MI	**Type 2 MI**	**Type 1 MI**	**Type 2 MI**	**Type 1 MI**	**Type 2 MI**
No. of participants (%)	1,826 (37)	131 (12)	1,511 (30)	305 (27)	1,644 (33)	685 (61)
Age (years), mean (SD)	55 (9)	51 (12)	70 (9)	68 (10)	80 (10)	81 (9)
Men, n (%)	1281 (70)	54 (41)	861 (57)	156 (51)	853 (52)	291 (42)
Past medical history						
Myocardial infarction, n (%)	194 (11)	6 (5)	188 (12)	45 (15)	285 (17)	112 (16)
Ischemic heart disease, n (%)	335 (18)	12 (9)	485 (32)	111 (36)	699 (43)	331 (48)
Cerebrovascular disease, n (%)	49 (3)	5 (4)	97 (6)	23 (8)	222 (14)	107 (16)
Diabetes mellitus, n (%)	205 (11)	6 (5)	264 (17)	35 (11)	333 (20)	106 (15)
Heart failure hospitalisation, n (%)	89 (5)	6 (5)	207 (14)	61 (20)	496 (30)	225 (33)
New medication						
Aspirin, n (%)	1217 (67)	33 (25)	635 (42)	40 (13)	388 (24)	44 (6)
DAPT, n (%)	1409 (77)	20 (15)	928 (61)	35 (11)	632 (38)	61 (9)
Statin, n (%)	1020 (56)	15 (11)	501 (33)	27 (9)	243 (15)	26 (4)
ACE inhibitor or ARB, n (%)	886 (49)	20 (15)	473 (31)	33 (11)	218 (13)	51 (7)
Beta-blocker, n (%)	961 (53)	39 (30)	560 (37)	74 (24)	357 (22)	106 (15)
Oral anti-coagulant, n (%)‡	18 (1)	23 (18)	55 (4)	62 (20)	56 (3)	124 (18)
Electrocardiogram§						
Myocardial ischemia	671 (37)	35 (27)	551 (36)	103 (34)	650 (40)	245 (36)
Physiological parameters§						
Heart rate, beats per minute	74 (16)	93 (36)	77 (19)	108 (40)	86 (21)	105 (32)
Systolic blood pressure, mmHg	149 (25)	148 (26)	142 (26)	140 (29)	134 (30)	126 (29)
Hematology and clinical chemistry						
Haemoglobin, g/L	146 (18)	138 (24)	136 (21)	132 (30)	126 (23)	120 (29)

eGFR, ml/min	59 (7)	56 (12)	54 (12)	54 (11)	43 (15)	42 (15)
Peak hs-cTn, ng/L	808 [132, 6255]	111 [44, 513]	787 [92, 5437]	128 [45, 672]	1063 [93, 8626]	124 [51, 609]

Table 7-4: Characteristics of Scottish cohort stratified by low, intermediate and high GRACE risk categories.

Table 7-5: Performance of GRACE 2.0 for the prediction of in-hospital death in the Scottish and the Swedish cohorts

	Scottish cohort		**Swedish cohort**	
	Type 1 MI (n=4,981)	**Type 2 MI (n=1,121)**	**Type 1 MI (n=1,080)**	**Type 2 MI (n=247)**
In-hospital death n (%)	74 (1.5)	25 (2.2)	27 (2.5)	14 (5.7)
AUC (95% CI)	0.85 (0.81-0.89)	0.67 (0.57-0.78)	0.85 (0.78-0.93)	0.82 (0.70-0.94)
$\chi 2$ and P-value for HL	100 <0.001	50 <0.001	26 0.01	444 <0.001
P value for DeLong test	0.002		0.65	

Table 7-6: Performance of high-sensitivity cardiac troponin assays alone for the prediction of death at one year

	Scottish cohort		**Swedish cohort**	
	Type 1 MI (n=4,981)	**Type 2 MI (n=1,121)**	**Type 1 MI (n=1,080)**	**Type 2 MI (n=247)**
Death at one year AUC (95% CI)	0.58 (0.56-0.61)	0.62 (0.58-0.65)	0.64 (0.58-0.69)	0.72 (0.65-0.80)
P value for DeLong test	0.18		0.65	

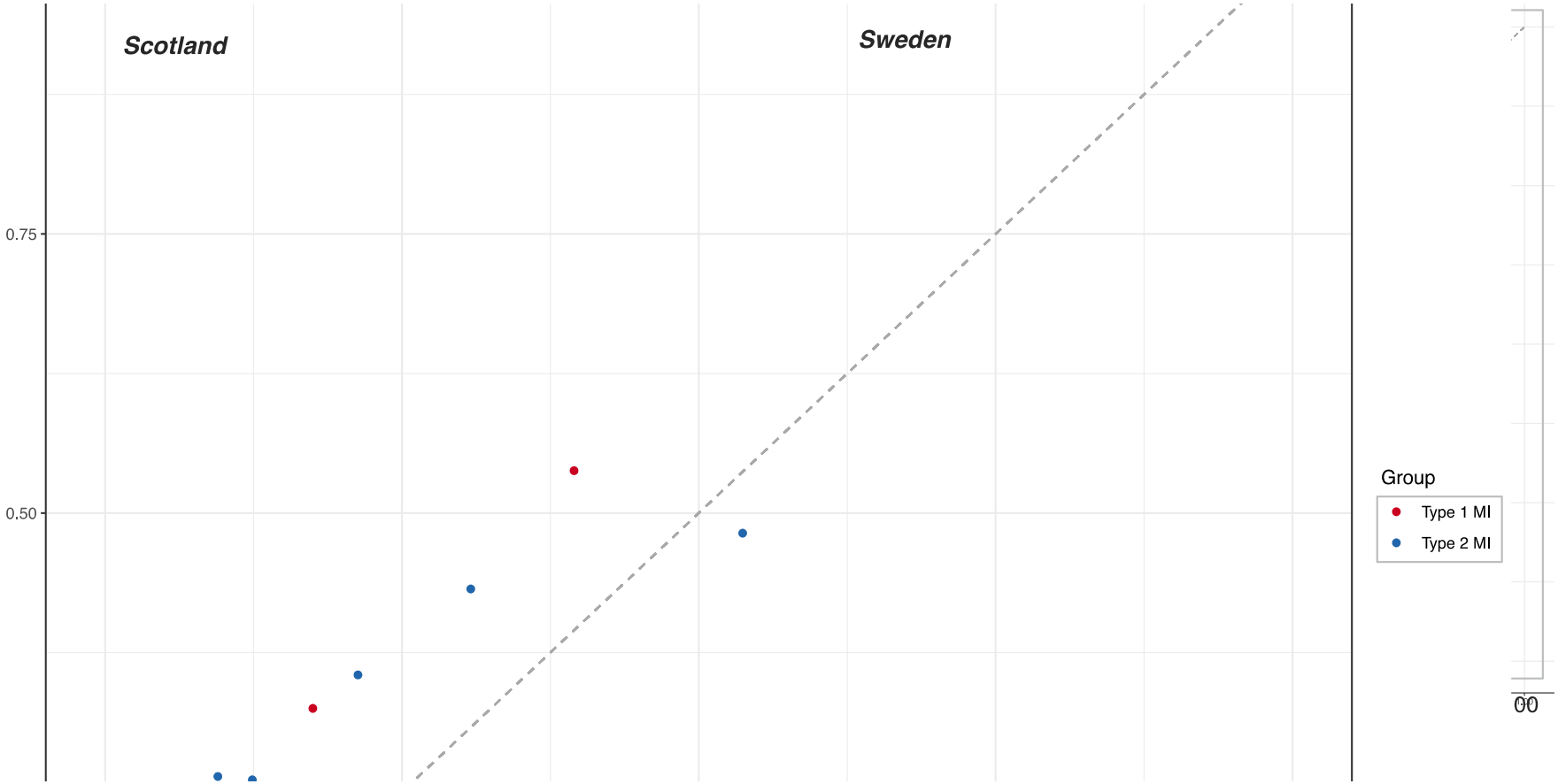

Figure 7-1: Observed versus predicted all-cause mortality or myocardial infarction events in type 1 and type 2 myocardial infarction according to the GRACE 2.0 algorithm in the Scottish and Swedish cohorts.

7.2 LINC01094 Data

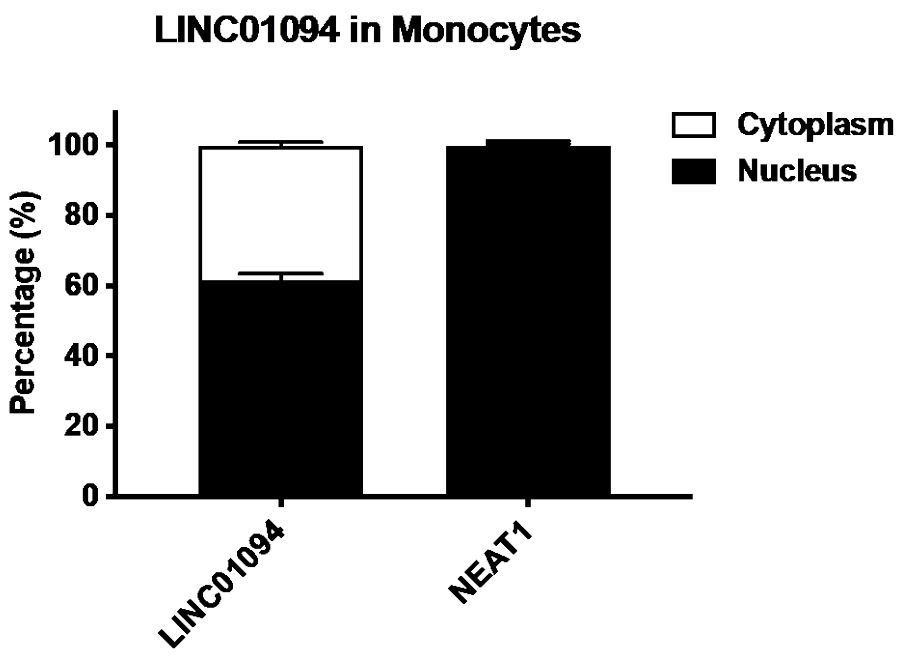

Figure 7-2: Intracellular localisation of LINC01094 in monocytes.
Fractionation by PARIS kit and RTqPCR demonstrates intra cellular localisation of LINC01272 is xx% nuclear in monocytes (n=3 technical replicates).

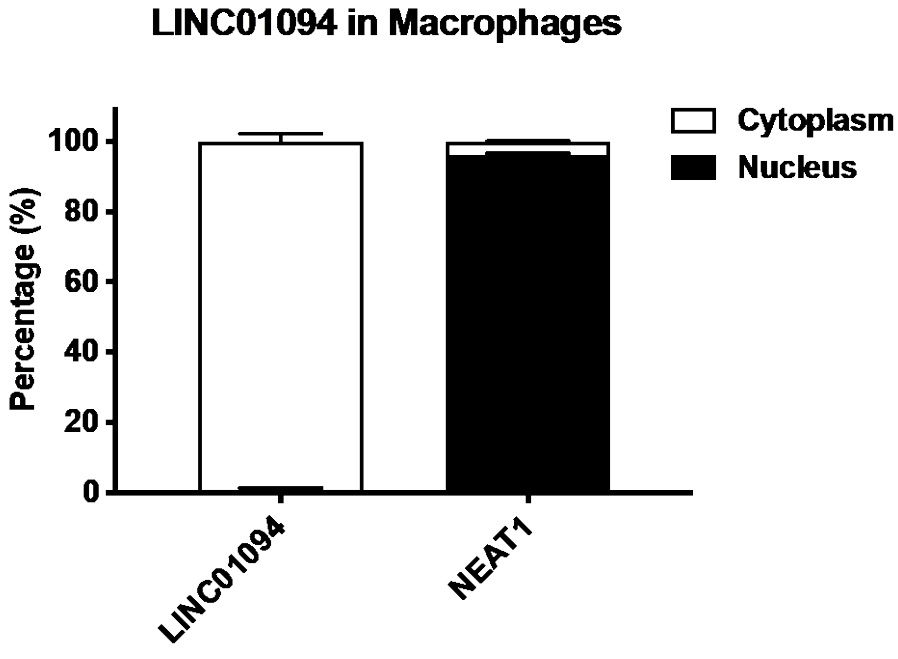

Figure 7-3: Intracellular localisation of LINC01094 in macrophages.

Fractionation by PARIS kit and RTqPCR demonstrates intra cellular localisation of LINC01272 is x% nuclear in macrophages (n=3 technical replicates).

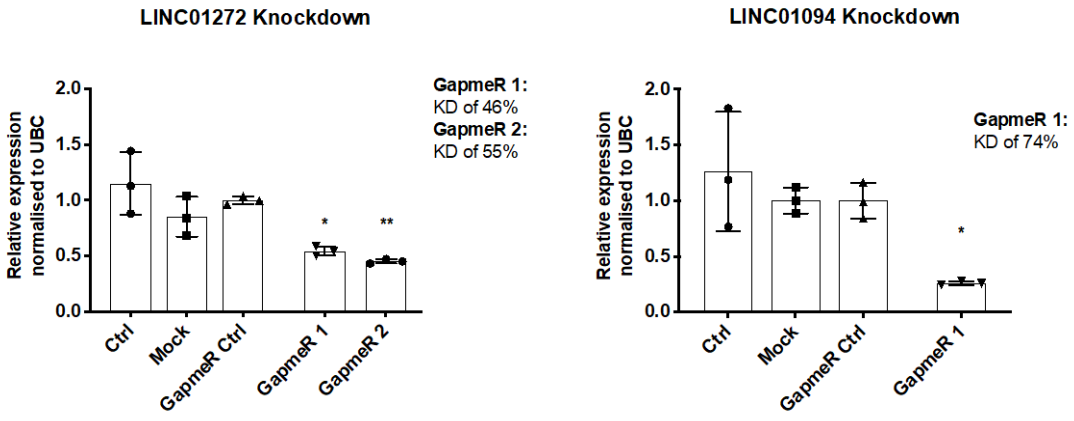

Bibliography

Publications

Hung J, Roos A, Kadesjö E et al. Performance of the GRACE 2.0 score in patients with type 1 and type 2 myocardial infarction.
European Heart Journal,
ehaa375, https://doi.org/10.1093/eurheartj/ehaa375

Hung J, Scanlon JP, Mahmoud AD, et al. Novel Plaque Enriched Long Noncoding RNA in Atherosclerotic Macrophage Regulation (PELATON).
Arterioscler Thromb Vasc Biol. 2020;40(3):697-713.
doi:10.1161/ATVBAHA.119.313430

Hung J, Miscianinov V, Sluimer JC, Newby DE, Baker AH. Targeting Non-coding RNA in Vascular Biology and Disease.
Frontiers in Physiology. 2018;9:1655. Published 2018 Nov 22.
doi:10.3389/fphys.2018.01655

Rashdan NA, Sim AM, Cui L, **Hung J** et al. Osteocalcin Regulates Arterial Calcification Via Altered Wnt Signaling and Glucose Metabolism.
J Bone Miner Res. 2020;35(2):357-367. doi:10.1002/jbmr.3888

Mahmoud AD, Ballantyne MD, Miscianinov V, **Hung J** et al. The Human-Specific and Smooth Muscle Cell-Enriched LncRNA SMILR Promotes Proliferation by Regulating Mitotic CENPF mRNA and Drives Cell-Cycle Progression Which Can Be Targeted to Limit Vascular Remodeling.
Circulation Research. 2019;125(5):535-551.
doi:10.1161/CIRCRESAHA.119.314876

Thompson CS, Pass M, Timothy T, **Hung J**, Egred M. Acute myocardial infarction in a young elite cyclist: a missed opportunity.
BMJ Case Rep. 2019;12(9):e228560. Published 2019 Sep 6.
doi:10.1136/bcr-2018-228560

Shah ASV, Anand A, Strachan FE, Ferry AV, Lee KK, Chapman AR, Sandeman D, Stables CL, Adamson PD, Andrews JPM, Anwar MS, **Hung J**, Moss AJ, O'Brien R, Berry C, Findlay I, Walker S, Cruickshank A, Reid A, Gray A, Collinson PO, Apple FS, McAllister DA, Maguire D, Fox KAA, Newby DE, Tuck C, Harkess R, Parker RA, Keerie C, Weir CJ, Mills NL.Investigators H-S. High-sensitivity troponin in the evaluation of patients with suspected acute coronary syndrome: A stepped-wedge, cluster-randomised controlled trial.
Lancet. 2018;392:919-928

Abstracts

J Hung, A Roos, E Kadesjo, D McAllister, ASV Shah, A Anand, FE Strachan, KA Fox, NL Mills, M Holzmann, AR Chapman. Performance of the grace 2.0 score in patients with type 1 and type 2 myocardial infarction**.**
Virtual abstract at BCS 2020

J Hung, A Roos, ASV Shah, A Anand, FE Strachan, KA Fox, NL Mills, AR Chapman, M Holzmann, on behalf of the High-STEACS Investigators. Performance of the GRACE score in patients with type 1 and type 2 myocardial infarction.
Presented at ESC 2019, Paris

J Hung, J Rodor, JP Scanlon, AD Mahmoud, M Fontaine, L Temmerman, J Kacynski, A Tavares, M Ballantyne, K Pinel, R Bhushan, DE Newby, EAL. Biessen, JC Sluimer, AH Baker. A novel macrophage long non-coding RNA in atherosclerosis.
Presented at ESM-EVBO Conference 2019, Maastricht.

J Hung, R Bhushan, J Rodor, K Pinel, M Ballantyne, A Mahmoud, A Tavares, J Kaczynski, JC Sluimer, D Newby, AH. Baker A novel macrophage long non-coding RNA in atherosclerosis.
Presented at Edinburgh Cardiovascular Centre Symposium June 2018. (Poster prize runner-up)

J Hung, S Murray, M Shaw, D Unwin. Moderated poster presentation, Impact of a low carbohydrate diet on traditional CVD risk factors in people with features of the metabolic syndrome and type 2 diabetes.
Presented at EuroPrevent, Slovenia, June 2018.

J Hung, R Bhushan, J Rodor et al. Integrative systems approach identifies novel lncRNA transcripts during atherosclerotic plaque development.
Presented at Non-Coding RNA Biochemistry Society Conference, Edinburgh, June 2017

J Hung, R Bhushan, J Rodor et al. Discovery of Novel Long Non-Coding RNAs: Therapeutic Targets in Atherosclerosis.
Presented at Edinburgh Cardiovascular Centre Symposium June 2017.

J Hung, S Murray, D Unwin et al. Impact of a low carbohydrate diet on traditional CVD risk factors in people with features of the metabolic syndrome and type 2 diabetes.
Moderated Poster presented at EuroPrevent, Slovenia, June 2018.

N Rashdan, A Sim, P Hohenstein, **J Hung** et al. Osteocalcin Regulates Arterial Calcification via altered Wnt signalling and Glucose Metabolism.

Presented at Bone Research Society, June 2018.

J Harrington, B Whittington, **J Hung** et al. The accuracy of hand-held echocardiography performed by non-cardiologists with limited echocardiography training.
Oral presentation at Scottish Cardiac Society, September 2018.

References

1. Sesso HD, Lee IM, Gaziano JM, Rexrode KM, Glynn RJ, Buring JE. Maternal and paternal history of myocardial infarction and risk of cardiovascular disease in men and women. Circulation. 2001;104(4):393-8.
2. O'Donnell CJ. Family history, subclinical atherosclerosis, and coronary heart disease risk: barriers and opportunities for the use of family history information in risk prediction and prevention. Circulation. 2004;110(15):2074-6.
3. Nasir K, Michos ED, Rumberger JA, Braunstein JB, Post WS, Budoff MJ, et al. Coronary artery calcification and family history of premature coronary heart disease: sibling history is more strongly associated than parental history. Circulation. 2004;110(15):2150-6.
4. De Castro-Orós I, Pocoví M, Civeira F. The genetic basis of familial hypercholesterolemia: inheritance, linkage, and mutations. Appl Clin Genet. 2010;3:53-64.
5. Brown MS, Goldstein JL. A receptor-mediated pathway for cholesterol homeostasis. Science. 1986;232(4746):34-47.
6. Ose L. [Müller-Harbitz disease--familial hypercholesterolemia]. Tidsskr Nor Laegeforen. 2002;122(9):924-5.
7. DuBroff R, de Lorgeril M. Fat or fiction: the diet-heart hypothesis. BMJ Evidence-Based Medicine. 2019:bmjebm-2019-111180.
8. Sturm AC, Knowles JW, Gidding SS, Ahmad ZS, Ahmed CD, Ballantyne CM, et al. Clinical Genetic Testing for Familial Hypercholesterolemia: JACC Scientific Expert Panel. J Am Coll Cardiol. 2018;72(6):662-80.
9. England N. Cardiovascular disease (CVD): Our ambition for CVD prevention [Available from: https://www.england.nhs.uk/ourwork/clinical-policy/cvd/.
10. Organisation) WWH. Raised cholesterol, Global Health Observatory data. 2020.
11. KANNEL WB, DAWBER TR, FRIEDMAN GD, GLENNON WE, MCNAMARA PM. RISK FACTORS IN CORONARY HEART DISEASE. AN EVALUATION OF SEVERAL SERUM LIPIDS AS PREDICTORS OF CORONARY HEART DISEASE; THE FRAMINGHAM STUDY. Ann Intern Med. 1964;61:888-99.
12. BJC. lipid metabolism and its role in atherosclerosis [Available from: https://bjcardio.co.uk/2015/07/lipids-module-1-lipid-metabolism-and-its-role-in-atherosclerosis-3/.
13. Chiva-Blanch G, Badimon L. Cross-Talk between Lipoproteins and Inflammation: The Role of Microvesicles. J Clin Med. 2019;8(12).
14. Stock J. Triglycerides and cardiovascular risk: Apolipoprotein B holds the key. Atherosclerosis. 2019;284:221-2.
15. Majesky MW, Dong XR, Hoglund V, Mahoney WM, Daum G. The adventitia: a dynamic interface containing resident progenitor cells. Arterioscler Thromb Vasc Biol. 2011;31(7):1530-9.
16. Virmani R, Kolodgie FD, Burke AP, Farb A, Schwartz SM. Lessons from sudden coronary death: a comprehensive morphological classification

scheme for atherosclerotic lesions. Arterioscler Thromb Vasc Biol. 2000;20(5):1262-75.
17. Velican D, Velican C. Atherosclerotic involvement of the coronary arteries of adolescents and young adults. Atherosclerosis. 1980;36(4):449-60.
18. VanderLaan PA, Reardon CA, Getz GS. Site specificity of atherosclerosis: site-selective responses to atherosclerotic modulators. Arterioscler Thromb Vasc Biol. 2004;24(1):12-22.
19. Bonetti PO, Lerman LO, Lerman A. Endothelial dysfunction: a marker of atherosclerotic risk. Arterioscler Thromb Vasc Biol. 2003;23(2):168-75.
20. Galkina E, Ley K. Vascular adhesion molecules in atherosclerosis. Arterioscler Thromb Vasc Biol. 2007;27(11):2292-301.
21. Libby P, Buring JE, Badimon L, Hansson GK, Deanfield J, Bittencourt MS, et al. Atherosclerosis. Nature Reviews Disease Primers. 2019;5(1):56.
22. Newby AC, George SJ, Ismail Y, Johnson JL, Sala-Newby GB, Thomas AC. Vulnerable atherosclerotic plaque metalloproteinases and foam cell phenotypes. Thromb Haemost. 2009;101(6):1006-11.
23. Woollard KJ, Geissmann F. Monocytes in atherosclerosis: subsets and functions. Nat Rev Cardiol. 2010;7(2):77-86.
24. Ley K, Miller YI, Hedrick CC. Monocyte and macrophage dynamics during atherogenesis. Arterioscler Thromb Vasc Biol. 2011;31(7):1506-16.
25. Gomez D, Owens GK. Smooth muscle cell phenotypic switching in atherosclerosis. Cardiovasc Res. 2012;95(2):156-64.
26. Allahverdian S, Chehroudi AC, McManus BM, Abraham T, Francis GA. Contribution of intimal smooth muscle cells to cholesterol accumulation and macrophage-like cells in human atherosclerosis. Circulation. 2014;129(15):1551-9.
27. Robbins CS, Hilgendorf I, Weber GF, Theurl I, Iwamoto Y, Figueiredo JL, et al. Local proliferation dominates lesional macrophage accumulation in atherosclerosis. Nat Med. 2013;19(9):1166-72.
28. Ruiz JL, Hutcheson JD, Aikawa E. Cardiovascular calcification: current controversies and novel concepts. Cardiovasc Pathol. 2015;24(4):207-12.
29. Huang H, Virmani R, Younis H, Burke AP, Kamm RD, Lee RT. The impact of calcification on the biomechanical stability of atherosclerotic plaques. Circulation. 2001;103(8):1051-6.
30. Aschoff L. Atherosclerosis. Lectures on Pathology. New York.1924. p. p. 131-53.
31. Arbab-Zadeh A, Nakano M, Virmani R, Fuster V. Acute coronary events. Circulation. 2012;125(9):1147-56.
32. Libby P. Mechanisms of acute coronary syndromes and their implications for therapy. N Engl J Med. 2013;368(21):2004-13.
33. Falk E, Nakano M, Bentzon JF, Finn AV, Virmani R. Update on acute coronary syndromes: the pathologists' view. Eur Heart J. 2013;34(10):719-28.
34. Libby P, Theroux P. Pathophysiology of coronary artery disease. Circulation. 2005;111(25):3481-8.

35. Davies MJ. Anatomic features in victims of sudden coronary death. Coronary artery pathology. Circulation. 1992;85(1 Suppl):I19-24.
36. Virmani R, Burke AP, Farb A, Kolodgie FD. Pathology of the vulnerable plaque. J Am Coll Cardiol. 2006;47(8 Suppl):C13-8.
37. Wilcox JN, Smith KM, Schwartz SM, Gordon D. Localization of tissue factor in the normal vessel wall and in the atherosclerotic plaque. Proc Natl Acad Sci U S A. 1989;86(8):2839-43.
38. Drake TA, Morrissey JH, Edgington TS. Selective cellular expression of tissue factor in human tissues. Implications for disorders of hemostasis and thrombosis. Am J Pathol. 1989;134(5):1087-97.
39. Yonetsu T, Kakuta T, Lee T, Takahashi K, Kawaguchi N, Yamamoto G, et al. In vivo critical fibrous cap thickness for rupture-prone coronary plaques assessed by optical coherence tomography. Eur Heart J. 2011;32(10):1251-9.
40. Amento EP, Ehsani N, Palmer H, Libby P. Cytokines and growth factors positively and negatively regulate interstitial collagen gene expression in human vascular smooth muscle cells. Arterioscler Thromb. 1991;11(5):1223-30.
41. Bauriedel G, Hutter R, Welsch U, Bach R, Sievert H, Lüderitz B. Role of smooth muscle cell death in advanced coronary primary lesions: implications for plaque instability. Cardiovasc Res. 1999;41(2):480-8.
42. Galis ZS, Sukhova GK, Lark MW, Libby P. Increased expression of matrix metalloproteinases and matrix degrading activity in vulnerable regions of human atherosclerotic plaques. J Clin Invest. 1994;94(6):2493-503.
43. Nikkari ST, O'Brien KD, Ferguson M, Hatsukami T, Welgus HG, Alpers CE, et al. Interstitial collagenase (MMP-1) expression in human carotid atherosclerosis. Circulation. 1995;92(6):1393-8.
44. Herman MP, Sukhova GK, Libby P, Gerdes N, Tang N, Horton DB, et al. Expression of neutrophil collagenase (matrix metalloproteinase-8) in human atheroma: a novel collagenolytic pathway suggested by transcriptional profiling. Circulation. 2001;104(16):1899-904.
45. Shah PK, Falk E, Badimon JJ, Fernandez-Ortiz A, Mailhac A, Villareal-Levy G, et al. Human monocyte-derived macrophages induce collagen breakdown in fibrous caps of atherosclerotic plaques. Potential role of matrix-degrading metalloproteinases and implications for plaque rupture. Circulation. 1995;92(6):1565-9.
46. Falk E, Shah PK, Fuster V. Coronary plaque disruption. Circulation. 1995;92(3):657-71.
47. Libby P. The molecular mechanisms of the thrombotic complications of atherosclerosis. J Intern Med. 2008;263(5):517-27.
48. Braunwald E. Coronary plaque erosion: recognition and management. JACC Cardiovasc Imaging. 2013;6(3):288-9.
49. Holmes DR, Lerman A, Moreno PR, King SB, Sharma SK. Diagnosis and management of STEMI arising from plaque erosion. JACC Cardiovasc Imaging. 2013;6(3):290-6.
50. Ozaki Y, Okumura M, Ismail TF, Motoyama S, Naruse H, Hattori K, et al. Coronary CT angiographic characteristics of culprit lesions in acute

coronary syndromes not related to plaque rupture as defined by optical coherence tomography and angioscopy. Eur Heart J. 2011;32(22):2814-23.
51. Kubo T, Imanishi T, Takarada S, Kuroi A, Ueno S, Yamano T, et al. Assessment of culprit lesion morphology in acute myocardial infarction: ability of optical coherence tomography compared with intravascular ultrasound and coronary angioscopy. J Am Coll Cardiol. 2007;50(10):933-9.
52. Clarkson TB, Prichard RW, Morgan TM, Petrick GS, Klein KP. Remodeling of coronary arteries in human and nonhuman primates. JAMA. 1994;271(4):289-94.
53. Glagov S, Weisenberg E, Zarins CK, Stankunavicius R, Kolettis GJ. Compensatory enlargement of human atherosclerotic coronary arteries. N Engl J Med. 1987;316(22):1371-5.
54. Stone GW, Maehara A, Lansky AJ, de Bruyne B, Cristea E, Mintz GS, et al. A prospective natural-history study of coronary atherosclerosis. N Engl J Med. 2011;364(3):226-35.
55. Mann J, Davies MJ. Mechanisms of progression in native coronary artery disease: role of healed plaque disruption. Heart. 1999;82(3):265-8.
56. Burke AP, Kolodgie FD, Farb A, Weber DK, Malcom GT, Smialek J, et al. Healed plaque ruptures and sudden coronary death: evidence that subclinical rupture has a role in plaque progression. Circulation. 2001;103(7):934-40.
57. Bruschke AV, Kramer JR, Bal ET, Haque IU, Detrano RC, Goormastic M. The dynamics of progression of coronary atherosclerosis studied in 168 medically treated patients who underwent coronary arteriography three times. Am Heart J. 1989;117(2):296-305.
58. Chatzizisis YS, Baker AB, Sukhova GK, Koskinas KC, Papafaklis MI, Beigel R, et al. Augmented expression and activity of extracellular matrix-degrading enzymes in regions of low endothelial shear stress colocalize with coronary atheromata with thin fibrous caps in pigs. Circulation. 2011;123(6):621-30.
59. Maldonado N, Kelly-Arnold A, Vengrenyuk Y, Laudier D, Fallon JT, Virmani R, et al. A mechanistic analysis of the role of microcalcifications in atherosclerotic plaque stability: potential implications for plaque rupture. 2012;303(5):H619-28.
60. Dutta P, Courties G, Wei Y, Leuschner F, Gorbatov R, Robbins CS, et al. Myocardial infarction accelerates atherosclerosis. Nature. 2012;487(7407):325-9.
61. Mittleman MA, Mostofsky E. Physical, psychological and chemical triggers of acute cardiovascular events: preventive strategies. Circulation. 2011;124(3):346-54.
62. Muller JE, Stone PH, Turi ZG, Rutherford JD, Czeisler CA, Parker C, et al. Circadian variation in the frequency of onset of acute myocardial infarction. N Engl J Med. 1985;313(21):1315-22.
63. Bentzon JF, Otsuka F, Virmani R, Falk E. Mechanisms of plaque formation and rupture. Circ Res. 2014;114(12):1852-66.
64. Motoyama S, Sarai M, Harigaya H, Anno H, Inoue K, Hara T, et al. Computed tomographic angiography characteristics of atherosclerotic

plaques subsequently resulting in acute coronary syndrome. J Am Coll Cardiol. 2009;54(1):49-57.
65. Hoffmann U, Moselewski F, Nieman K, Jang IK, Ferencik M, Rahman AM, et al. Noninvasive assessment of plaque morphology and composition in culprit and stable lesions in acute coronary syndrome and stable lesions in stable angina by multidetector computed tomography. J Am Coll Cardiol. 2006;47(8):1655-62.
66. Narula J, Achenbach S. Napkin-ring necrotic cores: defining circumferential extent of necrotic cores in unstable plaques. JACC Cardiovasc Imaging. 2009;2(12):1436-8.
67. Kashiwagi M, Tanaka A, Kitabata H, Tsujioka H, Kataiwa H, Komukai K, et al. Feasibility of noninvasive assessment of thin-cap fibroatheroma by multidetector computed tomography. JACC Cardiovasc Imaging. 2009;2(12):1412-9.
68. Sabatine MS, Giugliano RP, Keech AC, Honarpour N, Wiviott SD, Murphy SA, et al. Evolocumab and Clinical Outcomes in Patients with Cardiovascular Disease. N Engl J Med. 2017;376(18):1713-22.
69. Schwartz GG, Bessac L, Berdan LG, Bhatt DL, Bittner V, Diaz R, et al. Effect of alirocumab, a monoclonal antibody to PCSK9, on long-term cardiovascular outcomes following acute coronary syndromes: rationale and design of the ODYSSEY outcomes trial. Am Heart J. 2014;168(5):682-9.
70. Ridker PM, Everett BM, Thuren T, MacFadyen JG, Chang WH, Ballantyne C, et al. Antiinflammatory Therapy with Canakinumab for Atherosclerotic Disease. N Engl J Med. 2017;377(12):1119-31.
71. Thygesen K, Alpert JS, White HD, Jaffe AS, Apple FS, Galvani M, et al. Universal definition of myocardial infarction. Circulation. 2007;116(22):2634-53.
72. Shah AS, McAllister DA, Mills R, Lee KK, Churchhouse AM, Fleming KM, et al. Sensitive troponin assay and the classification of myocardial infarction. Am J Med. 2015;128(5):493-501.e3.
73. Sandoval Y, Thygesen K. Myocardial Infarction Type 2 and Myocardial Injury. Clin Chem. 2017;63(1):101-7.
74. Thygesen K, Alpert JS, Jaffe AS, Chaitman BR, Bax JJ, Morrow DA, et al. Fourth universal definition of myocardial infarction (2018). Eur Heart J. 2019;40(3):237-69.
75. Chapman AR, Shah ASV, Lee KK, Anand A, Francis O, Adamson P, et al. Long-Term Outcomes in Patients With Type 2 Myocardial Infarction and Myocardial Injury. Circulation. 2018;137(12):1236-45.
76. Shah ASV, Anand A, Strachan FE, Ferry AV, Lee KK, Chapman AR, et al. High-sensitivity troponin in the evaluation of patients with suspected acute coronary syndrome: a stepped-wedge, cluster-randomised controlled trial. Lancet. 2018;392(10151):919-28.
77. Januzzi JL, Sandoval Y. The Many Faces of
Type 2 Myocardial Infarction. J Am Coll Cardiol. 2017;70(13):1569-72.
78. Sandoval Y, Smith SW, Thordsen SE, Apple FS. Supply/demand type 2 myocardial infarction: should we be paying more attention? J Am Coll Cardiol. 2014;63(20):2079-87.

79. Uchida S, Dimmeler S. Long noncoding RNAs in cardiovascular diseases. Circ Res. 2015;116(4):737-50.
80. Taft RJ, Pheasant M, Mattick JS. The relationship between non-protein-coding DNA and eukaryotic complexity. Bioessays. 2007;29(3):288-99.
81. Jonas S, Izaurralde E. Towards a molecular understanding of microRNA-mediated gene silencing. Nat Rev Genet. 2015;16(7):421-33.
82. Lu Y, Thavarajah T, Gu W, Cai J, Xu Q. Impact of miRNA in Atherosclerosis. Arterioscler Thromb Vasc Biol. 2018;38(9):e159-e70.
83. Bostjancic E, Zidar N, Stajer D, Glavac D. MicroRNAs miR-1, miR-133a, miR-133b and miR-208 are dysregulated in human myocardial infarction. Cardiology. 2010;115(3):163-9.
84. Hayes J, Peruzzi PP, Lawler S. MicroRNAs in cancer: biomarkers, functions and therapy. Trends Mol Med. 2014;20(8):460-9.
85. Christopher AF, Kaur RP, Kaur G, Kaur A, Gupta V, Bansal P. MicroRNA therapeutics: Discovering novel targets and developing specific therapy. Perspect Clin Res. 2016;7(2):68-74.
86. Lee RC, Feinbaum RL, Ambros V. The C. elegans heterochronic gene lin-4 encodes small RNAs with antisense complementarity to lin-14. Cell. 1993;75(5):843-54.
87. Ozsolak F, Poling LL, Wang Z, Liu H, Liu XS, Roeder RG, et al. Chromatin structure analyses identify miRNA promoters. Genes & development. 2008;22(22):3172-83.
88. Monteys AM, Spengler RM, Wan J, Tecedor L, Lennox KA, Xing Y, et al. Structure and activity of putative intronic miRNA promoters. RNA (New York, NY). 2010;16(3):495-505.
89. Lee Y, Kim M, Han J, Yeom KH, Lee S, Baek SH, et al. MicroRNA genes are transcribed by RNA polymerase II. The EMBO journal. 2004;23(20):4051-60.
90. Lee Y, Ahn C, Han J, Choi H, Kim J, Yim J, et al. The nuclear RNase III Drosha initiates microRNA processing. Nature. 2003;425(6956):415-9.
91. Bohnsack MT, Czaplinski K, Gorlich D. Exportin 5 is a RanGTP-dependent dsRNA-binding protein that mediates nuclear export of pre-miRNAs. RNA (New York, NY). 2004;10(2):185-91.
92. Lund E, Guttinger S, Calado A, Dahlberg JE, Kutay U. Nuclear export of microRNA precursors. Science (New York, NY). 2004;303(5654):95-8.
93. Huntzinger E, Izaurralde E. Gene silencing by microRNAs: contributions of translational repression and mRNA decay. Nat Rev Genet. 2011;12(2):99-110.
94. Meijer Hedda A, Smith Ewan M, Bushell M. Regulation of miRNA strand selection: follow the leader? Biochemical Society Transactions. 2014;42(4):1135-40.
95. Fabian MR, Sonenberg N. The mechanics of miRNA-mediated gene silencing: a look under the hood of miRISC. Nature structural & molecular biology. 2012;19(6):586-93.
96. Eichhorn Stephen W, Guo H, McGeary Sean E, Rodriguez-Mias Ricard A, Shin C, Baek D, et al. mRNA Destabilization Is the Dominant Effect

of Mammalian MicroRNAs by the Time Substantial Repression Ensues. Molecular cell. 2014;56(1):104-15.
97. Mercer TR, Dinger ME, Mattick JS. Long non-coding RNAs: insights into functions. Nat Rev Genet. 2009;10(3):155-9.
98. Ponting CP, Oliver PL, Reik W. Evolution and functions of long noncoding RNAs. Cell. 2009;136(4):629-41.
99. Clark MB, Mercer TR, Bussotti G, Leonardi T, Haynes KR, Crawford J, et al. Quantitative gene profiling of long noncoding RNAs with targeted RNA sequencing. Nature methods. 2015;12(4):339-42.
100. Quinn JJ, Chang HY. Unique features of long non-coding RNA biogenesis and function. Nat Rev Genet. 2016;17(1):47-62.
101. Gascoigne DK, Cheetham SW, Cattenoz PB, Clark MB, Amaral PP, Taft RJ, et al. Pinstripe: a suite of programs for integrating transcriptomic and proteomic datasets identifies novel proteins and improves differentiation of protein-coding and non-coding genes. Bioinformatics (Oxford, England). 2012;28(23):3042-50.
102. Makarewich CA, Olson EN. Mining for Micropeptides. Trends in cell biology. 2017;27(9):685-96.
103. Anderson DM, Anderson KM, Chang CL, Makarewich CA, Nelson BR, McAnally JR, et al. A micropeptide encoded by a putative long noncoding RNA regulates muscle performance. Cell. 2015;160(4):595-606.
104. Matsumoto A, Pasut A, Matsumoto M, Yamashita R, Fung J, Monteleone E, et al. mTORC1 and muscle regeneration are regulated by the LINC00961-encoded SPAR polypeptide. Nature. 2016;541:228.
105. Spencer HL, Sanders R, Boulberdaa M, Meloni M, Cochrane A, Spiroski AM, et al. The LINC00961 transcript and its encoded micropeptide, small regulatory polypeptide of amino acid response, regulate endothelial cell function. Cardiovasc Res. 2020;116(12):1981-94.
106. Wu H, Yang L, Chen LL. The Diversity of Long Noncoding RNAs and Their Generation. Trends in genetics : TIG. 2017;33(8):540-52.
107. Hangauer MJ, Vaughn IW, McManus MT. Pervasive transcription of the human genome produces thousands of previously unidentified long intergenic noncoding RNAs. PLoS genetics. 2013;9(6):e1003569.
108. Wu H, Yin QF, Luo Z, Yao RW, Zheng CC, Zhang J, et al. Unusual Processing Generates SPA LncRNAs that Sequester Multiple RNA Binding Proteins. Molecular cell. 2016;64(3):534-48.
109. Yin QF, Yang L, Zhang Y, Xiang JF, Wu YW, Carmichael GG, et al. Long noncoding RNAs with snoRNA ends. Molecular cell. 2012;48(2):219-30.
110. Memczak S, Jens M, Elefsinioti A, Torti F, Krueger J, Rybak A, et al. Circular RNAs are a large class of animal RNAs with regulatory potency. Nature. 2013;495(7441):333-8.
111. Zhang Y, Zhang XO, Chen T, Xiang JF, Yin QF, Xing YH, et al. Circular intronic long noncoding RNAs. Molecular cell. 2013;51(6):792-806.
112. Zhang XO, Wang HB, Zhang Y, Lu X, Chen LL, Yang L. Complementary sequence-mediated exon circularization. Cell. 2014;159(1):134-47.

113. Zhang K, Shi ZM, Chang YN, Hu ZM, Qi HX, Hong W. The ways of action of long non-coding RNAs in cytoplasm and nucleus. Gene. 2014;547(1):1-9.
114. Kotake Y, Nakagawa T, Kitagawa K, Suzuki S, Liu N, Kitagawa M, et al. Long non-coding RNA ANRIL is required for the PRC2 recruitment to and silencing of p15INK4B tumor suppressor gene. Oncogene. 2010;30:1956.
115. Kim TK, Hemberg M, Gray JM, Costa AM, Bear DM, Wu J, et al. Widespread transcription at neuronal activity-regulated enhancers. Nature. 2010;465(7295):182-7.
116. Mousavi K, Zare H, Dell'orso S, Grontved L, Gutierrez-Cruz G, Derfoul A, et al. eRNAs promote transcription by establishing chromatin accessibility at defined genomic loci. Molecular cell. 2013;51(5):606-17.
117. Li W, Notani D, Ma Q, Tanasa B, Nunez E, Chen AY, et al. Functional roles of enhancer RNAs for oestrogen-dependent transcriptional activation. Nature. 2013;498(7455):516-20.
118. Orom UA, Derrien T, Beringer M, Gumireddy K, Gardini A, Bussotti G, et al. Long noncoding RNAs with enhancer-like function in human cells. Cell. 2010;143(1):46-58.
119. Bai M, Yuan M, Liao H, Chen J, Xie B, Yan D, et al. OCT4 pseudogene 5 upregulates OCT4 expression to promote proliferation by competing with miR-145 in endometrial carcinoma. Oncology reports. 2015;33(4):1745-52.
120. Mariner PD, Walters RD, Espinoza CA, Drullinger LF, Wagner SD, Kugel JF, et al. Human Alu RNA is a modular transacting repressor of mRNA transcription during heat shock. Molecular cell. 2008;29(4):499-509.
121. Tripathi V, Ellis JD, Shen Z, Song DY, Pan Q, Watt AT, et al. The nuclear-retained noncoding RNA MALAT1 regulates alternative splicing by modulating SR splicing factor phosphorylation. Molecular cell. 2010;39(6):925-38.
122. Park E, Maquat LE. Staufen-mediated mRNA decay. Wiley interdisciplinary reviews RNA. 2013;4(4):423-35.
123. Faghihi MA, Zhang M, Huang J, Modarresi F, Van der Brug MP, Nalls MA, et al. Evidence for natural antisense transcript-mediated inhibition of microRNA function. Genome biology. 2010;11(5):R56.
124. Carrieri C, Cimatti L, Biagioli M, Beugnet A, Zucchelli S, Fedele S, et al. Long non-coding antisense RNA controls Uchl1 translation through an embedded SINEB2 repeat. Nature. 2012;491(7424):454-7.
125. Gumireddy K, Li A, Yan J, Setoyama T, Johannes GJ, Orom UA, et al. Identification of a long non-coding RNA-associated RNP complex regulating metastasis at the translational step. The EMBO journal. 2013;32(20):2672-84.
126. Tsang WP, Ng EK, Ng SS, Jin H, Yu J, Sung JJ, et al. Oncofetal H19-derived miR-675 regulates tumor suppressor RB in human colorectal cancer. Carcinogenesis. 2010;31(3):350-8.
127. Li CX, Li HG, Huang LT, Kong YW, Chen FY, Liang JY, et al. H19 lncRNA regulates keratinocyte differentiation by targeting miR-130b-3p. Cell death & disease. 2017;8(11):e3174.

128. Hansen TB, Jensen TI, Clausen BH, Bramsen JB, Finsen B, Damgaard CK, et al. Natural RNA circles function as efficient microRNA sponges. Nature. 2013;495(7441):384-8.
129. Cheng J, Cai MY, Chen YN, Li ZC, Tang SS, Yang XL, et al. Variants in ANRIL gene correlated with its expression contribute to myocardial infarction risk. Oncotarget. 2017;8(8):12607-19.
130. Holdt LM, Beutner F, Scholz M, Gielen S, Gäbel G, Bergert H, et al. ANRIL expression is associated with atherosclerosis risk at chromosome 9p21. Arterioscler Thromb Vasc Biol. 2010;30(3):620-7.
131. Congrains A, Kamide K, Oguro R, Yasuda O, Miyata K, Yamamoto E, et al. Genetic variants at the 9p21 locus contribute to atherosclerosis through modulation of ANRIL and CDKN2A/B. Atherosclerosis. 2012;220(2):449-55.
132. Consortium WTCC. Genome-wide association study of 14,000 cases of seven common diseases and 3,000 shared controls. Nature. 2007;447(7145):661-78.
133. Samani NJ, Erdmann J, Hall AS, Hengstenberg C, Mangino M, Mayer B, et al. Genomewide association analysis of coronary artery disease. N Engl J Med. 2007;357(5):443-53.
134. Chen HH, Almontashiri NA, Antoine D, Stewart AF. Functional genomics of the 9p21.3 locus for atherosclerosis: clarity or confusion? Curr Cardiol Rep. 2014;16(7):502.
135. Song CL, Wang JP, Xue X, Liu N, Zhang XH, Zhao Z, et al. Effect of Circular ANRIL on the Inflammatory Response of Vascular Endothelial Cells in a Rat Model of Coronary Atherosclerosis. Cell Physiol Biochem. 2017;42(3):1202-12.
136. Holdt LM, Stahringer A, Sass K, Pichler G, Kulak NA, Wilfert W, et al. Circular non-coding RNA ANRIL modulates ribosomal RNA maturation and atherosclerosis in humans. Nat Commun. 2016;7:12429.
137. Raitoharju E, Lyytikäinen LP, Levula M, Oksala N, Mennander A, Tarkka M, et al. miR-21, miR-210, miR-34a, and miR-146a/b are up-regulated in human atherosclerotic plaques in the Tampere Vascular Study. Atherosclerosis. 2011;219(1):211-7.
138. Han H, Qu G, Han C, Wang Y, Sun T, Li F, et al. MiR-34a, miR-21 and miR-23a as potential biomarkers for coronary artery disease: a pilot microarray study and confirmation in a 32 patient cohort. Exp Mol Med. 2015;47:e138.
139. McDonald RA, White KM, Wu J, Cooley BC, Robertson KE, Halliday CA, et al. miRNA-21 is dysregulated in response to vein grafting in multiple models and genetic ablation in mice attenuates neointima formation. European heart journal. 2013;34(22):1636-43.
140. Wang S, Aurora AB, Johnson BA, Qi X, McAnally J, Hill JA, et al. The endothelial-specific microRNA miR-126 governs vascular integrity and angiogenesis. Dev Cell. 2008;15(2):261-71.
141. Schober A, Nazari-Jahantigh M, Wei Y, Bidzhekov K, Gremse F, Grommes J, et al. MicroRNA-126-5p promotes endothelial proliferation and limits atherosclerosis by suppressing Dlk1. Nature medicine. 2014;20(4):368-76.

142. Loyer X, Potteaux S, Vion AC, Guérin CL, Boulkroun S, Rautou PE, et al. Inhibition of microRNA-92a prevents endothelial dysfunction and atherosclerosis in mice. Circ Res. 2014;114(3):434-43.
143. Rayner KJ, Suárez Y, Dávalos A, Parathath S, Fitzgerald ML, Tamehiro N, et al. MiR-33 contributes to the regulation of cholesterol homeostasis. Science. 2010;328(5985):1570-3.
144. Horie T, Baba O, Kuwabara Y, Chujo Y, Watanabe S, Kinoshita M, et al. MicroRNA-33 deficiency reduces the progression of atherosclerotic plaque in ApoE-/- mice. J Am Heart Assoc. 2012;1(6):e003376.
145. Cipollone F, Felicioni L, Sarzani R, Ucchino S, Spigonardo F, Mandolini C, et al. A unique microRNA signature associated with plaque instability in humans. Stroke. 2011;42(9):2556-63.
146. Deng L, Blanco FJ, Stevens H, Lu R, Caudrillier A, McBride M, et al. MicroRNA-143 Activation Regulates Smooth Muscle and Endothelial Cell Crosstalk in Pulmonary Arterial Hypertension. Circ Res. 2015;117(10):870-83.
147. Maitrias P, Metzinger-Le Meuth V, Massy ZA, M'Baya-Moutoula E, Reix T, Caus T, et al. MicroRNA deregulation in symptomatic carotid plaque. J Vasc Surg. 2015;62(5):1245-50.e1.
148. Wang GK, Zhu JQ, Zhang JT, Li Q, Li Y, He J, et al. Circulating microRNA: a novel potential biomarker for early diagnosis of acute myocardial infarction in humans. Eur Heart J. 2010;31(6):659-66.
149. McManus DD, Ambros V. Circulating MicroRNAs in cardiovascular disease. Circulation. 2011;124(18):1908-10.
150. Matsumoto S, Sakata Y, Suna S, Nakatani D, Usami M, Hara M, et al. Circulating p53-responsive microRNAs are predictive indicators of heart failure after acute myocardial infarction. Circ Res. 2013;113(3):322-6.
151. Ishii N, Ozaki K, Sato H, Mizuno H, Saito S, Takahashi A, et al. Identification of a novel non-coding RNA, MIAT, that confers risk of myocardial infarction. J Hum Genet. 2006;51(12):1087-99.
152. Zangrando J, Zhang L, Vausort M, Maskali F, Marie PY, Wagner DR, et al. Identification of candidate long non-coding RNAs in response to myocardial infarction. BMC Genomics. 2014;15:460.
153. Vausort M, Wagner DR, Devaux Y. Long noncoding RNAs in patients with acute myocardial infarction. Circ Res. 2014;115(7):668-77.
154. Boulberdaa M, Scott E, Ballantyne M, Garcia R, Descamps B, Angelini GD, et al. A Role for the Long Noncoding RNA SENCR in Commitment and Function of Endothelial Cells. Mol Ther. 2016;24(5):978-90.
155. Ballantyne MD, Pinel K, Dakin R, Vesey AT, Diver L, Mackenzie R, et al. Smooth Muscle Enriched Long Noncoding RNA (SMILR) Regulates Cell Proliferation. Circulation. 2016;133(21):2050-65.
156. Sallam T, Jones M, Thomas BJ, Wu X, Gilliland T, Qian K, et al. Transcriptional regulation of macrophage cholesterol efflux and atherogenesis by a long noncoding RNA. Nat Med. 2018;24(3):304-12.
157. Arslan S, Berkan Ö, Lalem T, Özbilüm N, Göksel S, Korkmaz Ö, et al. Long non-coding RNAs in the atherosclerotic plaque. Atherosclerosis. 2017;266:176-81.

158. Kumarswamy R, Bauters C, Volkmann I, Maury F, Fetisch J, Holzmann A, et al. Circulating long noncoding RNA, LIPCAR, predicts survival in patients with heart failure. Circ Res. 2014;114(10):1569-75.
159. Bell RD, Long X, Lin M, Bergmann JH, Nanda V, Cowan SL, et al. Identification and initial functional characterization of a human vascular cell-enriched long noncoding RNA. Arterioscler Thromb Vasc Biol. 2014;34(6):1249-59.
160. Etienne PY, D'hoore W, Papadatos S, Mairy Y, El Khoury G, Noirhomme P, et al. Five-year follow-up of drug-eluting stents implantation vs minimally invasive direct coronary artery bypass for left anterior descending artery disease: a propensity score analysis. Eur J Cardiothorac Surg. 2013;44(5):884-90.
161. Gutschner T, Hämmerle M, Diederichs S. MALAT1 -- a paradigm for long noncoding RNA function in cancer. J Mol Med (Berl). 2013;91(7):791-801.
162. Ji P, Diederichs S, Wang W, Böing S, Metzger R, Schneider PM, et al. MALAT-1, a novel noncoding RNA, and thymosin beta4 predict metastasis and survival in early-stage non-small cell lung cancer. Oncogene. 2003;22(39):8031-41.
163. Michalik KM, You X, Manavski Y, Doddaballapur A, Zörnig M, Braun T, et al. Long noncoding RNA MALAT1 regulates endothelial cell function and vessel growth. Circ Res. 2014;114(9):1389-97.
164. Liu JY, Yao J, Li XM, Song YC, Wang XQ, Li YJ, et al. Pathogenic role of lncRNA-MALAT1 in endothelial cell dysfunction in diabetes mellitus. Cell Death Dis. 2014;5:e1506.
165. Zeliadt N. Big pharma shows signs of renewed interest in RNAi drugs. Nat Med. 2014;20(2):109.
166. Hutvagner G, Simard MJ, Mello CC, Zamore PD. Sequence-specific inhibition of small RNA function. PLoS biology. 2004;2(4):E98.
167. Elmen J, Lindow M, Schutz S, Lawrence M, Petri A, Obad S, et al. LNA-mediated microRNA silencing in non-human primates. Nature. 2008;452(7189):896-9.
168. Orom UA, Kauppinen S, Lund AH. LNA-modified oligonucleotides mediate specific inhibition of microRNA function. Gene. 2006;372:137-41.
169. Henry JC, Azevedo-Pouly AC, Schmittgen TD. MicroRNA replacement therapy for cancer. Pharmaceutical research. 2011;28(12):3030-42.
170. Davis S, Lollo B, Freier S, Esau C. Improved targeting of miRNA with antisense oligonucleotides. Nucleic acids research. 2006;34(8):2294-304.
171. Ji R, Cheng Y, Yue J, Yang J, Liu X, Chen H, et al. MicroRNA expression signature and antisense-mediated depletion reveal an essential role of MicroRNA in vascular neointimal lesion formation. Circulation research. 2007;100(11):1579-88.
172. Daniel JM, Penzkofer D, Teske R, Dutzmann J, Koch A, Bielenberg W, et al. Inhibition of miR-92a improves re-endothelialization and prevents neointima formation following vascular injury. Cardiovascular research. 2014;103(4):564-72.

173. Hullinger TG, Montgomery RL, Seto AG, Dickinson BA, Semus HM, Lynch JM, et al. Inhibition of miR-15 protects against cardiac ischemic injury. Circulation research. 2012;110(1):71-81.
174. Pirollo KF, Rait A, Zhou Q, Zhang XQ, Zhou J, Kim CS, et al. Tumor-targeting nanocomplex delivery of novel tumor suppressor RB94 chemosensitizes bladder carcinoma cells in vitro and in vivo. Clinical cancer research : an official journal of the American Association for Cancer Research. 2008;14(7):2190-8.
175. Trang P, Wiggins JF, Daige CL, Cho C, Omotola M, Brown D, et al. Systemic delivery of tumor suppressor microRNA mimics using a neutral lipid emulsion inhibits lung tumors in mice. Molecular therapy : the journal of the American Society of Gene Therapy. 2011;19(6):1116-22.
176. Miscianinov V, Martello A, Rose L, Parish E, Cathcart B, Mitic T, et al. MicroRNA-148b Targets the TGF-beta Pathway to Regulate Angiogenesis and Endothelial-to-Mesenchymal Transition during Skin Wound Healing. Molecular therapy : the journal of the American Society of Gene Therapy. 2018.
177. Woodrow KA, Cu Y, Booth CJ, Saucier-Sawyer JK, Wood MJ, Saltzman WM. Intravaginal gene silencing using biodegradable polymer nanoparticles densely loaded with small-interfering RNA. Nature materials. 2009;8(6):526-33.
178. Zhou J, Liu J, Cheng CJ, Patel TR, Weller CE, Piepmeier JM, et al. Biodegradable poly(amine-co-ester) terpolymers for targeted gene delivery. Nature materials. 2011;11(1):82-90.
179. Bellera N, Barba I, Rodriguez-Sinovas A, Ferret E, Asin MA, Gonzalez-Alujas MT, et al. Single intracoronary injection of encapsulated antagomir-92a promotes angiogenesis and prevents adverse infarct remodeling. Journal of the American Heart Association. 2014;3(5):e000946.
180. George SJ, Lloyd CT, Angelini GD, Newby AC, Baker AH. Inhibition of late vein graft neointima formation in human and porcine models by adenovirus-mediated overexpression of tissue inhibitor of metalloproteinase-3. Circulation. 2000;101(3):296-304.
181. Eulalio A, Mano M, Dal Ferro M, Zentilin L, Sinagra G, Zacchigna S, et al. Functional screening identifies miRNAs inducing cardiac regeneration. Nature. 2012;492(7429):376-81.
182. Wang D, Deuse T, Stubbendorff M, Chernogubova E, Erben RG, Eken SM, et al. Local MicroRNA Modulation Using a Novel Anti-miR-21-Eluting Stent Effectively Prevents Experimental In-Stent Restenosis. Arteriosclerosis, thrombosis, and vascular biology. 2015;35(9):1945-53.
183. Connelly CM, Uprety R, Hemphill J, Deiters A. Spatiotemporal control of microRNA function using light-activated antagomirs. Molecular bioSystems. 2012;8(11):2987-93.
184. Zheng G, Cochella L, Liu J, Hobert O, Li WH. Temporal and spatial regulation of microRNA activity with photoactivatable cantimirs. ACS chemical biology. 2011;6(12):1332-8.
185. Lucas T, Schafer F, Muller P, Eming SA, Heckel A, Dimmeler S. Light-inducible antimiR-92a as a therapeutic strategy to promote skin repair in healing-impaired diabetic mice. Nature communications. 2017;8:15162.

186. Ma S, Tian XY, Zhang Y, Mu C, Shen H, Bismuth J, et al. E-selectin-targeting delivery of microRNAs by microparticles ameliorates endothelial inflammation and atherosclerosis. Scientific reports. 2016;6:22910.
187. Jopling CL, Yi M, Lancaster AM, Lemon SM, Sarnow P. Modulation of hepatitis C virus RNA abundance by a liver-specific MicroRNA. Science (New York, NY). 2005;309(5740):1577-81.
188. Krutzfeldt J, Rajewsky N, Braich R, Rajeev KG, Tuschl T, Manoharan M, et al. Silencing of microRNAs in vivo with 'antagomirs'. Nature. 2005;438(7068):685-9.
189. Esau C, Davis S, Murray SF, Yu XX, Pandey SK, Pear M, et al. miR-122 regulation of lipid metabolism revealed by in vivo antisense targeting. Cell metabolism. 2006;3(2):87-98.
190. Elmen J, Lindow M, Silahtaroglu A, Bak M, Christensen M, Lind-Thomsen A, et al. Antagonism of microRNA-122 in mice by systemically administered LNA-antimiR leads to up-regulation of a large set of predicted target mRNAs in the liver. Nucleic acids research. 2008;36(4):1153-62.
191. Lanford RE, Hildebrandt-Eriksen ES, Petri A, Persson R, Lindow M, Munk ME, et al. Therapeutic silencing of microRNA-122 in primates with chronic hepatitis C virus infection. Science (New York, NY). 2010;327(5962):198-201.
192. Titze-de-Almeida R, David C, Titze-de-Almeida SS. The Race of 10 Synthetic RNAi-Based Drugs to the Pharmaceutical Market. Pharmaceutical research. 2017;34(7):1339-63.
193. Yin C, Salloum FN, Kukreja RC. A novel role of microRNA in late preconditioning: upregulation of endothelial nitric oxide synthase and heat shock protein 70. Circulation research. 2009;104(5):572-5.
194. Huang F, Li ML, Fang ZF, Hu XQ, Liu QM, Liu ZJ, et al. Overexpression of MicroRNA-1 improves the efficacy of mesenchymal stem cell transplantation after myocardial infarction. Cardiology. 2013;125(1):18-30.
195. Yang J, Brown ME, Zhang H, Martinez M, Zhao Z, Bhutani S, et al. High-throughput screening identifies microRNAs that target Nox2 and improve function after acute myocardial infarction. American journal of physiology Heart and circulatory physiology. 2017;312(5):H1002-h12.
196. Deng L, Blanco FJ, Stevens H, Lu R, Caudrillier A, McBride M, et al. MicroRNA-143 Activation Regulates Smooth Muscle and Endothelial Cell Crosstalk in Pulmonary Arterial Hypertension. Circulation research. 2015;117(10):870-83.
197. Gomez IG, MacKenna DA, Johnson BG, Kaimal V, Roach AM, Ren S, et al. Anti-microRNA-21 oligonucleotides prevent Alport nephropathy progression by stimulating metabolic pathways. The Journal of clinical investigation. 2015;125(1):141-56.
198. Bonauer A, Carmona G, Iwasaki M, Mione M, Koyanagi M, Fischer A, et al. MicroRNA-92a controls angiogenesis and functional recovery of ischemic tissues in mice. Science (New York, NY). 2009;324(5935):1710-3.
199. Hinkel R, Penzkofer D, Zuhlke S, Fischer A, Husada W, Xu QF, et al. Inhibition of microRNA-92a protects against ischemia/reperfusion injury in a large-animal model. Circulation. 2013;128(10):1066-75.

200. Abplanalp WT, Fischer A, John D, Zeiher AM, Gosgnach W, Darville H, et al. Efficiency and Target Derepression of Anti-miR-92a: Results of a First in Human Study. Nucleic Acid Ther. 2020.
201. Chang H, Yi B, Ma R, Zhang X, Zhao H, Xi Y. CRISPR/cas9, a novel genomic tool to knock down microRNA in vitro and in vivo. Scientific reports. 2016;6:22312.
202. Smaldone MC, Davies BJ. BC-819, a plasmid comprising the H19 gene regulatory sequences and diphtheria toxin A, for the potential targeted therapy of cancers. Current opinion in molecular therapeutics. 2010;12(5):607-16.
203. Halachmi S, Leibovitch I, Zisman A, Stein A, Benjamin S, Sidi A, et al. Phase II trial of BC-819 intravesical gene therapy in combination with BCG in patients with non-muscle invasive bladder cancer (NMIBC). Journal of Clinical Oncology. 2018;36(6_suppl):499-.
204. Haemmig S, Feinberg MW. Targeting LncRNAs in Cardiovascular Disease: Options and Expeditions. Circulation research. 2017;120(4):620-3.
205. Michalik KM, You X, Manavski Y, Doddaballapur A, Zornig M, Braun T, et al. Long noncoding RNA MALAT1 regulates endothelial cell function and vessel growth. Circulation research. 2014;114(9):1389-97.
206. Viereck J, Kumarswamy R, Foinquinos A, Xiao K, Avramopoulos P, Kunz M, et al. Long noncoding RNA Chast promotes cardiac remodeling. Science translational medicine. 2016;8(326):326ra22.
207. Gilbert LA, Horlbeck MA, Adamson B, Villalta JE, Chen Y, Whitehead EH, et al. Genome-Scale CRISPR-Mediated Control of Gene Repression and Activation. Cell. 2014;159(3):647-61.
208. Shah AS, Griffiths M, Lee KK, McAllister DA, Hunter AL, Ferry AV, et al. High sensitivity cardiac troponin and the under-diagnosis of myocardial infarction in women: prospective cohort study. BMJ. 2015;350:g7873.
209. Kadesjö E, Roos A, Siddiqui A, Desta L, Lundbäck M, Holzmann MJ. Acute versus chronic myocardial injury and long-term outcomes. Heart. 2019;105(24):1905-12.
210. Roos A, Sartipy U, Ljung R, Holzmann MJ. Relation of Chronic Myocardial Injury and Non-ST-Segment Elevation Myocardial Infarction to Mortality. Am J Cardiol. 2018;122(12):1989-95.
211. Livak KJ, Schmittgen TD. Analysis of relative gene expression data using real-time quantitative PCR and the 2(-Delta Delta C(T)) Method. Methods. 2001;25(4):402-8.
212. Townsend N, Wilson L, Bhatnagar P, Wickramasinghe K, Rayner M, Nichols M. Cardiovascular disease in Europe: epidemiological update 2016. Eur Heart J. 2016;37(42):3232-45.
213. Eagle KA, Lim MJ, Dabbous OH, Pieper KS, Goldberg RJ, Van de Werf F, et al. A validated prediction model for all forms of acute coronary syndrome: estimating the risk of 6-month postdischarge death in an international registry. JAMA. 2004;291(22):2727-33.
214. Fox KA, Dabbous OH, Goldberg RJ, Pieper KS, Eagle KA, Van de Werf F, et al. Prediction of risk of death and myocardial infarction in the six months after presentation with acute coronary syndrome: prospective multinational observational study (GRACE). BMJ. 2006;333(7578):1091.

215. Fox KA, Fitzgerald G, Puymirat E, Huang W, Carruthers K, Simon T, et al. Should patients with acute coronary disease be stratified for management according to their risk? Derivation, external validation and outcomes using the updated GRACE risk score. BMJ Open. 2014;4(2):e004425.
216. Granger CB, Goldberg RJ, Dabbous O, Pieper KS, Eagle KA, Cannon CP, et al. Predictors of hospital mortality in the global registry of acute coronary events. Arch Intern Med. 2003;163(19):2345-53.
217. NICE. Clinical Guideline 94: Unstable angina and NSTEMI: early management2010.
218. Roffi M, Patrono C, Collet JP, Mueller C, Valgimigli M, Andreotti F, et al. 2015 ESC Guidelines for the management of acute coronary syndromes in patients presenting without persistent ST-segment elevation: Task Force for the Management of Acute Coronary Syndromes in Patients Presenting without Persistent ST-Segment Elevation of the European Society of Cardiology (ESC). Eur Heart J. 2016;37(3):267-315.
219. Amsterdam EA, Wenger NK, Brindis RG, Casey DE, Ganiats TG, Holmes DR, et al. 2014 AHA/ACC guideline for the management of patients with non-ST-elevation acute coronary syndromes: a report of the American College of Cardiology/American Heart Association Task Force on Practice Guidelines. Circulation. 2014;130(25):e344-426.
220. DeFilippis AP, Chapman AR, Mills NL, de Lemos JA, Arbab-Zadeh A, Newby LK, et al. Assessment and Treatment of Patients With Type 2 Myocardial Infarction and Acute Nonischemic Myocardial Injury. Circulation. 2019;140(20):1661-78.
221. McCarthy CP, Raber I, Chapman AR, Sandoval Y, Apple FS, Mills NL, et al. Myocardial Injury in the Era of High-Sensitivity Cardiac Troponin Assays: A Practical Approach for Clinicians. JAMA Cardiol. 2019;4(10):1034-42.
222. Chapman AR, Adamson PD, Shah ASV, Anand A, Strachan FE, Ferry AV, et al. High-Sensitivity Cardiac Troponin and the Universal Definition of Myocardial Infarction. Circulation. 2020;141(3):161-71.
223. Sandoval Y, Smith SW, Sexter A, Thordsen SE, Bruen CA, Carlson MD, et al. Type 1 and 2 Myocardial Infarction and Myocardial Injury: Clinical Transition to High-Sensitivity Cardiac Troponin I. Am J Med. 2017;130(12):1431-9.e4.
224. Smilowitz NR, Subramanyam P, Gianos E, Reynolds HR, Shah B, Sedlis SP. Treatment and outcomes of type 2 myocardial infarction and myocardial injury compared with type 1 myocardial infarction. Coron Artery Dis. 2018;29(1):46-52.
225. Sarkisian L, Saaby L, Poulsen TS, Gerke O, Hosbond S, Jangaard N, et al. Prognostic Impact of Myocardial Injury Related to Various Cardiac and Noncardiac Conditions. Am J Med. 2016;129(5):506-14.e1.
226. Sarkisian L, Saaby L, Poulsen TS, Gerke O, Jangaard N, Hosbond S, et al. Clinical Characteristics and Outcomes of Patients with Myocardial Infarction, Myocardial Injury, and Nonelevated Troponins. Am J Med. 2016;129(4):446.e5-.e21.

227. Neumann JT, Sörensen NA, Rübsamen N, Ojeda F, Renné T, Qaderi V, et al. Discrimination of patients with type 2 myocardial infarction. Eur Heart J. 2017;38(47):3514-20.
228. Baron T, Hambraeus K, Sundström J, Erlinge D, Jernberg T, Lindahl B, et al. Impact on Long-Term Mortality of Presence of Obstructive Coronary Artery Disease and Classification of Myocardial Infarction. Am J Med. 2016;129(4):398-406.
229. Nestelberger T, Boeddinghaus J, Badertscher P, Twerenbold R, Wildi K, Breitenbücher D, et al. Effect of Definition on Incidence and Prognosis of Type 2 Myocardial Infarction. J Am Coll Cardiol. 2017;70(13):1558-68.
230. Cediel G, Sandoval Y, Sexter A, Carrasquer A, González-Del-Hoyo M, Bonet G, et al. Risk Estimation in Type 2 Myocardial Infarction and Myocardial Injury: The TARRACO Risk Score. Am J Med. 2019;132(2):217-26.
231. Murphy SP, McCarthy CP, Cohen JA, Rehman S, Jones-O'Connor M, Olshan DS, et al. Application of the GRACE, TIMI, and TARRACO Risk Scores in Type 2 Myocardial Infarction. J Am Coll Cardiol. 2020;75(3):344-5.
232. Myocardial Ischaemia National Audit Project SR. Published by National Institute for Cardiovascular Outcomes Research.
233. Szummer K, Wallentin L, Lindhagen L, Alfredsson J, Erlinge D, Held C, et al. Relations between implementation of new treatments and improved outcomes in patients with non-ST-elevation myocardial infarction during the last 20 years: experiences from SWEDEHEART registry 1995 to 2014. Eur Heart J. 2018;39(42):3766-76.
234. Ozsolak F, Milos PM. RNA sequencing: advances, challenges and opportunities. Nat Rev Genet. 2011;12(2):87-98.
235. Wang Z, Gerstein M, Snyder M. RNA-Seq: a revolutionary tool for transcriptomics. Nat Rev Genet. 2009;10(1):57-63.
236. Adams MD, Kelley JM, Gocayne JD, Dubnick M, Polymeropoulos MH, Xiao H, et al. Complementary DNA sequencing: expressed sequence tags and human genome project. Science. 1991;252(5013):1651-6.
237. Derrien T, Johnson R, Bussotti G, Tanzer A, Djebali S, Tilgner H, et al. The GENCODE v7 catalog of human long noncoding RNAs: analysis of their gene structure, evolution, and expression. Genome Res. 2012;22(9):1775-89.
238. Mahmoud AD, Ballantyne MD, Miscianinov V, Pinel K, Hung J, Scanlon JP, et al. The Human- and Smooth Muscle Cell-Enriched lncRNA SMILR Promotes Proliferation by Regulating Mitotic CENPF mRNA and Drives Cell-Cycle Progression Which Can Be Targeted to Limit Vascular Remodeling. Circ Res. 2019.
239. van der Wal AC, Becker AE. Atherosclerotic plaque rupture--pathologic basis of plaque stability and instability. Cardiovasc Res. 1999;41(2):334-44.
240. Tawakol A, Migrino RQ, Bashian GG, Bedri S, Vermylen D, Cury RC, et al. In vivo 18F-fluorodeoxyglucose positron emission tomography imaging provides a noninvasive measure of carotid plaque inflammation in patients. J Am Coll Cardiol. 2006;48(9):1818-24.

241. Joshi NV, Vesey AT, Williams MC, Shah AS, Calvert PA, Craighead FH, et al. 18F-fluoride positron emission tomography for identification of ruptured and high-risk coronary atherosclerotic plaques: a prospective clinical trial. Lancet. 2014;383(9918):705-13.
242. Dweck MR, Chow MW, Joshi NV, Williams MC, Jones C, Fletcher AM, et al. Coronary arterial 18F-sodium fluoride uptake: a novel marker of plaque biology. J Am Coll Cardiol. 2012;59(17):1539-48.
243. Vesey AT, Jenkins WS, Irkle A, Moss A, Sng G, Forsythe RO, et al. 18F-Fluoride and 18F-Fluorodeoxyglucose Positron Emission Tomography After Transient Ischemic Attack or Minor Ischemic Stroke: Case-Control Study. Circ Cardiovasc Imaging. 2017;10(3).
244. Ringnér M. What is principal component analysis? Nat Biotechnol. 2008;26(3):303-4.
245. Zhao H, Qin X, Wang S, Sun X, Dong B. Decreased cathepsin K levels in human atherosclerotic plaques are associated with plaque instability. Exp Ther Med. 2017;14(4):3471-6.
246. Abbas A, Aukrust P, Russell D, Krohg-Sørensen K, Almås T, Bundgaard D, et al. Matrix metalloproteinase 7 is associated with symptomatic lesions and adverse events in patients with carotid atherosclerosis. PLoS One. 2014;9(1):e84935.
247. Perisic L, Hedin E, Razuvaev A, Lengquist M, Osterholm C, Folkersen L, et al. Profiling of atherosclerotic lesions by gene and tissue microarrays reveals PCSK6 as a novel protease in unstable carotid atherosclerosis. Arterioscler Thromb Vasc Biol. 2013;33(10):2432-43.
248. Gil N, Ulitsky I. Regulation of gene expression by cis-acting long non-coding RNAs. Nat Rev Genet. 2020;21(2):102-17.
249. Ruffell D, Mourkioti F, Gambardella A, Kirstetter P, Lopez RG, Rosenthal N, et al. A CREB-C/EBPbeta cascade induces M2 macrophage-specific gene expression and promotes muscle injury repair. Proc Natl Acad Sci U S A. 2009;106(41):17475-80.
250. Gray MJ, Poljakovic M, Kepka-Lenhart D, Morris SM. Induction of arginase I transcription by IL-4 requires a composite DNA response element for STAT6 and C/EBPbeta. Gene. 2005;353(1):98-106.
251. Liu YW, Tseng HP, Chen LC, Chen BK, Chang WC. Functional cooperation of simian virus 40 promoter factor 1 and CCAAT/enhancer-binding protein beta and delta in lipopolysaccharide-induced gene activation of IL-10 in mouse macrophages. J Immunol. 2003;171(2):821-8.
252. Bence KK. Protein tyrosine phosphatase control of metabolism. New York: Springer; 2013. xi, 273 p. p.
253. Thompson D, Morrice N, Grant L, Le Sommer S, Lees EK, Mody N, et al. Pharmacological inhibition of protein tyrosine phosphatase 1B protects against atherosclerotic plaque formation in the LDLR. Clin Sci (Lond). 2017;131(20):2489-501.
254. Bärlund M, Monni O, Weaver JD, Kauraniemi P, Sauter G, Heiskanen M, et al. Cloning of BCAS3 (17q23) and BCAS4 (20q13) genes that undergo amplification, overexpression, and fusion in breast cancer. Genes Chromosomes Cancer. 2002;35(4):311-7.

255. Mercer TR, Gerhardt DJ, Dinger ME, Crawford J, Trapnell C, Jeddeloh JA, et al. Targeted RNA sequencing reveals the deep complexity of the human transcriptome. Nat Biotechnol. 2011;30(1):99-104.
256. Newby AC, Zaltsman AB. Fibrous cap formation or destruction--the critical importance of vascular smooth muscle cell proliferation, migration and matrix formation. Cardiovasc Res. 1999;41(2):345-60.
257. Lin Z, Zhou Z, Guo H, He Y, Pang X, Zhang X, et al. Long noncoding RNA gastric cancer-related lncRNA1 mediates gastric malignancy through miRNA-885-3p and cyclin-dependent kinase 4. Cell Death Dis. 2018;9(6):607.
258. Wang S, Hou Y, Chen W, Wang J, Xie W, Zhang X, et al. KIF9-AS1, LINC01272 and DIO3OS lncRNAs as novel biomarkers for inflammatory bowel disease. Mol Med Rep. 2018;17(2):2195-202.
259. Bronte V, Pittet MJ. The spleen in local and systemic regulation of immunity. Immunity. 2013;39(5):806-18.
260. Robinson MW, Harmon C, O'Farrelly C. Liver immunology and its role in inflammation and homeostasis. Cell Mol Immunol. 2016;13(3):267-76.
261. Kriebs A. Accumulation of macrophages in adipose tissue. Nat Rev Endocrinol. 2021;17(1):4.
262. Hung J, Miscianinov V, Sluimer JC, Newby DE, Baker AH. Targeting Non-coding RNA in Vascular Biology and Disease. Front Physiol. 2018;9:1655.
263. Dykes IM, Emanueli C. Transcriptional and Post-transcriptional Gene Regulation by Long Non-coding RNA. Genomics Proteomics Bioinformatics. 2017;15(3):177-86.
264. Rashid F, Shah A, Shan G. Long Non-coding RNAs in the Cytoplasm. Genomics Proteomics Bioinformatics. 2016;14(2):73-80.
265. Sasaki YT, Ideue T, Sano M, Mituyama T, Hirose T. MENepsilon/beta noncoding RNAs are essential for structural integrity of nuclear paraspeckles. Proc Natl Acad Sci U S A. 2009;106(8):2525-30.
266. Zhang P, Cao L, Zhou R, Yang X, Wu M. The lncRNA Neat1 promotes activation of inflammasomes in macrophages. Nat Commun. 2019;10(1):1495.
267. Moore KJ, Tabas I. Macrophages in the pathogenesis of atherosclerosis. Cell. 2011;145(3):341-55.
268. Moore KJ, Sheedy FJ, Fisher EA. Macrophages in atherosclerosis: a dynamic balance. Nat Rev Immunol. 2013;13(10):709-21.
269. Peled M, Fisher EA. Dynamic Aspects of Macrophage Polarization during Atherosclerosis Progression and Regression. Front Immunol. 2014;5:579.
270. Shioi A, Ikari Y. Plaque Calcification During Atherosclerosis Progression and Regression. J Atheroscler Thromb. 2018;25(4):294-303.
271. Martinez FO, Gordon S, Locati M, Mantovani A. Transcriptional profiling of the human monocyte-to-macrophage differentiation and polarization: new molecules and patterns of gene expression. J Immunol. 2006;177(10):7303-11.

272. Mantovani A, Sica A, Sozzani S, Allavena P, Vecchi A, Locati M. The chemokine system in diverse forms of macrophage activation and polarization. Trends Immunol. 2004;25(12):677-86.
273. Biswas SK, Mantovani A. Macrophage plasticity and interaction with lymphocyte subsets: cancer as a paradigm. Nat Immunol. 2010;11(10):889-96.
274. Gordon S. Alternative activation of macrophages. Nat Rev Immunol. 2003;3(1):23-35.
275. Sica A, Mantovani A. Macrophage plasticity and polarization: in vivo veritas. J Clin Invest. 2012;122(3):787-95.
276. Randolph GJ. Mechanisms that regulate macrophage burden in atherosclerosis. Circ Res. 2014;114(11):1757-71.
277. Lee SG, Oh J, Bong SK, Kim JS, Park S, Kim S, et al. Macrophage polarization and acceleration of atherosclerotic plaques in a swine model. PLoS One. 2018;13(3):e0193005.
278. Porta C, Rimoldi M, Raes G, Brys L, Ghezzi P, Di Liberto D, et al. Tolerance and M2 (alternative) macrophage polarization are related processes orchestrated by p50 nuclear factor kappaB. Proc Natl Acad Sci U S A. 2009;106(35):14978-83.
279. Kornienko AE, Guenzl PM, Barlow DP, Pauler FM. Gene regulation by the act of long non-coding RNA transcription. BMC Biol. 2013;11:59.
280. Akira S, Kishimoto T. NF-IL6 and NF-kappa B in cytokine gene regulation. Adv Immunol. 1997;65:1-46.
281. Etzion Y, Muslin AJ. The application of phenotypic high-throughput screening techniques to cardiovascular research. Trends Cardiovasc Med. 2009;19(6):207-12.
282. Soliman K. Super-Resolution High Content Screening and Analysis. Methods Mol Biol. 2017;1663:253-9.
283. Tripathi R, Chakraborty P, Varadwaj PK. Unraveling long non-coding RNAs through analysis of high-throughput RNA-sequencing data. Noncoding RNA Res. 2017;2(2):111-8.
284. Aderem A, Underhill DM. Mechanisms of phagocytosis in macrophages. Annu Rev Immunol. 1999;17:593-623.
285. Schrijvers DM, De Meyer GR, Herman AG, Martinet W. Phagocytosis in atherosclerosis: Molecular mechanisms and implications for plaque progression and stability. Cardiovasc Res. 2007;73(3):470-80.
286. Kapellos TS, Taylor L, Lee H, Cowley SA, James WS, Iqbal AJ, et al. A novel real time imaging platform to quantify macrophage phagocytosis. Biochem Pharmacol. 2016;116:107-19.
287. Matsuura E, Kobayashi K, Inoue K, Lopez LR, Shoenfeld Y. Oxidized LDL/beta2-glycoprotein I complexes: new aspects in atherosclerosis. Lupus. 2005;14(9):736-41.
288. Brown MS, Goldstein JL. Lipoprotein metabolism in the macrophage: implications for cholesterol deposition in atherosclerosis. Annu Rev Biochem. 1983;52:223-61.
289. Khoo JC, Miller E, McLoughlin P, Steinberg D. Enhanced macrophage uptake of low density lipoprotein after self-aggregation. Arteriosclerosis. 1988;8(4):348-58.

290. Steinberg D. Lewis A. Conner Memorial Lecture. Oxidative modification of LDL and atherogenesis. Circulation. 1997;95(4):1062-71.
291. Goldstein JL, Ho YK, Basu SK, Brown MS. Binding site on macrophages that mediates uptake and degradation of acetylated low density lipoprotein, producing massive cholesterol deposition. Proc Natl Acad Sci U S A. 1979;76(1):333-7.
292. Violi F, Carnevale R, Loffredo L, Pignatelli P, Gallin JI. NADPH Oxidase-2 and Atherothrombosis: Insight From Chronic Granulomatous Disease. Arterioscler Thromb Vasc Biol. 2017;37(2):218-25.
293. Nowak WN, Deng J, Ruan XZ, Xu Q. Reactive Oxygen Species Generation and Atherosclerosis. Arterioscler Thromb Vasc Biol. 2017;37(5):e41-e52.
294. Yurdagul A, Doran AC, Cai B, Fredman G, Tabas IA. Mechanisms and Consequences of Defective Efferocytosis in Atherosclerosis. Front Cardiovasc Med. 2017;4:86.
295. Kojima Y, Weissman IL, Leeper NJ. The Role of Efferocytosis in Atherosclerosis. Circulation. 2017;135(5):476-89.
296. Podrez EA, Febbraio M, Sheibani N, Schmitt D, Silverstein RL, Hajjar DP, et al. Macrophage scavenger receptor CD36 is the major receptor for LDL modified by monocyte-generated reactive nitrogen species. J Clin Invest. 2000;105(8):1095-108.
297. Kolodgie FD, Narula J, Burke AP, Haider N, Farb A, Hui-Liang Y, et al. Localization of apoptotic macrophages at the site of plaque rupture in sudden coronary death. Am J Pathol. 2000;157(4):1259-68.
298. Chistiakov DA, Killingsworth MC, Myasoedova VA, Orekhov AN, Bobryshev YV. CD68/macrosialin: not just a histochemical marker. Lab Invest. 2017;97(1):4-13.
299. Shah PK, Galis ZS. Matrix metalloproteinase hypothesis of plaque rupture: players keep piling up but questions remain. Circulation. 2001;104(16):1878-80.
300. Rao VH, Kansal V, Stoupa S, Agrawal DK. MMP-1 and MMP-9 regulate epidermal growth factor-dependent collagen loss in human carotid plaque smooth muscle cells. Physiol Rep. 2014;2(2):e00224.
301. Chanput W, Mes JJ, Wichers HJ. THP-1 cell line: an in vitro cell model for immune modulation approach. Int Immunopharmacol. 2014;23(1):37-45.
302. Bosshart H, Heinzelmann M. THP-1 cells as a model for human monocytes. Ann Transl Med. 2016;4(21):438.
303. Wang KC, Chang HY. Molecular mechanisms of long noncoding RNAs. Mol Cell. 2011;43(6):904-14.
304. Hung J, Scanlon JP, Mahmoud AD, Rodor J, Ballantyne M, Fontaine MAC, et al. Novel Plaque Enriched Long Noncoding RNA in Atherosclerotic Macrophage Regulation (PELATON). Arterioscler Thromb Vasc Biol. 2020;40(3):697-713.
305. Granger CB. Strategies of patient care in acute coronary syndromes: rationale for the Global Registry of Acute Coronary Events (GRACE) registry. Am J Cardiol. 2000;86(12B):4M-9M.
306. Huang W, FitzGerald G, Goldberg RJ, Gore J, McManus RH, Awad H, et al. Performance of the GRACE Risk Score 2.0 Simplified Algorithm for

Predicting 1-Year Death After Hospitalization for an Acute Coronary Syndrome in a Contemporary Multiracial Cohort. Am J Cardiol. 2016;118(8):1105-10.
307. Lin A, Devlin G, Lee M, Kerr AJ. Performance of the GRACE scores in a New Zealand acute coronary syndrome cohort. Heart. 2014;100(24):1960-6.
308. Correia LC, Garcia G, Kalil F, Ferreira F, Carvalhal M, Oliveira R, et al. Prognostic value of TIMI score versus GRACE score in ST-segment elevation myocardial infarction. Arq Bras Cardiol. 2014;103(2):98-106.
309. Hung J, Roos A, Kadesjö E, McAllister DA, Kimenai DM, Shah ASV, et al. Performance of the GRACE 2.0 score in patients with type 1 and type 2 myocardial infarction. Eur Heart J. 2020.
310. Sánchez E, Vidán MT, Serra JA, Fernández-Avilés F, Bueno H. Prevalence of geriatric syndromes and impact on clinical and functional outcomes in older patients with acute cardiac diseases. Heart. 2011;97(19):1602-6.
311. Pierce JB, Feinberg MW. Long Noncoding RNAs in Atherosclerosis and Vascular Injury: Pathobiology, Biomarkers, and Targets for Therapy. Arterioscler Thromb Vasc Biol. 2020;40(9):2002-17.
312. Chen J, Brunner AD, Cogan JZ, Nuñez JK, Fields AP, Adamson B, et al. Pervasive functional translation of noncanonical human open reading frames. Science. 2020;367(6482):1140-6.
313. Grelet S, Link LA, Howley B, Obellianne C, Palanisamy V, Gangaraju VK, et al. A regulated PNUTS mRNA to lncRNA splice switch mediates EMT and tumour progression. Nat Cell Biol. 2017;19(9):1105-15.
314. Novikova IV, Hennelly SP, Sanbonmatsu KY. Structural architecture of the human long non-coding RNA, steroid receptor RNA activator. Nucleic Acids Res. 2012;40(11):5034-51.
315. Chen L, Zhang YH, Pan X, Liu M, Wang S, Huang T, et al. Tissue Expression Difference between mRNAs and lncRNAs. Int J Mol Sci. 2018;19(11).
316. Schwartz GG, Steg PG, Szarek M, Bhatt DL, Bittner VA, Diaz R, et al. Alirocumab and Cardiovascular Outcomes after Acute Coronary Syndrome. N Engl J Med. 2018;379(22):2097-107.
317. Jain MK, Ridker PM. Anti-inflammatory effects of statins: clinical evidence and basic mechanisms. Nat Rev Drug Discov. 2005;4(12):977-87.
318. Chinetti-Gbaguidi G, Colin S, Staels B. Macrophage subsets in atherosclerosis. Nat Rev Cardiol. 2015;12(1):10-7.
319. Koelwyn GJ, Corr EM, Erbay E, Moore KJ. Regulation of macrophage immunometabolism in atherosclerosis. Nat Immunol. 2018;19(6):526-37.
320. Ye ZM, Yang S, Xia YP, Hu RT, Chen S, Li BW, et al. LncRNA MIAT sponges miR-149-5p to inhibit efferocytosis in advanced atherosclerosis through CD47 upregulation. Cell Death Dis. 2019;10(2):138.
321. Sun C, Fu Y, Gu X, Xi X, Peng X, Wang C, et al. Macrophage-Enriched lncRNA RAPIA: A Novel Therapeutic Target for Atherosclerosis. Arterioscler Thromb Vasc Biol. 2020;40(6):1464-78.

322. Wu X, Zheng X, Cheng J, Zhang K, Ma C. LncRNA TUG1 regulates proliferation and apoptosis by regulating miR-148b/IGF2 axis in ox-LDL-stimulated VSMC and HUVEC. Life Sci. 2020;243:117287.
323. Ylä-Herttuala S, Baker AH. Cardiovascular Gene Therapy: Past, Present, and Future. Mol Ther. 2017;25(5):1095-106.
324. White K, Nicklin SA, Baker AH. Novel vectors for in vivo gene delivery to vascular tissue. Expert Opin Biol Ther. 2007;7(6):809-21.
325. Amarzguioui M, Rossi JJ, Kim D. Approaches for chemically synthesized siRNA and vector-mediated RNAi. FEBS Lett. 2005;579(26):5974-81.
326. Shen X, Corey DR. Chemistry, mechanism and clinical status of antisense oligonucleotides and duplex RNAs. Nucleic Acids Res. 2018;46(4):1584-600.
327. Fitzgerald K, White S, Borodovsky A, Bettencourt BR, Strahs A, Clausen V, et al. A Highly Durable RNAi Therapeutic Inhibitor of PCSK9. N Engl J Med. 2017;376(1):41-51.
328. Ray KK, Landmesser U, Leiter LA, Kallend D, Dufour R, Karakas M, et al. Inclisiran in Patients at High Cardiovascular Risk with Elevated LDL Cholesterol. N Engl J Med. 2017;376(15):1430-40.